Bioconjugated Chitosan based DNA Nanoparticles – Non viral Approach of using Cationic polymer for Cancer Therapy

A THESIS PRESENTED BY

SUSAN M ALEX

TO

SREE CHITRA TIRUNAL INSTITUTE FOR MEDICAL
SCIENCES AND TECHNOLOGY
THIRUVANANTHAPURAM
INDIA

IN PARTIAL FULFILMENT OF THE REQUIREMENTS
FOR THE AWARD OF
DOCTOR OF PHILOSOPHY

2014

To

My Parents and My Dear Sisters

CERTIFICATE

I, ***SUSAN M ALEX***, hereby certify that I had personally carried out the work depicted in the thesis entitled, ***"Bioconjugated Chitosan based DNA Nanoparticles – Non viral Approach of using Cationic polymer for Cancer Therapy"***.

No part of the thesis has been submitted for the award of any other degree or diploma prior to this date.

13-08-2014 **Susan M Alex**

Thiruvananthapuram **Reg No: PhD/2010/22**

Tele : 0471-2340801
Fax : 0471-2341814

Grams : CHITRAMET
Telex : 0435 - 6290

श्री चित्रा तिरुनाल आयुर्विज्ञान तथा प्रौद्योगिकी संस्थान
बायो मेडिकल टैक्नोलॉजी विंग
पूजापुरा, तिरुवनन्तपुरम-695 012, इन्डिया

SREE CHITRA TIRUNAL INSTITUTE FOR MEDICAL SCIENCES AND TECHNOLOGY
BIO MEDICAL TECHNOLOGY WING
POOJAPPURA, THIRUVANANTHAPURAM-695 012, INDIA
(An Institute of National Importance under Govt. of India)

Ref: Dr. Chandra P. Sharma
Former Senior Scientist G & Head
Biosurface Technology Division & FADDS
sharmacp@sctimst.ac.in

Date: Aug13, 2014

This is to certify that **Ms. Susan M Alex** in the division of Biosurface Technology and FADDS of this Institute has fulfilled the requirements prescribed for the Ph.D Degree of Sree Chitra Tirunal Institute for Medical Sciences and Technology, Trivandrum.

The thesis entitled,"Bioconjugated Chitosan based DNA Nanoparticles – Non viral Approach of using Cationic polymer for Cancer Therapy" was carried out under my direct supervision. No part of the thesis was submitted for the award of any degree or diploma prior to this date.

*Clearance was obtained from the Institutional Ethics Committee/ Institutional Animal Ethics for carrying out the study

Chandra P Sharma

Dr. Chandra P. Sharma
Signed by Thesis Supervisor(s) with name(s) and date

The thesis entitled

"Bioconjugated Chitosan based DNA Nanoparticles – Non viral Approach of using Cationic polymer for Cancer Therapy"

Submitted by

SUSAN M ALEX

for the degree of

Doctor of Philosophy

Of

SREE CHITRA TIRUNAL INSTITUTE FOR MEDICAL SCIENCES AND TECHNOLOGY, THIRUVANANTHAPURAM - 695011

is evaluated and approved by

Dr. Chandra P. Sharma
(Research Supervisor)

Examiner

ACKNOWLEDGEMENT

I take this as an honour to thank many who have motivated and supported me during all those years of my PhD life and in the pursuit of my thesis compilation.

First of all, I would like to thank my supervisor, Dr. Chandra P. Sharma for his presence and guidance throughout my PhD period. It was only due to his great patience, critical evaluations and encouragement that I was able to complete my work.

I wish to express my gratitude and respect to the former and present Director of SCTIMST and the Head, BMT Wing for giving me the opportunity and the facilities during the course of my work. I am thankful to the Deputy Registrar Dr Sundar Jaysingh S, Associate Dean for PhD affairs Dr Prabha D Nair, Dean and all members of the academic division and Director's office for their assistance.

I owe my sincere gratitude to my Doctoral Advisory Committee members Dr. Mira Mohanty, Dr K Sreenivasan and Dr M.R Rekha for the valuable suggestions and critical comments in each stage of my work. I am grateful to Council of Scientific and Industrial Research (CSIR), India for the research fellowship and Department of Science & technology, Govt of India for the financial assistance through the project Facility for nano/microparticle based biomaterials- advanced drug delivery systems (FADDS) #8013, under the Drugs & pharmaceuticals Research Programme.

I thank Dr. M.R Rekha once again, Mr Willi Paul and Dr. Kaladhar Kamalasanan for their timely support and assistance from our laboratory. I warmly thank Dr. T Anoopkumar and his students for molecular biology works needed for

my study. I wish to thank Dr Roy Joseph for lyophilisation of my samples. I am grateful to Dr. Anilkumar P.R for giving me assistance in confocal microscopy. I wish to thank Dr. Lissy K. Krishnan and Mr. Renjith Kartha for FACS analysis. Also I wish to acknowledge Dr Annie John and her staff for TEM analysis and other facilities. My sincere gratitude also goes to the entire personnel and staff of BMT Wing, administration office and library for their cooperation.

Also I am really thankful for the love and support that I received from the past and present lab mates of BST to complete my work. And I'm deeply indebted to my past and present friends in FADDS who was with me through the ups and downs of my work. Together we had laughed, debated, worried and motivated ourselves to face the daily uncertainty and toil of our PhD years. My appreciation also extends to all my SCTIMST friends for their friendship throughtout my study period. And it is a privilege to thank my friends outside my PhD circle who were there for me always without fail.

Finally, and most importantly my deepest appreciation and gratitude goes to my parents, Mrs. Aleyamma Alex and Mr. Alexander, for their unending love, prayers, faith and patience that encouraged me to accomplish my task. I greatly value the love and care that my sisters and elders bestowed on me to stay calm and sane through these difficult years.

Words are not enough to thank my Lord Jesus whose benevolence and grace sustained me always. His invincible presence in my life is as true as mentioned…

"For our life is a matter of faith, not of sight (2 Corinthians 5:7)".

TABLE OF CONTENTS

Declaration by the Student	i
Certificate of Guide	ii
Approval of Thesis	iii
Acknowledgements	iv
Table of Contents	vi
List of Figures	xv
List of Tables	xviii
Abbreviations	xix
Synopsis	xx
1. Introduction	**1**
1.1 Cancer- An overview	1
1.2 Genetics and Biology of cancer	2
1.2.1. The Tumour	3
1.3 Existing Treatments for Cancer	5
1.4 Gene Therapy	7
1.4.1 Viral Systems Verses Non viral	8
1.5 Nanotechnology in Gene therapy	10
1.6 Barriers to gene delivery	11
1.6.1 Stable Polymer and DNA condensates	12
1.6.2 Systemic delivery	13
1.6.3 Cellular binding	14
1.6.4 Endosomal Release	14
1.6.5 Nuclear Entry	15

1.7 Aims 16

1.8 Hypothesis 16

1.9 Objective 17

2. Literature Review

2.1 Natural polymer based nanoparticles: Significance of chitosan as the polymer back bone …… 18

2.2 Importance of Ligand Conjugation into Chitosan Polymer…… 25

2.2.1 Conjugation with Galactose and spermine……. 27

2.2.2 Conjugation with Protamine and Polyethylene glycol…… 28

2.2.3 Conjugation with Ornithine…… 30

2.2.4 Conjugation of Chitosan Ornithine with Spermine…… 31

2.3. Uptake of Chitosan nanoparticles via Endocytic pathway……. 33

3. Materials and Methods

3.1 Depolymerisation of Chitosan

3.1.1 Materials……..... 37

3.1.2 Depolymerisation by Sodium nitrite…… 37

3.2 Spermine grafted galactosylated chitosan

3.2.1 Materials…… 38

3.2.2 Preparation of galactosylated chitosan with spermine coupling (GCSM) ……... 38

3.2.3 Colorimetric determination of primary amine groups …… 39

3.2.4 Analysis by Fourier transform infrared spectroscopy..... 40

3.2.5 Analysis by Proton Nuclear Magnetic Resonance spectroscopy.... 40

3.2.6 Buffering capacity of GCSM……... 41

3.2.7 Amplification and Purification of plasmid DNA and calf thymus DNA…….. 41

3.2.8 Preparation of GCSM complexes…… 42

3.2.9 Determination of particle size and zeta potential……. 42

3.2.10 Transmission Electron microscopy analysis……..... 43

3.2.11 Atomic Force microscopy analysis……..... 43

3.2.12 DNA Gel retardation…… 44

3.2.13 DNase I protection and release assay…… 44

3.2.14 Interaction of GCSM with Red blood cells (RBC) ……. 45

3.2.15 Electrophoretic analysis of GCSM polymer with plasma protein interactions..... 46

3.2.16 Cell Culture…….. 46

3.2.17 Cytotoxicity assay…… 47

3.2.18 Cellular uptake of GCSM nanoparticles…… 48

3.2.19 Cell uptake studies in the presence of endocytic inhibitors…… 48

3.2.20 In vitro transfection - Luciferace gene expression……. 49

3.2.21 In vitro transfection- p53 gene expression……. 50

3.3 Synthesis and Characterisation of Protamine PEG diamine chitosan

3.3.1 Materials…….. 51

3.3.2 Preparation of chitosan diaminopolyethylene glycol with protamine grafting (CDP)……. 52

3.3.3 Colorimetric determination of primary amine groups…… 53

3.3.4 Analysis by Fourier transform infrared spectroscopy……. 54

3.3.5 Analysis by Proton Nuclear Magnetic Resonance spectroscopy.... 54

3.3.6 Analysis by Differential Scanning Calorimeter…… 54

3.3.7 Buffering capacity of CDP…… 54

3.3.8 Amplification and Purification of plasmid DNA and calf thymus DNA…… 55

3.3.9 Preparation of CDP nanoparticles……. 55

3.3.10 Determination of size and zeta potential……. 56

3.3.11 Transmission Electron microscopy analysis…… 56

3.3.12 DNA Gel retardation…… 57

3.3.13 DNase I protection and release assay…….. 57

3.3.14 Interaction of CDP polymer with Red blood cells (RBC)…… 58

3.3.15 Electrophoretic analysis of CDP polymer with plasma protein interactions…….. 59

3.3.16 Cell Culture……. 59

3.3.17 Cytotoxicity assay…… 60

3.3.18 Cellular uptake of CDP nanoparticles……. 60

3.3.19 Cell uptake studies in the presence of endocytic inhibitors…….. 61

3.3.20 In vitro transfection- p53 gene expression……. 62

3.4 Synthesis and Characterisation of Chitosan Ornithine conjugate

3.4.1 Materials ……. 62

3.4.2 Preparation of chitosan ornithine conjugate (CON)…… 63

3.4.3 Colorimetric determination of primary amine groups…… 63

3.4.4 Analysis by Fourier transform infrared spectroscopy…… 64

3.4.5 Analysis by Proton Nuclear Magnetic Resonance spectroscopy…. 64

3.4.6 Analysis by Differential Scanning Calorimeter…….. 65

3.4.7 Buffering capacity of CON…… 65

3.4.8 Amplification and Purification of plasmid DNA and calf thymus DNA…… 66

3.4.9 Preparation of CON nanoparticles……. 66

3.4.10 Determination of particle size and zeta potential……. 67

3.4.11 Transmission Electron microscopy analysis…….. 67

3.4.12 Atomic Force microscopy analysis…… 67

3.4.13 DNA Gel retardation…….. 68

3.4.14 DNase I protection and release assay……. 68

3.4.15 Interaction of CON with Red blood cells (RBC)…… 69

3.4.16 Electrophoretic analysis of CON polymer with plasma protein interactions…….. 70

3.4.17 Cell Culture……. 70

3.4.18 Cytotoxicity assay…… 70

3.4.19 Cellular uptake of CON nanoparticles…… 71

3.4.20 Cell uptake studies in the presence of endocytic inhibitors……. 72

3.4.21 In vitro transfection- p53 gene expression……... 73

3.5 Synthesis and Characterisation of Spermine derivatised Chitosan Ornithine conjugate

3.5.1 Materials…… 74

3.5.2 Preparation of spermine derivatised chitosan ornithine Conjugate (COSM)…… 75

3.5.3 Colorimetric determination of primary amine groups…… 75

3.5.4 Analysis by Fourier transform infrared spectroscopy……. 76

3.5.5 Analysis by Proton Nuclear Magnetic Resonance spectroscopy…. 76

3.5.6 Analysis by Differential Scanning Calorimeter…… 76

3.5.7 Buffering capacity of COSM…… 77

3.5.8 Amplification and Purification of plasmid DNA and calf thymus DNA……. 77

3.5.9 Preparation of COSM nanoparticles……... 77

3.5.10 Determination of particle size and zeta potential…….. 78

3.5.11 Transmission Electron microscopy analysis……. 78

3.5.12 DNA Gel retardation……. 79

3.5.13 DNase I protection and release assay…… 79

3.5.14 Interaction of COSM with Red blood cells (RBC)…… 80

3.5.15 Electrophoretic analysis of COSM polymer with plasma protein interactions…….. 81

3.5.16 Cell Culture…… 81

3.5.17 Cytotoxicity assay…… 82

3.5.18 Cellular uptake of COSM nanoparticles……. 82

3.5.19 Cell uptake studies in the presence of endocytic inhibitors…….. 83

3.5.20 In vitro transfection- p53 gene expression…… 84

3.5.21 Intracellular trafficking of Nanoplex……. 85

4. Results

4.1 Depolymerisarion of Chitosan ……..... 86

4.2. Spermine grafted galactosylated chitosan (GCSM) polymer for gene delivery

4.2.1 Synthesis and characterisation of GCSM……. 86

4.2.2 Characterisation of Nanoparticle: GCSM and DNA interaction

4.2.2.1 Nanoparticle size measurement and zeta potential…… 91

4.2.2.2 Morphological observation by TEM and AFM…… 92

4.2.2.3 Electrophoretic analysis of GCSM nanoparticle……. ., 92

4.2.3 Blood compatibility and Cytotoxicity study of GCSM polymer

4.2.3.1 Hemolysis and RBC aggregation…… 94

4.2.3.2 Plasma protein interaction with GCSM polymer…… 94

4.2.3.3 Cytotoxicity evaluation of GCSM polymer…… 95

4.2.4. In vitro analysis of GCSM/pDNA nanoparticle

4.2.4.1 Evaluation of Cellular Uptake …… 96

4.2.4.2 Endocytosis inhibition Study…….. 97

4.2.4.3 Transfection with Luciferase Gene expression…….. 98

4.2.4.4 Transfection with p53 Gene expression …… 99

4.3 Protamine conjugated diamine PEGylated Chitosan (CDP) polymer for gene delivery

4.3.1 Synthesis and characterisation of CDP ……. 100

4.3.2 Characterisation of Nanoparticle: CDP and DNA interaction

4.3.2.1 Nanoparticle size measurement and zeta potential…… 105

4.3.2.2 Morphological observation by TEM ……..…… 106

4.3.2.3 Electrophoretic analysis of CDP nanoparticle…… 107

4.3.3 Blood compatibility and Cytotoxicity study of CDP polymer

4.3.3.1 Hemolysis and RBC aggregation…… 108

4.3.3.2 Plasma protein interaction with CDP polymer…… 109

4.3.3.3 Cytotoxicity evaluation of CDP polymer…… 110

4.3.4 In vitro cell study with CDP/pDNA nanoparticle

4.3.4.1 Evaluation of Cellular Uptake…… 111

4.3.4.2 Endocytosis inhibition Study…… 112

4.3.4.3 Transfection with p53 Gene expression…… 114

4.4 Ornithine grafted chitosan polycation (CON) for gene delivery

4.4.1 Synthesis and chemical characterisation of CON……. 115

4.4.2 Characterisation of Nanoparticle: CON and DNA interaction

4.4.2.1 Nanoparticle size determination and zeta size potential…….. 120

4.4.2.2 Morphological Observation by TEM and AFM…… 121

4.4.2.3 Electrophoretic analysis of CON nanoparticle …… 122

4.4.3 Blood compatibility and Cytotoxicity study of CON polymer

4.4.3.1 Hemolysis and RBC aggregation……. 123

4.4.3.2 Plasma protein interaction with CON polymer…… 124

4.4.3.3 Cytotoxicity evaluation of CON polymer…….. 125

4.4.4 In vitro cell study with CON/pDNA nanoparticle

4.4.4.1 Evaluation of Cellular Uptake…… 126

4.4.4.2 Endocytosis inhibition Study…… 127

4.4.4.3 Transfection with p53 Gene expression…… 130

4.5 Spermine derivatized chitosan ornithine conjugate for gene delivery

4.5.1 Synthesis and chemical characterisation of (COSM)…….. 131

4.5.2 Characterisation of Nanoparticle: COSM and DNA interaction

4.5.2.1 Nanoparticle size determination and zeta size potential…… 136

4.5.2.2 Morphological observation by TEM…… 138

4.5.2.3 Electrophoretic analysis of COSM nanoparticle……. 138

4.5.3 Blood compatibility and Cytotoxicity study of COSM polymer

4.5.3.1 Hemolysis and RBC aggregation…… …… 139

4.5.3.2 Plasma protein interaction with COSM polymer…… 140

4.5.3.2 Cytotoxicity evaluation of COSM polymer…… 141

4.5.4 In vitro cell study with COSM/pDNA nanoparticle

4.5.4.1 Evaluation of Cellular Uptake……..... 142

4.5.4.2 Endocytosis inhibition Study…….. 144

4.5.4.3 Transfection with p53 Gene expression…….. 147

4.5.4.4 Intracellular Nanoparticle trafficking……. 148

5. Discussion

5.1 Spermine grafted galactosylated chitosan for improved nanoparticle mediated gene delivery …… 151

5.2 Protamine conjugated diamine PEGylated chitosan derived polyplex for enhanced cell uptake and gene delivery…….. 159

5.3 Enhanced intracellular uptake and endocytic pathway selection mediated by ornithine grafted chitosan polycation for gene delivery…….. 169

5.4 Nanoparticle mediated gene expression and intracellular trafficking by spermine derivatized chitosan ornithine conjugate……. 174

6. Summary and Conclusion…… 184

7. References……. 191

8. List of Publications & Conferences…… 214

9. Appendices…… 215

List of Figures

1. Schematic representation of synthesis of GCSM polymer ……. 87
2. TNBS assay for determination of free amine groups in GCSM, GC, chitosan and glucosamine as the reference…….. 87
3. Infrared spectroscopy for evaluation of chemical groups in the functional entities of the GCSM derivative……... 89
4. ^{1}H NMR spectra of GCSM polymer …… 90
5. Analysis of the buffering capacity of GCSM ……... 90
6. (A)TEM observation GCSM nanoparticles in 1:15 ratio. Scale bar is 200nm. (B) AFM observation of nanoparticle of 1:15 ratio…… 92
7. Agarose gel electrophoresis performed on ctDNA/GCSM complexes…. 93
8. RBC aggregation studies with (A) GCSM derivative (B) with normal saline (C) with PEI 25 kDa (20 X magnification for RBC) (D) Plasma Protein interaction with GCSM (1 mg/mL); Lanes GCSM1, GCSM2 represent polymer in 50 &100 µg and lane NS is normal saline, the control…..... 95
9. Cytotoxicity of GCSM polymer…… 96
10. Cell uptake of GCSM nanoparticles in HepG2 cells…… 97
11. Endocytosis inhibition of cell uptake of GCSM nanoparticles in HepG2 cells…… 98
12. Luciferase expression in HepG2 cells transfected by DNA/GCSM complexes and DNA/PEI complexes taken at two different ratios (1:15 and 1:16)…….. 99
13. Transfection Assessment via Live Dead assay in C6 cells……. 100
14. Proposed reaction scheme of synthesis of CDP…… 101
15. TNBS assay for determination of free amine groups in CHI (chitosan), CD (PEG diamineylated chitosan) CDP (protamine conjugated diaminePEGylated chitosan) along with glucosamine as the reference… 101
16. Infrared spectroscopy for evaluation of chemical groups in the conjugated CDP derivative…… 103
17. ^{1}H NMR spectra of protamine grafted PEG diamineylated chitosan… 104
18. DSC analysis of CDP and chitosan…….. 104
19. Analysis of buffering capacity of CDP derivative…… 105
20. TEM observation of CDP polyplex…….. 107
21. Agarose gel electrophoresis performed on CDP/pDNA complexes…… 108
22. RBC aggregation studies with (A) CDP derivative (B) with normal saline (C) with PEI 25 kDa (20 X magnification for RBC). (D) Plasma Protein interaction with CDP (1 mg/mL); Lanes CDP1, CDP2 represent polymer in 50 &100 µg and lane NS is normal saline, the control.…… 110
23. Cytotoxicity of CDP polymer…… 111

24. A) Fluorescent image of cellular uptake of CDP nanoparticles. B) Flow-cytometric analysis of the cell uptake of CDP nanoparticles by C6 glioma cells upon incubation for 3 h in comparison with C) control C6 cells…… 112
25. Endocytosis inhibition study of CDP nanoparticles…… 113
26. Transfection Assessment via Live Dead assay in C6 cells…….. 114
27. Illustration scheme of synthesis of CON…… 115
28. TNBS assay for determination of free amine groups in Chitosan ornithine conjugate CON, chitosan (CHI) and glucosamine as the reference…… 116
29. Infrared spectroscopy for evaluation of chemical groups in the functional entities of the CON derivative. FTIR of chitosan, ornithine and chitosan ornithine conjugate (CON)……..... 117
30. ^{1}H NMR spectra of CON……. 118
31. DSC analysis of CON and chitosan……. 119
32. Analysis of buffering capacity of CON derivative…… 120
33. Nanoparticle Morphological analysis…… 121
34. Agarose gel electrophoresis performed on CON/pDNA complexes…… 123
35. RBC aggregation studies with (A) CON derivative (B) with normal saline (C) with PEI 25 kDa (20 X magnification for RBC) (D) Plasma Protein interaction with CON (1 mg/mL); Lanes CON1, CON2 represent polymer in 50 &100 μg and lane saline is the control…… 125
36. Cytotoxicity of CON evaluated by MTT assay…… 126
37. Cell uptake of CON/p53 plasmid nanoparticles…… 127
38. Fluorescent images of endocytosis inhibition study with CON/pDNA complexes in ratio 1:3 (DNA/CON) in C6 glioma cells……. 130
39. Transfection Assessment via Live Dead assay in C6 cells…… 131
40. Schematic representation of synthesis of COSM polymer…… 132
41. TNBS assay of COSM polymer compared to chitosan (CHI), chitosan ornithine (CON) and reference glucosamine……. 133
42. Infrared spectroscopy for evaluation of chemical groups in the functional entities of the COSM derivative…… 134
43. ^{1}H NMR spectra of COSM polymer…….. 135
44. DSC analysis of COSM and chitosan……. 135
45. Evaluation of the buffering capacity of COSM…….. 136
46. Nanoparticle Morphological analysis……... 138
47. Agarose gel electrophoresis performed on pDNA/COSM nanoparticles…… 139
48. RBC aggregation studies with (A) COSM derivative (B) with normal saline (C) with PEI 25 kDa (20 X magnification for RBC) (D) Plasma Protein interaction with COSM (1 mg/mL); Lanes COSM1, COSM2 represent polymer in 50 &100 μg and lane NS is normal saline, the control…. 141

49. Cytotoxicity of COSM evaluated by MTT assay……. 142
50. Fluorescence microscopic image of A) control C6 cells with only YOYO tagged pDNA and B) YOYO labelled pDNA/COSM nanoparticles in 1:15 ratio (w/w) after 4h incubation. C) Confocal fluorescent images of cell uptake of YOYO labelled pDNA/COSM nanoparticles merging images of both the bright field and green filter after 4h. . Magnigication is 40X and the bar size is 20μm. Representative histograms of pDNA fluorescence from flow cytometry analysis of D) cells incubated with COSM/pDNA nanoparticles E) Unstained cells as control……. 143
51. Representative fluorescent and confocal images of endocytosis inhibition study with COSM/pDNA complexes in ratio 1:16 (DNA/COSM) in C6 glioma cells. Magnification and scale bar is 40X and 20 μm respectively. Fluorescent images of cells from (A) to (F) treated with a separate endocytic inhibitor prior incubation with COSM nanoparticles. Therefore (A) represent chlorpromazine treated cells B) Dynasore treated cells C) Amiloride treated cells D) Filipin treated cells E) Ornithine and F) spermine treated cells. Images A1 to F1 represented the z-stacking confocal images of the same inhibitor studies…….. 147
52. Transfection Assessment via Live Dead assay in C6 cells…… 148
53. Nanoparticle trafficking in the cell…… 149

List of Tables

1. Particle size and zeta potential of GCSM/ctDNA nanoparticle…… 91
2. Particle size and zeta potential of CDP/ctDNA nanoparticles…….. 106
3. Particle size and zeta potential of CON/ctDNA nanoparticles…….. 120
4. Particle size and zeta potential of COSM/ctDNA nanoparticles…… 137

Abbreviations

Abs	Absorbance
AFM	Atomic force microscopy
CDP	Protamine PEG diamine chitosan conjugate
CPP	Cell penetrating peptides
CON	Chitosan Ornithine conjugate
COSM	Spermine derivatised Chitosan Ornithine conjugate (COSM).
ctdna	calf thymus DNA
DLS	Dynamic light scattering
DMAP	Dimethylaminopyridine
DMEM	Dulbecco's modified Eagle's medium
DMF	Dimethylformamide (DMF)
DNA	Deoxyribonucleic acid
DSC	Differential scanning calorimetry
DSC	N, N'-Disuccinimidyl carbonate
EDC	1-Ethyl-3-(3-dimethylaminopropyl) carbodiimide hydrochloride
EDTA	Ethylene diamine tetra acetic acid
EPR	Enhanced permeability and retention effect
FBS	Foetal bovine serum
FTIR	Fourier transform infrared spectroscopy
GCSM	Spermine grafted galactosylated chitosan
h	hours
kDa	kilo Dalton
MEM	Minimal essential medium
MTT	3-(4, 5-Dimethylthiazol-2-yl)-2, 5-diphenyltetrazolium bromide
mV	milli Volt
Mw	Molecular weight
NHS	N-hydroxy succinimidyl ester
nm	nano meter
NMR	Nuclear magnetic spectroscopy
PBS	Phosphate buffered saline
pDNA	plasmid DNA
PEG	Polyethylene glycol
PEI	Polyethyleneimine
ppm	parts per million
RES	Reticulo endothelial system
RLU	Relative light units
TEM	Transmission electron microscopy
TNBS	Trinitrobenzenesulfonic acid
UV	Ultraviolet

SYNOPSIS

Cancer is a deadly disease that has genes responsible for the onset of an infectious and malignant condition which adversely affect human health. The incidence of cancer has been on the rise since the longevity of people has been improved giving more time for genetic mutations to occur and get accumulated in the cells. Extensive knowledge and understanding have been gathered over the years regarding the biology and progression of cancer which aimed to advance several therapeutic strategies against cancer. Cancer cells show individual traits and genetic alterations that differ from organ to organ which indicate that cancer cells are heterogeneous in nature, giving rise to divergent cancer types depending on the affected organs. Hence cancer treatment is commonly approached using a combined effect of chemotherapy, radiation or surgical removal. However all this treatments has its own demerits which still makes cancer incurable.

Gene therapy stands as a promising alternative strategy for cancer treatment. The field of gene therapy revolve around the concept of gene delivery which focuses on the transfer of therapeutic genes that encode genetic expression to either kill the cells or inhibit production of proteins that are harmful to cells. The past few decades witnessed the discovery of several tumor suppressor genes, oncogenes and onco-related genes that regulate in the signal transduction pathways which added to the optimistic hope of utilising gene therapy for cancer treatment. Given the fact that tumour cells are capable of genetic redundancy and massive proliferation, therapy using genes for replacing the defectives ones would be futile and therefore genes that cause apoptosis or killing of the cells are preferred. Eventually a stable delivery of

the interested gene to the appropriate site of action is the most sought after goal for gene therapy. In the current scenario, clinical trials for gene therapy against cancer are being undertaken worldwide and consensus success has yet to be attained. The lacuna for this is the absence of an ideal and effective vector system for gene delivery. Continued effort is reported in the making of suitable gene vectors and my area of research interest falls in the design of a non viral delivery system for cancer therapy.

Therefore my synopsis include the chapters that deal with an introduction to the topic, review of literature on the concerned topic, methodology adopted for this study and discussion of the major findings in the study.

The first chapter portray an overview of cancer, its present status quo in affecting world health and the several strategies adopted against the deadly disease. One such strategy that came into research interest was the field of gene therapy. As cancer is fundamentally a genetic disease, the treatment at the genetic level would be a real boon if the gene of interest has been delivered rightly to the site of action. However naked genes lack specificity to discriminate tumour cells from healthy cells and when introduced into the body, are susceptible to nuclease degradation. Therefore carrier systems are necessary to ensure proper gene delivery in the body. For the past decade, both viral and non viral systems are widely explored to facilitate gene delivery. Viruses were found to be suitable as they were able to recombine and integrate into host genome during growth in host cells. This made viral delivery a promising vehicle to transfer the functional genes to the defective cells. The inherent property of viruses to undergo spontaneous recombination is at the same time a

matter of concern as there is the likelihood for them to revert back into any infective form that may induce pathogenesis.

Development of non viral systems was opted to overcome the risk associated with viruses and this led to the use of polymer matrixes for generation of non viral gene vectors. Later section of this chapter explain the convergence of natural polymers and the concept of nanotechnology to produce suitable carrier systems that would be small enough in nano dimensions to get internalised in the cells. Natural polymers with cationic nature are considered for their desirable traits that make them a potential vector for carrying genes. By means of nanoscience, the polymer based vectors form nanoparticles that have to overcome the various biological hurdles inside the body. The first chapter ends with the discussion of the aims of the study, projection of hypothesis and objectives considered for the PhD study.

The second chapter discussed the pros and cons of choosing chitosan for the study, a polymer derived from the naturally present chitin abundantly found in the shells of crustaceans. The polymer have cationic charge density that would help in effective DNA binding and is versatile in nature as a lot of physicochemical parameters are there which could be exploited for chemical modification. Chitosan can also degrade like starch as the polymer consists of glucosamine subunits and is subjected to lysosomal degradation. However it is soluble only in acidic conditions and the acidic chitosan solution would prove to be toxic for systemic administration as wells as for *in vitro* cell lines. In addition to this chitosan based nanoparticles has low transfection efficiency that is influenced by its physicochemical attributes. Although such drawbacks hinder its widespread application, the scope to alter the chemical parameters in chitosan with different modifications is immense which once

again make it useful for extensive research study. As a result several chitosan derivatives are synthesised based on differing objectives which are reported and cited.

Chitosan does not possess any cell targeting ability and modifications that include ligand conjugation will provide sensitivity to the polymer. This feature will enable chitosan nanoparticles to bind to specific receptors abundantly found in tumor cell lines that would facilitate enhanced transfection ability and also allow solubility in neutral pH. The significance of chemical conjugation into chitosan backbone with ligands such as the sugar moiety galactose, cationic compounds like the protein protamine that is known to have DNA condensing property, polyamine such as spermine and its precursor amino acid ornithine, have their implications highlighted in the later section of this chapter. Once the nanoparticles reach the target cells, they are internalised through the cellular phenomenon known as endocytosis which consists of multiple pathways. Among those pathways, the most known and studied four pathways are discussed for nanoparticle cell uptake. The literature has therefore helped to understand that ligand modification with suitable functional residues would address the negative traits in chitosan and enable a feasible nanoparticle based gene delivery system.

The third chapter involved the methodology employed to produce the four chitosan based derivatives. Each derivative is then mixed with DNA in appropriate varying ratios to result in the nanoparticles also known as nanoplexes or polyplexes. First derivative included ligand modification with galactose residue that provided dissolution property to chitosan at neutral pH and further grafting with spermine, a polyamine gave excess amine groups to maintain the cationic density of chitosan that

got reduced by galactose incorporation. The derivative was labelled as GCSM and the presence of spermine would also provide targeting specificity for tumour cells that showed abundant polyamine metabolism. Second derivative named as CDP included the grafting of protamine and PEG diamine into the chitosan backbone to ensure integrity and solubility respectively. Chemical modification of chitosan with ornithine resulted in the third derivative labelled as CON. Ornithine is an amino acid biologically present in the cells and a precursor of cellular polyamines that would provide enhanced solubility, reduced toxicity and cationic density for effective nanoparticle mediated cellular uptake. The fourth derivative COSM included the grafting of spermine into the synthesised CON derivative to further enhance the targeting ability of the nanoparticles.

Each derivative was subjected to physicochemical characterisation, biological evaluation and *in vitro* application to establish the feasibility of nanoparticle mediated gene delivery. Physicochemical characterisation included techniques such as FTIR, ^{1}H NMR, and DSC to establish the successful conjugation of each ligand into the chitosan backbone. Size and zeta potential was determined by dynamic light scattering phenomenon with the complexes formed of chitosan derivative and DNA in the corresponding ratios (w/w) by keeping the gene as constant. Buffering capacity of each derivative was determined in comparison with the parent chitosan compound. The morphological observation by TEM and AFM confirmed the nanoparticle sizes of each chitosan derivatives. The integrity of the nanoparticle was examined by performing agarose gel electrophoresis that had wells loaded with complexes comprising of DNA and chitosan derivative. The samples were further treated with the enzyme deoxyribonuclease (DNase) to investigate the ability of the polymer to

package the DNA in a condensed manner so as to protect the DNA from any nuclease attack. Heparin treatment is carried out on the sample complexes to confirm the release and presence of earlier tightly bound DNA in the chitosan nanoparticles. *In vitro* cell culture study was performed in cancer cell lines to assess the compatibility of the polymer which is followed by cell uptake study of the nanoparticle. Uptake was performed with fluorescent tagged gene complexed with the chitosan derivative and observed by fluorescent microscopy while the percentage uptake of nanoparticles was ascertained by FACS analysis. The determination of endocytosis pathways was followed next by treating the cells with respective inhibitors of the known endocytosis pathways prior to treatment with nanoparticles. Finally to establish the gene delivery efficacy of the polymer based nanoparticle, live dead expression analysis was performed by transfecting the cells with chitosan based nanoparticles complexed with the therapeutic gene p53 that would cause apoptosis to the cells. The transfected cells that had the plasma membrane damaged allowed the entry of the ethidium homodimer dye into the cells and stained the dead cells as red.

The fourth chapter discussed the results obtained for each chitosan derivative and their significant implications. In spermine grafted galactosylated chitosan (GCSM), the solubility of chitosan derivative was enhanced and optimal sizes within 150 nm and 24 mV cationic zeta potential was obtained. The nanoparticles retarded the movement of DNA in agarose gel electrophoresis and protected DNA against nuclease attack. More than 80 % cell viability was seen when MTT assay was performed for cells treated with GCSM derivative. Effective cellular uptake of GCSM nanoparticles was assessed by fluorescent microscopy and FACS analysis. Endocytosis pathway inhibition study revealed that the ligand receptor mediated

pathway was mostly regulated for GCSM nanoparticle uptake than the other pathways. Transfection study by fluorescent microscopy also showed enhanced gene expression in cancer cell lines. In the second derivative CDP, favourable findings were observed with improved stability for nanoparticle, enhanced buffering capacity that would provide feasible endosomal escape, reduced toxicity with more than 85 % cell viability, enhanced cellular uptake and transfection efficiency. Among the pathways, caveolae mediated pathway was found to be the most regulated and specific for CDP nanoparticle mediated cellular endocytosis. The derivative of chitosan ornithine (CON) had the advantage of a biologically relevant amino acid ornithine as conjugate. This provided enhanced solubility, desirable cationic zeta potential and size that would facilitate cell uptake. Buffering capacity was also observed to be enhanced than the parent compound. Agarose gel electrophoresis also showed good DNA retention ability of nanoparticle and protection against nuclease attack. Cell viabilty was analysed to be more than 80 % and cellular uptake was confirmed by fluorescent microscopy and FACS analysis. Profound apoptotic expression was mediated by p53 vector that was successfully transfected into the cells using chitosan ornithine nanoparticle. Since this conjugate had provided favourable results, the fourth matrix had spermine conjugated to chitosan ornithine derivative (COSM). Physicochemical evaluation confirmed the grafting and enhanced buffering capacity was observed. Gel retardation was significantly observed for the nanoparticles from COSM derivative with sizes coming within the range 200 nm and a favourable high positive charge. Cell viability was much similar to the normal growth medium control and enhanced cell uptake was observed under the fluorescent microscope and measured with FACS analysis. Apoptosis gene

expression was strikingly observed with COSM/p53 gene vector nanoparticle indicating the enhanced transfection efficiency. Fluorescent and confocal observation also revealed the pathways that are mostly adopted for COSM nanoparticle cellular internalisation.

In the last chapter of my thesis, the major findings related to the efficacy of the four derivatives are summarized. The efficacy of bioconjugated chitosan DNA based nanoparticles are shown to be influenced by the type of ligand modification and the specificity of endocytosis pathways are also dependent on the functional conjugate attached to the chitosan backbone. Among the four derivatives, spermine derivatised chitosan ornithine conjugate has the potential scope to be exploited for futuristic purposes of non viral approach for cancer therapy.

CHAPTER 1 INTRODUCTION

1.1 Cancer- An overview

The unscheduled abnormal proliferation of normal cells has paved way to a life threatening condition known as Cancer. The disease is a major leading cause of death in almost every country in the world. According to the press report released by (WHO) World health Organisation and the International Agency for Research on Cancer, the global cancer burden rose to 14.1 million new cases in 2012 and 8.2 million cancer deaths in the same year **(**Bray et al., 2012). The Human Development Index (HDI), an excellent surveyor of globalisation of cancer has projected a huge leap of 22.2 million new cancer cases by 2030 from 12.7 million cases of 2008 indicating the alliance of incidence and prevalence of cancer to the rapid reforms in the economy and lifestyle typical of an urbanised society (Vineis & Wild, 2014). The health scenario has been greatly affected by the burdens of cancer and to develop an affordable and effectual treatment for cancer is an urgent need of the situation (Jemal et al., 2011)**.**

In India, nationwide survey around 2010 estimated 70 % of fatal cancers that has occurred in the age group of 30-69 years, confirming that cancer is an important cause of adult deaths **(**Dikshit et al., 2012). This frequency of occurrence has increased from the 6 % of cancer deaths in 2008 which also represented 8 % of estimated global cancer death. However, there has been impressive progression in the health sectors with the advent of novel technologies for diagnosis and treatment which has improved the survival rate of the cancer patients. Still cancer remains as

an incurable disease worldwide and is leading to untimely deaths, ranking second to cardiovascular diseases.

1.2 Genetics and Biology of cancer

Cancer is referred in medical terms as a form of malignant neoplasm which is entirely influenced by genetic alterations that have a deleterious effect on human health. The inherent damage accumulated over a period of time in the cells is the bottom line for cancer initiation and progression. The malfunctioning of three types of genes is the root cause for tumour initiation and progression. They are the proto oncogenes that encode for proteins that stimulate cell division, tumour suppressor genes that inhibit the cell to grow continuously and DNA repair genes that prevent mutations to occur (Vermeulen et al., 2003; Lahtz & Pfeifer, 2011) . The abnormality of cancer results from mutations in these genes that take place both exclusively and coherently. For instance infinite cell growth is manifested when genes responsible for encoding proteins that stimulate cell division are mutated and this genome aberration escapes from the scrutiny of the cell due to the mutations present in the genes encoding the DNA repair mechanism.

Other multiple reasons that lead to cancer are exposure to carcinogens (Soto & Sonnenschein et al., 2010), radiation, acquired or inherited genetic defects, aneuploidy (Gordon et al., 2012), abnormal hormone stimulation (Chlebowski & Anderson, 2012) and most of them complement each other for sporadic development of cancer. Eventually these factors induced genome aberrations which generate inappropriate stimuli for proto-oncogenes, genes that code for cell division, to become activated oncogenes. The oncogenic activites can be random gene recombinations, copy number variations and viral inserted chromosome

rearrangements, with most of them being irreversible and leading to tumorigenesis (Floor et al., 2012). Consequently, normal cells become tumorigenic that lacks cell adhesion, have change in cell morphology and grow in an independent and infinite pattern. The new characteristics will be heritable and the primary cancer cells become the progenitor cells that have a predisposition for mutations and culminate for tumour clonal expansion. Evidently, the most prominent features noticed in cancer cells are rapid cell division and maturation, insusceptibility to normal cell death regulation, ability to cross the lymphatic and blood circulatory system for metastasis and tissue invasion, promoting simultaneous angiogenesis and hypoxic condition and eventually genome fidelity and instability (Chari, 1998; Hanahan & Weinberg, 2000; 2011). Depending on the tissue origin, tumour cells are referred accordingly and therefore tumours derived from epithelial cells in skin and internal organs are named as carcinomas, those arising from soft tissues like muscles, blood vessels are mentioned as sarcomas and cancerous form of brain glial cells are known as gliomas.

1.2.1. The Tumour

Tumour cells possess various versions of mutated genes that encode downstream signals of growth factors which activate the signal transduction pathway and activate nuclear transcription factors to enter the cell cycle. Dysregulation of cell cycle is also caused by the mutated genes which disable several checkpoints in the cycle that prevent unwanted replication and be conducive for tumour cells to continually enter the cell cycle phases for proliferation (Cairns et al., 2011). Another strategy for tumour cells is to be insensitive to growth inhibitory signals, apoptosis and autophagy factors and tumour suppressing proteins. This leads to absence of cell

to cell contact inhibition that grows in number to displace the healthy cells surrounding that region. The endothelial cells primarily mediate the remodelling of new blood vessels that aid in continuous supply of nutrients depending on the signals released from the tumour microenvironment (Bergens & Benjamin, 2003; Acheampong et al., 2013).

The extracellular matrix determine the tumour microenvironment as it is deregulated from the normal ECM and is highly dynamic with constant remodelling of protein and sugar composition consisting of pro-angiogenic factors such as VEGF, FGF and cell bound signals that act as building blocks for the survival of tumours in nutrient depleted environment (Pietras & Östman, 2010). Once tumour cells have completely invaded the local tissues and exhausted the nutrient supply, they exploit proteolytic enzymes for matrix dissolution that result in tumour cells getting detached from the parent site, transit through the spaces of the leaking tumour microenvironment, intravasate into the proximal vasculature and migrate to distant locations. This stage, known as the metastasis condition of cancer cells, is the most dangerous phase of the disease. During circulatory migration, homing of tumour cells occurs in the nascent sites in response to favourable signals of cell adhesion and there they extravaste and colonizes the tissues and organs with metastatic objective. Importantly in cancer, the frequency of gene mutations seems to rise exponentially and this affects the DNA repair mechanism that induces malfunctioned DNA machinery. In course of time, the tissue architecture is damaged, interstitial space and stromal cells are polluted with circulating tumour cells and inflammatory signals are elicited for further tumour invasion at both primary tumour and distant locations with

cells becoming immortal and organs non functional towards the demise of the living organism (Lu et al., 2012).

1.3 Existing Treatments for Cancer

With such disparate events of malignancy, treatment for cancer remains elusive with farfetched success. Cell heterogeneity is prevalent in tumours and numerous genotypic and phenotypic differences might affect drug sensitivity and hinder the efficacy and sustained exposure of the drug for cure. Another stumbling block is that the disease varies from organ to organ and therefore the strategy for treatment depends on several factors such as the person's genetic disposition, his/her physique and age, stage of the disease and access to the particular affected organ. Nevertheless, conventional forms of treatment are invariably used and are successful to a reasonable extent depending on the type and location of cancer and the stage of advancement in the disease. Surgery has been the oldest from of treatment and is effective to remove solid and benign form of tumors. Surgical removal is highly appreciated for tumours at the initial outgrowth or for precancerous lesions which have an increased risk of becoming cancerous. However not every part of the body is accessible for surgical incision and even after removal there are cases of distant recurrence of tumour growth (Chua et al., 2011).

Chemotherapy uses drugs to kill the cancer cells and the drugs are administered either intravenously or by oral pills. The main disadvantage of chemotherapy is that it act on dividing cells and as it can not discriminate normal dividing cells, healthy cells are too killed. Tumour cells are destroyed by intervention of anticancer drugs at several stages of molecular mechanisms for tumorigenesis but this can also lead to other health complications like alopecia, anaemia,

thrombocytopenia and gastrointestinal problems (Preissner et al., 2012; McMahon et al., 2012). It is seen that over 50 % of cancer patients require radiotherapy at some point of time during their illness. Radiation therapy employs radiation or beam energy to destroy tumour cells which impair the DNA integrity thus making them unable to divide further. Generally radiation is given in adjunct with chemotherapy and surgery, depending on the advanced stages of cancer. An essential component for efficacy of the treatment is requirement of a quality assured linear accelerators for the high ionising radiations which demands repeated quality checks that is quite expensive. Of late, certain radiations such as linear energy transfer (LET) have proved to be highly toxic or logistically too complex to be implemented (Niemantsverdrie et al., 2012). However surrounding normal cells cannot be spared from the ionised high beams while irradiation.

Immunotherapy uses the principle of immunization and vaccines to boost the immune system of patients to combat the tumours. Advances in the field of antibody discovery has motivated the Food and Drug Agency, USA (FDA) approval for humanized monoclonal anitibodies like Rituximab, Trastuzumab, Cetuximab to eradicate different cancer cells based on antibody or complement dependent cellular cytotoxicity (Soliman, 2013). The therapy functions in response to the tumour associated antigens but there is likelihood of inducing undesired responses to antigens that are exhibited by normal tissues, which remains as a challenge to be overcome. Unlike the treatments discussed above, patients who have been diagnosed with the final stages of cancer can find solace only on palliative and supportive care. At the cross road of diverse cancer treatment approaches, it has now been considered that the use of ‘genes’ as therapeutic medicine is a promising alternative.

1.4 Gene Therapy

The recognition of mutated genes responsible for cancer manifestation and discovery of potent sequence selective inhibition by genes led to the emergence of gene therapy. Therapeutic genes are delivered to diseased cells for gene expression or modification of the diseased gene is the underlying principle of gene therapy. In theory, introduction of genes will allow controlled downstream expression of desired genes by associating with mRNA and suppress tumour progression. Moreover gene expression is likely to be transient and short lived which is sufficient to eradicate the tumours unlike other genetic disorders which require sustained expression.

Over the years extensive research has been carried out for making gene therapy a remedy to alleviate inherited diseases. In the year 1990 the first FDA-approved gene therapy experiment was conducted in an ADA-SCID affected patient in the United States. From then onwards, it has been reported that almost 2000 clinical trials had been sanctioned and implemented for gene therapy (Edelstein et al., 2007). There were reports of failed clinical trials which resulted either as manifestation of other ailments or as unexpected deaths caused either by the experiment or microorganism related infections. The first mortality was met in the year 1999 for the patient affected with the genetic disorder that resulted in ornithine transcarbamylase deficiency. Although for a period of time gene therapy was halted, the ban was later lifted around 2000 and since then several clinical trials have been attempted with slight assurance of success (Ginn et al., 2013). However advanced improvisation in gene therapy has led to less failure in clinical trials. Currently immunotherapy is benefitted with the arrival of gene therapy as cancer cells could be

engineered with genes that produce pro-inflammatory stimuli or antigen proteins that is used for vaccines development (Vile et al., 2000).

Initially transfer of naked DNA by simple injection was attempted directly to the tissues but it proved futile as nucleic acids were susceptible to enzymatic degradation and encountered intense physical and pharmacological hurdles during their circulation in the body. Recent exploration of delivering cancer therapeutic genes like siRNA for gene silencing was also hampered due to systemic exposure of the nucleic acid that induced non-specific responses. This reinforced the need for a carrier system that would cargo the gene of interest to the site of action where the gene could resume its functional role. Therefore the primary focus is to develop a suitable delivery system or vector that masks and shield nucleic acids from enzymatic attack during its systemic circulation. Secondly the carrier has to overcome extracellular barriers by diffusion through vasculature and tissues without evoking any immune and prophylactic responses. Thirdly, these carriers have to reach the target cells and execute formidable tasks such as cellular uptake, endosomal escape and import to the nucleus.

1.4.1 Viral Systems Verses Non viral

In the beginning, viruses were considered promising vector system as they were evolved by nature to escape the cellular barriers and traverse the cytosol to transfer the gene and allocate functional roles exploiting the host cellular and genetic machinery. Efforts were concentrated on using recombinant technology in engineering viral vectors that included both adenoviruses and retroviruses which were non virulent and displayed high efficacy to deliver the oligonucleotides to cancer cell lines (Zhang et al., 2011). For instance, oncolytic viruses were

extensively studied for gene transfer as they multiply selectively in tumour cells, lead to cell death at the end of the replicative cycle, evade the cell defence mechanisms and release matured viruses to the neighbouring cancer cells (Wang & Pham, 2008; Liu & Kirn, 2008). Unfortunately, a recurring issue with viral vectors is the risk of reversion of virulence capability as there is the possibility of insertional mutagenesis which turns out to be the fundamental challenge against its application. Problems such as toxicity and immunogenicity were also faced during the studies. Limitations of scale up procedures for viral vectors, size restriction of transgene that can be the payload and expensive methods for manufacture were other reasons that discouraged viral approach of gene delivery system. This gave rise to non viral systems which manipulated polymers to perform as gene vectors and is devoid of the risks associated with viral vectors.

Being the counter part of the viral systems, non viral vectors are based on synthetic molecules that exploit the dynamic interactions that occur at the interface between materials and biological systems (for example blood, body fluid, tissues, cells, proteins and nucleic acids). Polymers are highly recognized non viral vectors as they hold high degree of molecular weight and structure and could be subjected to different modifications dependent on the chemical rationale of design. Most of them have cationic charge and can interact conveniently with negatively charged biological entities (Parhiza et al., 2013). Polymers with polysaccharide constituency have been found to be a suitable matrix for non viral systems due to their heterogeneous chemical composition with monomers being natural in origin. Besides, the monomers present in the natural polymers are ubiquitously seen in the biological system and therefore these polysaccharide based polymers are capable of

intrinsic modulation in response to the environment for degradation and restructuring by enzymes of the cells (Nazir et al., 2014).

Therefore the natural polymers are both biocompatible and biodegradable with minimal immunogenicity. These polymers are generally abundant in nature and hence will be cost effective and available for large scale production. Another merit in natural polymers are the presence of hydrophilic end groups that would enable diverse associations at atomic and molecular levels such as the non covalent interactions with biological membranes providing an adhesive property as well as an electrostatic bonding with nucleotide fragments which help in accommodating large size genes and conjugate attachment that would help to devise tumour specificity and targetability (Elsabahy et al., 2011; Alexis et al., 2010).

1.5 Nanotechnology in Gene therapy

Unfortunately polymer based non viral gene therapy has a major drawback of yielding low transgene expression when compared to a viral vector. This is surpassed by introducing the concept of 'nano' into polymers that would mimic the viral characteristics. The recent emergence of nanotechnology as a promising tool in the field of biology and medicine has led to the development of polymer based non viral systems into nanoscale forms (Cuenca et al, 2006; Wagner et al., 2006). A recent review highlights the scope of polymeric nanomaterials designed with a focus on amenable pharmacological and therapeutic attributes (Kamaly et al., 2012). In line with this, attention has been diverted to polymers which could be designed into particulate sizes that would be similar to the cellular components (DNA, protein, cell membrane) with atleast one dimension range below 100 nm. Often the polymer that has been modified to avail nano size dimension is combined with genes to yield as

nanoparticles, also known in other names as *polyplexes, nanoplexes and nanoconjugates*. These entities open up vast possibilities to incorporate various compounds or drugs that can be transported effectively to the desired tumour site which otherwise are compromised by several external parameters. The colloidal particle existing in the nanoscale range itself is an interesting highlight since the surface areas shrink in comparison to their volumes providing a larger surface-to-volume ratio. This enables the nanoparticles to be exposed and interact at ease with more proteins or biomolecules than a particle of bulk size. The most noted functions that nanoparticles offer are better stability for long term storage, high loading capacity for integrating diverse drug and target molecules, modulation in the particle matrix for both hydrophilic and hydrophobic domains, different administration routes could be entertained such as parental, oral and inhalation, sustained and controlled release of the packaged bioactive groups and time regulated effective clearance from the body (Goesmann & Feldmann, 2010). These advantages therefore have attracted the attention of polymer based nanoparticles for cancer therapy. However, in the biological system the true potential of nanoparticles is questioned as they have to confront both extra and intracellular hurdles which reduce their efficacy.

1.6 Barriers to gene delivery

Unlike viruses which have inherent strategy to escape from the defense mechanisms of the body, polymeric nanoparticles do not possess any natural instinct to evade the biological barriers which is responsible for the low transgene expression. At present these barriers pose challenges for the nanoparticles which need to be understood and overcome. Effective gene delivery requires overcoming a series of barriers that include stable binding of DNA and the polycation in the

external milieu, feasible diffusion though the cell membrane, escape endosomal entrapment, and evade lysosomal degradation and lastly nuclear import for gene expression (Mintzer & Simanek, 2009). Presently the design of various polymers with multifunctional attributes is based on the information gathered regarding the intracellular barriers to achieve the desired transfection efficiency (Jeong et al., 2007).

1.6.1 Stable Polymer and DNA condensates

There should be close association between DNA and polymer to form polyelectrolyte complexes such that the two components may behave as a single unit which is defined as polyplex or nanoplex (Verma & Stellacci, 2010). This interaction is present when polycations are used as non viral vectors as the nucleotides are wound and squeezed into the core by the dissumulation of amine groups that the polycations carry (Morille et al., 2008). The complexation affects the physical properties of the nanoparticles that lead to colloidal stability and safe guard the nucleic acids from nucleolytic degradation. Polycations become protonated at neutral pH and form electrostatic interaction with the phosphate groups of DNA, where charge neutralization and size is modulated by the varying ratios of the two constituents. The compaction of the nucleic acid is well maintained by the excess positive charge distributed by the polycation and prevents any chance of vulnerability for nuclease degradation during systemic translocation (Arvizo et al., 2011). This advantage also has a negative shade as the cationic property of the nanoparticle encounter certain ionic interactions in the fluid system that may cause either aggregation or adsorption with the blood stream components that may be blood cells, proteins, enzymes and complement factors. Proteins in the serum known

as opsonins bind on the surface of nanoparticle that will result in their recognition as foreign substances for macrophage phagocytosis and will be removed immediately from circulation by reticuloendothelial system followed by renal clearance (Nel et al., 2009). Ideally strict solution to this problem is absent but the attachment of certain polysaccharide residues and PEG groups to the polycation nanoparticles has brought considerable reduction in the blood polymer interaction (Huynh et al., 2010). Polyethylene glycol chains are either adsorbed or grafted onto the surface of nanoparticle and the extended chains in solution act as a shield and block the adherence of opsonins to the nanoparticle surface. Indeed they become camouflaged and avoid the mononuclear phagocytic system (MPS) clearance system (Jokerst et al., 2011).

1.6.2 Systemic delivery

In tumour cells, rapid angiogenesis disrupt the endothelial lining of blood and tissue vasculature and lymphatic system is collapsed with improper fluid drainage. This defect in the tumour tissues is a blessing in disguise for cancer therapy as there will be irregular spaces at intervals making the region highly permeable to the passing nanoparticles and without proper lymphatic drainage, the substance get retained in the tumour areas. This concept of enhanced permeation and retention effect will extend the duration of nanoparticles to be exposed to tumour cells, giving ample time to make its way inside the tumour cells (Prabhakar et al., 2013). But in clinical studies, exploiting the concept alone for therapy has failed to achieve the required efficacy. The main reason for this is that EPR effect strategy for nanoparticles to reach the tumour site is therapeutic for tumour cells that are in the vicinity of circulation (Jain & Stylianopoulos, 2010). Meanwhile extensive blood

flow also lead to hydrostatic pressure on the micro vessels which impede further perfusion and create a hypoxic environment at the distal end where tumour cells proliferate in the anaerobic state (Bertrand et al., 2014). And access to these type of tumour cells are denied for the circulating nanoparticles.

1.6.3 Cellular binding

The anionic nature and hydrophilicity of plain nucleic acid is actually hindered from crossing the cellular membrane and this could be overcome when they are transported as cationic nanoparticles. To gain access inside the cell, nanoparticles should form electrostatic interactions with the proteoglyacans and lipid composition of the cell membrane (Xu et al., 2009; Neamnark et al., 2009). Viruses adopt this membrane interaction strategy for its cellular entry and therefore cationic lipids and polymers could interact preferentially in the same manner. Nanoparticles generated from polymers that is conjugated with tissue specific ligands, polysaccharides, PEG and cell penetrating pepetide, amino acids, polyamines could specifically enable facile cellular uptake (Verma & Stellacci, 2010).

1.6.4 Endosomal Release

Once bound to cell surface, the targeted and non targeted nanoparticles are internalized by certain vesicles termed endosomes, an entity of a multifaceted cytoplasmic trafficking pathway known as endocytosis (Canton & Battaglia, 2012). Depending on the nature of the cargo engulfed, its cellular fate is decided and endosomes traverse the cytosol by exchanging the payload with other endosomes till it is either released to organelles or to lyososmal for degradation. This enforced endocytosis should be breached and several escape mechanisms has to be introduced to the nanoparticles. One such strategy is to exploit the ATP driven proton pump in

the endosomes. Entrapped polymeric nanoparticles that contribute protonation, buffer the endosome and the ATPase system, allow rapid influx of ions to counter balance the increased protons in the vesicle. Macromolecules that constitute the polymeric nanoparticles will have amine groups that convey low pKa values which provide high buffering capacity. As a result, endosomes swell enough to cause membrane leakage and rupture releasing the nanoparticles into the intracellular space (Sonawane et al., 2003; Dominska & Dykxhoorn, 2010). Similar style is followed by Simian virus 40 to promote endosomal membrane disruption (Engel et al., 2011). Cationic polymers such as polyethyleneimine, PAMAM, protamine, dendrimers are capable of inducing this characteristic, among which PEI claims to be the most buffering agent (Morille et al, 2008; Benjaminsen et al., 2013). Other approaches are to design amphiphilic polymers with tunable pH sensitivity (Wang et al., 2009a) or decorate with endosomolytic and fusogenic peptides like CPP (cell penetrating peptides) (Endoh & Ohtsuki, 2009) that would create perturbations in the endosomal membrane and cause burst release.

1.6.5 Nuclear Entry

Vector unpacking is a crucial factor for the nanoparticle to dissociate itself from the bound gene to allow the nucleic acid import to the nucleus (Tan et al., 2006). Disassembly of nanoparticles for the nucleotide fragment to enter the nucleus is by far the most daunting task for nanoparticle mediated gene delivery. The transcription machinery along with the factors and proteins associated with it are located within the nucleus and therefore it is mandatory for nanoparticles to find their way through the nuclear membrane from the cytosol. This part of nanoparticle transport is barely understood and different routes of entry are suggested. Certain

histidine and lysine rich polymers (Yu et al., 2011) which promote excellent buffering capacity are able to facilitate disassociation of the polymer and DNA once they reached the nuclear target. In parallel to this it is likely that when cells undergo division, the chromatin and nuclear envelope are loosened and relaxed rather being rigid and tightly regulated. During such instances, nanoparticles unpack the wound DNA and gain entry inside the nucleus. Incorporating certain sequences known as nuclear localisation signals and transcription promoter fragments to the transgene would allow better expression.

1.7 Aims

Gene therapy is still in vogue for the scientific community to treat cancer and for this a plethora of gene delivery systems with diverse features are explored. Despite having issues of toxicity and low transfection efficiency, polymers are a much sought after non viral approach for addressing cancer therapy. Chitosan is a widely studied natural cationic polymer whose potentiality continues to be exploited. The thesis follows this trend and aims to develop a chitosan based matrix for nanoparticle formulations which after conjugation with targeting ligands, amino acid and polyamines ensure enhanced solubility, maintain cationic zeta potential after DNA complexation, convey low cytoxicity and enhanced transgene expression. Eventually the study will compliment the large pool of information and continued research regarding chitosan based gene vectors.

1.8 Hypothesis

In this thesis it is hypothesized that derivatisation of chitosan with conjugates that have biological and physiological significance would lead to gene delivery

vectors that have a natural proclivity to promote enhanced gene delivery to cancer cells.

1.9 Objective

In order to investigate the hypothesis, the following objectives are accomplished.

a) Develop chitosan derivatives with incorporation of ligands for targeted delivery.
b) Ensure a nano based gene delivery systems with the bioconjugated chitosan.
c) Demonstrate the gene expression of a therapeutic gene delivered by the conjugated chitosan nanoparticles.
d) Identify the specific endocytic pathways adopted by the chitosan derivatives for nanoparticle mediated intracellular gene delivery.

The objectives has been accomplished and summarized in the thesis into the following chapters. ***Chapter 1*** introduces cancer biology and existing therapy along with the emergence of nanomedicine with polymer based non viral delivery systems. ***Chapter 2*** describes the relevant literature and lacuna that exist related to the topic of interest. ***Chapter 3*** explains the materials and methodology adopted to execute the study. ***Chapter 4*** examines the results and draws inference from the data collected at the end of each experiment. ***Chapter 5*** discusses and interprets the results for establishing the objectives. ***Chapter 6*** summarizes the study on the whole in terms of the generated data and depicts the major conclusions from each studies bringing out the significance of relevant elements for designing future projects.

CHAPTER 2 LITERATURE REVIEW

2.1 Natural polymer based nanoparticles: Significance of chitosan as the polymer back bone

Among many natural polysaccharides, chitosan is a veteran polymer with enormous commercial applications in the food, pharmaceutical, biomedical and chemical industry. The polymer is obtained from natural marine source and therefore considered biocompatible and biodegradable. The physicochemical properties of chitosan that include molecular weight, degree of deacetylation, amphiphillic nature, high permeability and presence of reactive groups which attribute a positive charge are exploited for producing diverse derivatives with multifaceted purposes. Interestingly chitosan exhibit certain inherent traits of pH sensitivity, viscosity, adhesivity to mucosal membrane, permeability towards mammalian membranes that stimulate the opening of tight junctions of the intestinal barrier , tend to form gels and films, chelates metal ions, form electrostatic interactions with oppositely charged macromolecules and above all antimicrobial action against fungi and certain bacteria. Therefore they have displayed roles that included stabilizing agents and protective biofilms in food preservatives and packaging (No et al., 2007), flocculation and filtration for water purification, as emulsifiers and adhesives in moisturisers and cosmetics, enzyme immobilization, catalysts for 'green' and reusable synthetic reactions, pH responsive attribute for biosensors and bio-microelectromechanical (bioMEMS) systems (Cheng et al., 2010) and antimicrobial and mucoadhesive property for agriculture and oral care therapeutics (Pedro et al., 2009).

Beyond these applications, concurrent research reports are continued to be published regarding the versatility of chitosan and it is now very well established as pharmaceutical excipient (Illum, 1998), scaffolds for cell and tissue seeding in regenerative medicine (Muzzarelli, 2009) and recently as carrier systems for biopharmaceuticals (Illum et al., 2001). Most of the active ingredients for cancer therapy involve anticancer agents and therapeutic proteins that manipulate the different aspects of tumour for treatment such as the EPR effect of tumour vasculature, tumour specific receptors for angiogenesis factors and tumour homing molecules that can avoid the reticuloendothelial cells and allow targeted delivery. The primary focus for delivery of biopharmaceutical agent recommends the use of a biodegradable polymer that can form colloid like particles and convey controlled and sustained drug release. Similar prerequisites exist for gene delivery systems also and the aforementioned attributes of chitosan have encouraged ongoing scientific investigations related to chitosan and its derivatives based gene delivery, making it an undisputable candidate in the arena of gene therapy for cancer. One of the favourable traits in chitosan is the provision to control the parameters that influence its physicochemical property and the modification is designed according to the need. The fine tuned specifications reform the way in which chitosan merge with DNA for gene delivery (Jayakumar et al., 2010) forming complexes with size and charge allied to overcome the biological hurdles to gene transfer.

Chitosan is derived from chitin, a natural polysaccharide which is abundantly found in the exoskeleton of marine crustaceans. Chitin is a byproduct waste resource of the marine industry and when subjected to alkaline deacetylation result in the linear copolymer of chitosan (Hamman, 2010; Dash et al., 2011). Chitosan has

random distribution of β-1,4 linked N acetyl-D-glucosamine (GlcNAc) and D-glucosamine (GlcN) subunits and chemical modifications are feasible to occur due to the availability of reactive functional groups of amine and hydroxyl in the polymer. The groups allow chitosan to initiate reactions such as substitution with acyl or alkyl groups, quaternization, O-carboxymethylation, N-carboxyalkylation, graft copolymerization with chemical residues and attachment of side groups that alter the physical and biological features of the chitosan backbone (Buschmann et al., 2013). Chitosan is found to be insoluble in neutral and alkaline pH since the solubility nature of chitosan is influenced by the varying amount of acetylated monomers and the amine groups. However under dilute acidic conditions chitosan becomes soluble as the primary amine groups offer a pKa value of ~6.5 and tend to get protonated providing an overall positive charge for the polymer. The intrinsic pKa value of chitosan in aqueous or mild acidic conditions seem to be invariably depending on the extent of degree of deacetylation and the ionic strength imparted by the protonated amine groups. This is of advantage as the reactive amine groups is responsible for gelation and metal chelation nature of chitosan, both phenomenon help in creating cross linkages between the polymer chains and provide hydration and sorption property (Sudheesh et al., 2013; Riva et al., 2011).

Chitosan is a polyelectrolyte with a cationic charge that enables the polymer to have electrostatic interactions with anionic macromolecules like glycosaminoglycans or nucleic acids which proves to be useful for contributing the DNA condensing property of chitosan. As a result, stable complexes are formed with the negatively charged polyelectrolyte DNA wound by the polymer in a tightly packaged state. The mixing of oppositely charged two polyelectrolytes (PEC) leads

to the immediate binding of charged ions to form polyelectrolyte complexes. The spontaneity of PEC formation and the stability is directly related to the structural composition of the polyelectrolyte and the stochiometric concentrations of both components. In a matter of fact, the integrity of this affinity binding depends upon the varying ratio of the polymer and DNA (Leong et al., 1998). This principle has been of intense research interest in the synthesis of non viral delivery systems so as so to generate polymers with positive charges in order to bind via electrostatic interactions with negative charged nucleotides. This association has been investigated in the context of several parameter changes with different polymers showing that the strength of polyelectrolyte interaction is dependent on the nature of polymer and the suspended medium. Change in polymer structural properties of length and charge spacing, method of mixing and the molar ratios, ionic strength and pH of the dissolution medium, salt inclusion are some of the parameters that influence the polycation and polyanion binding.

Several articles related to polycation based gene delivery has enthused that electrostatic surface modifications have the potential to circumvent the physiological barriers by improving serum resistance, cell targeting, cellular uptake, endosomal escape, controlled release, and reduced toxicity (Shmueli et al., 2010). Fortunately, the ionisable groups in the chitosan backbone is succumbed to protonation at acidic and near neutral pH and they tend to associate with oppositely charged ions. At this state an increase in entropy is witnessed and the balance is integrated between the charges so as to maintain charge fractionalization leading to the formation of polyelectrolyte complexes otherwise also referred to as polyplexes or nanoparticles. Apparently the DNA is highly condensed and covered with the excess charges of

chitosan to appear as an encapsulated cargo that facilitate gene delivery. Chitosan as gene delivery system utilising the nucleic acid condensing ability was first claimed by Mumper et al. (1995) which was later followed with numerous such attempts that suggested the suitability of implementing chitosan as carrier system for gene delivery.

It was observed that the amount of nitrogen atoms in chitosan to the phosphate groups in the DNA and the range of molecular weight used determine the topographical formation of the DNA and polymer complexes. As part of charge neutralization, the polycations surround the phosphate groups of DNA and cause distortion and bending leading to compilation of both polyelectrolytes into orderly particles. The DNA condensation is reversible process favoured by the competitive binding and net charge on the DNA and cations. As a result the structures of the colloidal particles will be in the form of rods, toroids like structures or as mentioned as scrambled egg like structures with exceeding amount of protonated amines of chitosan in binding the nucleotide fragments (Buschmann et al., 2013). Though chitosan promotes DNA condensation to form self assembled polyplexes, it is yet to be confirmed the particular criteria by which any polycation will affect the packing formation and unpacking of polyplexes

The integrity of chitosan nanoparticle is pertained to molecular weight, degree of deacetylation, polycation /DNA ratio. Chitosan is known to be non toxic and biocompatible but at very high molecular weights the polymer is found to be toxic (Kean & Thanou, 2010). In such cases, reduction in chain length is suggested to reduce toxicity in cells where it is also reported to affect the strong binding of chitosan and plasmid DNA complexes. This would enable disassembly of the

chitosan polyplexes in the intracellular environment even though the polyplexes were tightly wound while traversing in the body to reach the target site inside the cell. An ideal polyplex for gene transfer should adopt an optimised approach that include better polycation/DNA association during cellular transport and upon reaching the nucleus should be able to breakup that affinity bond and release DNA for expression. Currently this part of research has to be studied in depth and therefore the nature of the dissociation of polyplexes once inside the cell remains a crucial factor to be discovered that would determine the extent of gene expression by polycation mediated nanoparticle gene delivery (Won et al., 2009). Another parameter that greatly influences the ability of gene transfer by chitosan is the effect of molecular weight. Three types of chitosan with varying molecular weight were studied with results showing that quarternised chitosan had better transfection efficiency than the other two. Quaternization in chitosan proved to enhance solubility with more protonated amines binding effectively to either DNA or the cell membranes (Zheng et al., 2007). Another way of molecular tailoring in chitosan is glycosyl substituted chitosan oligomers which revealed improved gene transfer efficacy (Strand et al., 2008).

Moreover the glucosamine backbone of chitosan also conveniently forms chemical bonds with the surface proteins of cells which enable cellular entry of chitosan based complexes (Venkatesh & Smith, 1998). This association is responsible for the membrane perturbant nature in chitosan in the cells transfected, which is also explained with respect to the degree of protonation on chitosan (Fang et al., 2001). Upon cellular entry, chitosan polyplexes cannot move freely instead they are engulfed by certain vesicles that constitute the different endocytosis pathways of

the cell. Internalization of molecules in the cell from the external environment is regulated by the process of endocytosis. This major intracellular trafficking cascade is a collection of pathways that has gained immense attention of being considered as the "master organizer of cell signalling", playing a key role in deciding, sorting and organising the final localisation and subcellular destination of the engulfed cargo material. In case where the engulfed cargo is not identified for any cellular purpose, then the cargo containing endosome will be directed towards lysosome for degradation. Exchange of cargo occurs via fusion of endosomes with each vesicle getting matured at each stage of transport. The pH of the endosome is in acidic range and it increases as the maturation of the endosome rises. This is detrimental to effective gene delivery as the endosomes that contain the polyplexes will follow the general sequestrial cascade of endosomal lysosomal degradation (Conner & Schmid, 2003; Sigismund et al., 2012).

In the lysososmes, the gene packaged in the polyplexes will be degraded by the endonucleases. Hence it is a necessity that the polyplexes should escape into the cytosol to avoid enzymatic degradation of the polyplexes once it is transported to the lysosome. It is now widely supported that certain cationic polymers are able to cause endosomal escape by following the proposed hypothesis "proton sponge" put forward by Behr (Behr, 1997). According to the hypothesis, polymers with cationic groups would be protonated when they come in contact with the slightly below physiological pH in the endosome and invoke continuous influx of chloride ions and protons with excessive movement of water. As a result osmotic swelling occurs in the endosome leading to its destabilization and disruption followed by the release of the polyplexes (Yang & May, 2008; Moreira et al, 2009). It is evident that many of

the cationic polymers are able to induce the buffering mechanism in the endosome such as in the case of polymer PEI, being the most accomplished and known buffering polymer. However the buffering capacity of chitosan is reduced due to the fewer amounts of free amines that are available after forming bonds with the nucleotides during polyplex formation. Despite this, functionalization of chitosan with imidazole moieties or with histidine residues has improved the buffering capacity and transfection efficiency (Moreira et al., 2009; Chang et al., 2010). This suggests a role for the guanidium ring in both the chemical residues to increase the proton acidification in the endosome.

2.2 Importance of Ligand Conjugation into Chitosan Polymer

A formidable challenge faced in chitosan based nanoparticles is to convey targeted gene delivery. Targeted delivery of chitosan nanoparticles is a requirement which the polymer chitosan is lacking. Cell specific recognition by polycation polyplexes is essential to avoid any unwanted cellular interactions with the nanoparticles. In general chitosan do not possess any chemical group that is cell or tissue specific. Chitosan is able to generate self assembled polyplexes but as such these are unable to provide targeted gene delivery. An essential prerequisite in gene delivery is to transfer the gene of interest to site of action and chitosan polycations do not possess any kind of cell specificity that will impart targeting ability to the polycation. In this situation, chemical modifications in chitosan with certain cell specific ligands and chemical groups will be able to fulfill the functional role. The ligands are selected based on the functional role it has in the cells in the form of substrates, carbohydrate or polyamine end groups that will enable recognition to specific cells. Another asset of ligand modification in chitosan is the enhancement of

solubility to the polycation. Much of the ligands will be of biological significance and hence are soluble in body fluids. Chemical conjuation with such ligands would impart enhanced solubility to chitosan at physiological pH. Enhanced solubility would also allow chitosan nanoparticles to be stable while circulating in the body. Chitosan in native form tends to cause less endosome swelling and rupture when compared to other polymers like PEI. However with appropriate ligand conjugation, the buffering ability of chitosan has found to be enhanced (Hongliang et al., 2013) which is another advantage.

In general, tumour cells differ from normal cells in many pathophysiological aspects which include a leaky architecture in endothelial cells lining the blood vasculature and poor lymphatic drainage system. The whole tumour environment therefore becomes a favourable ground for nanoparticles to get accumulated during its movement in the circulatory system. Like any other biomolecule, nanoparticles will be entrapped in the tumour vasculature and thus gain an entry into the tumour cells. This physiological state observed in tumour environment is named as enhanced permeability and retention effect (EPR) which imparts an indispensable tool for cancer therapy. Another trait that would direct nanoparticles further into the tumour cells is the possession of specificity towards the cancer cells. The main principle behind active targeting using ligand modified nanoparticles is to utilise the specific receptor binding sites that is over expressed in cancer cells when compared to normal cells which would enable feasible intracellular delivery. For this, different steps have been employed to manifest targeted gene delivery by chitosan nanoparticles. Active targeting includes conjugation with targeting components like folic acid, transferrin, mannose (Kim et al., 2006) and RGD peptide (Cai et al., 2011)

that would recognize the respective receptors on the cell surface. Conjugation with multiple ligands is another strategy of ensuring effective and targeted cellular uptake. Similar studies were attempted to functionalise and decorate a single polymer derivative with unique side conjugates of tumour specificity so as to acquire sensitivity and efficacy in gene delivery.

2.2.1 Conjugation with Galactose and spermine

It is well known that tumour cells have high metabolism than normal cells and therefore the cells display an increased amount of membrane bound sugar transporters to aid in binding of circulating sugar moieties. The induction of glucose transporters is detected as a sign of cell's malfunction to transform into tumour cells. Therefore extensive consumption of sugars and enhanced activity of glycolytic enzymes are manifested in tumour cells. Sugar transporters known as GLUT are responsible for the translocation of carbohydrate residues across the plasma membrane dependent on the sugar concentration gradient inside the cells. However in tumour cells, the particular concentration gradient is disrupted and blocks the exit of glucose outside the cells while the GLUT transporter is impaired and fails to recognize the saturation of sugar uptake in the tumour cells. The GLUT transporters vary in number in different tissues and are specific to distinct sugar moiety such as glucose, galactose, lactose etc (Calvo et al., 2010, Hashimoto et al., 2006). Certain sugar compounds like galactose act as cell binding ligands that would target the carbohydrate specific receptors like asialoglycoprotein receptors in the case of hepatocytes (Mao et al., 2010).

Dual targeting is an acceptable approach for ensuring specificity to the polymeric system as in the case of a chitosan derivative with grafted PEI which was

conjugated with polyethylene glycol and further with galactose (Jiang et al., 2008) to convey two attributes namely better hepatocyte specificity and further reduction in cytotoxicity. And with this similar thought, another conjugate of tumour relevance was considered, a polyamine spermine that has functional role of cellular association with nuclear DNA that prescribe DNA binding and delivery. A comparative study has been carried out with spermine polysaccharide conjugation in varying combinations which explained the significance of spermine in the polymer for transfection (Eliyahu et al., 2006). The same group also delved further in modifying dextran with spermine and demonstrated the role of secondary amines in achieving transgene expression in *in vivo* condition (Eliyahu, 2007).

2.2.2 Conjugation with Protamine and Diamino Polyethylene glycol

Most of the biological conjugates are prevented from having an easy diffusion across the cell membrane since they are polar and hydrophilic due to their proteinaceous composition. In such instances, certain peptides known as cell penetrating peptides or protein transduction domains are capable to penetrate the membrane and facilitate cellular internalization. Hence attachment of these short peptides to biological cargoes has become popular as the linkage promises effective intracellular translocation. Surprisingly it is revealed that arginine is the most predominant amino acid in several of the various sequences of the CPP (Ma et al., 2011) which include the TAT peptide, the first known cationic protein transduction domain (PTD) (Jiao et al., 2009), Antp and Hph, penetratin and polyarginine. Additional reports also supported the capability of arginine constituted nanoparticles (Khalil et al., 2006; Kosuge et al., 2008) to mediate efficient cellular uptake. Likewise conjugation of chitosan with arginine has also enthused to be an

anticoagulant biomaterial which also showed enhanced transfection efficiency. Therefore any biomolecules with arginine rich composition bestow an effective conjugate for polymer derivitisation that enable feasible gene delivery (Zhang et al., 2011; Youn et al., 2008).

Potentially, identification of protamine (Tsuchiya et al., 2006) another cationic polypeptide which has arginine rich sequence became a suitable conjugate for grafting into chitosan backbone. These small polypeptides, isolated from mature fishes, are concerned with binding to nuclear chromatin structures in the sperm for feasible DNA delivery to the egg nucleus during fertilization. This desirable characteristic is exploited for cytosolic delivery of exogenous DNA using non viral delivery of chitosan based nanomaterial (El-Sayed et al., 2008, Hayashi et al., 2011). The efficacy is contributed by the arginine-rich content of protamine that devise different ways of endosomal escape avoiding prolonged entrapment of the engulfed cargo in the endosomes (El-Sayed et al., 2009). Initial research efforts carried out with protamine-oligonucleotide complexes reflected poor intracellular dissociation and transgene expression (Junghans et al., 2000; Junghans et al., 2001)**.** This was overcome by additional introduction of amphiphilic molecules like albumin to generate a ternary system which presented profound cellular uptake with cent percent transfection. The incorporation of protamine into other polysaccharides like dextran and pullulan also featured nanoparticles that produced gene expression and preferential endocytic pathway uptake (Thomas et al., 2010; Priya et al., 2014).

Grafting of polyethylene glycol into the chitosan backbone is an established strategy for creating biocompatible gene delivery systems. Polyethylene glycol chains are hydrophilic molecules with hydroxyl end groups that convey a neutral

charge. They are available in varied size range from 200 to 40000 Da and when conjugated to polymers, these linear chains can cause steric repulsion. Hence while the nanoparticles traverse in the blood circulation, PEG grafted nanoparticles is able to mask the chemical groups from any unwanted protein interactions (Zhang et al., 2008). Thereby less immune response would be elicited and the duration of nanoparticles to be present in the system would be extended for a long period rather than be cleared immediately by the reticuloendothelial system (RES). The steric stabilization is attributed due to the arrangement of PEG chains in a brush like appearance on the outer surface of the formed nanoparticle thus avoiding any chance of serum proteins to come into contact with the reactive groups of the polymer backbone (Erbacher et al., 1999a). Nowadays diamine functionalised PEG is adopted that would cater to the reactions specific for amine end groups and enable desired chemical modifications. This strategy was implemented to synthesize PEGylated superparamagnetic iron oxide nanoparticles (SPIONs) which used its surface carboxylic roups to form amide bonds with PEG diamine (Liu et al., 2011).

2.2.3 Conjugation with Ornithine

Studies have shown that incorporation of basic amino acids such as arginine and lysine into the polymer backbone showed enhanced transfection efficiency than the parent polymer. Similar transfection efficiency was observed when chitosan was conjugated with the cell penetrating peptides like TAT which consisted of these amino acid residues (Lee et al., 2011). This supported the fact that arginine conjugated delivery vectors performed significant transgene expression indicating the preference of arginine by the endocytosis pathway for cell internalization. Simultaneously it is also reported that the polypeptide form of another amino

acid ornithine, a byproduct of arginine breakdown in human system, is known to promote high cellular uptake (Kumar et al., 2010). The biogenesis and metabolic pathway of arginine and ornithine occur in parallel as per the need of supply in the cells (Soetens et al., 1998). Though ornithine is not an essential amino acid coded in protein synthesis, the biological requirement is correspondingly as significant as arginine. It was also interesting to discover the work that involved ornithine conjugated dendrimers which investigated the mechanism of cell uptake and elucidated a promising role of polyamine transporter system besides the charge-mediated endocytosis in the internalization of ornithine-conjugated dendriplexes (Kumar et al., 2011). This holds true as the polyamine transport system is considered as a potent tumour targeted pathway for selective translocation of polyamines into the tumour cells which could be exploited for ornithine uptake (Palmer & Wallace, 2010). Moreover ornithine is also acted upon by enzyme ornithine decarboxylase (ODC) whose encoded gene is highly present in tumour cell lines and regarded to be a plausible biomarker for targeting cancer and this characteristic is taken advantage to gain preferential uptake in cancer cell line.

2.2.4 Conjugation of Chitosan Ornithine with Spermine

Since ornithine gained cellular internalization via cationic transport system, the likelihood of polyamine transport system to be involved was greatly anticipated. Hence further conjugation of chitosan ornithine derivative with the polyamine spermine served the purpose of acquiring as much as preferential and enhanced cellular uptake of nanoparticle that might influence transfection efficiency.

In early period of cancer research, it was reported that tumour cells required large amount of polyamine for metabolism as observed by other normal cells. On these

findings, tumour cells are known to have increased metabolism. Fundamentally, polyamines are low molecular weight biomolecules required for the normal cellular metabolism. Several cellular functions are mediated by polyamines with the most acclaimed to be cell proliferation and differentiation. They are soluble in water with positive charges at physiological pH and therefore are prone to interact with anionic macromolecules. Free polyamines as such is reported to be very negligible in the cell as they tend to bind to proteins, DNA, RNA, enzymes and phosphorylated molecules and so are proposed to play even more significant roles in signal transduction, cell cycle regulation, preserve the chromatin framework, intercede in DNA transcription and cytoskeleton movement.

The three most prominent known polyamines that are widely studied are putrescine, spermine and spermidine. The body maintains a constant supply of polyamines by highly coordinated, complex and circuitous independent cycles of metabolism, synthesis and degradation. Arginine and methionine are the initial precursors for polyamine synthesis with ornithine and S-adenosyl methionine as intermediate substrates that are able to enter the cycle at several checkpoints. Additionally the pathways are complex enough that they are modulated towards equilibirium according to the need and excess level of polyamines. Although the polyamine biogenesis pathways are conserved against evolution, it is reported that polyamines, putrescine and spermidine are found to dominate in prokaryotic cells while spermine is seen abundantly in eukaryotic and mammalian cells (Igarashi & Kashiwagi, 2010). Endogenous spermine is postulated to have direct involvement in regulating the gated ion channels and can modulate the opening and closure of membrane bound receptors (Williams, 1997). And it is already known that spermine

can effectively bind to DNA, RNA and chromatin and caused stabilization and destabilisation of the complexes formed. This attribute is exploited to design cationic polymers that would readily condense the nucleic acid for gene transfer which is observed in grafting the polysaccharides chitosan, dextran and pullulan (Jiang et al., 2011; Eliyahu et al., 2005; Eliyahu et al., 2006, Kanatani et al., 2006). The studies have exhibited that incorporation of polysaccharide with spermine conjugates evidently improved transfection and enhanced DNA expression.

2.3 Uptake of Chitosan nanoparticles via Endocytic pathway

It is highly necessary that once the nanoparticles reach the tumour cells, they should be recognised as host materials to gain cellular entry. In other words, the nanoparticles should be decorated with cell specific active compounds that allow feasible recognition of the target cells. These protruded bioactive molecules would act either as substrates or antigens that will be analogous to the normal biomolecules that interact with the cell surface receptors. This association is the key to enter inside the cell, by the formation of inward invagination of the plasma membrane, mediated by the well organised and highly orchestrated cellular mechanism known as endocytosis (Sahay et al., 2010). It is characterised by a repertoire of pathways with distinct features for specialized functions. In a nut shell, endocytosis engulf the external material in membrane bounded compartments called vesicles which are shuttled across the cytosol and the payload is exchanged between themselves until they reach the predetermined subcellular locations for their utilization. Unlike the process to be a single movement, multiple pathways are involved featuring variable endosomes with distinct signal molecules and domains that sort and translocate the cargo dependent on the nature of the cargo and pathway chosen (Verma & Stellacci,

2010). Correspondingly non viral biomaterial are also internalised in the cells by the same phenomenon and it has been realised that intracellular sorting and trafficking determine the intracellular destination of polymeric nanoparticles which correlate to the efficacy of gene delivery. Hence it is necessary to learn the significance of endocytosis and investigate the emphasis of the diverse pathways adopted by chitosan nanoparticles enabling us to achieve a sound understanding of the relationship between the ligand attachment and intracellular trafficking. Although endocytosis is actually a normal and universal route of entry for any macromolecule to enter the cell, the predominance of the various pathways may differ depending on the cell type specific variation. For instance, hepatoma cancer cell line exploits certain receptors on the cell surfaces that have high affinitiy binding to the sugar containing compounds (Mao et al., 2010). Since multitude endocytosis pathways exist, the commonly discussed entry portals are the clathrin mediated, caveolae mediated endocytosis, macropinocytosis and receptor mediated pathways.

Clathrin mediated pathway is very much known to engage in the uptake of certain nutrients like cholesterol that is bound to low density lipoproterin and iron bound to transferrrin, both of which are recognised by specific cell surface receptors via LDL and transferrin respectively (Rejman et al., 2005). The vesicles pinch off from the plasma membrane towards the cell interior with the internalized cargo engulfed within the vesicle. These are referred to as endosomes where the cargo is transported by the fusion with similar vesicles till it reaches the lysosome for degradation. Another prominent regulator molecule is dynamin which causes the scission of the endosomes to bud off from the membrane. There are cases where dynamin independent endocytosis is also reported to occur (Haugsten et al., 2011).

Unlike clathrin vesicles which have coated pits, the caveolae pathway initiates with flask shaped vesicle which has lipid rich raft domains that are lined with proteins called caveolin in the interior. Most likely the caveolae are found to be cell dependent and these hydrophobic membrane domains are encountered in endothelial cells, fibroblasts and adipocytes. The pathway is ascribed to be non acidic without leading to lysosomal degradation, which is yet to be ascertained. In that case, the caveolae portal will be nondigestive without any pH variations making it suitable for gene delivery. This might be the reason that viruses like simian 40 (SV40) and bacterial toxins find their way into the cell through this pathway (Vercauteren et al., 2012). Certain cationic polymer and PTD peptides combined with nucleic acid also showed the presence of caveolar mediated uptake for the complexes (Youn et al., 2008).

At other times when nanoparticles do not have any kind of specificity, they enter the cells as part of the fluid drinking mechanism called macropinocytosis which is characterised by membrane ruffling that lead to large invaginations from the plasma membrane with extracellular fluid intake (Vercauteren et al., 2012). Macropinosomes formed is devoid of any inner lining of coat proteins and receptors and adopts a non selective pathway of internalization of submicron substances. The pathway is assumed not to include phagocytosis and therefore is preferred by some pathogens and viruses as it is invariably present in almost all kinds of cells. Since the route permits non specificity, it is suggested that polymeric nanoconjugates utilize this pathway also along with other specific endocytosis portals.

Most of vesicles of the aforementioned pathways contain receptors which constitute the receptor mediate pathway of endocytosis. In this mode of entry,

selectivity and specificity play a crucial role for internalization and certain essential biomolecules such as folic acid, transferrin and glycoconjugates follow the receptor mediated pathway (RME) of cellular uptake. Indeed this promised a definite approach for transfer of gene to the cell by introducing the ligands in the polymeric matrixes to be recognized by the receptor specific for the ligand conjugate and achieve cellular entry. Large amount of work related to ligand targeted delivery has been implemented in tumour cell lines, of which the main cited are folic conjugated (Yang et al., 2010) transferrin mediated (Dufes et al., 2004) and galactose attached polymeric nanocarriers (Song et al., 2009; Zhu et al., 2013). It is accepted that that most of the polymeric nanomaterials benefit from multiple endocytosis pathways for accomplishing cellular uptake. Hydrophobically modified chitosan supported this since the cationic nanoparticles utilised clathrin as well as caveolae and macropinocytosis for cellular internalization (Nam et al., 2009).

Therefore a comprehensive understanding of these pathways alone does not improve the gene delivery efficacy as it also informed that other parameters such as nanoparticle size, charge, shape, type of cell lines used and even culture conditions dictate the selection of the uptake pathways. Nonetheless these parameters do have certain well defined specifications in defining the characteristics required for an efficient cell uptake and seem to vary with the physicochemical properties of the nature of the carriers. The relationship of these factors with the intracellular trafficking and transfection continue to be active area of research and therefore extensive research is still ongoing to unearth even more interesting aspects and unknown facts related to endocytosis.

CHAPTER 3 MATERIALS AND METHODS

3.1 Depolymerisation of Chitosan

3.1.1 Materials

High molecular weight chitosan polymer (Mw- $3x10^4$ Da; deacetylation degree-90 %) was obtained from CIFT Kochi and absolute methanol was purchased from Merck, India.

3.1.2 Depolymerisation by Sodium nitrite

Usually chitosan, purchased in bulk amounts, comes with very high molecular weight ranging between 3×10^4 Da and 2×10^6 Da which often fail to be feasible for medical applications (Mourya & Inamdar, 2008). For gene delivery purposes, chitosan either with low or intermediate molecular weight is desirous, ranging either within 30–90 kDa or within 100–150 kDa. The degree of deacetylation was not modified but the molecular weight was reduced. Reduction is obtained by oxidative degradation of chitosan with $NaNO_2$ as performed in the work of Mao et al. (2004). In brief, raw chitosan flakes was filtered through nylon membrane of pore size of 120 μm, to remove any unwanted debris and dissolved in 1 % acetic acid solution. The prepared chitosan solution was reacted with 0.1 M $NaNO_2$ under constant magnetic stirring of 500 rpm, at room temperature for 3 h. The reaction mixture was subsequently neutralized with 1 N NaOH to pH 8.0 to precipitate chitosan. The precipitated chitosan was recovered by centrifugation at 3350×g for 10 min, washed thrice with deionised water, followed by two times wash with 75 % methanol wash. Chitosan was then dried in vacuum oven at 60˚C for 5 h. The molecular weight was then determined using the Ubbelohde viscometer (Ventek,

India). The molecular weight is calculated on the basis of intrinsic viscosity of the chitosan polymer solution against the viscosity of the 0.25 M sodium acetate solution. The depolymerised chitosan is adopted for the synthesis of four derivatives.

3.2 Spermine grafted galactosylated chitosan

3.2.1 Materials

Spermine tetrahydrochloride, N, N'-Disuccinimidyl carbonate (DSC), 4-dimethylaminopyridine (DMAP) and glucosamine were purchased from Fluka. N, N-Dimethylformamide (DMF) and acetone was purchased from Merck, India. Lactobionic acid, branched PEI (25 kDa), 1-ethyl-3-(3-dimethylaminopropyl) carbodiimide hydrochloride (EDC), N-hydroxysuccinimide (NHS), fluorescein isothiocyanate (FITC), 3-(4, 5-dimethylthiazol-2-yl)-2, 5-diphenyl tetrazolium bromide (MTT), Dulbecco's modified Eagle's medium (DMEM), F12 Ham, chlorpromazine, filipin, asialofetuin, galactose from Sigma-Aldrich, USA. Fetal bovine serum (FBS) was from GIBCO (USA). YOYO iodide, Hoechst 33342 and Live Dead assay kit from Invitrogen. Others were Calf thymus DNA (Worthington Biochemical Corp.), pGL3 DNA, Luciferase Assay (Promega, USA) and p53 Dominant-Negative Vector (Clonetech, USA). The HepG2 cell lines and C6 glioma cells lines were supplied by the National Centre for Cell Science (NCCS), Pune, India. Human blood was collected from the unmedicated healthy volunteers. All other chemicals were of AR grade.

3.2.2 Preparation of galactosylated chitosan with spermine coupling

To obtain galactosylated chitosan (GC), the dried chitosan was coupled with lactobionic acid in the presence of coupling agents EDC and NHS at room temperature (Kim et al., 2004). Initially 500 mg chitosan (1 %) was dissolved 0.25 N

HCl and stirred for 1 h. The pH was adjusted to 6.5 with 2 N NaOH and should see to that the pH does not go beyond 6.7. To this solution, lactobionic acid of 250 mg was added to chitosan, in the presence of the activating agent EDC (0.1 M) and NHS (0.1 M) and kept under magnetic stirring at 500 rpm overnight. The solution was then dialyzed against distilled water for 2 days and transferred into lyophilising glass flasks. The flasks were fitted into cold vacuum based lyophiliser (LABCONO, USA) for two days to obtain moisture driven galactosylated chitosan (GC). The GC obtained was dissolved in mild acidic condition of 0.5 % HCl (w/w) as it is insoluble in organic solvents. Further reaction was carried out in DMF, with initial dissolving of GC (0.25 %) in HCl that will be 20 % the total volume in DMF. GC was then activated with 6 mM DSC and 6 mM DMAP for 4 h (Kim et al., 2008). Activated GC was conjugated with spermine, added in equal amount as GC and kept for overnight stirring at 4˚C. The precipitate was recovered by acetone wash, centrifuged at 3350×g for 10 min, followed by dialysis and lyophilization. The dried product appeared to be white, thin, mesh form with paper like texture and it was coded as GCSM. The polymer was prepared in concentration 1 mg/mL MilliQ H_2O in order to be used for further experiments, unless stated otherwise.

3.2.3 Colorimetric determination of primary amine groups

The free primary amine groups present in the chitosan determine the intensity of positive charge that resides in the derivatised polymer. Therefore modified chitosan was evaluated by the presence of primary amine groups that is left unreacted after the grafting reaction and this was measured using the standard procedure of a biochemical assay using TNBS (Snyder and Sobocinski, 1975). All samples were taken in 1 mg/mL concentration. GCSM was dissolved in MilliQ water, GC in 0.5 %

HCl (w/w) while unmodified chitosan was suspended in 1N HCl. Chemical reactions occur at the free amine group of glucosamine subunits present in chitosan and hence glucosamine was taken as the reference, whose concentration was fixed as 100. To the sample, 200 µL 0.1 % (TNBS) 2, 4, 6-trinitrobenzenesulfonic acid and 4 % sodium bicarbonate was added. Triplicates were carried out for each sample and after incubation for 2 h at 37˚C, 200 µL of 2 N HCl was added to stop the reaction. Absorbance was read at 344 nm with the UV-Vis spectroscope (UV Varian Cary, USA). Triplicates were done and statistical analysis was performed with respective standard deviations being provided. The result calculations were determined as follows: Percentage of free amine groups = $\left(Ab_S \div Ab_R\right) \times 100$

Where Ab_S represent absorbance of sample; Ab_R represent absorbance of reference

3.2.4 Analysis by Fourier transform infrared spectroscopy

The functional groups in the derivative was analysed with the Infrared (FTIR) spectra of chitosan, lactobionic acid, spermine and GCSM which were recorded on a Fourier transform infrared spectrometer (Shimadzu spectrophotometer) in the range of 4000−400 cm^{-1}. The dried samples were grounded with KBr powder and compressed into pellets containing ca. 2 wt % samples for FTIR examination.

3.2.5 Analysis by Proton Nuclear Magnetic Resonance spectroscopy

A proton nuclear magnetic resonanace (^{1}H NMR) spectrum of the chitosan derivative GCSM was measured in D_2O using a 500MHz spectrometer (Bruker Avance DPX 300). The analysis was performed at 22˚C and the number of transients during the measurements was set as 16. The relaxation time of the instrument during measurements was 3.17s. All other parameters were in the default settings of the instrument as per the specifications of Bruker Avance DPX 300.

3.2.6 Buffering capacity of GCSM

The extent of protonation of the polymer is a notable feature for the polymer to escape endosomes delivery to lysosome degradation. To study this, 6mg of GCSM was dissolved in 30 ml MilliQ to get a final concentration of 0.2 mg/mL. At the initial stage, the pH of the polymer solution was adjusted to 10 with sodium hydroxide which was then titrated against 0.1N hydrogen chloride, adding 50 μL gradually to record the pH changes of the polymer solution (Benns et al., 2002). The pH profile of both branched PEI (25 kDa) (0.2 mg/mL), a cationic polymer reported to have the most buffering capacity and unmodified chitosan 120 kDa (0.2 mg/mL) prepared in 1 N HCl, was also recorded to compare with the buffering ability of GCSM solution.

3.2.7 Amplification and Purification of plasmid DNA and calf thymus DNA

Dynamic light scattering used calf thymus DNA (ctDNA) for nanoparticle formulation with GCSM polymer as large number of varying ratios is performed for optimisation. The calf thymus DNA was prepared at 1mg/mL concentration and dialyzed in 0.1 M sodium acetate buffer prior to nanoparticle formulation for determination of size and zeta potential. Plasmid DNA p53 and pGL3 were used for other experiments and they were isolated separately from Ecoli cells that were transformed with the respective plasmid. Using the Qiagen QIA filter plasmid Mega kit, the isolation and purification of the plasmid DNA was implemented and plasmid integrity was determined by both agarose gel electrophoresis and UV-Vis spectroscope (UV Varian Cary, USA). The final purity is determined to be 1.83 (OD 260/280) and 2.08 (OD 260/235).

3.2.8 Preparation of GCSM complexes

The dried GCSM product obtained after the modification reactions was soluble in MilliQ water. Cationic polymers showed a rapid condensation with negatively charged DNA to form compact complexes which were nanoparticles that could be also addressed as nanoplexes or polyplexes. GCSM was prepared in a concentration of 1mg/mL before combining with calf thymus DNA (ctDNA). The solution was filtered through a 0.22 μm filter and kept sterile. Calf thymus DNA was also prepared in the same concentration 1mg/mL. Nanoparticles were prepared in normal saline (NS, 0.9 % sterile sodium chloride) by mixing ctDNA with varying concentration of polymer solution equivalent to DNA:polymer ratio (w/w), i.e. DNA/GCSM, expressed in terms with concentration of both ctDNA and polymer solution. Calf thymus DNA concentration is kept constant for all ratios. The system was vortexed for 15 s and incubated for 20 min at room temperature for complex formation to occur. It was made particular during complex preparation, the concentration of DNA to be constant and concentration of polymer solution to be varied to adjust the theoretical charge ratio. Likewise nanoparticles that used plasmid DNA for formulation with GCSM polymer also followed the above procedure. The complexes employed for further experiments cited below were prepared in terms of this method unless otherwise stated.

3.2.9 Determination of particle size and zeta potential

Nanoplexes prepared was checked for size and surface charge using the Zetasizer Nano ZS (Malvern Instruments Ltd., UK) at a temperature of 25˚C. The complexes were prepared in saline (NS, 0.9 % sterile sodium chloride) with increasing DNA/polymer ratio (w/w), with ctDNA at a constant concentration of

1mg/mL (Case et al., 2009). The average particle size was evaluated based on dynamic light scattering phenomenon of the Zetasizer Nano ZS (Malvern Instruments Ltd., UK). The size of polyplexes was expressed as the mean diameter (z-average) obtained by cumulant analysis of the correlation function using the viscosity and refractive index of water in calculations (Strand et al., 2010). Zeta potential is a function of the surface charge present on the nanoparticle and was also measured with Zetasizer Nano ZS (Malvern Instruments Ltd., UK) at a temperature of 25˚C.

3.2.10. Transmission Electron microscopy analysis

The morphology of the GCSM nanoplexes were observed using Transmission electron microscopy (TEM) and the nanoparticle suspension of 10 µL, complexed at DNA/polymer ratio (w/w) of 15 was placed on a copper grid removing excess liquid with a piece of filter paper and grid was then air dried. Samples were visualized with a Hitachi 226 H 7650 instrument at 100 kV.

3.2.11 Atomic Force microscopy analysis

Furthermore the samples were subjected to Atomic force microscopy (AFM) (WITEC Confocal Raman Microscope System with Atomic Force Microscope Extension, Germany) that enabled a closer visualization of the GCSM nanoparticle. Plasmid pLG3 was mixed with GCSM polymer solution in the DNA/polymer ratio (w/w) of 15 and was deposited on mica substrates to be operated in the contact mode of the instrument with cantilevers that operated between 0.6-1 Hz at a resonant frequency approximately 320 Hz.

3.2.12 DNA Gel retardation

Nanoplexes were prepared with GCSM polymer and ctDNA which was then loaded onto agarose gel to analyze the condensation ability of the polymer to retard the bound ctDNA. Increasing ratios of the GCSM nanoplexes were analysed on 1 % agarose gel prepared in 1X TBE buffer (89 mM Tris–HCl pH 8.3, 89 mM borate and 2 mM EDTA), staining with 2 µL of 10 mg/mL ethidium bromide. Electrophoresis was carried out in a Bio-Rad electrophoresis system (Bio-Rad laboratories, CA, USA) at 100 V for 60 min. The DNA bands were then visualized and photographed using MultiImage TM Light Cabinet (Alpha Innotech Corporation, San Leandro, CA, USA). Sample ratios 6, 8, 10, 12, 14, 15, 16, 17, and 18 were considered for loading into the wells.

3.2.13 DNase I protection and release assay

DNase was prepared in digestion buffer containing 0.1 M sodium acetate and 5 mM magnesium sulfate at pH 7.4. Nanoplexes of varying ratios 4, 6, 8, 10, 12, 14, 15, 16, 17 and 18 were prepared. The complexes were incubated with DNase of concentration 569 U/mL. For 2 µg DNA, usually 2.28 µL of DNAse is taken. The reaction was terminated using termination buffer containing 0.5 M EDTA, 2M NaOH and 0.5 M NaCl. Nanoplex stability was confirmed further by treating the samples with heparin of 5 µL at concentration 1000 U/mL, for 30 min. It is previously reported that heparin, a highly charged polyanion have the property to displace DNA competitively from DNA-chitosan polyplexes (Srinivasachari et al., 2007). The protection rate of GCSM polymer to retain the DNA from degradation and its release was detected by visualizing the bands run on a 1% agarose gel electrophoresis (Bio-Rad Laboratories, CA, USA).

3.2.14 Interaction of GCSM with Red blood cells (RBC)

Blood was compiled from a healthy volunteer and anticoagulated with sodium citrate (3.8 %) at ratio 9:1. Isolation of RBC was done as explained in the following protocol (Joshy & Sharma, 2012) to conduct hemolysis and red blood cell aggregation. Hemolysis was performed with erythrocytes which were washed with saline thrice, diluted with saline in the ratio 1:8 and around 100 µL was transferred to separate tubes. The polymer GCSM (1 mg/mL) was added to the RBC collected tubes in replicates of desired four concentrations of 25 µg, 50 µg, 75 µg and 100 µg. The samples were incubated for 2 h at 37˚C followed by centrifugation at 1500 rpm for 5min. Subsequent absorbance of amount of haemoglobin released was monitored in UV-Vis spectroscope (UV Varian Cary, USA) at 541 nm. The absorbance was measured in relative to the positive control Triton X-100 (100 %) and negative control saline (0 %). Hemolysis was calculated with the following equation

$$\text{Percentage hemolysis} = \left(\frac{Ab_T - Ab_N}{Ab_X - Ab_N} \right) \times 100$$

Where Ab_T represent absorbance of test, Ab_N represent absorbance of normal saline, Ab_X represent absorbance of Triton X-100.

Microscopic observation of RBC in response to addition of polymer GCSM in concentrations 100 µg was carried out. Saline washed RBC was diluted to 1:9 and 100 µL RBC was incubated with GCSM for 30 min. Saline and PEI treated RBC was taken as the controls. Images were captured with phase contrast microscope Leica DMI3000 B (Leica, Germany).

3.2.15 Electrophoretic analysis of GCSM polymer with plasma protein interactions

A polymer is considered to be suitable for systemic delivery when they are capable to evade serum protein adsorption at its surface. To assess this, blood plasma was diluted with saline and incubated with GCSM polymer (1mg/mL) prepared in two concentrations 50 µg and 100 µg for 1 h at normal temperature. This was followed by a quick centrifugation and subjected to native gel electrophoresis with 20 µL of samples loaded on 7 % resolving and 4 % stacking gel. Samples were run at 90 V for 90 min using Mini-Protean II electrophoresis system (Bio-Rad, CA, United States). Staining was done with Coomassie blue and the proteins bands were visible that was captured in image analyser (LAS 4000, Fuji). Normal saline (0.9 % sterile sodium chloride NaCl) treated plasma proteins also revealed protein bands and was therefore considered for reference.

3.2.16 Cell Culture

The influence of GCSM nanoparticle on biological system was analysed by performing cell culture studies. The study was attempted in human liver carcinoma cell lines (HepG2) cells seeded in culture flasks with DMEM medium along with 10 % FBS and incubated for 24 h at 37˚C in 5 % CO_2 and 95 % humidity to attain a cell growth of 80 % confluency. Prior to the following culture experiments, the cells were trypsinised and transferred to multi well tissue culture plates in the density of 1×10^5 cells/well. Reports from our lab (Morris and Sharma 2010; Rekha and Sharma 2009) were used as reference for performing the cell culture experiments. For fluorescent imaging GCSM polymer (2 mg/mL) was tagged with FITC (FCP) (Sigma) separately and prepared as per the manufacturers' protocol in the dye conjugation kit. FCP was

then purified by dialysis using membrane of molecular weight cut off of 12,000 Da (Sigma) against distilled water.

3.2.17 Cytotoxicity assay

Cell viability is a significant parameter to be evaluated in order to determine any toxic effect of the novel chitosan derivative in in vitro settings. The cytotoxicity was assessed by the MTT assay which contains the reagent, 3-(4, 5-dimethylthialzol-2-yl)-2.5- diphenyl tetrazolium bromide (MTT) prepared in deionised water. The trypsinised HepG2 cells, seeded into multi well tissue culture plate were kept for incubation in the same lab culture conditions of temperature and pressure. GCSM polymer corresponding to 1 mg/mL was added in triplicates at a very high concentration of 100 µg. After 24 h incubation, GCSM with the media were removed and MTT reagent (0.2 mg/mL) was added to each well. After 3 h incubation, the reagent removed and dimethyl sulfoxide (DMSO) was added to dissolve the MTT formazan crystals. Plates were incubated for 5 min and the resultant solution was measured in an automated microplate reader at 540 nm (Finstruments Microplate Reader, MTX Labs, USA). Cells in DMEM medium without GSCM sample treatment were selected as the negative control to acquire viable cell measurement. For comparative analysis, the cells were treated with 100 µL of unmodified chitosan (1 mg/mL, 1 N HCl). Cell viability was expressed as the mean percentage of sample absorbance relative to untreated cells.

$$\text{Percentage cell viability \%} = \left(\frac{Ab_S}{Ab_C}\right) X 100$$

Where Ab_S represent absorbance of sample, Ab_C represent absorbance of medium control.

3.2.18 Cellular uptake of GCSM nanoparticles

In the four-well plate, Hep G2 cells were seeded at a density of $1x10^5$ cells/well and allowed to grow for 24 h to attain 80 % confluency. Plasmid DNA was tagged with YOYO as YOYO iodide is a DNA labeling dye with high sensitivity and affinity towards double stranded DNA. The plasmid DNA was incubated for 30 min with YOYO iodide, with 2.5 µL of 10 µM YOYO labeled for 1.0 µg DNA/well. Two nanoplex combinations, in ratio 15, were made for observing plasmid trafficking. In one combination, FITC labeled GCSM was complexed with unlabelled pGL3 plasmid and in the other, YOYO tagged pGL3 plasmid, was mixed with unlabelled GCSM polymer. After 20 min complexation, HepG2 cells were treated with the above mentioned combination of GCSM nanoparticles. After 3.5 h the cells were treated with 15 µL of Hoechst 33342 (final concentration to be 1mM) for nucleus staining, followed by half hour incubation. The cells were then washed in saline, replaced with fresh media and immediately viewed under a fluorescence microscope (Leica DMI 3000B, Germany). Similar cell treatment was performed to implement quantification of cell uptake by flow cytometry (Becton Dickinson FACS Aria, USA). For each measurement ten thousand cells were counted and the percentage of positive cells was calculated by setting the background population as 98 % negative when analyzing untreated control cells (Kanatani et al., 2006).

3.2.19 Cell uptake studies in the presence of endocytic inhibitors

HepG2 cells were seeded to a 4-well plate at a density of $1x10^5$ cells/well and uptake study was carried out in the cells after 80 % confluent growth. Nanoparticle entry inside the cell, in general, is mediated by a mechanism known as endocytosis that comprised a number of trafficking channels, among which clathrin dependent,

caveolae-mediated and receptor mediated internalization are prominent endocytic pathways. The intracellular movement of GCSM nanoparticle was investigated by adopting four endocytic inhibitors that is reported to cause inhibition to endocytic motion (Rejman et al., 2005, Orlandi & Fishman 1998). To begin with, the cells were rinsed with PBS and incubated for 30 min with clathrin mediated inhibitor chlorpromazine and caveolae mediated inhibitor filipin at a concentration of 1 µg/mL and 2.5 µg/mL respectively (Rekha and Sharma 2009, Kanatani et al., 2006). During the 30 min incubation of the cells at 37˚C in 5 % CO2 pressure, the nanoplexes were prepared with FITC tagged GCSM polymer with pGL3 plasmid in the ratio 1:15. This is then followed by the removal of inhibitors containing media and cells were rinsed with fresh media. Nanoplexes tagged with FITC were added to the cells before adding the fresh media with serum for 4 h incubation. It is known, that polymeric nanoparticle with attached sugar residues is engulfed by cell through asialoglycoprotein receptor that is present in liver cells. Hence, two ligands asialofeutin and glucose were added to separate wells in 1µg/mL concentration, to study the inhibition caused by these receptor specific ligands. To the pre-treated cells, the prepared FITC labeled nanoplex ratio was added and incubated with fresh media with serum. Nucleus staining was done with Hoechst 33342. After 4 h incubation, the four inhibitor samples were subjected to twice PBS (pH 7.4) wash and the uptake mechanism inside the cell was observed using the 40 X objective of fluorescence microscope (Leica DMI 3000B, Germany).

3.2.20. In vitro transfection - Luciferace gene expression

The harvested HepG2 cells after trypsinisation were plated onto a 4-well tissue culture plate with a density of 1×10^5 cells/well in DMEM containing 10%

FBS, incubating for 24 h at 37˚C in 5% CO_2. Transfection was carried out to investigate the gene transfer efficiency of the GCSM nanoplexes. The nanoplexes were prepared, by mixing plasmid pGL3 with GCSM polymer solution in ratios of 1:15 and 1:16 and diluted rest with DMEM medium containing 10 % FBS serum. These ratios showed consistent optimum size and zeta potential, and hence was selected for transfection. Nanoplexes were added to the cells and incubated at 37˚C for 4 h in 5 % CO_2. Following this the nanoplexes were removed, cells further incubated with fresh medium containing serum and kept for 24 h incubation. As PEI was reported (Neu et al., 2005) to show high transfection ability, plasmid pGL3 was coupled with PEI to be used as positive control. Triplicates were carried out for the ratios and control. The medium was then removed, followed by rinsing cells with phosphate buffered saline (pH 7.4) and lysed with 100 µL of lysis reagent (Promega). The lysed cells were treated with luciferase assay substrate and cell extract was measured for luciferase activity expression. The relative luminance expression (RLU) was determined using the luminometer (Chamaleon, Hidex). The lysate was subjected to Micro BCA Protein Assay Reagent Kit (Pierce) for elucidating the total protein content. Gene expression efficiency was presented as percentage of observed luminance expression count to the cellular protein (mg) obtained for each sample.

3.2.21 In vitro transfection- p53 gene expression

Glioma C6 cells derived from murine fibroblasts were harvested and seeded at a density of $1x10^5$ cells/well in a 4-well plate. The cells were cultured in MEM: DMEM/F12 Ham medium (1:1) supplemented with 10 % serum and grown for 24 h to attain 80 % confluency. The medium was replaced the next day with fresh medium

containing the desired amount of GCSM nanoplexes consisting of the plasmid p53 which express the gene for apoptosis in cells. After 4 h incubation the old medium was discarded and the cells were allowed to grow in fresh medium for additional 24 h incubation. The cells were followed with a phosphate buffered saline wash pH 7.4 and treated with 200 μL of a solution mixture of 2 μM calcein AM and 4 μM ethidium homodimer (EthD-1) reagent of the Live Dead assay kit as per the manufacturer's protocol. After 25 min of incubation, cells were again washed with PBS twice and visualised in the fluorescence microscope Leica DMI3000 B (Leica, Germany). The principle behind the assay is that the intracellular esterase activity of live cells would convert the cell-permeant calcein AM to fluorescent calcein which will provide green fluorescence to live cells. On the other hand, EthD-1 which is generally excluded by the intact plasma membrane of viable cells, is able to enter cells with damaged membranes and bind to nucleic acids, thereby producing a bright red fluorescence in dead cells

3.3 Synthesis and Characterisation of Protamine PEG diamine chitosan

3.3.1 Materials

Protamine chloride, N, N$^{\llcorner}$-disuccinimidyl carbonate (DSC), 4-dimethylaminopyridine (DMAP), glucosamine and PEG diamine 3000 Da were purchased from Fluka. N, Ndimethylformamide (DMF) and acetone was purchased from Merck, India. Branched PEI (25 kDa), 1-ethyl-3-(3-dimethylaminopropyl) carbodiimide hydrochloride (EDC), N-hydroxysuccinimide (NHS), 3-(4, 5-dimethylthiazol-2-yl)-2, 5-diphenyl tetrazolium bromide (MTT), Mnimum essential

medium Eagle (MEM), Dulbecco's modified Eagle's medium (DMEM), F12 Ham, chlorpromazine, filipin, amiloride and dynasore monohydrate from Sigma-Aldrich, USA. Other chemicals were Fetal bovine serum (FBS) was from GIBCO (USA), YOYO iodide, Hoechst 33342 and Live Dead assay kit from Invitrogen, Calf thymus DNA (Worthington Biochemical Corp.) and p53 Dominant-Negative Vector (Clonetech, USA). All other chemicals were of AR grade. The C6 glioma cells lines were supplied by the National Centre for Cell Science (NCCS), Pune, India. Human blood was collected from the unmedicated healthy volunteers. Deionised Milli Q water (DI) with a resistivity of 18.Ωcm^{-1} was used throughout the experiments.

3.3.2 Preparation of Chitosan Diaminopolyethylene glycol with protamine grafting

The derivative was synthesised in two step procedure. Firstly, the hydroxyl group of depolymerised chitosan of 120 kDa was activated for 4 hour in the presence of 6 mM DSC and 6mM DMAP (Kim et al., 2008). Activated chitosan of 200 mg was reacted with 100 mg PEG diamine and kept for overnight magnetic stirring. The amount of chitosan and PEG diamine was taken in 2:1 mole ratio. After 16 h reaction, acetone wash was given to the reacting solution and a soft gel like precipitate was resulted. Dialysis was performed for 2 days with the product to remove any unreacted chemicals. This was followed by freeze drying, lyophilisation and storage at 4˚C. In the second step, equal amount of chitosan PEG diamine conjugate and protamine was taken for the reaction. Initially protamine was activated with EDC (0.1M) and NHS (0.1M) for one hour while chitosan PEG diamine conjugate was allowed to stir for some time to get solubilised (Alex et al., 2011). Activated protamine was added to chitosan PEG diamine conjugate and kept for

overnight stirring. The precipitate was revived with acetone rinse and the product was then subjected to dialysis against distilled water and lyophilised. The derivative appeared to be white thin film, labelled as CDP and stored in cold condition.

3.3.3 Colorimetric determination of primary amine groups

The presence of free amine groups in chitosan has a great influence in providing cationic potential to the polymer which helps the polycation to interact with anionic molecules. The amount of amine groups that exist in the parent compound and in the modified was investigated by following the protocol described elsewhere (Snyder and Sobocinski, 1975). The polymers diamine PEGylated chitosan (CD) and protamine grafted diamine PEGylated chitosan (CDP) were suspended in MilliQ water while unmodified chitosan was suspended in 1N HCl. All samples were prepared in 1 mg/mL concentration. Chitosan has glucosamine as one of its substituent and hence was regarded as the reference to be compared. Equal volumes of the polymer samples were treated with 200 µL 0.1 % (TNBS) 2, 4, 6-trinitrobenzenesulfonic acid and 4 % sodium bicarbonate. Incubation was carried at 37˚C for 2 h after which the reaction was halted by 200 µL of 2 N HCl. The absorbance recorded at 344 nm with the UV-Vis spectroscope (UV Varian Cary, USA). Triplicates were done and statistical analysis was performed with respective standard deviations being provided. The result calculations were determined as follows:

Percentage of free amine group = $\left(Ab_S \div Ab_R\right) \times 100$

Where Ab_S represent absorbance of sample; Ab_R represent absorbance of reference.

3.3.4 Analysis by Fourier transform infrared spectroscopy

The dried sample of chitosan, PEG diamine, protamine and CDP were powdered with KBr pellets for Fourier transform infrared (FTIR) analysis. The measurement was performed over 4000- 400 cm^{-1} on a Fourier transform infrared spectrometer (Shimadzu spectrophotometer).

3.3.5 Analysis by Proton Nuclear Magnetic Resonance spectroscopy

A proton nuclear magnetic resonanace (^1H NMR) spectrum of of protamine conjugated diamine PEGylated chitosan (CDP) was measured in D_2O/0.5 (w/w) DCl using a 500MHz spectrometer (Bruker Avance DPX 300). The analysis was performed at 22˚C and the number of transients during the measurements was set as 16. The relaxation time of the instrument during measurements was 3.17s. All other parameters were in the default settings of the instrument as per the specifications of Bruker Avance DPX 300.

3.3.6 Analysis by Differential Scanning Calorimeter

Differential scanning calorimeter (DSC) was implemented to analyse the thermal behaviour of protamine conjugated diamine PEGylated chitosan (CDP) in comparison to the parent compound unmodified depolymerised chitosan. Approximately 5 mg of the samples were encapsulated in aluminium pans, heating at a rate of 10˚C/min from 20 to 250˚C and the measurements were conducted using a Waters differential scanning calorimeter with a mass flow control calibrated using indium as the standard.

3.3.7 Buffering capacity of CDP

The ability of the polymer to provide protonation over a pH profile range from 10-3 was determined with acid base titration analysis. In brief, CDP polymer

about 6 mg was dissolved in 30 ml MilliQ to obtain a final concentration of 0.2 mg/mL. Firstly, the pH of the polymer solution was set to pH 10 using 1N NaOH and titrated against 0.1 N HCl to record the pH decrement. The pH of the solution was measured after each 50 µL addition of 0.1 N HCl using a pH meter (Benns et al., 2002). Unmodified chitosan and PEI was also experimented like wise to compare with the chitosan derivative CDP.

3.3.8 Amplification and Purification of plasmid DNA and calf thymus DNA

Bacterial E coli cells were transformed with p53 plasmid DNA and colonies were picked up for extraction of the plasmid. Isolation and purification of the plasmid DNA was carried out with the protocol manual of Qiagen QIA filter plasmid Mega kit. The purity of the plasmid was assessed by running a 1% agarose gel electrophoresis. Calf thymus DNA was suspended in 0.1 M sodium acetate buffer corresponding to 1 mg/mL concentration and dialyzed in the same molar concentration of sodium acetate buffer before storing in refrigerated condition. Calf thymus DNA is adopted for nanoparticle preparation that is used for DLS measurement and plasmid DNA for the other discussed experiments. The final purity is determined to be 1.83 (OD 260/280) and 2.08 (OD 260/235) by UV-Vis spectroscope (UV Varian Cary, USA).

3.3.9 Preparation of CDP nanoparticles

Cationic polymers when mixed with the anionic nucleic acid in suspension tend to bind and form compact constructs known as nanoparticles or polyplexes. CDP solution was prepared in 1mg/mL MilliQ water, filtered through a 0.22 µm filter and kept sterile. The complexes also known as nanoplexes or polyplexes are formed by varying the ratios with the derivative CDP in appropriate concentrations

with respect to the constant amount of DNA. Calf thymus DNA was also prepared in the same concentration 1 mg/mL. The solution consisting of both the polymer and CDP is vortexed and incubated for 20 min before using it for the characterisation experiments unless stated otherwise. Both plasmid and calf thymus DNA followed the same procedure for polyplex formation.

3.3.10 Determination of size and zeta potential

Surface charge and the size of nanoparticles are crucial parameters that need to be determined for a gene delivery vector. Calf thymus DNA (1 mg/mL) and CDP (1mg/mL) were used for nanoparticle formulation and suspended in saline normal saline (NS, 0.9 % sterile sodium chloride). The nanoparticles ratios are prepared as explained before in the corresponding concentrations of CDP/DNA (w/w). They were subjected to dynamic light scattering measurement using a Zetasizer NanoZS (Malvern Instruments Ltd, UK). The surface charge was also measured and is expressed as the zeta potential which is estimated with the Zetasizer NanoZS (Malvern Instruments Ltd, UK). Both size and surface charge were evaluated at a temperature of 25˚C. Triplicates were also simultaneously carried out. Statistical analysis was performed and provided with respective standard deviations.

3.3.11 Transmission Electron microscopy analysis

The optimal mixing of CDP polymer and plasmid p53 DNA at w/w ratio 7 yielded nanoparticles that were mounted on a copper grid, removing excess liquid with a piece of filter paper and air dried at room conditions. Transmission electron microscopy (TEM) analysis was performed in a JEOL JEM-1230 (Japan) electron microscope at accelerating voltage of 200 kV and images were captured.

3.3.12 DNA Gel retardation

The polymer should have a strong binding affinity to DNA so as to maintain a cationic density around the nanoparticle which would enable the CDP derivative to hold fast onto the tightly twined DNA. For this, the derivative CDP was combined with plasmid DNA p53 to avail the polyplexes in the ratios 1 till 10 and vortexed for 15 sec with 20 min incubation at room temperature. Agarose gel electrophoresis was performed with nanoparticles loaded on to 1 % agarose gel run at 100 V for 60 min in 1X TBE buffer (89 mM Tris–HCl pH 8.3, 89 mM borate and 2 mM EDTA). Gel retardation of the nanoparticles were visualised by the aid of ethidium bromide staining (2 μL of 10 mg/mL) and image captured in a Image Analyser (LAS 4000, Fuji).

3.3.13 DNase I protection and release assay

The same nanoparticle ratios consisting of pDNA from 1-10 were treated with DNase solution consisting of 569 U/mL of DNase in 0.1M sodium acetate and 5mM magnesium sulphate at pH 7.4. Incubation was carried out for 15 min at room temperature and the activity of the enzyme was stopped with termination buffer containing 0.5 M EDTA, 2 M NaOH and 0.5 M NaCl. Electrophoresis was carried out in BioRad system with the samples run in 1X TBE buffer and gel stained with EtBr. The stability was probed further by subjecting the nanoparticles to heparin treatment 5 μL at a concentration of 1000 U/mL for 30 min. Heparin a negatively charged polyanion capable causing competitive binding with the charged groups of CDP derivative thus displacing the DNA from the compacted complexes (Srinivasachari et al 2007). The displaced DNA was viewed in 1 % agarose gel after its run in the electrophoresis system.

3.3.14 Interaction of CDP polymer with Red blood cells (RBC)

The effect of polymer CDP on the integrity of red blood cells were evaluated by hemolysis and aggregation study. Hemolysis was carried out with the blood provided by non medicated volunteers and was suspended in the ratio 9:1 (blood: anticoagulant) with 3.8 % sodium citrate. The blood components were segregated following the protocol as discussed (Joshy & Sharma, 2012). The polymer CDP was prepared in normal saline (NS, 0.9 % sterile sodium chloride) in 1mg/mL concentration. Equal volumes of saline diluted RBC (8:1) were incubated with varying concentrations of 25 µg, 50 µg, 75 µg and 100 µg of CDP polymer. The controls used for comparison were normal saline (NS, 0.9 % sterile sodium chloride) that did not give any cell lysis and Triton X-100 (1 %) that gave 100 % lysis. Any disruption in the cell would release haemoglobin and the absorbance corresponding to it was monitored at 541 nm with a UV-visible spectrophotometer (Varian). Hemolysis was calculated with the following equation.

$$\text{Percentage hemolysis} = \left(\frac{Ab_T - Ab_N}{Ab_X - Ab_N} \right) \times 100$$

Where Ab_T represent absorbance of test, Ab_N represent absorbance of normal saline, Ab_X represent absorbance of Triton X-100.

Further evaluation was performed by erythrocyte aggregation study in which separate tubes of 100 µL of 9: 1 saline diluted blood sample was incubated for 25 min with 100 µg of CDP polymer (1 mg/mL), normal saline (NS, 0.9 % sterile sodium chloride) and PEI 25 kDa (1 mg/mL) as the controls. Samples were mounted on slides and images were procured from phase contrast microscope (Leica DMIRB, Germany).

3.3.15 Electrophoretic analysis of CDP polymer with plasma protein interactions

Interaction of CDP derivative with blood serum proteins is an essential criterion that needs to be assessed. The plasma protein interactions with CDP polymer was identified using native gel electrophoresis. Plasma was diluted with saline and incubated with two concentrations of 50 and 100 µg of CDP for 1 h at room temperature. After a brief spinning, 20 µL of samples were loaded on 7 % resolving and 4 % stacking gel at 90 V for 90 min using Mini-Protean II electrophoresis system (Bio-Rad, CA, United States). Gel picture was taken of the Coomassie stained gel using an image analyser (LAS 4000, Fuji). The presence of serum proteins was compared with the control which consisted of plasma incubated with normal saline (0.9 % sterile sodium chloride).

3.3.16 Cell Culture

The impact of chitosan derived nanoparticles in the *in vitro* system is an important assessment to be carried out. The investigation was carried out in murine derived glioma cells C6, seeded in culture flasks with MEM: DMEM/F12 Ham medium in 1:1 combination along with 10 % FBS. Cells were grown for 24 h at 37˚C in 5 % CO_2 and 95 % humidity to achieve around 80 % cell confluency. Cells were harvested from the flasks, transferred to culture plates with a density of 1×10^5 cells/well and grown for 24 h under the same incubation conditions before initiating each cell experiment. For all cell culture experiments, the polymer CDP was prepared in 1 mg/mL in F12 Ham medium before DNA complexation. Reports from our lab (Morris and Sharma, 2010; Rekha and Sharma, 2009) were used as reference for performing the cell culture experiments.

3.3.17 Cytotoxicity assay

At first the toxic effect of the chitosan derivative CDP on the cell lines was assessed with the help of MTT assay. Glioma C6 cells were seeded in a density 1×10^5 cells/well into 24-well plate and allowed to be confluent for 24 h. The polymer CDP prepared in 1mg/mL in MEM: DMEM/F12 Ham medium (1:1) was added to the cells in triplicates in the desired concentration of 25 µg, 50 µg, 75 µg, 100 µg and incubated at 37°C for 24 h along with the control which is untreated cells with medium alone. The samples were then discarded and MTT reagent (0.2 mg/mL) was added to each well for 3 h incubation. The MTT formazan crystals resulted was dissolved in DMSO for 5 min after the removal of the reagent. The absorbance was read at 540 nm using the automated microplate reader (Tecan Microplate Reader, Switzerland) and the readings were used for calculating the mean % cell viability with respect to the untreated cells with medium alone. For comparative analysis, the cells were treated separately with 50 µL of other controls such as Triton X-100 (1 %), PEI 25 kDa (1 mg/mL) and unmodified chitosan (1 mg/mL, 1 N HCl).

$$\text{Percentage cell viability \%} = \left(\frac{Ab_S}{Ab_C}\right)X100$$

Where Ab_S represent absorbance of sample, Ab_C represent absorbance of medium control.

3.3.18 Cellular uptake of CDP nanoparticles

Glioma C6 cells were harvested from the stock culture and seeded at a density of $1x10^5$ cells/well into 4-well plates and incubated for a day. The plasmid p53 was tagged with the YOYO iodide dye that imparts the green fluorescence. The plasmid DNA was incubated for 30 min with YOYO iodide, with 2.5 µL of 10 µM

YOYO labelled for 1.0 µg DNA/well. Nanoparticle formulation was done with 2.5 µg of plasmid DNA p53 mixed with the corresponding polymer amount of CDP in the ratio 1:7 to obtain the nanoparticles. The media in the four-well plates were replaced with fresh medium containing the nanoparticles and kept for 4 h incubation. Nuclear staining is provided with Hoechst 33342 (15 µL of 1mM solution) for half an hour just before completing the incubation period. Cells were rinsed with PBS (pH 7.4) twice and fixed in 1% formaldehyde. The cellular internalization of the nanoparticles was observed and photographed using fluorescence microscope (Leica DM IRB, Germany). Similar cell treatment was performed to implement quantification of cell uptake by flow cytometry (Becton Dickinson FACS Aria, USA). For each measurement ten thousand cells were counted and the percentage of positive cells was calculated by setting the background population as 98 % negative when analyzing untreated control cells (Kanatani et al., 2006).

3.3.19 Cell uptake studies in the presence of endocytic inhibitors

Initial cell seeding into 4-well plates was repeated for inhibition study that would identify the pathways that regulate the translocation of nanoparticles across the cell. Each well was treated with individual inhibitors in the corresponding amounts of chlorpromazine (1 µg/mL), dynasore (8-200 nM), filipin (2.5 µg/mL), amiloride (2 µg/mL) and the substrate protamine (1 µg/mL) for 30 min which was later discarded, following as described in Alex et al., 2011. Cells were then treated with polyplexes prepared with YOYO tagged plasmid p53 and CDP in the particular 1:7 ratio and kept for 4 h incubation. Hoeschst staining was done for the nucleus followed by PBS wash and fixation of cells in 1 % formaldehyde. Images were collected with fluorescence microscope (Leica DM IRB, Germany).

3.3.20 In vitro transfection- p53 gene expression

C6 cells were grown for 24 h and incubated with the desired amount of CDP nanoplexes consisting of the plasmid p53 which express the apoptosis condition for the cells. After 4 h incubation the medium was exchanged for fresh medium and kept for further 24 h incubation. The cells were washed with PBS twice and the Live Dead assay was performed using the Live and Dead kit. The reagent, constituted of 2 μM calcein AM and 4 μM ethidium homodimer (EthD-1) that would specifically stain live and dead cells respectively, was added to the cells and left for staining for approximately 25 min at room temperature. Fluorescent microscope (Leica DMI3000 B, Germany) observation depicted the state of the cells after the assay. The principle behind the assay is that the intracellular esterase activity of live cells would convert the cell-permeant calcein AM to fluorescent calcein which will provide green fluorescence to live cells. On the other hand, EthD-1 which is in general excluded by the intact plasma membrane of viable cells, is able to enter cells with damaged membranes and bind to nucleic acids, thereby producing a bright red fluorescence in dead cells.

3.4 Synthesis and Characterisation of Chitosan Ornithine conjugate

3.4.1 Materials

L-Ornithine dihydrochloride, 1-ethyl-3-(3-dimethylaminopropyl) carbodiimide hydrochloride (EDC), 3-(4, 5-dimethylthiazol-2-yl)-2, 5-diphenyl tetrazolium bromide (MTT), Mnimum essential medium Eagle (MEM), Dulbecco's modified Eagle's medium (DMEM), F12 Ham, Polyethyleneimine (PEI 25 kDa), Chlorpromazine, amiloride, filipin and dynasore monohydrate were procured from Sigma-Aldrich Chemicals Co., USA. Glucosamine was purchased from Fluka, Fetal

bovine serum (FBS) was from GIBCO (USA). Others were YOYO iodide, Hoechst 33342 and Live Dead assay (Invitrogen), Calf thymus DNA (Worthington Biochemical Corp.) and p53 Dominant-Negative Vector (Clonetech, USA). The C6 glioma cells lines were supplied by the National Centre for Cell Science (NCCS), Pune, India. Human blood was collected from the unmedicated healthy volunteers. All other chemicals were of AR grade.

3.4.2 Preparation of chitosan ornithine conjugate (CON)

Dried depolymerised intermediate molecular weight range chitosan was coupled with ornithine in the presence of coupling agent EDC at room temperature. Briefly, 200 mg of depolymerised chitosan (1 %) was dissolved in 0.25 N HCl and stirred for 1 h. Ornithine was added to chitosan in 2:1 equivalence and coupling was carried out in the presence of EDC, which gets activated at pH between 4.5 and 6.5. The pH of the reaction was maintained in this range and the precipitate resulted was dialysed against distilled water. The conjugate was then lyophilised and a white derivative (labelled as CON) was obtained with thin, mesh-like texture. For further experiments, the polymer was prepared in concentration of 1 mg/mL MilliQ H_2O, unless stated otherwise.

3.4.3 Colorimetric determination of primary amine groups

The free amine groups that reside in chitosan convey the positive charge in the polymer and on each chemical modification, variation in the amount of amine groups has an impact in the cationic potential of the derivative. A biochemical assay described in (Snyder and Sobocinski, 1975) which uses the TNBS chemical to assess the free amine groups is adopted for the study. Glucosamine is considered for comparison as it is present in the chemical structure of chitosan. All samples are

prepared in 1 mg/mL concentration and except for unmodified chitosan suspended in aqueous 1 N HCl, both glucoamine and chitosan ornithine is dissolved in MilliQ water. In brief, 200 µL 0.1 % (TNBS) 2, 4, 6-trinitrobenzenesulfonic acid and 4 % sodium bicarbonate was added to equal volumes of the polymer samples and made up to one ml. The reaction was continued for 2 h incubation at at 37˚C. Triplicates were carried out and using 200 µL of 2 N HCl, the reaction was stopped. The absorbance of the reagent was read at 344 nm with the aid of UV-Vis spectroscope (UV Varian Cary, USA). The percentage of amine groups was determined from the readings acquired for the test samples in relative to the reading of the reference which is assumed to have 100 % amine groups. The percentage of free amine groups is calculated as

$$= \left(Ab_S \div Ab_R\right) \times 100$$

Where Ab_S represent absorbance of sample; Ab_R represent absorbance of reference

3.4.4 Analysis by Fourier transform infrared spectroscopy

The presence of conjugated groups in the modified compound CON was evaluated by Fourier transform infrared **(**FTIR) technique. Samples were powdered with KBr and recorded on a Fourier transform infrared spectrometer (Shimadzu spectrophotometer). Parent compounds depolymerised chitosan and ornithine were also recorded for comparison.

3.4.5 Analysis by Proton Nuclear Magnetic Resonance spectroscopy

Further characterisation of CON polymer was performed with Proton nuclear magnetic resonanace (^{1}H NMR) spectrophotometer (Bruker Advance DPX 300). The sample was dissolved in D_2O/0.5 (w/w) DCl and measured at 22º C with rest of the parameters set as default settings in the instrument. The number of transients during

the measurements was set as 16 and relaxation time of the instrument during measurements was 3.17s.

3.4.6 Analysis by Differential Scanning Calorimeter

Differential scanning calorimeter (DSC) was implemented to analyse the thermal behaviour of chitosan ornithine (CON) in comparison to the unmodified depolymerised parent compound chitosan. Approximately 5mg of the samples were encapsulated in aluminium pans, heating at a rate of 10˚C/min from 20 to 250˚C and the measurements were conducted using the Waters differential scanning calorimeter with a mass flow control calibrated using indium as the standard.

3.4.7 Buffering capacity of CON

Acid base titration was attempted to determine the extent of buffering capacity of the polymer. Protonation of the polymer is a prerequisite to avoid delivery to the lysosome via late endosomal trafficking. Six milligram of CON was dissolved in 30 ml MilliQ to get a final concentration of 0.2 mg/mL. At the initial stage, pH of the polymer solution was set to pH 10 with 1N sodium hydroxide and was then titrated against 0.1 N hydrogen chloride to reach till pH 3 by adding 50 µL of 0.1 N HCl gradually to the solution (Benns et al., 2002). Similarly unmodified 120 kDa chitosan (0.2 mg/mL) and PEI 25 kDa (0.2 mg/mL) prepared in the same concentration were also titrated individually to compare the buffering ability of CON solution. The pH changes were recorded and plotted graphically. Triplicates were also performed and statistical analysis was performed and respective standard deviations were provided.

3.4.8 Amplification and Purification of plasmid DNA and calf thymus DNA

Dynamic light scattering used calf thymus DNA for nanoparticle formulation with CON polymer as large number of varying ratios is performed for optimisation. The calf thymus DNA was prepared at 1mg/mL concentration and dialyzed in 0.1 M sodium acetate buffer prior to nanoparticle formulation for determination of size and zeta potential. Plasmid DNA p53 and pGL3 were used for other experiments and they were isolated separately from Ecoli cells that were transformed with the respective plasmid. Using the Qiagen QIA filter plasmid Mega kit, the isolation and purification of the plasmid DNA was implemented and plasmid integrity was determined by both agarose gel electrophoresis and UV-Vis spectroscope (UV Varian Cary, USA). The final purity is determined to be 1.83 (OD 260/280) and 2.08 (OD 260/235).

3.4.9 Preparation of CON nanoparticles

The dried CON product obtained was soluble in MilliQ water. CON solution was prepared in a concentration of 1 mg/mL, filtered through a 0.22 μm filter and kept sterile. The calf thymus DNA (ctDNA) was also prepared in the same concentration. Nanoparticles were prepared in normal saline (NS, 0.9 % sterile sodium chloride) by combining ctDNA, which is kept constant, with varying concentrations of polymer solution corresponding to the concentration of DNA: polymer ratio (w/w). The polymer condensed rapidly with negatively charged DNA to form nanoparticles. At room temperature, each nanoparticle was vortexed for 15 s and then incubated for 20 min to obtain the desired complexes. Both plasmid and calf thymus DNA followed the same procedure for nanoplex formation.

3.4.10 Determination of particle size and zeta potential

Size determination and surface charge measurements were carried out using the Zetasizer Nano ZS (Malvern Instruments Ltd., UK) at a temperature of 25˚C. The complexes were prepared in increasing DNA/polymer ratio (w/w), having ctDNA at a constant concentration in 1 mg/mL saline ((NS, 0.9 % sterile sodium chloride). The nanoparticles are prepared in saline and subjected to the nanoparticle size determination. The surface charge of the nanoparticles correspond to zeta potential that represents its electrophoretic mobility and is determined by the Zetasizer Nano ZS (Malvern Instruments Ltd., UK) at a temperature of 25˚C. Triplicates were also simultaneously carried out. Statistical analysis was performed and provided with respective standard deviations.

3.4.11 Transmission Electron microscopy analysis

Transmission electron microscopy (TEM) imaging was carried out to visualise the nanoparticles and the measurements were performed in a JEOL JEM-1230 (Japan) electron microscope at accelerating voltage of 200 kV. Samples were mounted as a solution of nanoparticles generated by the CON polymer when complexed with DNA at a DNA/polymer ratio (w/w) of 3, on a copper grid coated by an amorphous carbon film and air dried at at room temperature.

3.4.12 Atomic Force microscopy analysis

The effect of interaction of chitosan ornithine (CON) with plasmid DNA on size and shape is examined under the Atomic force microscopy (AFM) (WITEC Confocal Raman Microscope System with Atomic Force Microscope Extension, Germany) that enabled a close visualization of the CON nanoplex. The polymer/ plasmid DNA was combined in the ratio (w/w) of 1:3 and was deposited on mica

substrates. The dried sample stored in a desiccator at room temperature was operated in the contact mode of the instrument with cantilevers that operated between 0.6-1 Hz at a resonant frequency approximately 320 Hz.

3.4.13 DNA Gel retardation

The effect of nanoparticle condensation with DNA was assessed by agarose gel electrophoresis. Agarose gel was prepared in 1X TBE buffer (89 mM Tris–HCl pH 8.3, 89 mM borate and 2 mM EDTA), staining with 2 µL of 10 mg/mL ethidium bromide. Increasing ratios of CON complexes were loaded onto 1 % agarose gel and run in the same buffer in a Bio-Rad Electrophoresis system (Bio-Rad laboratories, CA, USA) at 100 V for 60 min. The DNA bands were then visualized and photographed using image analyser (LAS 4000, Fuji). Sample ratios 1, 2, 3, 4, 5, 6, 7, 8 and 9 were considered for loading into the wells.

3.4.14 DNase I protection and release assay

The same nanoparticle ratios from 1-10 were treated with DNase solution consisting of 569 U/mL of DNase in 0.1 M sodium acetate and 5 mM magnesium sulphate at pH 7.4. Incubation was carried out for 15 min at room temperature and the activity of the enzyme was stopped with termination buffer containing 0.5 M EDTA, 2 M NaOH and 0.5 M NaCl. Electrophoresis was carried out in BioRad system with the samples run in 1X TBE buffer and gel stained with ethidium bromide. The stability was probed further by subjecting the nanoparticles to heparin treatment at a concentration of 1000 U/mL for 30 min. Heparin a negatively charged polyanion is caused competitive binding with the charged groups of CDP derivative thus displacing the DNA from the compacted complexes. The displaced DNA was viewed in 1 % agarose gel after its run in the electrophoresis system.

3.4.15 Interaction of CON with Red blood cells (RBC)

A blood compatibility study of the chitosan ornthine conjugate was performed using whole blood from healthy donors. In the presence of sodium citrate 3.8 %, 10mL blood was collected (ratio of blood to anticoagulant taken was 9:1), followed by isolation of blood components carried out as described elsewhere (Joshy & Sharma, 2012). The polymer CON was prepared in normal saline (NS, 0.9 % sterile sodium chloride) in 1 mg/mL concentration. A hemolysis study with saline diluted RBC (8:1) was performed using the derivative at four concentrations 25 µg, 50 µg, 75 µg and 100 µg to observe the effect on RBC cells. The absorbance of released haemoglobin was monitored at 541 nm with a UV-visible spectrophotometer (Varian). Here normal saline (NS, 0.9 % sterile sodium chloride) was used as negative control (0 % lysis) and Triton X-100 (1 %) as positive control (100 % lysis). Hemolysis was calculated with the following equation:

$$\text{Percentage hemolysis} = \left(\frac{Ab_T - Ab_N}{Ab_X - Ab_N} \right) \times 100$$

Where Ab_T represent absorbance of test, Ab_N represent absorbance of normal saline, Ab_X represent absorbance of Triton X-100.

In addition to this, erythrocyte aggregation study was also performed by treating 100 µL of saline diluted RBC (9:1) with 100 µg of CON polymer (1 mg/mL), normal saline (NS, 0.9 % sterile sodium chloride) and PEI 25 kDa (1 mg/mL) as the controls. Samples were mounted on slides and images were procured from phase contrast microscope (Leica DMIRB, Germany).

3.4.16 Electrophoretic analysis of CON polymer with plasma protein interactions

Native PAGE gel electrophoresis was adopted to identify plasma protein interactions with chitosan-ornithine (CON) polymer. Two sample concentrations were incubated with human plasma (diluted with saline) for 1 h at 37°C. The samples were briefly centrifuged for 10 min and 20 μL of the supernatant was loaded on 7 % resolving and 4 % stacking gel at 90 V for 90 min using Mini-Protean II electrophoresis system (Bio-Rad, CA, United States). The gel was stained with Coomassie blue and documented using an image analyser (LAS 4000, Fuji). Plasma incubated with normal saline (0.9 % sodium chloride NaCl) was considered as the control.

3.4.17 Cell Culture

The influence of CON nanoparticle on biological systems was evaluated by performing cell culture studies. The study was attempted in the murine derived glioma C6 cell lines. The cells were harvested in DMEM medium / F12 Ham: MEM (1:1) medium supplemented with 10 % FBS at 37°C in 5 % CO_2 and 95 % humidity and incubated for 24 h to attain a cell growth of 80 % confluency. The cells were trypsinised and transferred to multi well tissue culture plates in the density of 1×10^5 cells per well prior 24 h for experiments that followed, unless mentioned othewise. For all cell culture experiments, the polymer CON was prepared in 1 mg/mL in F12 Ham medium before DNA complexation.

3.4.18 Cytotoxicity assay

Chitosan ornithine polymer should be non toxic to cells in *in vitro* condition in order to be used for further cell culture studies. Cell viability was analysed using

the reagent 3-(4, 5-dimethylthialzol-2-yl)-2.5- diphenyl tetrazolium bromide (MTT) prepared in deionised water. The C6 cells were trypsinised and seeded into multiwell tissue culture plate. After 24 h incubation, CON polymer corresponding to 1 mg/mL was added to cells in triplicates at four different concentrations of 25 µg, 50 µg, 75 µg and 100 µg. After 24 h incubation, polymer CON with the media was removed and MTT reagent (0.2 mg/mL) was added to each well. The reagent was discarded after 3 h incubation and dimethyl sulfoxide (DMSO) was added for dissolution of MTT formazan crystals. This was measured in an automated microplate reader at 540nm (Tecan Microplate Reader, Switzerland) and cells containing medium alone without polymer sample was considered as control. Cell viability was expressed as the mean percentage of sample absorbance relative to untreated cells. For comparative analysis, the cells were treated separately with 50 µL of other controls such as Triton X-100 (1 %), PEI 25 kDa (1 mg/mL) and unmodified chitosan (1 mg/mL, 1 N HCl).

$$\text{Percentage cell viability \%} = \left(\frac{Ab_S}{Ab_C} \right) X\ 100$$

Where Ab_S represent absorbance of sample, Ab_C represent absorbance of medium control.

3.4.19 Cellular uptake of CON nanoparticles

C6 cells were subcultured from the stock culture and seeded into four well plates for 24 h incubation. Plasmid p53 was rendered fluorescent by tagging it with a high affinity intercalating fluorescent labelling dye, YOYO iodide by incubation for 1 h. The plasmid DNA was incubated for 30 min with YOYO iodide, with 2.5 µL of10 µM YOYO labeled for 1.0 µg DNA/well. Nanoparticles were prepared with 2.5

μg YOYO tagged plasmid DNA and corresponding CON concentration at ratio of 1:3. The cells were incubated with the fluorescent labelled nanoparticles for 4 h at 37˚C in DMEM/Ham F12: MEM (1:1) medium with 10 % FBS. Half an hour before the end of incubation time, 15 μL of Hoechst 33342 dye (1 mM) was applied to enable nuclear staining. Later cells were washed with phosphate buffered saline (pH 7.4) and fixed in 1% formaldehyde. The localisation of plasmid was visualized and photographed using a fluorescent microscope (Leica DM IRB, Germany) and confocal laser scanning microscope (Zeiss LSM 510 Meta, Germany). Z-stacking image analysis was performed using LSM 510 software image analyser (version 5). Similar cell treatment was performed to implement quantification of cell uptake by flow cytometry (Becton Dickinson FACS Aria, USA). For each measurement ten thousand cells were counted and the percentage of positive cells was calculated by setting the background population as 98 % negative when analyzing untreated control cells (Kanatani et al., 2006).

3.4.20 Cell uptake studies in the presence of endocytic inhibitors

C6 cells were seeded with a density of $1x10^5$ cells one day prior to the uptake experiment. The inhibitors used were specific to block each of the known major endocytic pathways. Mainly four inhibitors were used, chlorpromazine (1 μg/mL) specific for inhibiting Rho GTPase that could block the clathrin mediated delivery, filipin (2.5 μg/mL), the inhibitor for caveolae mediated endocytosis, macropinocytosis pathway inhibitor amiloride (2 μg/mL) and dynasore (8-200 nM) that inhibits dynamin function (Alex et al., 2011). To assess receptor mediated endocytic pathway, ornithine (1 μg/mL) was also tested against the cells. The cells were incubated for thirty minutes with the optimised concentrations of the different

inhibitors suspended in 1 mL of serum free medium. Afterwards the medium was discarded and cells were rinsed with either PBS pH 7.4 or serum free medium alone to remove any trace of inhibitors. Fresh serum free medium containing chitosan ornithine nanoparticles in the ratio 1:3 were added to cells for further 4 h incubation. Hoechst staining was performed for the nucleus, with cells later washed with PBS and fixed with 1 % formaldehyde and viewed with a 40 X objective of fluorescent microscope. Detailed examination of intracellular localisation of CON nanoparticle within the cells inhibited by the endocytosis inhibitors was confirmed by confocal laser scanning microscopy. Cells were harvested and treated with the same inhibitors followed by removal and addition of CON nanoparticles ratio prepared in the same manner as mentioned before. Cells were incubated for 4 h without nuclear staining followed by PBS wash and fixation. Images were visualized in the confocal laser scanning microscope (Zeiss LSM 510 Meta, Germany) and z-stacking image analysis was performed using LSM 510 software image analyser (version 5).

3.4.21 In vitro transfection- p53 gene expression

C6 cells were cultured in the same conditions as mentioned earlier and incubated for 4 h with CON nanoparticles of ratio 3. Old medium is replaced with fresh and cells were again incubated for 24 h. After this the cells were given PBS wash and since the nanoparticles were devoid of any tagging, the expression was qualitatively assessed by the Live/Dead assay kit (Invitrogen). According to its manual, the cells were incubated for 25 min with the reagent containing 2 μM calcein AM and 4 μM ethidium homodimer (EthD-1) that would stain the live and dead cells respectively. Cells were washed with PBS pH 7.4 and images were captured by fluorescence microscopy (Leica DM IRB, Germany). The principle

behind the assay is that the intracellular esterase activity of live cells would convert the cell-permeant calcein AM to fluorescent calcein which will provide green fluorescence to live cells. On the other hand, EthD-1 which is in general excluded by the intact plasma membrane of viable cells, is able to enter cells with damaged membranes and bind to nucleic acids, thereby producing a bright red fluorescence in dead cells.

3.5 Synthesis and Characterisation of Spermine derivatised Chitosan Ornithine conjugate (COSM).

3.5.1 Materials

Spermine tetrahydrochloride, 1-ethyl-3-(3-dimethylaminopropyl) carbodiimide hydrochloride (EDC), fluorescein isothiocyanate (FITC), Tetramethylrhodamine (TRITC), 3-(4, 5-dimethylthiazol-2-yl)-2, 5-diphenyl tetrazolium bromide (MTT), Minimum essential medium Eagle, Dulbecco's modified Eagle's medium (DMEM), F12 Ham, Polyethyleneimine (PEI-25 kDa), Chlorpromazine, amiloride, filipin and dynasore monohydrate were also purchased from Sigma-Aldrich Chemicals Co., USA. Glucosamine was purchased from Fluka, Fetal bovine serum (FBS) was from GIBCO (USA). YOYO iodide, Hoechst 33342 and Live Dead assay kit from (Invitrogen), Calf thymus DNA (Worthington Biochemical Corp.) and p53 Dominant-Negative Vector from (Clonetech, USA). The C6 glioma cells lines were supplied by the National Centre for Cell Science (NCCS), Pune, India. Human blood was collected from the unmedicated healthy volunteers. All other chemicals were of AR grade.

3.5.2 Preparation of spermine derivatised chitosan ornithine conjugate

Chitosan ornithine conjugate prepared earlier was activated with 6 mM DSC and 6 mM DMAP (Kim et al., 2008) for four hour and then reacted with spermine. Amount of chitosan ornithine and spermine were taken in in the ratio 1:1 equivalent molar for the reaction. The reaction was kept on magnetic stirring at 500 rpm in room conditions for 16 h. Precipitation of the derivative was achieved by repeated rinse with cold acetone followed by freeze drying and lyophilisation. The product yielded was white, thin film, labelled as COSM and it was suspended in MilliQ water in 1mg/mL for the following reactions, unless mentioned otherwise.

3.5.3 Colorimetric determination of primary amine groups

The density of free amine groups in the polymer chitosan provides the positive charges that determine the interactions of the polymer with the negative charged biological molecules. Chemical modification in chitosan causes a variation in the amount of amine groups that is responsible for promoting the surface charge in chitosan and hence using the reagent TNBS, the quantification of the amine groups in the modified chitosan was evaluated. The samples were prepared at 1 mg/mL concentration and glucosamine was used as the reference control as it is the one of the substituents in chitosan. Glucosamine, chitosan ornithine (CON) and spermine derivatised chitosan ornithine (COSM) were prepared in Milli Q water while unmodified chitosan was suspended in 1N HCl. Based on the procedure mentioned in the article (Azzam et al., 2004)), the assay was performed by incubating the polymer samples for 2 h at 37˚C with 200 µL 0.1 % (TNBS) 2, 4, 6-trinitrobenzenesulfonic acid and 4 % sodium bicarbonate. The reaction was later stopped on addition of 200 µL of 2 N HCl and the OD was measured at 344 nm with the UV-Vis spectroscope

(UV Varian Cary, USA). Triplicates were carried for each polymer sample and statistical analysis was performed along with respective standard deviations. The following equation was employed to derive at the results. Percentage of free amine groups % = $\left(Ab_S \div Ab_R\right) \times 100$

Where Ab_S represent absorbance of sample; Ab_R represent absorbance of reference.

3.5.4 Analysis by Fourier transform infrared spectroscopy

The presence of conjugated groups in the modified compound COSM along with spermine and chitosan ornithine conjugate was evaluated by Fourier transform infrared (FTIR) technique. Samples COSM were powdered with KBr and recorded on a Fourier transform infrared spectrometer (Shimadzu spectrophotometer). Parent compounds chitosan ornithine and spermine were also treated with KBr and recorded for comparison.

3.5.5 Analysis by Proton Nuclear Magnetic Resonance spectroscopy

A proton nuclear magnetic resonanace (^{1}H NMR) spectrum of of COSM was measured in D_2O/0.5 (w/w) DCl using a 500MHz spectrometer (Bruker Avance DPX 300). The analysis was performed at 22˚C and the number of transients during the measurements was set as 16. The relaxation time of the instrument during measurements was 3.17s. All other parameters were in the default settings of the instrument as per the specifications of Bruker Avance DPX 300.

3.5.6 Analysis by Differential Scanning Calorimeter

Differential scanning calorimeter (DSC) was implemented to analyse the thermal behaviour of spermine derivatised chitosan ornithine conjugate (COSM) in comparison to unmodified chitosan. Samples were encapsulated in aluminium pellets, heating at a rate of 10˚C/min from 20 to 250˚C. The measurements were

conducted using a Waters differential scanning calorimeter with a mass flow control calibrated using indium as the standard.

3.5.7 Buffering capacity of COSM

The ability of the polymer to become protonated at pH range of 10 to 3 was determined by following a previously reported procedure (Benns et al., 2002). In brief, 6 mg of each polymer was dissolved in 30 mL MilliQ water to give a final concentration of 0.2 mg/mL. The solution was titrated against 0.1 M NaOH to reach pH 10 and then titrated with 0.1 N HCL to reach till 3. The values were recorded by a pH meter and plotted in a graph. The pH profile of spermine derivatised chitosan ornithine along with unmodified chitosan and PEI, a highly buffering polymer was also measured. Triplicates were also performed. Statistical analysis was performed and respective standard deviations were provided.

3.5.8 Amplification and Purification of plasmid DNA and calf thymus DNA

Calf thymus DNA was dissolved and dialysed in 0.1M sodium acetate buffer. The nanoparticle size and zeta potential determination was carried out with nanoparticles that had calf thymus DNA and p53 plasmid DNA. Plasmid DNA p53 was isolated from JM109 cells and purified using Qiagen QIA filter plasmid Mega kit according to the manufacturer's instruction and re-suspended in TE buffer. The purity was confirmed by 1% agarose gel electrophoresis and pDNA concentration was measured in UV-Vis spectroscope (UV Varian Cary, USA). The final purity is determined to be 1.83 (OD 260/280) and 2.08 (OD 260/235).

3.5.9 Preparation of COSM nanoparticles

COSM was dissolved in MilliQ water at a concentration of 1mg/mL, filtered through a 0.22 μm filter and kept sterile. Calf thymus DNA was taken in 1mg/mL.

Both the derivative and DNA were mixed in the desired ratios corresponding to their w/w amounts. The nanoparticles, also referred as nanoplexes were suspended in normal saline (0.9% sterile sosium chloridel) and each nanoparticle ratio consisted of an increasing concentration of the polymer with respect to the constant amount of the DNA. The w/w ratio of the polymer and DNA determined the varying nanoparticle ratios. Once mixed, both the solutions were vortexed for 15 sec and incubated at room temperature for 20 min to avail the nanoparticles or polyplexes. The solution was then made up to 1 mL and analysed for the size and zeta potential. Both plasmid DNA and calf thymus DNA followed the same procedure as mentioned above during nanoparticle preparation.

3.5.10 Determination of particle size and zeta potential

The nanoparticles prepared with calf thymus DNA (1mg/mL) and COSM (1mg/mL) in increasing ratios and subjected to dynamic light scattering measurement (DLS) using the Zetasizer Nano ZS (Malvern Instruments Ltd., UK) to determine their size. The ratios 1 – 20 were adopted for the study but as the values of smaller ratios were inconsistent in size and surface charge, only higher ratios from 11-20 were included. Triplicates were also simultaneously carried out. Statistical analysis was performed and provided with respective standard deviations. Zeta potential represented the surface charge of the nanoparticles and with the same ratios 11-20, the charge density was analysed in Zetasizer Nano ZS (Malvern Instruments Ltd., UK).

3.5.11 Transmission Electron microscopy analysis

The morphology of COSM-pDNA nanoparticles was observed with the the aid of Transmission electron microscopy (TEM) analysis. Nanoparticles were

prepared at DNA/polymer ratio (w/w) 15 and suspended on a copper grid. The excess liquid was removed with tissue paper and the grid was left to dry. The samples were visualized with a Hitachi H 7650 instrument at 100 kV.

3.5.12 DNA Gel retardation

The nanoparticle formed should embark on the binding capacity of the chitosan derivative with DNA which should be reasonably strong enough to withstand other non specific interactions. The complexes with COSM and pDNA prepared in increasing ratios from 11-20 were loaded onto a 0.8 % agarose gel with plain pDNA on either sides of the gel and run in 1 X TBE buffer (89 mM Tris–HCl pH 8.3, 89 mM borate and 2 mM EDTA). The gel was run on at 100 V for 60 min and stained with ethidium bromide (2 µL of 10 mg/mL) and photographed using the Image analyser (LAS 4000, Fuji).

3.5.13 DNase I protection and release assay

The retention ability of COSM polymer with pDNA was further confirmed by treating the same ratios with DNase with concentration of 569 U/mL (digestion buffer 0.1 M sodium acetate and 5 mM magnesium sulphate at pH 7.4) for 15 min at 37˚C. The nanoparticles that consist of 2 µg DNA is incubated with 2.28 µL of DNase I. The reaction was then inactivated by termination buffer containing 0.5 M EDTA, 2 M NaOH and 0.5 M NaCl. The integrity of pDNA/COSM complex was ascertained by running agarose gel electrophoresis at 60 V for 1 h. Furthermore it is observed that the polymer-DNA interaction is abruped in the presence a strong negative charged polyanion heparin that would displace the bound DNA from the nanoparticle. The same sample ratios were treated with 5 µL hepain at concentration of 1000 U/mL for 30 min. The released DNA from COSM nanoparticle was analysed

by running the samples in 1 % agarose gel in a Bio-Rad electrophoresis system (Bio-Rad laboratories, CA, USA).

3.5.14 Interaction of COSM with Red blood cells (RBC)

The blood compatibility of COSM polymer was evaluated in terms of hemolysis by the method described elsewhere (Joshy & Sharma, 2012). The blood was obtained from healthy adult volunteers and collected in the presence of an anticoagulant sodium citrate as nine volumes of blood to one volume of 3.8 % sodium citrate. The blood is then centrifuged to isolate red blood cells (RBCs) and was washed and diluted with saline (1:8) to obtain RBC stock solution. Polymer COSM prepared in saline (1 mg/mL) was added in the corresponding volumes of concentration 25 µg, 50 µg, 75 µg and 100 µg to constant volume of diluted RBC and whole solution made up to one mL by saline. The mixture incubated for 2 hr and centrifuged. Saline and Triton X-100 was used as negative (0 % lysis) and positive controls (100 %). Absorbance reading was determined at 541 nm by UV spectrophotometer (Varian). Hemolysis was calculated with the following equation:

$$\text{Percentage hemolysis} = \left(\frac{Ab_T - Ab_N}{Ab_X - Ab_N} \right) \times 100$$

Where Ab_T represent absorbance of test, Ab_N represent absorbance of normal saline, Ab_X represent absorbance of Triton X-100.

Further RBC aggregation studies was carried out by incubating 100 µL of saline diluted RBC (9:1) with 100 µg of COSM polymer solution (1 mg/mL), normal saline (NS, 0.9 % sterile sodium chloride) and PEI 25 kDa (1 mg/mL) as the controls for 25 min and then mounted on a glass slide for microscope observation through phase contrast microscope (Leica DM IRB, Germany) at 20 times magnification.

3.5.15 Electrophoretic analysis of COSM polymer with plasma protein interactions

Native PAGE gel electrophoresis was performed to determine the effect of polymer COSM compatibility towards blood plasma proteins. The polymer COSM prepared in 1mg/mL was added in volume 50 µL and 100 µL to 100 µL of blood plasma diluted with saline. After a brief centrifugation, the supernatant of the samples were run in the 7 % resolving and 4 % stacking gel at 90 V for 90 min using Mini-Protean II electrophoresis system (Bio-Rad, CA, United States). Gel was stained in Coomassie blue and the protein bands were visualised in the Image analyser (LAS 4000 Fuji). Normal saline treated blood plasma was considered as the control for comparison.

3.5.16 Cell Culture

In vitro analysis is carried out with murine derived glioma C6 cells seeded in culture flasks and maintained in equal volume of DMEM/F12 Ham medium and MEM (1:1) supplemented with 10 % FBS and 1 % antibiotic under 5 % CO_2 and 95 % humidity at 37˚C. The cells were grown till they became 80 % confluent and trypsinised to be transferred to multiwall tissue culture plates with at a density of 1×10^5 cells/well. Each experiment was conducted after 24 h incubation of the cell culture plates which had the same count of cells. For all cell culture experiments, the polymer COSM was prepared in 1 mg/mL in F12 Ham medium (1:1) before DNA complexation.

3.5.17 Cytotoxicity assay

It is necessary to determine the toxic effect of the chitosan derivative, COSM in glioma cell lines. Hence cells were seeded in 24-well tissue culture plate suspended in MEM: DMEM/F12 Ham medium containing 10 % FBS. After 24 h incubation, cells attained 70-80 % confluency and polymer COSM was added in 1 mg/mL concentration in the particular volumes of 25 µL, 50 µL, 75 µL and 100 µL. Cells incubated with medium were taken as the negative control and Triton X-100 (1%) treated cells were considered to be the positive control. The derivative with the medium was discarded after 24 h and the cells were treated with 200 µL of MTT reagent (0.2 mg/mL) for 4 h incubation at 37˚C. The formazan crystals formed were then dissolved by DMSO and the lysed cells were kept for 10 min. The results were assessed as the mean % cell viability relative to untreated cells by measuring the absorbance of the samples at 540 nm using an automated microplate reader (Tecan Micro plate Reader, Switzerland). For comparative analysis, the cells were treated separately with 50 µL of other controls such as PEI 25 kDa (1 mg/mL) and unmodified chitosan (1 mg/mL, 1 N HCl). The following equation was adopted to arrive at the results.

$$\text{Percentage cell viability \%} = \left(\frac{Ab_S}{Ab_C} \right) X\ 100$$

Where Ab_S represent absorbance of sample, Ab_C represent absorbance of medium control

3.5.18 Cellular uptake of COSM nanoparticles

Glioma C6 cells were seeded in four well plates at a density of 1×10^5 cells/well and incubated for 24 h. The plasmid DNA was incubated for 30 min with

YOYO iodide which required 2.5 μL of 10 μM YOYO labeled for 1.0 μg DNA/well. COSM nanoparticles were formulated in F12 Ham medium by combining 2.5 μg tagged plasmid DNA with the corresponding amounts of COSM polymer in the ratio 15. The medium in the 4-well plate was replaced with fresh medium containing COSM nanoparticles. Nuclear staining was done with 15 μL of Hoechst 33342 dye (final concentration to be 1mM) just half an hour before the allotted 4 h incubation time and the medium was discarded followed by PBS pH7.4 wash. The cells were fixed with 1 % formaldehyde for 20 min before taking fluorescent images by both fluorescent microscope (Leica DMI3000 B, Germany) and confocal laser scanning microscope (Zeiss LSM 510 Meta, Germany). Z-stacking image analysis was performed using LSM 510 software image analyser (version 5). Similar cell treatment was performed to implement quantification of cell uptake by flow cytometry (Becton Dickinson FACS Aria, USA). For each measurement ten thousand cells were counted and the percentage of positive cells was calculated by setting the background population as 98% negative when analyzing untreated control cells (Kanatani et al., 2006).

3.5.19 Cell uptake studies in the presence of endocytic inhibitors

In this study five inhibitors specific to each pathway were employed to identify the particular endocytosis pathway that promote cellular uptake. C6 cells were grown in MEM: DMEM/F12 Ham (1:1) culture medium under the normal cell culture parameters and treated at first with inhibitors, each well for separate inhibitor. The inhibitors used were chlorpromazine (1 μg/mL) that block the clathrin mediated pathway, dynasore monohydrate (8-200 nM) inhibit the dynamin dependent clathrin mediated pathway, filipin (2.5 μg/mL) the inhibitor for caveolae mediated

endocytosis, amiloride is the macropinocytosis pathway inhibitor (2 μg/mL) (Alex et al., 2011). Ornithine (1 μg/mL) and spermine (1 μg/mL) was also adopted to inhibit the receptor mediated pathway. After 30 min treatment, the medium with inhibitors were discarded and cells were then incubated for 4 h with COSM/pDNA nanoparticles of ratio 1:15. The medium was removed and washed twice with PBS followed by formaldehyde fixation for microscopic visualisation. Images were captured in (Leica DMI 3000B, Germany). Detailed examination of intracellular localisation of COSM nanoparticle within the cells inhibited by these inhibitors was furthermore confirmed by confocal laser scanning microscopy. Cells were harvested and treated with the same inhibitors and COSM nanoparticles ratio prepared in the same manner as mentioned above. Cells were incubated for 4 h without nuclear staining followed by PBS wash and fixation. Images were visualized in the confocal laser scanning microscope (Zeiss LSM 510 Meta, Germany) and z-stacking image analysis was performed using LSM 510 software image analyser (version 5).

3.5.20 In vitro transfection- p53 gene expression

C6 cells were harvested for growth in a 4-well plate and incubated for 24 h under the regulated cell culture conditions. COSM nanoparticles were prepared with p53 plasmid and supplemented to cells for 4 h incubation. Later the medium was replaced with fresh MEM: DMEM/F12 Ham with 10 % serum and left for 24 h incubation in $C0_2$ incubator. Next day the cells were washed twice with PBS pH 7.4 and following the protocol of the Live Dead assay kit (Invitrogen), about 200 μL of the reagent consisting of 2 μM calcein AM and 4 μM ethidium homodimer (EthD-1) was added to the cells and incubated for 25 min at 37˚C. Next the cells were rinsed with PBS and visualized under the fluorescence microscope (Leica DMI 3000B,

Germany). The principle behind the assay is that the intracellular esterase activity of live cells would convert the cell-permeant calcein AM to fluorescent calcein which will provide green fluorescence to live cells. On the other hand, EthD-1 which is in general excluded by the intact plasma membrane of viable cells, is able to enter cells with damaged membranes and bind to nucleic acids, thereby producing a bright red fluorescence in dead cells

3.5.21 Intracellular trafficking of Nanoplex

C6 cells were seeded in the same density of 1 X 10^5 and grown for 24 h to achieve the desired 80 % confluency. The polymer COSM was tagged with TRITCI for 2 h incubation and dialysed using membrane of molecular weight cut off of 12,000 Da (Sigma) against PBS pH 7.4 to remove any unbound TRITCI from the polymer. COSM nanoparticles were prepared in ratio 1:15 (w/w) with YOYO tagged plasmid and TRITCI tagged polymer to visualize the intracellular path of the nanoparticle. C6 cells were exposed to the nanoparticles for 4 h followed by adition of Hoeschst stain, added half an hour prior to the completion of incubation time. The cells were washed with PBS, fixed and viewed under fluorescence microscope (Leica DMI 3000B, Germany).

CHAPTER 4 RESULTS

4.1 Depolymerisarion of Chitosan

Depolymerisation of very high molecular weight of chitosan was carried out repeatedly to result in an intermediate molecular weight range. Using the Ubbelohde viscometer, the molecular weight was determined using intrinsic viscosity method in 0.25 M acetic acid/0.25 M sodium acetate with 'k' and 'a' values of 15.7x 10^5 and 0.79 (Kasaai et al., 2000). Only the molecular weight parameter was subjected to transition while the degree of deacetylation about 90 % was kept constant. The molecular weight was calculated to be in the range of 120–130 kDa. This particular depolymerised chitosan was adopted for the derivatisation study with conjugates of biological significance.

4.2. Spermine grafted galactosylated chitosan (GCSM)

4.2.1 Synthesis and characterisation of GCSM

Chitosan has a pKa value of about 6.2–7.0 which makes it soluble in acidic pH and insoluble in neutral as well as alkaline solutions. Ligand modification in chitosan is suggestive for improving the solubility and therefore conjugation with lactobionic acid into the 120 kDa depolymerised chitosan was carried out to incorporate galactose groups into the polymer backbone. Further coupling of the derivative with spermine was performed and the solubility of the chitosan derivative was enhanced. An illustration of the scheme of synthesis of GCSM is given in Fig 1.

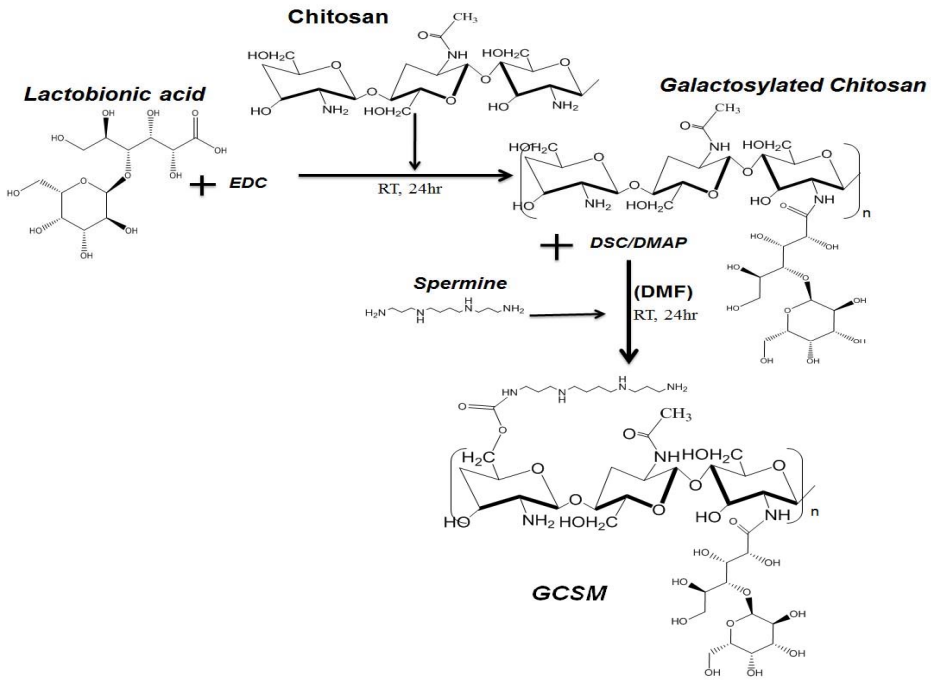

Fig 1: Proposed reaction scheme of synthesis of GCSM polymer. Chitosan reacted with lactobionic acid to give galactosylated chitosan (GC) which on further reaction with spermine resulted in GCSM derivative.

The extent of substitution of the conjugates in the chitosan was determined by the amount of free primary amine groups in the depolymerised chitosan available after the coupling reaction. A colorimetric biochemical assay, TNBS determined the amount of free amine groups in chitosan, gal-chitosan (GC) and GCSM polymer. Results indicated that GC consisted of less free amine groups when compared to the parent compound due to the binding of galactose moiety at the reactive amine position. However, on conjugation with spermine resulted in replacing almost the reacted primary amine groups in GC by the primary groups of spermine and hence a slight increase in free amine groups is observed in the gal-chitosan-spermine derivative, GCSM as depicted in Fig. 2.

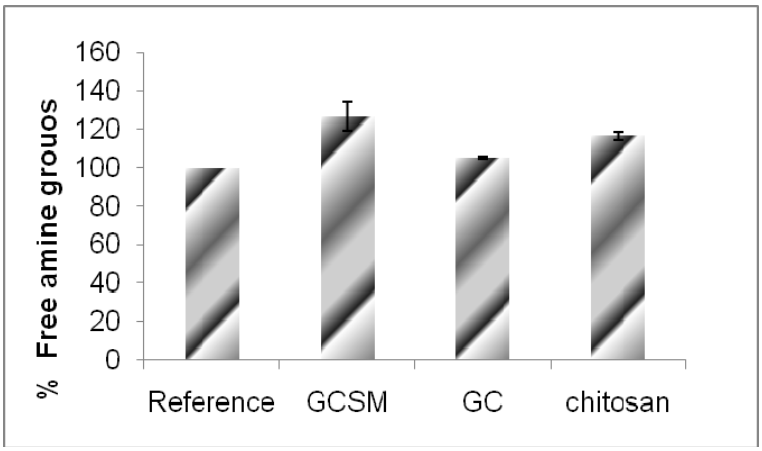

Fig.2: TNBS assay for determination of free amine groups in GCSM, GC, chitosan and glucosamine as the reference. The values given are mean ± SD and n= 3.

FTIR evaluation, displayed in Fig. 3A-D indicated chitosan stacked with the other functional conjugates along with the GCSM derivative of chitosan. The IR spectra of GC & GCSM displayed the required peaks used for conjugation in chitosan. In GC derivative, lactobionic acid on reaction with chitosan resulted in hydroxyl peak at 3416 cm^{-1} along with a new amide I stretch at 1635.8 $cm^{-1}$and amide II stretch at 1522 cm^{-1} that clearly correlated to substitution of galactose. Subsequent conjugation of GC with spermine revealed peaks at 3116.8 cm^{-1} for amine stretch of spermine and an additional peak at 1648 cm^{-1} was due to the CN stretching of amide. A broad peak at 3346 cm^{-1} was due to OH stretching of parent compounds in GCSM. The spectrum of galactosylated chitosan (GC) is given in Appendix A5-Fig 1.

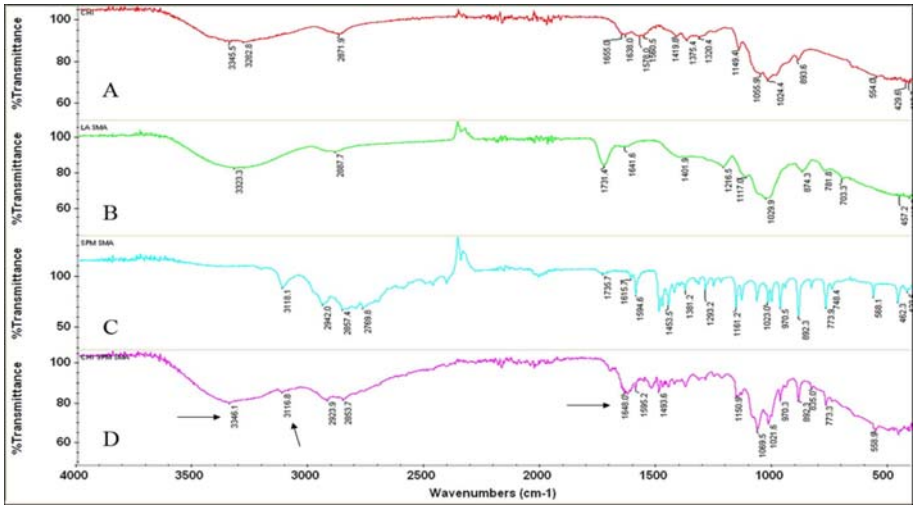

Fig 3: Infrared spectroscopy for evaluation of chemical groups in the functional entities of the GCSM derivative. FT-IR of (A) chitosan (B) lactobionic acid (C) spermine (D) GCSM.

Aready a lot of previous articles have presented the ^{1}H NMR results of chitosan (Tian et al., 2003; Knight et al., 2007) and galactosylated chitosan (Jiang et al., 2008) which enabled for comparison with ^{1}H NMR of GCSM polymer. In Fig. 4, the signals at 3.811 ppm and 3.645 ppm were assigned for protons of lactobionic acid. And within 2.006–1.974 ppm, the signals corresponded to the CH_3 proton of chitosan. The signals 1.7012–1.671 ppm corresponded to protons of spermine (Ha et al., 1998). In accordance with Jintapattanakit et al. (2008), the degree of substitution of galactose and spermine was calculated to be 15 % and 32 %, respectively, which illustrated the successful formulation of GCSM polymer variant.

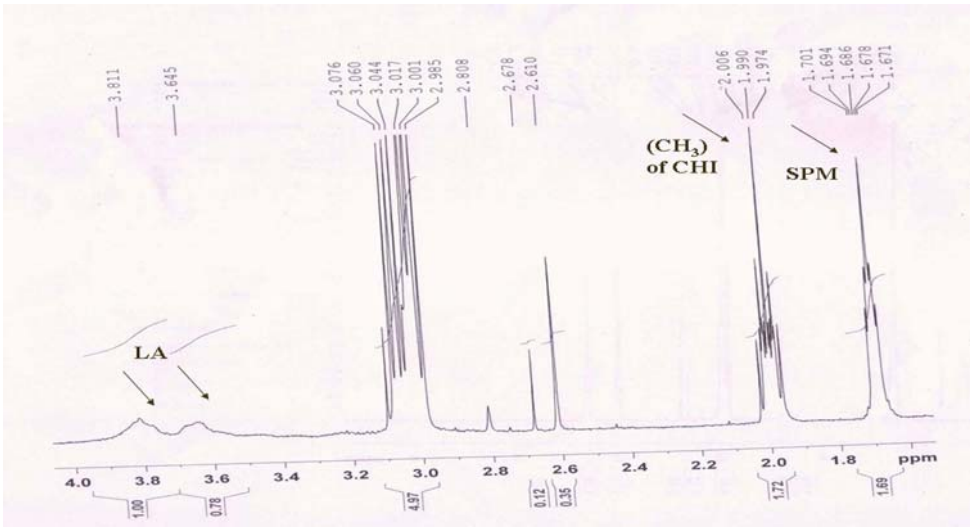

Fig 4: ^{1}H NMR spectra of GCSM polymer.

The result shown in Fig.5 revealed that GCSM conjugate has buffering capacity over a pH range of 10–5 against 950 µL of 0.1 N HCl titration. This was found to be slightly higher than normal buffering capacity of unmodified chitosan that showed resistance around pH 7–5 with 650 µL of the acid. PEI showed the maximum buffering capacity of pH range 10–5 with higher volume of acid titration.

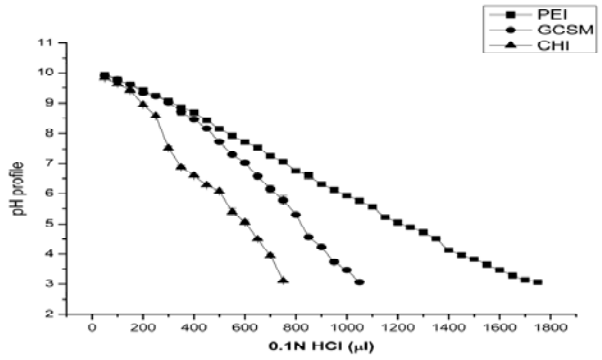

Fig 5: Analysis of the buffering capacity of GCSM. Acid base titration of PEI, GCSM and chitosan (CHI) polymer against 0.1 N HCl. The values given are mean ± SD and n= 3, with standard deviation found to be very negligible.

4.2.2 Characterisation of Nanoparticle: GCSM and DNA interaction

4.2.2.1 Nanoparticle size measurement and zeta potential

The size of the nanoparticle is a detrimental factor to be used for gene transfer studies. The hydrodynamic diameter of the complexes indicated the size of the nanoplexes. The five ratios gave sizes of 328 nm, 258 nm, 241 nm, 241 nm, and 559 nm. Ratios 15 and 16 showed an optimum size of 241 nm generally preferred for in vitro studies. Nanoplexes prepared in ratios DNA/GCSM (w/w) below 12 and above 17 were very large and inconsistent, and could not be used for *in vitro* studies, hence data is not shown. The mean hydrodynamic diameter of the complexes of different weight ratios along with their zeta potential is given in Table 1. The surface charge for complexes made of varying ctDNA and GCSM ratios were found to be 10.4 mV, 11.7 mV, 13.8 mV, 7.81 mV, and 10.4 mV. Fortunately, ratios 15 and 16 showed a fairly good positive charge of 13 and 7 mV, respectively that enabled its further use.

Table 1: Particle size and zeta potential of GCSM/ctDNA nanoparticles. The values given are Mean ± SD and n=3.

DNA/polymer ratio	Size (nm) ±sd	Zeta potential (mV) ± sd
1:12	328 ± 8.4	10.4 ± 0.58
1:14	258 ± 35.5	11.7 ± 2.08
1:15	241± 33.2	13.8 ± 3.41
1:16	241 ± 28.9	7.81 ± 4.09
1:17	559 ± 158.3	10.4 ± 1.48

4.2.2.2 Morphological observation by TEM and AFM

In transmission electron micrographs, the chitosan derivative nanoplexes did not form aggregates and distinct sizes were visualized, clearly showing the shape of the nanoparticles (Fig. 6A). Simultaneous shapes of spheroid like globular structures were seen with an average diameter of 170–215 nm. AFM technique was adopted to attain a surface topography image of the GCSM nanoparticle. The image (Fig. 6B) further confirmed the absence of aggregates and adhesion between the nanoplexes. Distinct nanoplexes with slight irregularities were distributed and a kind of ellipsoidal shape was observed, drawing a similarity in the existing kind of shapes achieved through TEM observation.

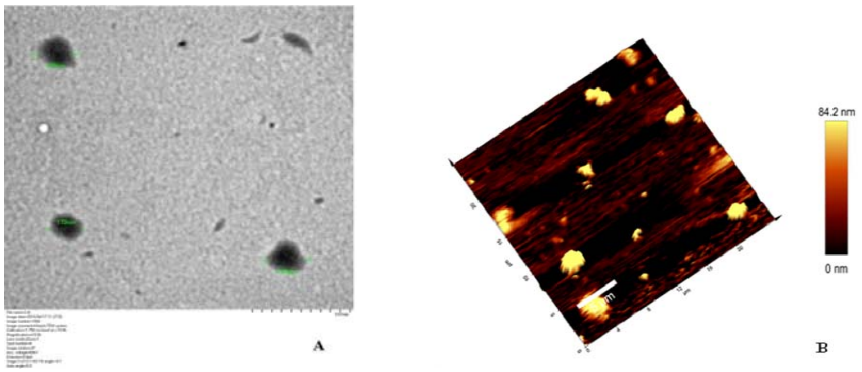

Fig 6: (A) TEM observation GCSM nanoparticles in 1:15 ratio. Scale bar is 200 nm. (B) AFM observation of nanoparticle of 1:15 ratio.

4.2.2.3 Electrophoretic analysis of GCSM nanoparticle

The binding ability of GCSM polymer with calf thymus DNA was investigated by running agarose gel electrophoresis. GCSM nanoplexes resulted after mixing varying proportions of GCSM solution with a constant concentration of calf thymus DNA, showed no release of DNA in the lanes. The bright intensity of DNA was retained in the wells as shown in Fig. 7(A) which confirmed the strong interaction between the

GCSM and ctDNA that retarded the movement of DNA towards the positive electrode. DNA alone without complexation was loaded in the first well resulting in a DNA smear in the first lane. And rest of the wells were loaded with the nanoplex ratios 6, 8, 10, 12, 14, 15, 16, 17, and 18. Except for ratios 6 and 17 which had an appearance of slight degradation, all the other ratios showed luminance in the wells. Electrostatic interaction between DNA and the polymer need to be stable in order to obtain nanoplexes that can be consistent for a time period. Therefore, the integrity of nanoplex with ctDNA was confirmed by treating the nanoparticles with DNase for degradation study. The faint fluorescence seen in the wells in Fig. 7(B) indicated that DNA was retained in the wells and was condensed tightly into the polymer nanosize configuration, thus protecting it from DNase attack. On treatment with heparin, the DNA was released from the bound nanoplexes as observed in Fig. 7(C). Ratios 4, 6, 8, 10, 12, 14, 15, 16, 17, and 18 loaded in the wells revealed the stability of the nanoplexes to remain bound to DNA. Control DNA treated with DNase was completely degraded in its lane. The voltage fluctuations in between caused slight bend in the DNA streaks.

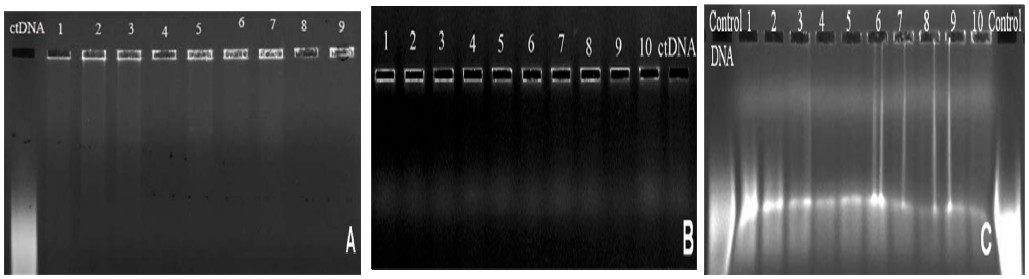

Fig 7 Agarose gel electrophoresis performed on ctDNA/GCSM complexes. The DNA retardation ability of the nanoplex was determined. In Fig 7 (A) Lane ctDNA is control (2 μL DNA). Lanes 1–9 have nanoplex ratios 1:6, 1:8, 1:10, 1:12, 1:14, 1:15,

1:16, 1:17 and 1:18. (B) Protection of pDNA against DNase I after complexation with GCSM. Lanes 1–10 have nanoplex ratios 1:4, 1:6, 1:8, 1:10, 1:12, 1:14, 1:15, 1:16, 1:17 and 1:18 and lane ctDNA refers to DNA treated with enzyme (C) heparin affinity for COSM polymer and DNA released from nanoplexes. Lanes 1–10 have nanoplex ratios 1:4, 1:6, 1:8, 1:10, 1:12, 1:14, 1:15, 1:16, 1:17 and 1:18. The first and last lanes consisted of control ctDNA.

4.2.3 Blood compatibility and Cytotoxicity study of GCSM polymer

4.2.3.1 Hemolysis and RBC aggregation

The effect of the polymer on RBC showed negligible haemolytic activity for varying concentrations of GCSM (1 mg/mL). The hemolysis level was well within the acceptable range of 1 % which was comparatively non toxic when compared to the positive control Triton X-100 (Appendix A1-Table 1). Further non toxicity of the polymer was confirmed by performing RBC aggregation study that resulted with images Fig 8A and B showing the absence of aggregation of red blood cells as similar to the negative control saline. At high concentration of 100 µg, GCSM proved to be non toxic and maintained the integrity of red blood cells. Meanwhile PEI treated RBC cells Fig 8C showed aggregation and lysis of cells, which was therefore taken as the positive control.

4.2.3.2 Plasma protein interaction with GCSM polymer

Another case is where the presence of any foreign material in the plasma would interact with the serum proteins to form complexes and thereby reduce the amount of free proteins in the plasma. This was assessed by PAGE analysis Fig 8D in which the normal saline was considered as the positive control for comparing the chitosan derivative since saline do not have any affinity interaction with the serum

proteins and does not remove them from the blood serum. And therefore the protein bands were visible in the gel. Similarly the presence of GCSM polymer did not cause adsorption of plasma proteins and this was indicated by the presence of the serum protein bands in the two lanes of the gel. The bands represented that GCSM polymer does not lead to any undesired reactions with the plasma proteins and could be considered for systemic administration.

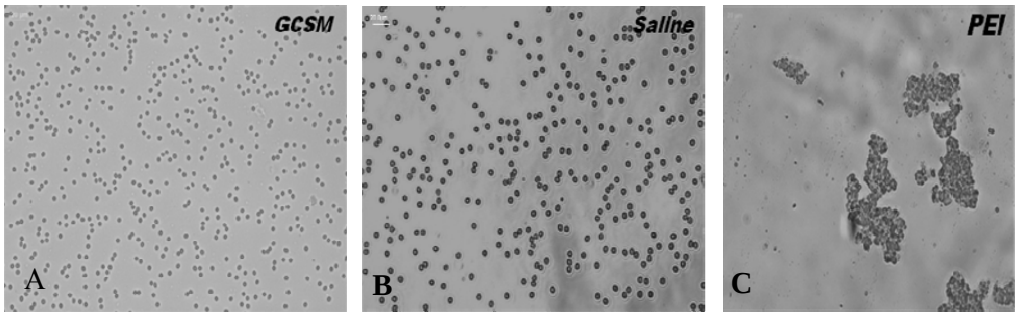

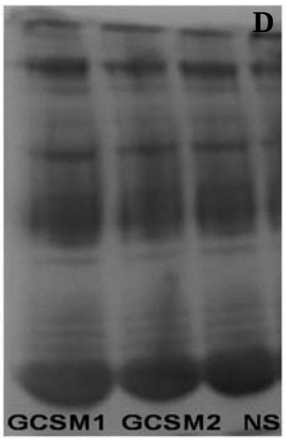

Fig 8: RBC aggregation studies with (A) GCSM derivative (B) with normal saline (C) with PEI 25 kDa (20 X magnification for RBC) (D) Plasma Protein interaction with GCSM (1 mg/mL); Lanes GCSM1, GCSM2 represent polymer in 50 &100 µg and lane NS is normal saline, the control

4.2.3.3 Cytotoxicity evaluation of GCSM polymer

The cytotoxicity of GCSM polymer was evaluated by the MTT method, which measured the intracellular dehydrogenase activity in cells to determine the cell viability response to the concentration of GCSM polymer. Significant cytotoxicity was not observed for GCSM in the cell lines. The % viability of GCSM polymer was compared with chitosan and control in triplicates. The graphical representation of

GCSM polymer as depicted in Fig 9 showed 80 % cell viability in presence of GCSM polymer. Even at high concentration of 100 µg, GCSM treated cells continued to show viability almost in comparison to the medium control of untreated cells. On the other hand chitosan treated cell lines had cell viablity below 60 % and this was because chitosan was dissolved in slight acidic pH that becomes toxic to the cells.

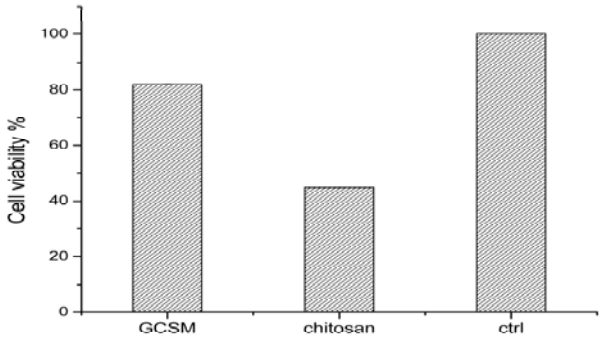

Fig 9: Cytotoxicity of GCSM polymer. Medium was the control. The values given are mean ± SD and n= 3, with standard deviation found to be very negligible.

4.2.4. In vitro analysis of GCSM/pDNA nanoparticle

4.2.4.1 Evaluation of Cellular Uptake

Cell uptake of FITC tagged nanoplexes were demonstrated in Fig 10. In Fig. 10A, there was absence of fluorescence inside the cells in the control which was supplemented with only FITC tagged polymer without plasmid complexation. Cell uptake did not occur in these cells. Meanwhile the image displayed Fig 10B showed the accumulation of FITC labelled nanoplexes inside the cells which illustrated the transfer of plasmid into the cytoplasm and finally to the Hoechst stained nucleus. The high distribution of nanoplexes within the cell and nucleus was observed by flow

cytometry also, which represented more than 100 % of efficient cellular uptake of the GCSM nanoplexes.

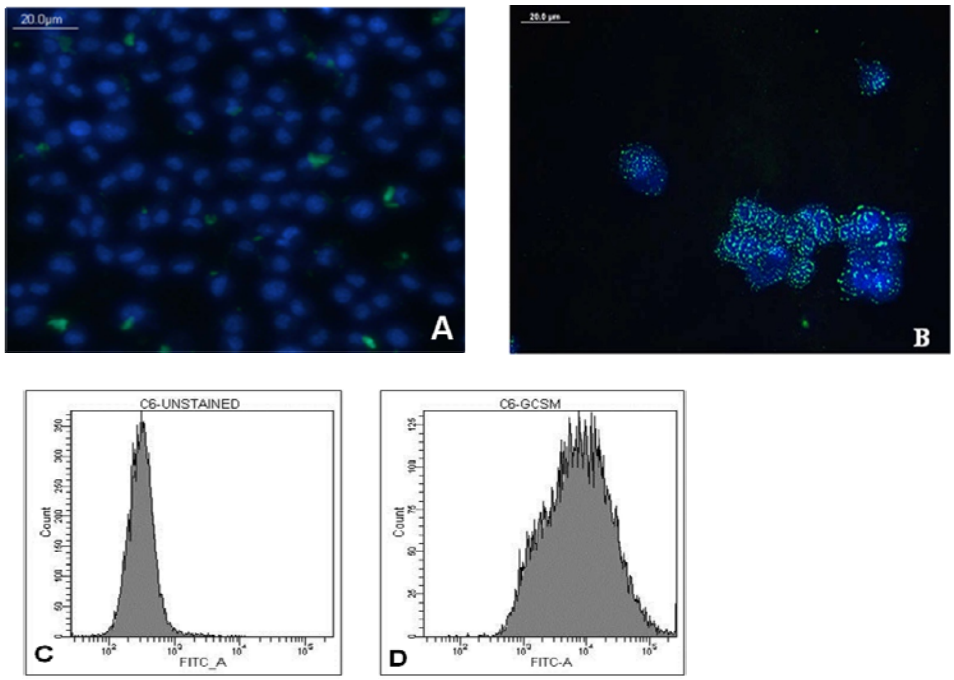

Fig 10: Cell uptake of GCSM nanoparticles in HepG2 cells. Fluorescent microscope observation of cell uptake of A) FITC tagged GCSM polymer without plasmid complexation B) YOYO tagged GCSM/pDNA nanoparticle. Flow cytometry of C) Unstained control cells D) FITC tagged GCSM nanoparticles

4.2.4.2 Endocytosis inhibition Study

Cell uptake inhibition by blocking the endocytosis pathway enabled recognition of the pathways chosen by GCSM nanoparticles for cell internalization. The GCSM/DNA complexes were found to be localized in the nucleus of the cells in Fig. 11A and 11B, though the presence of inhibitors namely chlorpromazine and filipin were made available in the cells. On the contrary, application of ligands such as asialofeutin and galactose in Fig 11C and D, revealed localization of nanoplexes around the peripheral regions of the nucleus. High intensity of fluorescence around

the nucleus indicated a crowd of nanoparticles in the extracellular region where smooth passage of the nanoplex through the cytoplasm to the nucleus would have been hindered due to the presence of asialofeutin and galactose.

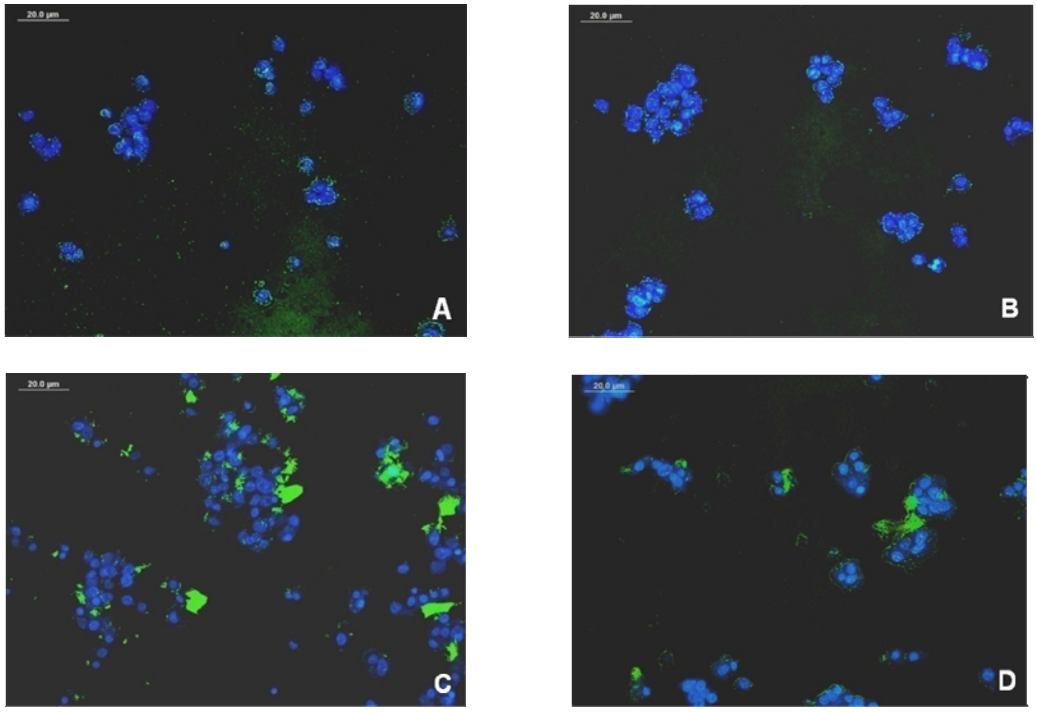

Fig 11: Endocytosis inhibition of cell uptake of GCSM nanoparticles in HepG2 cells. Fluorescent microscope observation of cell uptake treated with the inhibitors A) chlorpromazine B) Filipin C) Asialofeutin D) Galactose.

4.2.4.3 Transfection with Luciferase Gene expression

Transfection efficiency of GCSM nanoparticle was evaluated with ratios 1:16 and 1:15 combined with pGL3. Control PEI was adopted for comparison with the samples. A considerable high level of transfection in Fig. 12 was resulted with the ratios and negligible differences existed between the two ratios. Spermine coupling to galactosylated chitosan therefore attributed an efficient targeted gene expression in HepG2 cells even in the presence of serum in the medium. On other hand, ratios

below the considered and higher did not provide a favourable gene expression and hence not presented here.

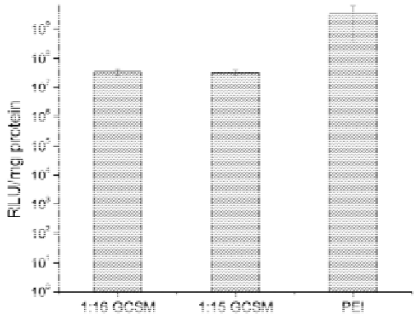

Fig 12: Luciferase expression in HepG2 cells transfected by DNA/GCSM complexes and DNA/PEI complexes taken at two different ratios (1:15 and 1:16). The values given are mean ± SD and n=3.

4.2.4.4 Transfection with p53 Gene expression

The successful delivery of gene by GCSM nanoparticle is reflected by the qualititative assessment of the expression of p53 which was analysed by means of the Live Dead Assay. Since p53 gene facilitate apoptosis, those cells in which the gene was effectively been transferred caused the cell membrane leakage. The reagent that contains both calcein AM and ethidium homodimer stained the live and dead cells respectively. After 24 h incubation, most of the cells had apoptosis expression and the damaged cell membrane of those cells allowed the movement of ethidium homodimer dye into the cell, staining them in red colour (Fig 13A). Live cells were not observed at all in GCSM treated cells. In Fig 13B, the live cells that had only p53 treated showed complete live cells in green colour. PEI polymer which is strong transfecting agent was considered as the positive control (Fig 13C) that had cells transfected with PEI/p53 nanoplexes and showed maximum cell death.

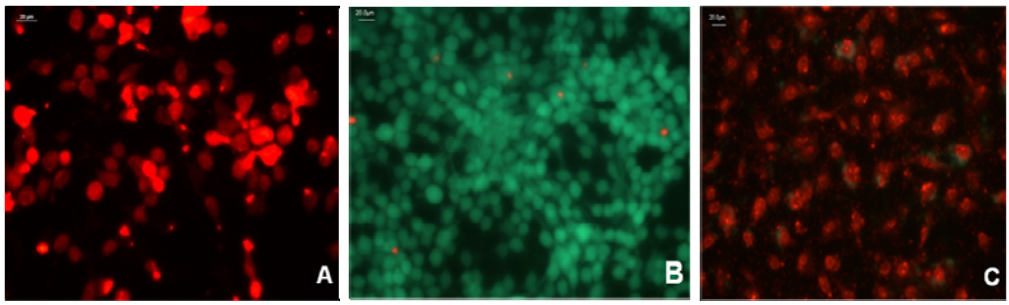

Fig 13: Transfection Assessment via Live Dead assay in C6 cells. Live Dead assay showed the staining of live cells by calcein (green) and dead cells by ethidium homodimer (red). Glioma cells treated with A) GCSM/p53 nanoparticles B) only p53 plasmid C) PEI/p53 nanoparticles.

4.3 Protamine conjugated diamine PEGylated chitosan (CDP)

4.3.1 Synthesis and characterisation of CDP

Chitosan was reacted with PEG diamine initially to derive the chitosan backbone with PEG units containing free amine groups. This particular derivative was sparingly soluble and was reacted with EDC activated protamine to acquire protamine conjugated diamine PEGylated chitosan coded as CDP which turned out to be soluble at neutral pH. The lyophilised product appeared as white thin flake substance. A representation of the synthesis is illustrated in Fig 14.

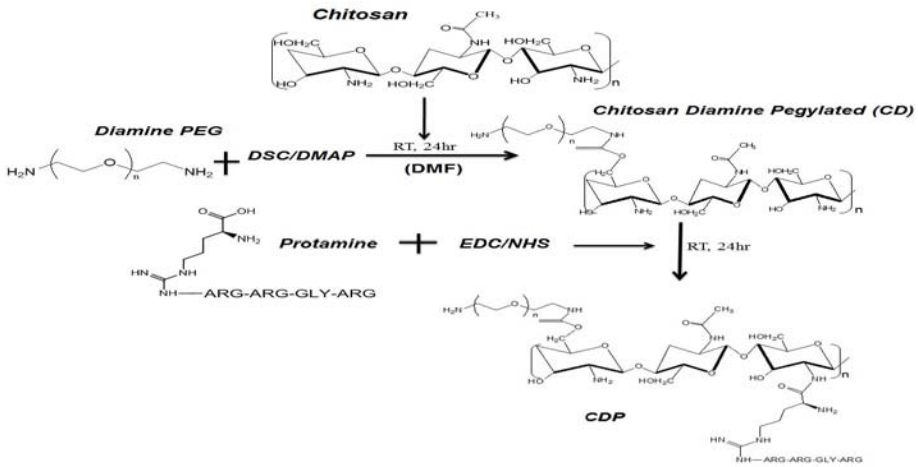

Fig 14: Proposed reaction scheme of synthesis of CDP. Depolymerised chitosan is reacted with PEG diamine to yield diamine PEGylated chitosan. This is then reacted with protamine to derive the final product CDP.

The degree of amine substitution in the synthesized chitosan derivative was determined through primary amine reaction with 6-trinitrobenzenesulfonic acid solution (TNBS). The primary amine composition in the chitosan derivative was measured in relative to the reference glucosamine that is allocated to have cent percent free primary amines. The graphical calculation of the assay showed the number of primary groups of CDP to be much higher than that of the parent compound chitosan and the diamine PEGylated chitosan. Coupling of PEG diamine had increased the primary amine in chitosan which got further enhanced with protamine conjugation. As protamine is an arginine rich protein, excess amount of primary amine was provided by the arginine residues and the extra primary amine composition of nearly 120 % was found in CDP in Fig 15 than that of the chitosan and CD polymer.

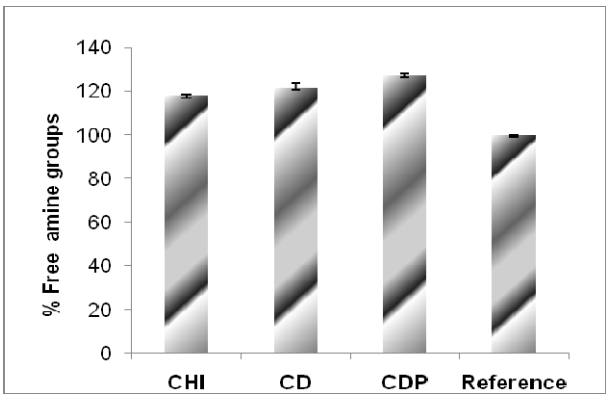

Fig 15: TNBS assay for determination of free amine groups in CHI (chitosan), CD (diamine PEGylated chitosan) CDP (protamine conjugated diamine Pegylated

chitosan) along with glucosamine as the reference. The values given are mean ± SD and n= 3.

The chitosan conjugate was characterised with FTIR and ^{1}H NMR to confirm the conjugation of the different residues in chitosan. In the FTIR spectra in Fig 16, the stacked spectra of chitosan and the reacted conjugate along with the final derivative has been showcased. In chitosan spectra the peak at 3284 cm^{-1} represented the hydroxyl groups of chitosan and the amide peaks at 1641 cm^{-1} and 1581 cm^{-1}. In protamine grafted chitosan PEG diamine conjugate the peaks at 3271 cm^{-1} highlight the O-H stretch of chitosan. The shift occurred due to the enhanced alcohol substitution in the chitosan backbone by the incorporation of the peaks of PEG diamine which was observed at 2934 cm^{-1} referring to the C-O stretch Excess of amine groups from protamine and the amide coupling has been depicted by the peak at 1637 cm^{-1} and 1527 cm^{-1} along with additional peaks at 1360 cm^{-1}, 1244 cm^{-1} and 1449 cm^{-1} that depicted the carbon of chitosan having the carboxylic and hydroxyl stretches. The marked shift in the amide bond (N-H bend) and extended peaks of hydroxyl in the formed CDP derivative clearly represented the successful conjugation of protamine and PEG diamine into the chitosan backbone. The spectrum of diamine PEGylated chitosan (CD) is given in Appendix A6-Fig 2

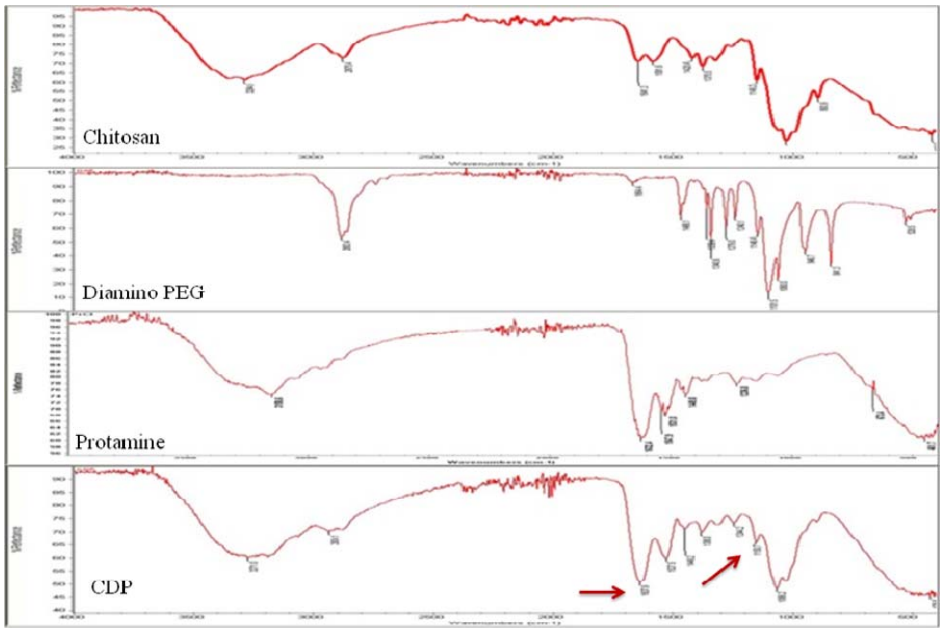

Fig 16 Infrared spectroscopy for evaluation of chemical groups in the conjugated CDP derivative. FTIR spectrum of chitosan, PEG diamine, protamine and the conjugated product CDP is displayed.

Furthermore the conjugation was affirmed by ^{1}H NMR in Fig 17 that revealed distinct peaks corresponding to the methylene protons of PEG diamine at 3.5 ppm (Liu & Lin, 2012). The peak at 4.9 ppm was attributed to the protons of the anomeric carbon of chitosan and the peak at 3.2 ppm was attributed to the proton connected to C-OH group of chitosan. Peak at 1.7 ppm corresponded to the methylene protons of protamine (Awotwe-Otoo et al., 2012). The presence of the peaks related to protamine and PEG diamine in the NMR spectrum suggested the successful conjugation of these moieties onto the chitosan polymer backbone. In accordance with Jintapattanakit et al. (2008), the degree of substitution of PEG diamine and protamine was calculated to be 28.75 % and 37.75 %. respectively which illustrated the successful conjugation.

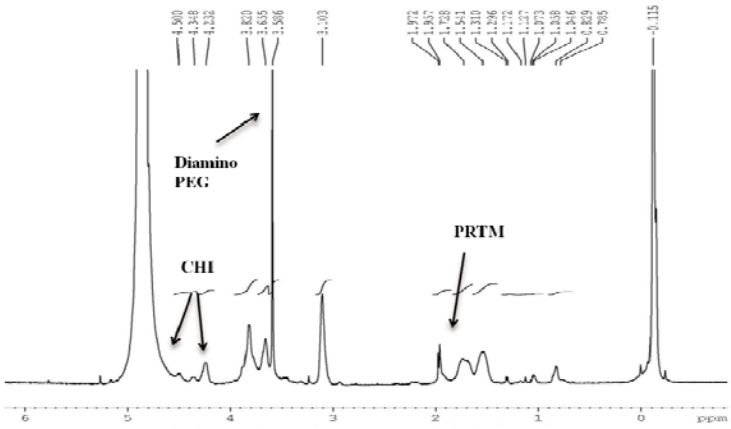

Fig 17: ^{1}H NMR of protamine grafted PEG diamineylated chitosan.

The thermal property of CDP was evaluated by DSC analysis by comparing with the parent chitosan compound. From the DSC curve in Fig 18, it was clear that the crystalline nature of CDP was different from that of chitosan. In chitosan, the DSC curve showed a sharp peak at 163.08˚C which indicated the melting point of depolymerised chitosan derivative. The DSC curve of the synthesised conjugate CDP gave a melting peak at 186.16˚C and the shift in the endothermic peak from the parent compound is due to the successful incorporation of PEG diamine and protamine in the chitosan.

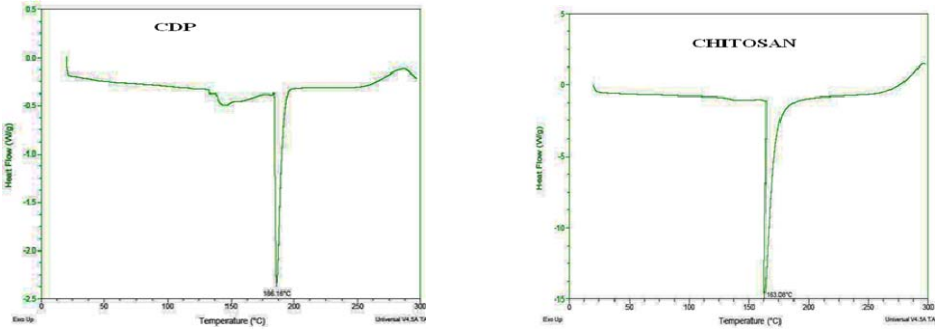

Fig 18: DSC analysis of CDP and chitosan

The effect of the polymer CDP to induce endosomal escape in the cell was investigated with acid base titration method. In Fig 19, against the addition of 0.1 N

HCl, the pH of CDP solution initially reached the acidic pH at a quick pace but then started to resist acid titration in the range between 4-3 which indeed required excess amount of HCl. Nearly 1200 µL of 0.1N HCl was required to reach till pH 3 and the buffering ability was compared to unmodified chitosan which had very less buffering capacity whereas PEI had exceedingly good amount of buffering range. Therefore substitution of protamine and PEG diamine into the chitosan polymer has benefitted the parent polymer with enhanced buffering capacity.

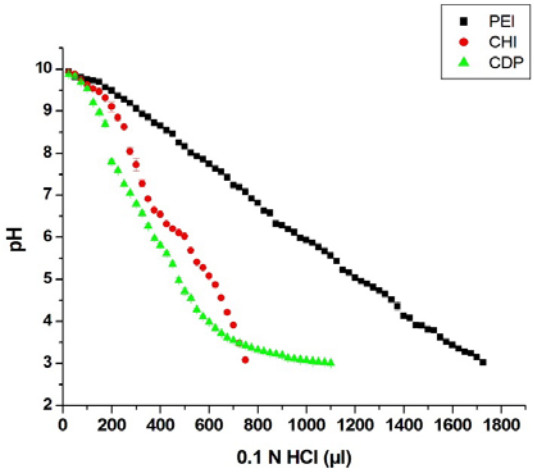

Fig 19. Analysis of buffering capacity of CDP derivative. Acid base titration of PEI 25 kDa, unmodifiedchitosan (CHI) and CDP polymer against 0.1 N HCl. The values provided are mean ± SD and n=3 with standard deviation found to be very negligible.

4.3.2 Characterisation of Nanoparticle-CDP and DNA interaction

4.3.2.1 Nanoparticle size measurement and zeta potential

By means of dynamic light scattering (DLS), the nanoparticles that fell in the ratios between 1:4 and 1:8 had size within the range of 200nm. The triplicates performed maintained the size range within the same polyplex ratios and ratios beyond the mentioned values on either side gave inconsistent values for size. Zeta

potential was found to be positive for the polyplex ratios even after being bound to negatively charged DNA and charges were optimised in triplicates. Table 2 listed both nanoparticle size and zeta potential. It was also observed that 1:7 had a size range coming close to 100 nm and an appreciable surface charge of +21 mV that was considered effective for cell uptake. The particular CDP/DNA ratio of 1:7 corresponding to their w/w amounts was adopted therefore for further nanoparticle characterisation study.

Table 2: Particle size and zeta potential of CDP/ctDNA nanoparticles. The values given are Mean ± SD and n=3.

DNA/polymer ratio	Size (nm) ±sd	Zeta potential (mV) ± sd
1:4	271 ± 2.82	19.6 ± 3.3
1:5	170 ± 9.2	21.3 ± 6.4
1:6	203 ± 1.5	15.7 ± 9.3
1:7	117± 0.56	21.8 ± 3.85
1:8	136± 0.43	25.2 ± 1.25
1:9	396 ± 6.31	4.45 ± 3.3

4.3.2.2 Morphological observation by TEM analysis

With the help of transmission electron microscope, protamine conjugated diamine PEGylated chitosan (CDP) nanoparticles that consisted of plasmid DNA showed sizes much smaller than those obtained from the DLS data. Sizes less than 150nm were observed and the nanoparticles appeared as an assortment of spherical and ellipsoidal shapes. An average diameter of 80-150 nm was observed in the TEM

image in Fig 20. The size range came within the limits that were suitable for gene delivery applications.

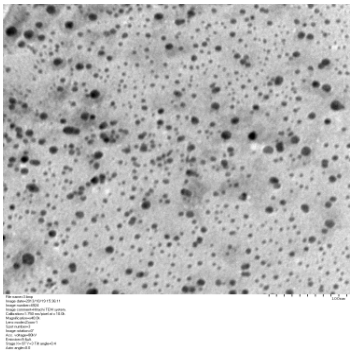

Fig 20: TEM observation of CDP polyplex. Scale bar is 200 nm.

4.3.2.3 Electrophoretic analysis of CDP nanoparticle

The binding strength of protamine grafted diamine PEGylated chitosan (CDP) with plasmid DNA was assessed by running the polyplexes formed in varying ratios in an agarose gel immersed in TBE buffer. It was revealed that except for the last two ratios all the rest had excellent retardation ability with the luminance seen inside the wells indicating DNA to be bound to the polymer with electrostatic bonds (Fig 21A). From ratio 1:3 to 1:9 the gel retardation was obvious with very little invincible leaking of DNA. The control lane had control plasmid DNA which appeared in the lane. Meanwhile the ratios treated with DNase enzyme did not show any release of the DNA in the lanes in Fig 21B and faint white halo like appearance was seen around the wells. The pDNA was well protected by the polymer, hidden inside the wells and hence any sort of DNA trail was absent in the lanes. The presence of the protected or hidden nucleic acid in the DNase treated CDP nanoparticles were further established by heparin affinity binding. The same polyplex samples after incubation with DNase was then treated with heparin to create

preferential affinity binding for the chitosan derivative (Fig 21C). Since heparin is highly negative anion, the interaction between heparin and CDP polymer would be possible. Hence the bound DNA was released and therefore the lanes had smear kind appearance of the released DNA.

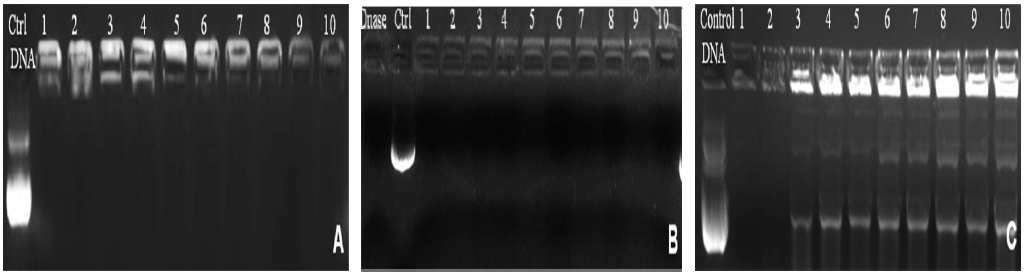

Fig 21: Agarose gel electrophoresis performed on CDP/pDNA complexes. The DNA retardation ability of the polyplex was determined. In Fig 17(A) Lane ctrl DNA consists of the control (2 µL DNA). Lanes 1–10 have polyplex ratios 1:1 to 1:10 (B) Protection of pDNA against DNase I after complexation with CDP. Lane DNase refers to DNA treated with enzyme; lane ctrl refers to plasmid alone, lanes 1-10: CDP polyplex ratios 1-10. (C) heparin binding affinity for CDP polymer and DNA released from polyplexes. Lane control DNA consists of plasmid DNA alone; Lane 1: pDNA treated with 2U of DNase. Lane 2-10: CDP polyplex ratios 1-9.

4.3.3 Blood compatibility and Cytotoxicity study of CDP polymer

4.3.3.1 Hemolysis and RBC aggregation

The blood compatibility was analysed by performing hemolysis, RBC aggregation study and protein adsorption. Although being cationic in nature, CDP did not show any hemolysis which indicated that red blood cells were not likely to get damaged on interaction with chitosan derivative. The % haemolytic activity was well within the permissible range of below 1 % for four different concentrations of

CDP treated red blood cells (Appendix A2-Table 2). Further criteria to be investigated were the tendency of eythrocyrtes to get aggregated during any intravenous administration of polymer materials. Hence CDP (1 mg/mL) at a maximum concentration of 100 μg was incubated with equal volume of saline rinsed red blood cells. In Fig 22A, RBC aggregation was completely ruled out with the cells showing intact morphology. Saline treated RBC (Fig 22B) represented the negative control devoid of any RBC aggregation that was similar to the RBC morphology as seen in CDP treated RBC. Meanwhile PEI treated RBC (Fig 22C) exemplified the kind of aggregation that occurred when the polymer was toxic and considered positive for reference.

4.3.3.2 Plasma protein interaction with CDP polymer

Furthermore analysis was performed to assess the association of serum proteins in response to CDP in blood. Plasma proteins incubated with two varying concentrations of CDP was run in native gel electrophoresis. Absence of any interactions with CDP polymer and the plasma proteins would lead to the visualization of protein bands in the gel indicating that the derivative does not result in the removal of serum proteins from the blood plasma as the polymer is incapable of forming complexes with plasma proteins. In CDP loaded plasma samples the lanes of Fig 22D showed the serum proteins in stacked arrangement in the gel after Coomassie blue staining. Normal saline does not cause any protein adsorption in the blood plasma and therefore saline treated plasma was taken as the control that showed the stack of protein bands which was similar to the lanes of CDP treated samples. Both concentrations of chitosan derivative revealed all the protein bands in

the gel as seen in the normal saline which reflected that CDP polymer was not likely to cause any protein adsorption.

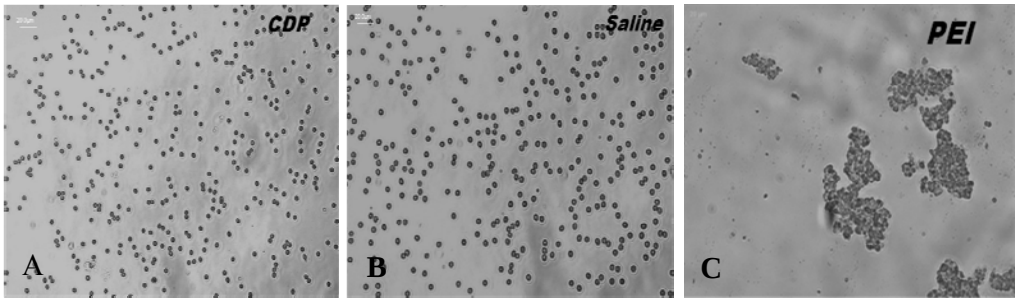

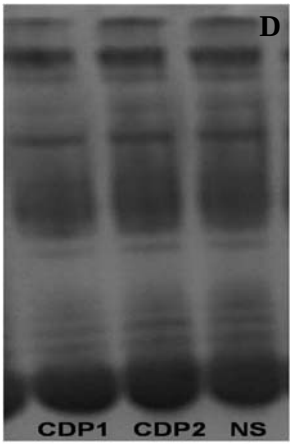

Fig 22: RBC aggregation studies with (A) CDP derivative (B) with normal saline (C) with PEI 25 kDa (20 X magnification for RBC) (D) Plasma protein interaction with CDP (1 mg/mL); Lanes CDP1, CDP2 represent polymer in 50 &100 µg and lane NS is normal saline, the control.

4.3.3.3 Cytotoxicity evaluation of CDP polymer

Before implementing for further *in vitro* studies, the toxicity of CDP (1 mg/mL) polymer in varying concentrations was tested in glioma C6 cells. All the four concentrations showed more than 85 % cell viability in Fig 23 which affirmed that the chitosan derivative did not cause any lysis or damage to the cell integrity. The positive control Triton X-100 represented the toxic effect on cells while medium MEM: DMEM/F12 Ham alone was considered to be the negative control. Cell viability of CDP was found to be comparable to the medium control. Both chitosan (CHI) and PEI 25 kDa added in 50 µg concentration displayed toxicity to the cells. Toxicity of unmodified chitosan is due to its solubilisation in acidic medium.

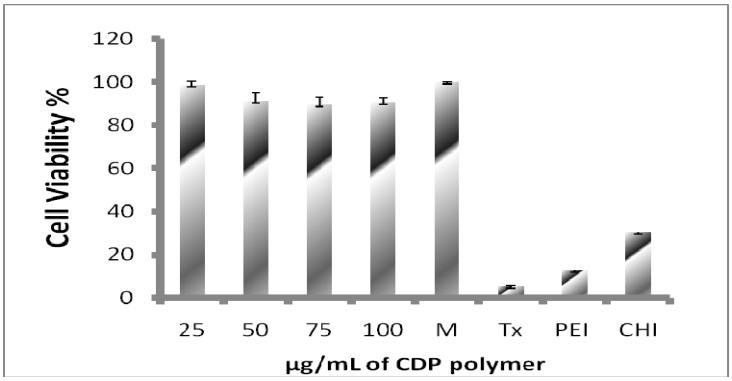

Fig 23: Cytotoxicity of CDP polymer. **M** refers to medium MEM: DMEM/F12 Ham was the control and **TX** coded for Triton X-100. Other controls were **CHI**: unmodified chitosan (50 µg) and **PEI** (25 kDa) (50 µg). The values given are mean ± SD and n= 3.

4.3.4 In vitro cell study with CDP/pDNA nanoparticle

4.3.4.1 Evaluation of Cellular Uptake

A four well plate seeded with the glioma C6 cells were treated with two ratios of CDP polymer 7 and 8 as they had the optimum size and zeta potential. Cellular uptake of CDP polyplexes with the YOYO tagged plasmid DNA was very impressive with fluorescence distribution observed in most of the cells. The image of one of the CDP nanoparticle ratio is represented here (Fig 24A). Quantitative estimation of the cell uptake of CDP nanoparticles was performed in flow cytometry that revealed more than 90 % of cellular uptake. The cell lines displayed a clear shift in the fluorescence in Fig 24B which depicted the enhanced cell uptake of CDP/YOYO tagged pDNA nanoparticles when compared to the unstained cells in Fig 24C.

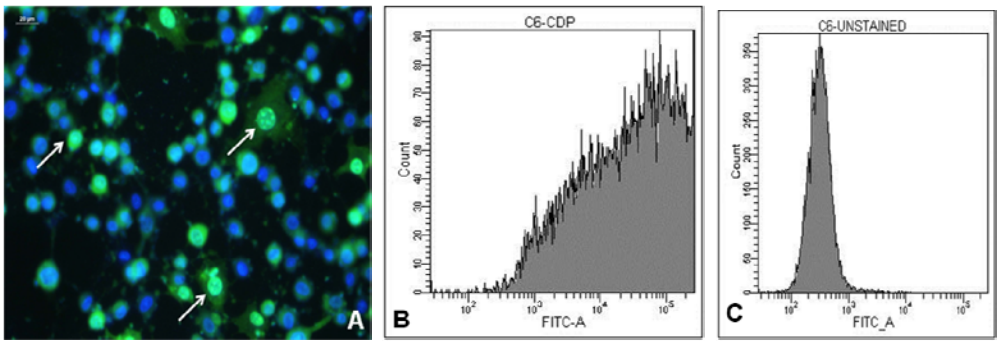

Fig 24: A) Fluorescent image of cellular uptake of CDP nanoparticles. B) Flow-cytometric analysis of the cell uptake of CDP nanoparticles by C6 glioma cells upon incubation for 3 h in comparison with C) control C6 cells.

4.3.4.2 Endocytosis inhibition Study

It is a matter of interest to evaluate the specific pathways of endocytosis for the uptake of CDP polyplexes in glioma cells. Inhibitors such as chlorpromazine that is specific for clathrin pathway revealed accumulation of fluorescent nanoparticles in peripheral regions of the cells rather than being inside the nucleus (Fig 25A). Dynasore inhibitor that is specific for dynamin dependent clathrin pathway showed reasonable amount of CDP nanoparticle uptake (Fig 25B). Meanwhile macropinocytosis also has not been inhibited by the addition of amiloride inhibitor for uptake (Fig 25C). And the receptor mediated pathway also was hardly inhibited by the conjugate protamine and cell uptake of CDP polyplexes was therefore observed (Fig 25D). In fact it was noticed that the inhibitor filipin had blocked the caveolae pathway which caused reduction of entry of CDP nanoparticles into the cells (Fig 25E). Consequently it is discernible that caveolae pathway would be the most engaged pathway among the other pathways for CDP nanoparticle uptake.

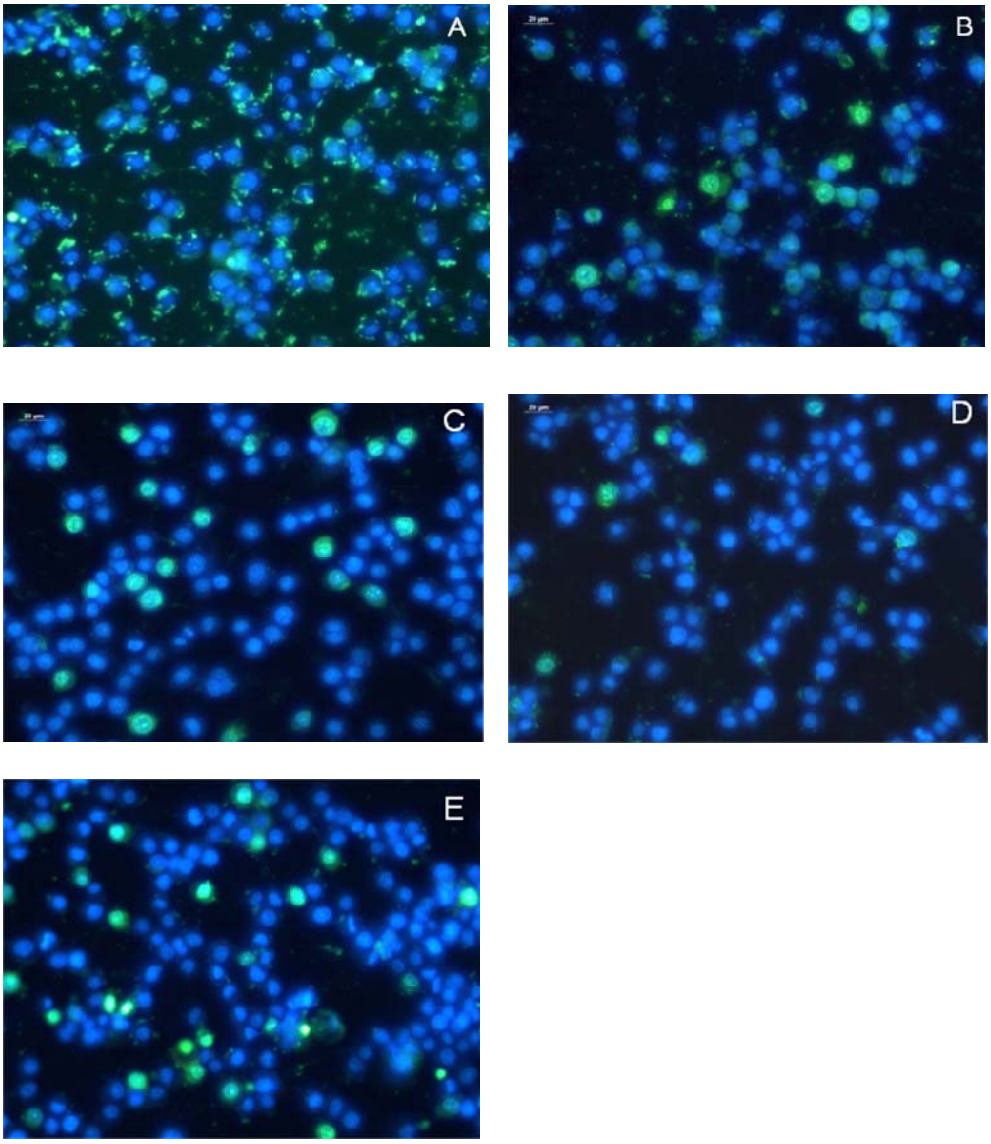

Fig 25: Endocytosis inhibition study of CDP nanoparticles. Fluorescent images of the efficacy of cell uptake were evaluated by blocking the endocytosis pathways, prior treatment with CDP/DNA complexes in ratio 7:1 (CON/YOYO tagged pDNA) in C6 glioma cells, with the following inhibitors A) represent chlorpromazine treated cells B) Dynasore treated cells C) Amiloride treated (D) Filipin treated cells showed very less accumulation of polyplexes around the cells (E) Protamine treated cells. Magnification and scale bar represent 40 X and 20 μm respectively.

4.3.4.3 Transfection with p53 Gene expression

After the cellular uptake of CDP polyplexes, it is necessary that the gene of interest should be expressed in order to testify the gene delivery efficacy of protamine conjugated PEG diamineylated chitosan nanoparticle. Hence the transfection activity was assessed by the expression of p53 plasmid which led to the apoptosis condition of cells and this was evaluated by the live dead assay kit. CDP was complexed with p53 gene and added to C6 cells in the ratio 7:1. Apoptosis expression of p53 was observed in Fig 26A after 24 h incubation where the cells transfected with p53 gene displayed the red dye stain of ethidium homodimer that gained entry into those cells whose cell membranes were perturbed due to apoptosis. The same nanoplex ratio 7 that had shown enhanced cellular uptake before exhibited the significant cell death. Almost 90 % cell death has occurred without any trace of live cells. The cells emitted fully red fluorescence due to the dispersion of ethidium homodimer uniformly in the cells. Plasmid alone treated cells (fig 26B) did not bring about transfection and hence cells were live and stained green colour by calcein AM. PEI transfected nanoparticles (Fig 26C) also showed cell death and the result was comparable to that obtained with the chitosan derivative, CDP.

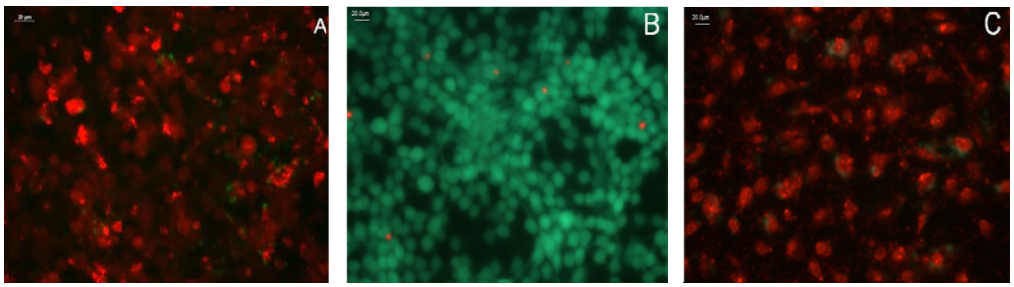

Fig 26: Transfection Assessment via Live Dead assay in C6 cells. Live Dead assay showed the staining of live cells by calcein (green) and dead cells by ethidium

homodimer (red). Glioma cells treated with A) CDP/p53 polyplexes in ratio 7 B) only plasmid p53 C) PEI/p53 nanoparticles. Magnification and scale bar represent 40 X and 20 μm respectively.

4.4 Ornithine grafted chitosan polycation (CON) for gene delivery

4.4.1 Synthesis and chemical characterisation of CON

As part of chemical modification in 120 kDa chitosan, the amino acid ornithine was mainly selected for derivitisation to enhance the solubility of chitosan as well as to possess excess concentration of free primary amines that would help in series of chemical interaction with genes for nanoparticle formulations. The lyophilised product was labelled CON, a thin white material which was powdered for dissolution. An illustrative representation of the synthesis of CON is depicted in Fig 27.

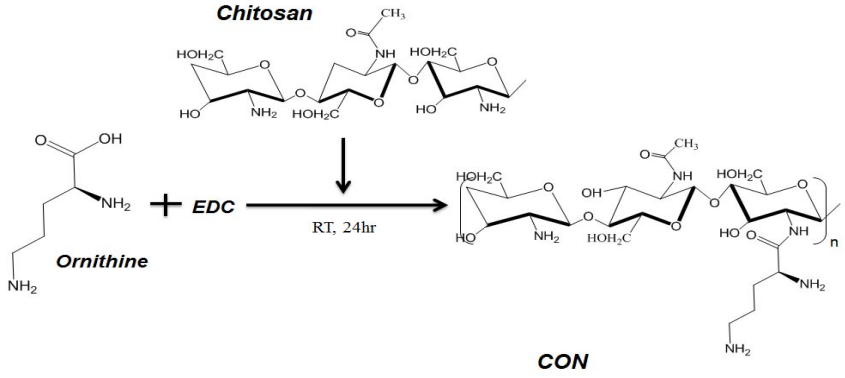

Fig 27: Proposed reaction scheme of synthesis of CON. Depolymerised chitosan is reacted with ornithine to yield chitosan ornithine conjugate (CON).

The extent of conjugation of ornithine in chitosan was estimated by the percentage of free primary amine groups in the modified chitosan. The colorimetric biochemical assay TNBS allowed the comparison of the amount of amines in chitosan, glucosamine as the reference and chitosan ornithine. Graphical

representation of the percentage of free primary groups in Fig 28 revealed that unmodified chitosan of 120 kDa had good share of free amine group than glucoamine that was regarded to be 100 %. However the graph showed an increase in the amount of amine groups in the chitosan derivative which was contributed by the substitution of ornithine into the chitosan backbone. CON on reaction with 2,4,6-trinitrobenzenesulfonic acid (TNBS) showed the absorbance corresponding to the available free amine groups that signify the affluence of ornithine substitution.

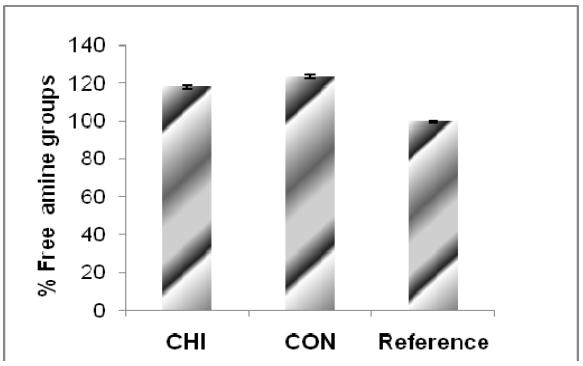

Fig. 28: TNBS assay for determination of free amine groups in chitosan (CHI), chitosan ornithine conjugate CON and glucosamine as the reference. The values given are mean ± SD and n= 3.

The IR spectra displayed the distinct peaks of chitosan, ornithine and CON in Fig 29 stacked together. In chitosan, bands were observed at 3284 cm^{-1} and 1581 cm^{-1} which could be assigned to stretching vibrations of hydroxyl group and bending vibrations of amine groups respectively. The peaks around 893 cm^{-1} and 1149 cm^{-1} correspond to saccharide structure of chitosan. The characteristic carbonyl stretching of primary amide in chitosan has also been observed at 1641 cm^{-1} . In ornithine, the spectrum revealed carboxyl stretching at 1736 cm^{-1} and amine stretching peaks at 3015 cm^{-1}. Finally the conjugate IR spectra revealed the presence of hydroxyl

stretching vibration around 3293 cm^{-1}. The characteristic NH bending vibration of amide is also observed at 1535 cm^{-1} and the amide C=O at 1631 cm^{-1}. The main chemistry is the amide formation between chitosan amine group and carboxylic acid group of ornithine. Further we also observed a change in the C-O stretching due to conjuagation with ornithine. The absence of the carboxyl stretching at 1736 cm^{-1} in the conjugate and the presence of hydroxyl stretching at 3293 cm^{-1} were consistent with the formation of amide group. In short, the IR bands observed in the conjugate spectra were very consistent with amide formation and covalent coupling of chitosan and ornithine.

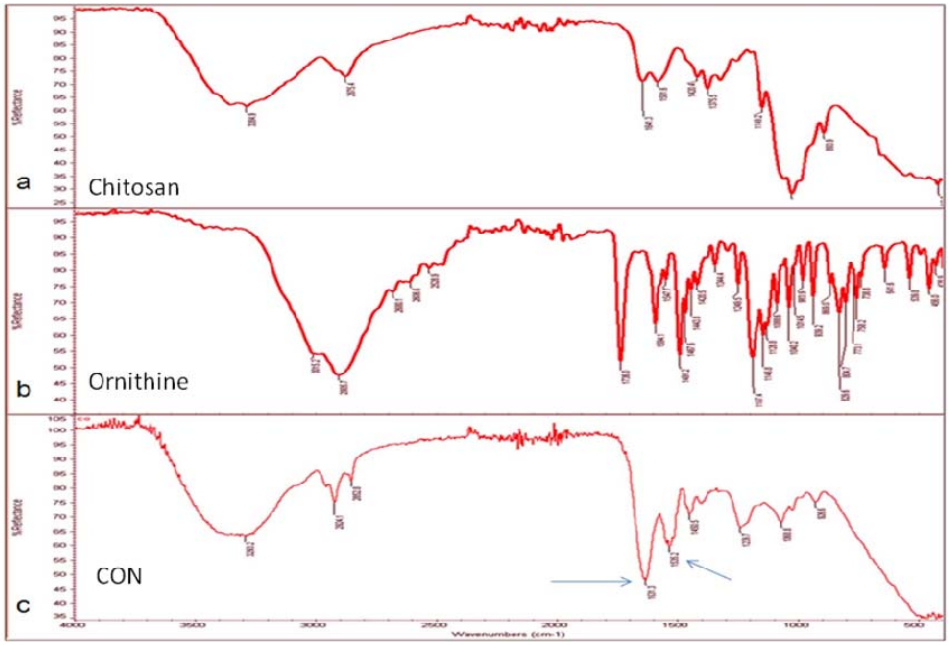

Fig 29**:** Infrared spectroscopy for evaluation of chemical groups in the functional entities of the CON derivative. FTIR of chitosan, ornithine and chitosan ornithine conjugate (CON).

The conjugation of chitosan to ornithine was further supported by ^{1}H NMR analysis. In Fig 30, the protons contributed by methyl group of chitosan occured at

2.63 ppm (Knight et al., 2007) along with proton chemical shift at 3.3 ppm and 4.85 ppm which corresponds to the protons of glucosamine residue (Shelma & Sharma, 2011). In comparison to ornithine (Williams et al., 1982) and (Kumar et al., 2010), the CON spectrum had proton chemical shift occur at 1.5 ppm since the proton intensity provided by both β and γ- carbons of ornithine fall in the region between 2 and 1 ppm in the conjugate. And integration of protons of δ-carbon of ornithine into the chitosan backbone was also found to resonate at 3.2 ppm. Furthermore, the degree of substitution of ornithine was determined to be 30.8 % which demonstrated the successful conjugation of CON polymer derivative.

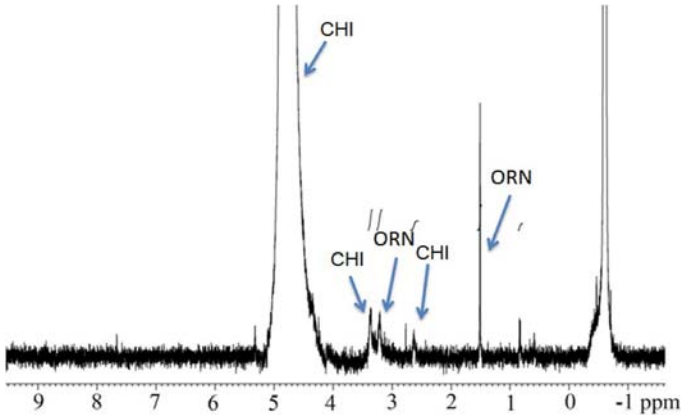

Fig 30: ^{1}H NMR spectra of CON.

The melting temperature of CON was determined by DSC analysis and compared to that of the parent compound chitosan. The thermal property of the polymers was represented by the DSC curve in Fig 31 that suggested the difference in the crystalline nature between CON and chitosan. The DSC curve of CON exhibited a sharp peak at 175.84˚C which was different from the distinct peak of chitosan at 163.08˚C. The change in the peak has been literally contributed by the

incorporation of ornithine into the chitosan structure that has raised the melting temperature of the synthesised derivative CON.

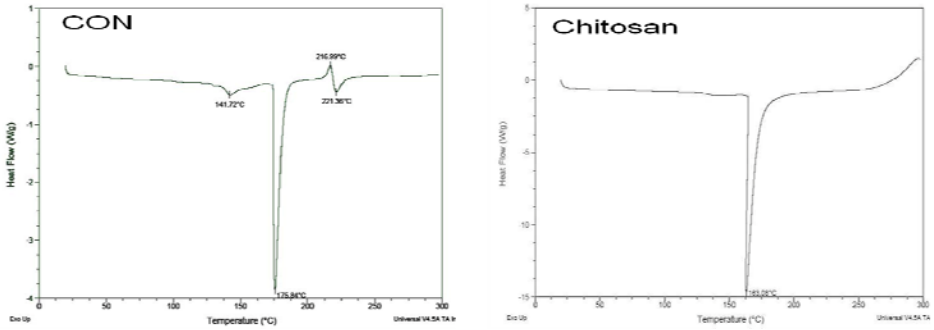

Fig 31: DSC analysis of CON and chitosan.

The presence of protonable amine groups in chitosan ornithine conjugate would enable significant buffering activity of CON nanoparticles that could lead to endosomal disruption and cause nanoparticles escape into the cytosol. In Fig 32, chitosan ornithine conjugate resisted acid titration within pH 6-4 and therefore a titration volume nearly 950 µL exceeding the unmodified chitosan was observed. Acid titration of CON was performed against parent compound chitosan 120 kDa and PEI (25 kDa) for comparison. The presence of excess amine groups in PEI attributed to its high buffering capacity.

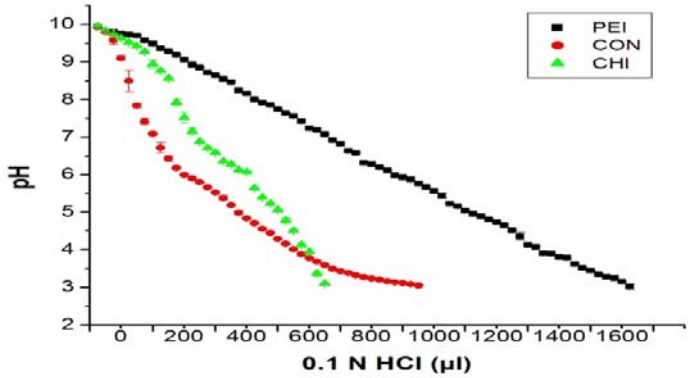

Fig 32: Analysis of buffering capacity of CON derivative. Acid base titration of PEI 25 kDa, unmodified chitosan (CHI) and CON polymer against 0.1 N HCl. The values provided are mean ± SD and n=3 with standard deviation found to be very negligible.

4.4.2 Characterisation of Nanoparticle: CON and DNA interaction

4.4.2.1 Nanoparticle size determination and zeta size potential

Table 3 displayed the sizes and the zeta potential of the nanoparticles in the prepared ratios. It was seen that except for the lowest ratios 1 and 2, all the rest had sizes in the range of 100nm and 150nm. After the compact folding of oppositely charged DNA and CON polymer, an overall cationic charge density of +17mV to +21mV was formed on the nanoparticle surface. Ratios above 9 had certain inconsistency in both size and zeta potential and are not shown here. *In vitro* cell studies were performed using nanoparticles with a ratio of 3 and a size of 100 nm with a favorable overall positive charge.

Table 3: Particle size and zeta potential of CON/ctDNA nanoparticles. The values given are Mean ± SD and n=3.

DNA/polymer ratio	Size (nm) ±sd	Zeta potential (mV) ± sd
1:3	99.6 ± 1.8	17.1 ± 2.5
1:4	143 ± 6.1	17.5 ± 3.96
1:5	137 ± 7.7	22 ± 1.4
1:6	145 ± 10.9	20.6 ± 2.56
1:7	181 ± 10.7	21.9 ± 1.83
1:8	131 ± 6.6	21.1 ± 2.4
1:9	118 ± 9.09	17.8 ± 5.76

4.4.2.2 Morphological Observation by TEM and AFM

The size and shape of CON nanoparticle was established from Fig 33A where TEM analysis showed nanoplexes within 100 nm range having an appearance as of a pattern of distinct speckles. It has been assigned that the shape of nanoplex is dependent on the affinity binding of opposite charges present in both polymer and DNA and thereby a perfect spherical shape is hardly found as both the components are dynamic in the suspension state. Coincidently similar type of distorted shapes of chitosan DNA constructs has also been reported (Sajomsang et al., 2011). Direct confirmation of size was possible by observing the surface topography image of CON nanoplex using AFM technique. Although there was a large density of nanoplexes in the given surface area, the image (Fig 33B) showed a uniform distribution of the complexes, having size measurement with atleast one dimension of the nanoplex falling below 100nm range.

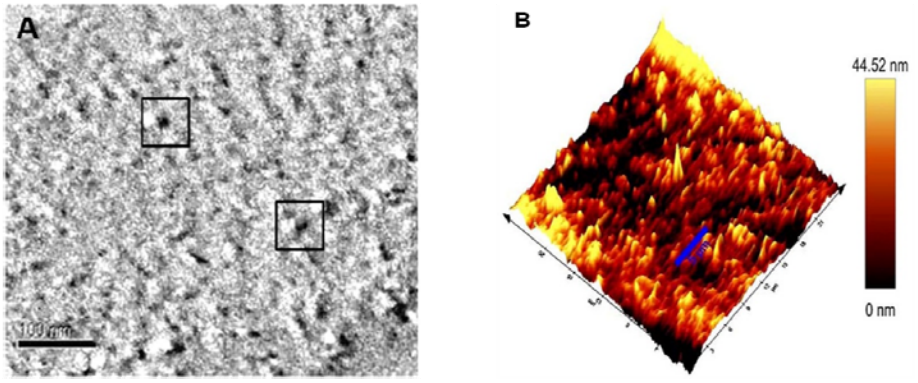

Fig 33: Nanoparticle Morphological analysis. A) TEM observation. CON nanoparticle 1:3 ratio show size range within 100nm B) AFM surface topography of CON nanoparticles in 1:3 ratio.

4.4.2.3 Electrophoretic analysis of CON nanoparticle

The same ratios that were used for size determination was adopted to run the 1 % agarose gel for checking DNA polymer stability. The gel image, Fig 34A clearly showed that DNA was retarded inside the wells when compared to the control in the first and last lane having freely moving DNA without the polymer. The lane which had DNA alone appeared as smear while bright intensity was observed in the wells that retained the nanoparticles. The stability was further tested by subjugating the same ratios for DNase degradation and it was seen in Fig 34B that pDNA was completely protected against enzymatic attack. The luminance was observed in the wells as broken and faint with absolutely no smear of DNA in the lanes. The first lane had the pDNA alone degraded by DNase and the last well consisted of pDNA alone with the DNA smear in the lane. For heparin binding affinity study (Fig 34C), the same nanoplex ratios were again treated with DNase followed by heparin incubation and the samples showed the DNA released in the lanes. This emphasized that CON nanoplexes had masked the DNA well against nuclease attack but in contact with heparin, the protected DNA got released from the nanoparticles indicated by the DNA smear in the lanes since cationic CON showed competitive affinity binding towards a highly negative anion as heparin.

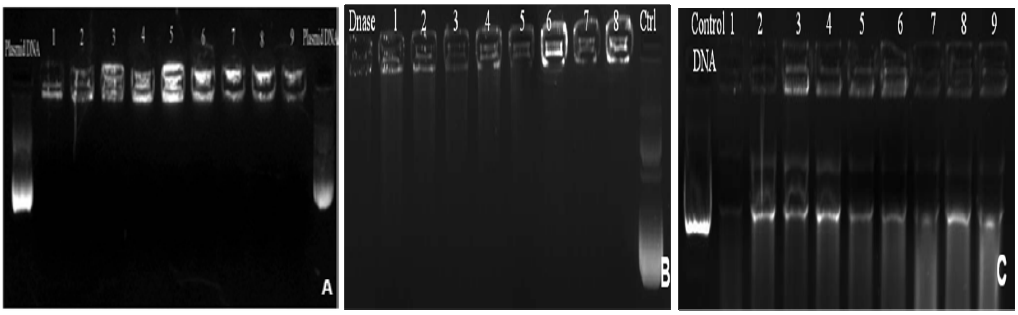

Fig 34: Agarose gel electrophoresis performed on CON/pDNA complexes. The DNA retardation ability of the polyplex was determined. A) Agarose gel electrophoresis has chitosan ornithine (CON) nanoplex loaded from lanes 1-9 in the nanoplex ratios 1:1 to 1:9. Plasmid DNA is loaded in the first and last lanes which act as control. B) Protection of pDNA against DNase I after complexation with CON. Lane DNase refers to DNA treated with enzyme; lane ctrl refers to plasmid alone and lanes 1-8 is loaded with CON nanoparticle ratios 1-8 (C) heparin binding affinity for CON polymer and DNA released from nanoparticles. Lane control DNA consists of plasmid DNA alone; Lane 1: pDNA treated with 2U of DNase. Lane 2-9: CDP nanoparticle ratios 1:1 to 1:8.

4.4.3 Blood compatibility and Cytotoxicity study of CON polymer

4.4.3.1 Hemolysis and RBC aggregation.

Red blood cells incubated with varying concentrations of CON polymer showed negligible aggregation with hardly any cell lyses. The percent hemolysis of CON conjugate was far below the permissible index value of 1 % hemolysis for all the four concentrations of CON polymer while positive control elicited 100 % hemolysis (Appendix A3-Table 3). Hence CON polymer could be declared biocompatible which was further supported by visualisation of RBC (Fig. 35A and B) treated with 100 µg concentration of CON (1 mg/mL) conjugate. There was no aggregation and cells were intact much similar to as observed with the control normal saline treated RBC cells. PEI treated RBC was regarded as the positive control that showed agglomeration of cells that indicated the hemotoxic effect of the polymer (Fig 35C).

4.4.3.2 Plasma protein interaction with CON polymer

To rule out any undesired interactions with the binding of plasma proteins with CON polymer, the extent of plasma protein adsorption was established by analysing native PAGE electrophoresis. Reactive polymers that interact with plasma proteins would result in formation of complexes and eventually lead to the removal of free plasma proteins from the blood. Since normal saline does not have any effect on the plasma proteins, the serum proteins remain in the plasma and would be presented as bands in the gel. In Fig 35D, the lanes loaded with concentrations at 50 µg and 100 µg of CON (1 mg/mL) showed an array of protein bands of the plasma as observed similarly in the saline control referring to absence of protein adsorption by the polymer. Therefore the stacked protein bands in the gel lanes indicated that CON polymer did not cause any undesirable responses when in contact with blood serum and was likely to be considered non toxic for *in vivo* studies.

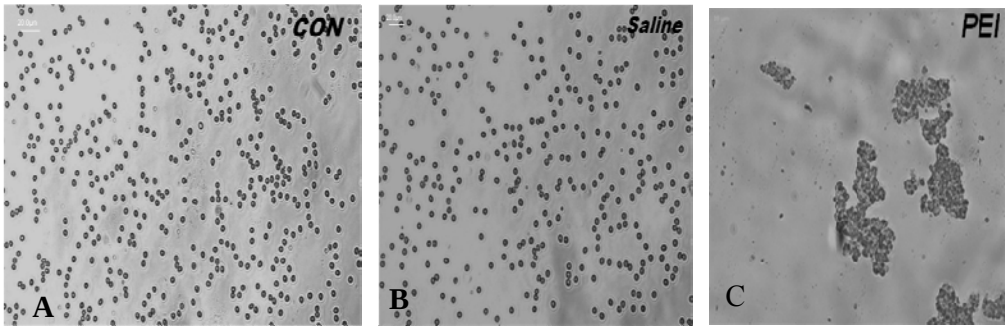

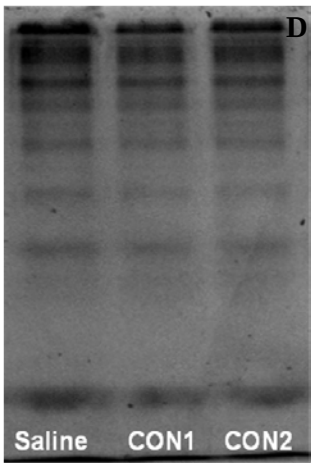

Fig 35: RBC aggregation studies with (A) CON derivative (B) with normal saline (C) with PEI 25 kDa (20 X magnification for RBC) (D) Plasma protein interaction with CON (1 mg/mL); Lanes CON1, CON2 represent polymer in 50 &100 µg and lane saline is the control

4.4.3.3 Cytotoxicity evaluation of CON polymer

The toxicity of the chitosan derivative in *in vitro* was assessed by performing MTT (3-(4,5-dimethylthiazol-2-yl)-2,5-diphenyl tetrazolium bromide) assay. The intracellular dehydrogenase activity of the CON treated cells was expressed in relative to that of the control (untreated) cells. The cells which were incubated with CON (1 mg/mL) polymer for 24 h had showed more than 80% viablity as deciphered from the graph (Fig. 36). The viability % was determined as percent of the viable cells with respect to the 100 % live cells of the control which was treated with medium alone. Triton X-100 that proved to be highly toxic for cells was the control for cytotoxic condition. Both chitosan (CHI) and PEI 25 kDa added in 50 µg concentration displayed toxicity to the cells. Toxicity of unmodified chitosan is due to its solubilisation in acidic medium. Triplicates were performed and statistical analysis was performed with respective standard deviations calculated.

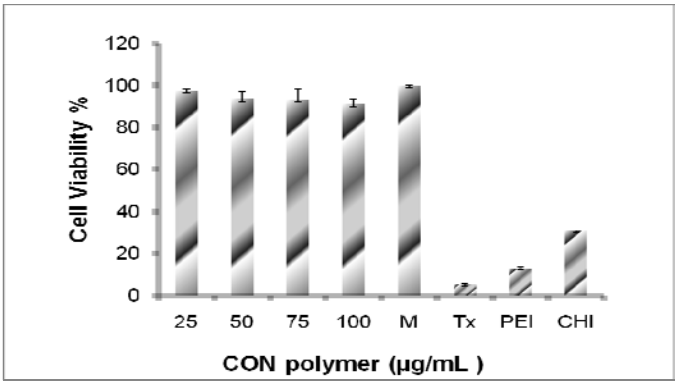

Fig 36: Cytotoxicity of CON evaluated by MTT assay. Cell viability % of C6 glioma cells after incubation with CON in four different concentrations. Controls were **M** that referred to medium alone and **TX** coded for Triton X-100. Other controls were **CHI**: unmodified chitosan and **PEI** (25 kDa). The values given are mean±SD and n=3.

4.4.4 In vitro cell study with CON/pDNA nanoparticle

4.4.4.1 Evaluation of Cellular Uptake

Glioma cells were treated with CON nanoparticle which consisted of the YOYO labelled plasmid. Enhanced cell uptake was observed after 4 h incubation with bright green fluorescence inside most of the cells which had internalized CON nanoparticles. Meanwhile cells treated with YOYO tagged plasmid alone showed very faint fluorescence in the outer regions of the cell and was compared as the control (Fig.37A and B). Orthogonal z-stacking analysis by confocal microscope also provided the same result with green fluorescence explicitly present in the cells (Fig 37C) and showed the in depth accumulation of the nanoparticles throughout the cell. Also quantitative estimation of the internalization was projected by flow cytometric analysis in Fig 37D with cell lines treated with CON nanoparticles having cells more than 90 % uptake. Flow cytometry count the fluorescence emitted from each cell and

therefore the unstained cells (Fig 37E) did not have the fluorescence as it was not treated by fluorescent tagged nanoparticles. In comparison to this control, the histogram of YOYO tagged CON/pDNA nanoparticles had the shift in the fluorescence range which counted the cells that internalized the tagged nanoparticles. Both fluorescent and confocal images supported the flow cytometry histogram

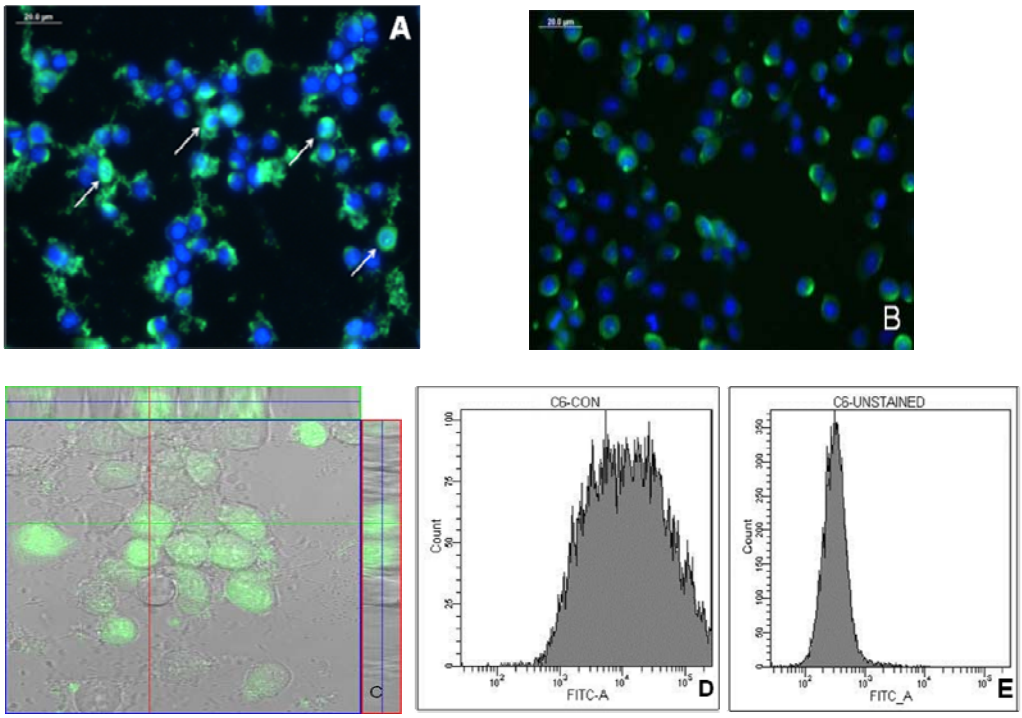

Fig 37: Cell uptake of CON/p53 plasmid nanoparticles. A) Fluorescent images of C6 cells treated with CON nanoparticles. Arrows indicate the uptake of CON in the nucleus. B) Control cells with tagged plasmid alone C) Confocal observation of nanoparticles. Flow cytometry estimation of D) cells stained with the tagged CON nanoparticles E) Unstained cells.

4.4.4.2 Endocytosis inhibition Study

Meanwhile, cells were treated with each inhibitor of the endocytosis pathway that would affect the rate of cell uptake of CON nanoparticles. This is featured by

both fluorescent and confocal microscopic images in Fig 38 which unveiled the actual pathways adopted by the CON/pDNA nanoparticles. Orthogonal analysis by z-stacking helped in identifying the localization of nanoparticles within and around the cells. Chlorpromazine treated cells showed very less uptake of nanoparticles in Fig 36A which indicated that blocking of clathrin mediated pathway prevented the access of nanoparticles inside the cells. The confocal image 38A1 gave evidence of very less amount of nanoparticle localisation only in the peripheral region of the cell. Modest movement of nanoparticles were viewed within the cytoplasm and perinuclear regions when cells were treated with filipin (Fig 38B and B1) and amiloride (Fig 38C and C1) which caused selective inhibition to caveolae and macropinocytosis pathway respectively. Dynasore, another specific inhibitor, seen in the clathrin mediated pathway also displayed accumulation of fluorescent labelled nanoparticles (Fig 38D and D1) at the peripheral regions of the cell. Cells treated with ornithine also did not show much inhibition which referred that receptor mediated pathway had less influence in cell uptake (Fig 38E and E1). Examining the orthogonal analysis of the z-stacks by confocal microscope demonstrated the cell uptake to be deducted on treatment with which inhibitor.

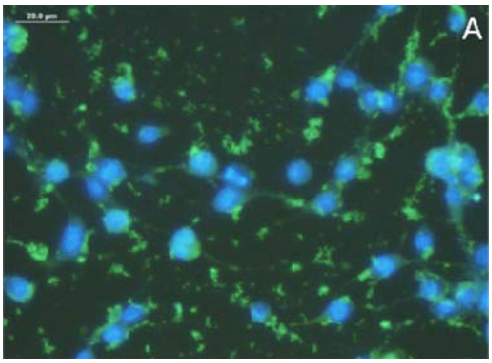

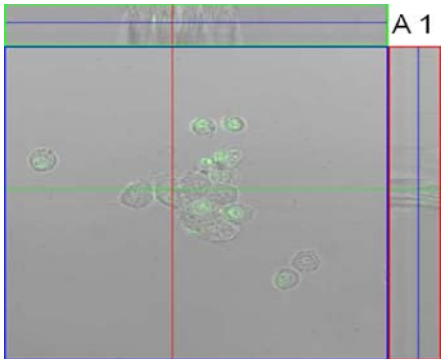

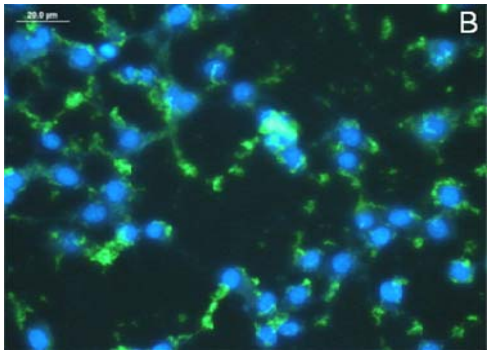
B

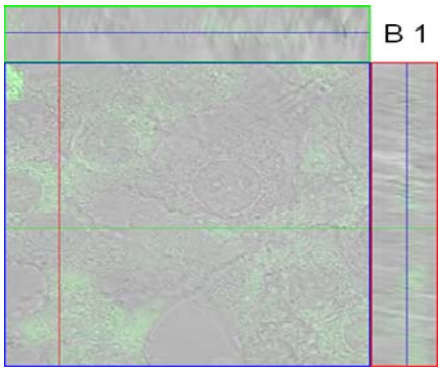
B 1

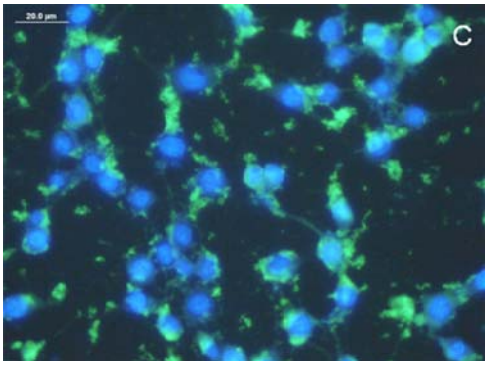
C

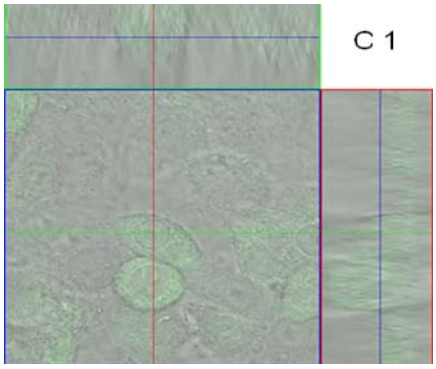
C 1

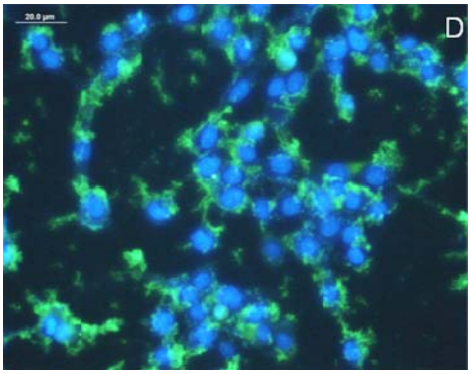
D

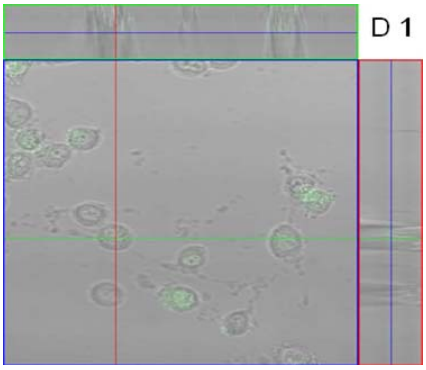
D 1

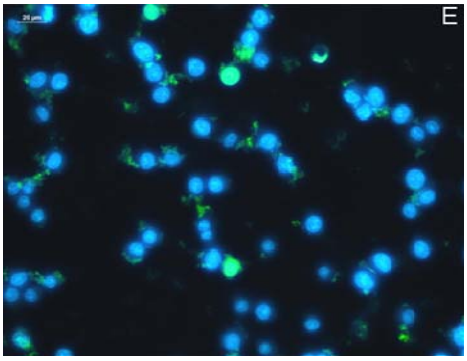
E

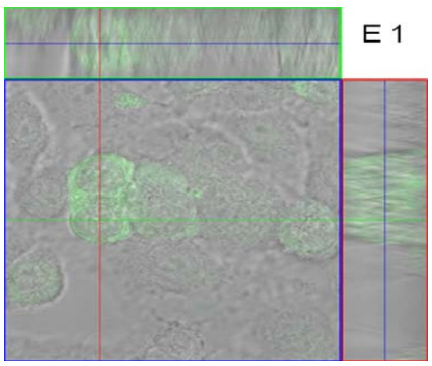
E 1

Fig 38: Fluorescent images of endocytosis inhibition study with CON/pDNA complexes in ratio 1:3 (DNA/CON) in C6 glioma cells. Magnification and scale bar is 40X and 20 μm respectively. Images (A) to (E) represented cells treated with a separate endocytic inhibitor prior incubation with CON nanoparticles. Therefore (A) represent chlorpromazine treated cells. (B) Filipin treated cells. (C) Amiloride treated cells. (D) Dynasore treated cells and (E) ornithine treated cells. Images A1 to E1 represented the z-stacking confocal images of the same inhibitor study.

4.4.4.3 Transfection with p53 Gene expression

Transfection efficiency of CON gene delivery system was evaluated with the Live Dead assay kit (Invitrogen). At a very low nanoparticle ratio 3:1, significant cell death was caused by CON nanoparticles and observed at the end of 24 h incubation. The image is shown Fig 39A with dead cells stained in red which had p53 apoptosis expression to be prominent. Cell line treated with CON nanoparticles had practically no live cells which would have been stained as green by the calcein AM dye as seen in the control cells that was treated with p53 plasmid alone (Fig 39B). Cells transfected with CON nanoparticles was able to unpack the p53 gene and release into the nucleus that led to its expression for apoptosis. Cells transfected with PEI also showed similar cell death (Fig 39C) and compared as positive control for establishing the gene delivery efficacy of CON nanoparticles.

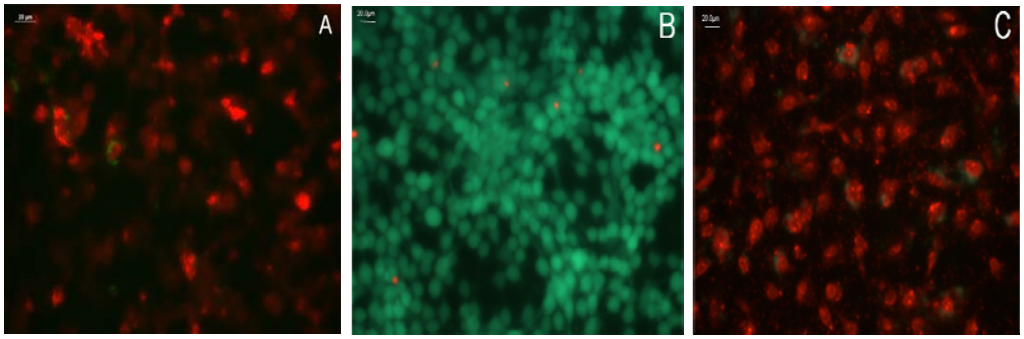

Fig 39: Transfection Assessment via Live Dead assay in C6 cells. Cells which were transfected with p53 plasmid had undergone cell death and were stained red while non transfected cells with p53 plasmid alone had live cells showing the green stain. Cells were transfected with A) CON nanoparticles in ratio 3 B) only the gene plasmid p53 and without nanoparticles C) with PEI/p53 nanoparticles. Magnification and scale bar represent 40 X and 20 μm respectively.

4.5 Spermine derivatized chitosan ornithine conjugate (COSM) for gene delivery

4.5.1 Synthesis and chemical characterisation of COSM

Since chitosan ornithine was found to be a promising gene delivery system, a targeted approach of conjugation in this delivery system was attempted. Polyamine such as spermine is one of the most sought after substrate for tumour cells metabolism and therefore was employed to conjugate chitosan-ornithine using DSC-DMAP coupling. The lyophilised product had a thin white film like appearance referred to as COSM. The scheme of synthesis is illustrated in Fig 40.

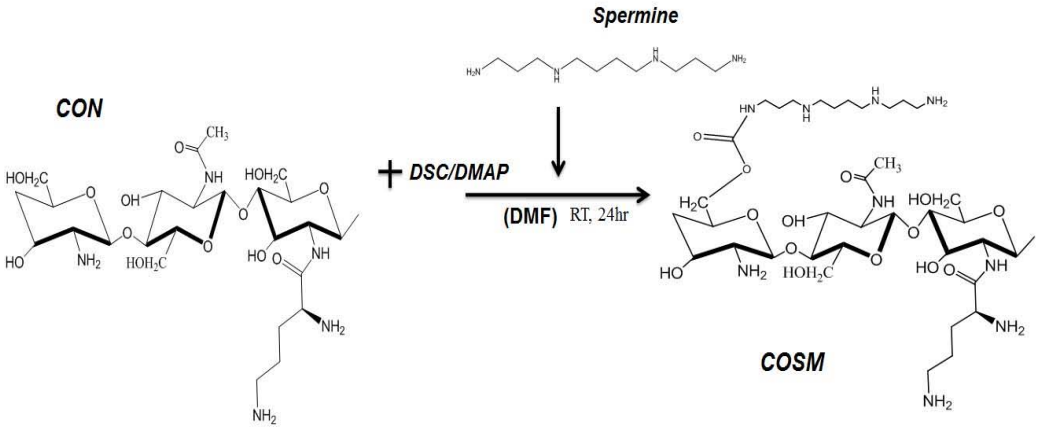

Fig 40: Schematic representation of synthesis of COSM polymer. Chitosan ornithine conjugate (CON) was reacted with spermine to yield spermine derivatised chitosan ornithine conjugate (COSM).

The percentage of free primary amine that is present in the synthesized chitosan derivative asserted the conjugation of spermine into the chitosan-ornithine backbone. In the biochemical assay, 2,4,6-trinitrobenzenesulfonic acid (TNBS) reacted with COSM and the absorbance correlated to the free primary amines available in the derivative. Graphical representation of the derivative COSM showed primary amine content of 126 % which indicated the excess amount of free primary amines contributed to chitosan ornithine conjugate by spermine substitution as in Fig 41. The conjugate was compared with glucosamine and the unmodified depolymerised chitosan of 120 kDa. Hence spermine derivatised chitosan ornithine polymer has achieved more free primary amines that would promote the cationic density for polymer protonation and strong electrostatic interactions with nucleic acids.

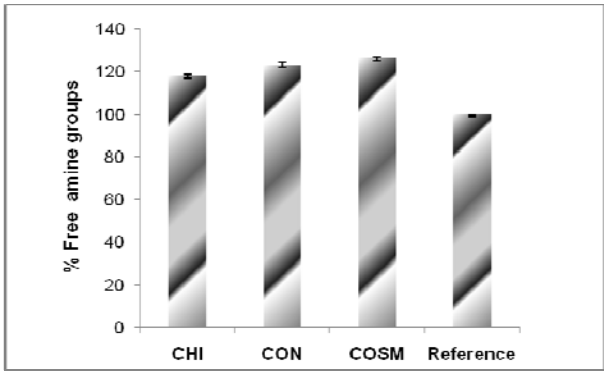

Fig 41: TNBS assay of COSM polymer compared to chitosan (CHI), chitosan ornithine (CON) and reference glucosamine. The values given are mean ± SD and n= 3.

The efficiency of conjugation was confirmed with FTIR spectra in Fig 42 in which the stacked array of chitosan ornithine conjugate, spermine and COSM was arranged. In chitosan ornithine conjugate, the characteristic NH bending vibration of amide was observed at 1535 cm^{-1} and the amide C=O at 1631 cm^{-1} revealing the amide formation between chitosan amine group and carboxylic acid group of ornithine. The COSM polymer displayed peaks at 3386 cm^{-1} and 1647 cm^{-1} which could be assigned to stretching vibrations of hydroxyl group and amine groups. And the C-H stretch of spermine at 2857 cm^{-1} was shifted to 2869 cm^{-1} in the COSM derivative. The chitosan ornithine complex on conjugation with spermine further formed additional amide linkages at 1637 cm^{-1} , 1597 cm^{-1} and 1560 cm^{-1} while the saccharide structure of chitosan was retained at 1075 cm^{-1} (skeletal vibrations of C-O-C stretching).

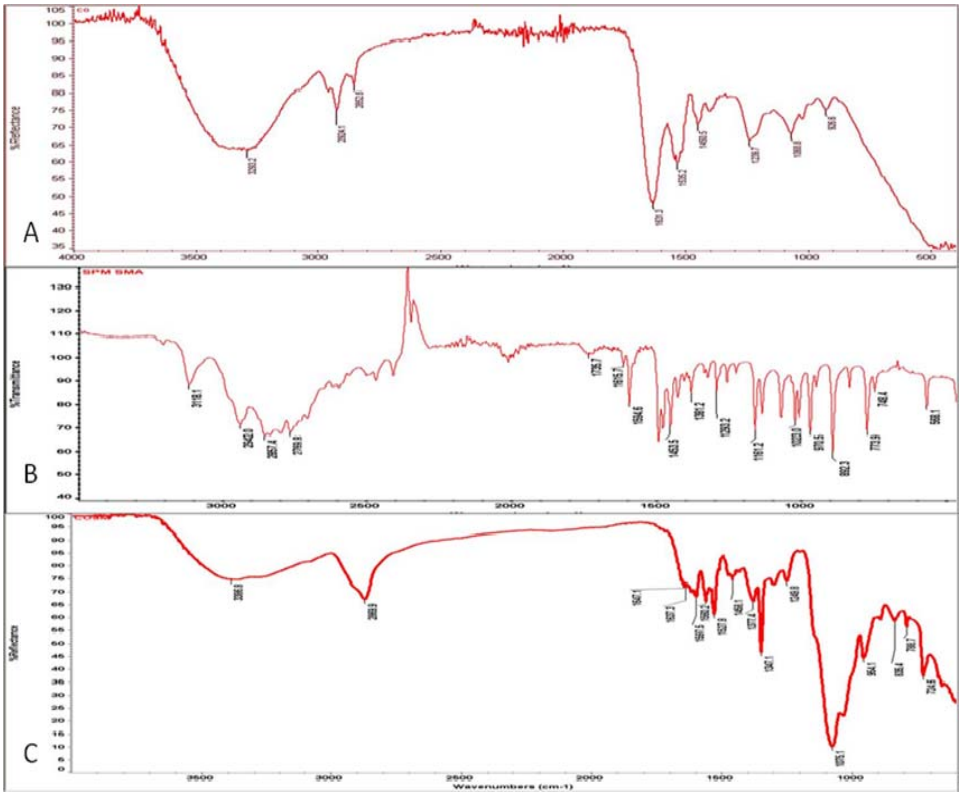

Fig 42**:** Infrared spectroscopy for evaluation of chemical groups in the functional entities of the COSM derivative. FTIR of A) chitosan ornithine conjugate B) spermine and C) COSM conjugate.

In COSM, the ^{1}H NMR spectra of Fig 43 had peaks at 2.5 ppm and 2.39 ppm that belonged to the protons of the methyl group of chitosan and the multiple peaks at 3.10 ppm to 2.88 pm are attributed to protons of the -CH_2- group that resided both in spermine and CON. The proton peak that corresponded to the ornithine group in CON remained in the COSM derivative at 1.5 ppm and the presence of –CH_2 protons of spermine signals occurred at 1.8 ppm and 1.79 ppm. The proton chemical shift at 3.49 ppm and 3.66 ppm correspond to the glucosamine residue. Finally the degree of substitution of spermine was determined to be 11 % which indicated the successful conjugation of COSM polymer variant.

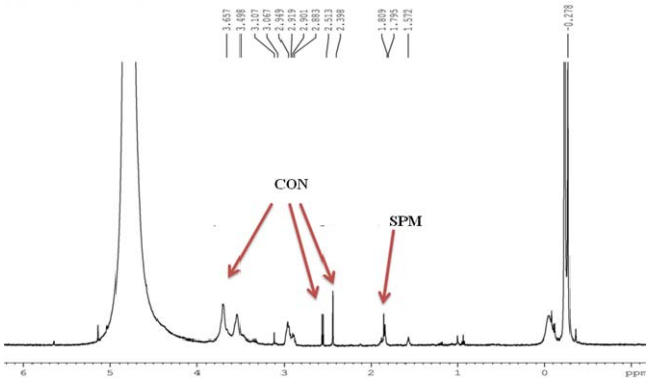

Fig 43: ^{1}H NMR spectra of COSM polymer

Another confirmation of the formation of COSM derivative was established by DSC analysis of the COSM derivative and the unmodified depolymerised chitosan as figured in Fig 44. The changes in the thermal properties of the two compounds cite the dissimilarity in the crystalline nature of COSM and chitosan which is mainly due to the addition of conjugates into chitosan polymer. The DSC curve of COSM has portrayed a sharp peak at 178.12˚C whereas the parent chitosan has the peak at 163.08˚C, comparatively lower melting temperature than the chitosan derivative. The increase in the temperature in COSM indicated that chitosan conjugation with the functional residues ornithine and spermine has been successfully accomplished.

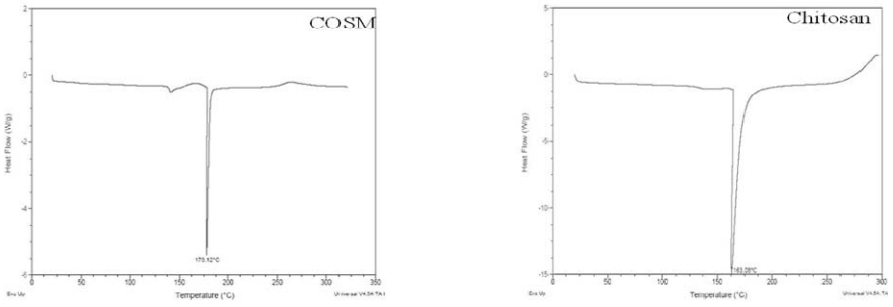

Fig 44: DSC analysis of COSM and chitosan

It was noticed that the CON polymer did show an optimal buffering capacity that enabled the nanoparticles to create swelling of the endosome that would lead to its rupture. However after conjugation with spermine to the CON matrix, the buffering capacity have been further enhanced which was seen in the Fig 45. A total volume of 1400 µL of 0.1 N HCl was required to finally reach the COSM solution at pH 3 and the polymer protonation resisted the influx of H+ ions at pH range between 4-3. In comparison with the parent compound chitosan, the derivative COSM had a beneficial buffering capacity that could induce the proton sponge effect in cells. The polymer PEI (25 kDa) had a very high titration curve with respect to COSM derivative but due to this, however PEI is also considered as a toxic polymer to the cells.

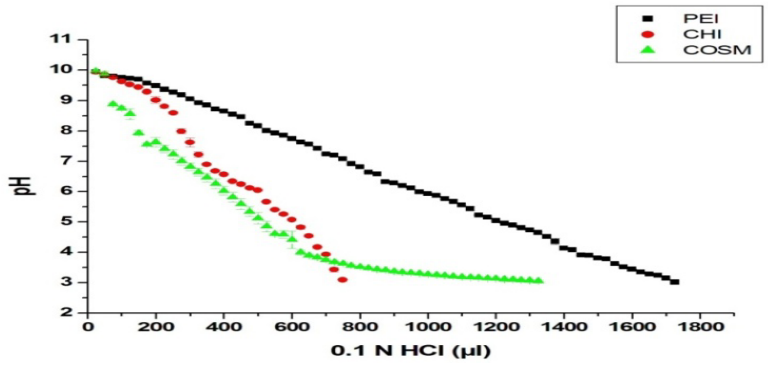

Fig 45: Evaluation of the buffering capacity of COSM. Acid base titration of PEI, CHI and COSM polymers against 0.1N HCl. The values given are in ±SD and n=3, with standard deviation calculated to be very negligible.

4.5.2 Characterisation of Nanoparticle- COSM and DNA interaction

4.5.2.1 Nanoparticle size determination and zeta size potential

Spermine functionalised chitosan ornithine formed nanoparticles by the electrostatic interactions with negative charged DNA which was precisely measured

by dynamic light scattering technique that revealed size and zeta potential range as displayed in Table 4. Triplicates were conducted and COSM/pDNA (w/w) ratios from 1:1 till 12 gave fluctuating values for both size and zeta potential. Hence nanoparticles from 13 to 18 is put here which had consistency throughout the triplicates. It was observed that sizes were within 200-300 nm except for two ratios. Since the size is elucidated in an aqueous environment, the hydrodynamic diameter around the nanoparticle could influence the size measurement and might have resulted in the larger sizes. Meanwhile the zeta potential came within the range of 30mV to 37mV which explained that the nanoparticle have the DNA excellently compressed by the COSM positive groups. The polymer/DNA weight ratio 1:16 was found to be acceptable for further morphological and in vitro studies due to comparatively suitable size dimension and a good surface charge that could act as a driving force to penetrate into the cells.

Table 4: Particle size and zeta potential of COSM/ctDNA nanoparticles. The values given are Mean ± SD and n=3.

DNA/polymer ratio	Size (nm) ±sd	Zeta potential (mV) ± sd
1:13	740 ± 23.2	37.5 ± 5.25
1:14	271 ± 2.82	36 ± 5.5
1:15	292 ± 7.3	36.3 ± 5.69
1:16	287 ± 2.2	30.2± 5.39
1:17	293± 6.1	34.5 ± 6.54
1:18	334± 18.3	34.5 ± 5.33
1:19	432 ± 21.2	33 ± 14.1

4.5.2.2 Morphological observation by TEM

The TEM image in Fig 46 exhibited COSM nanoparticles with a diameter range within 200nm and they appeared to have a distorted spheroid shape. The size range was suitable for a feasible entry into the cell.

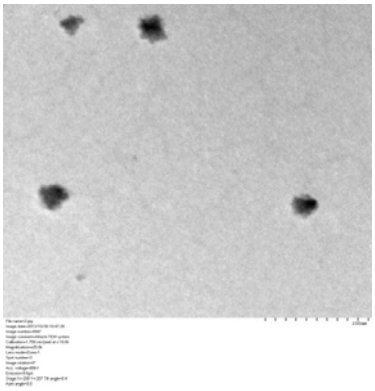

Fig 46: Nanoparticle Morphological analysis. A) TEM observation of COSM nanoparticle 1:16 ratio showed size range within 100nm. Scale bar is 200 nm.

4.5.2.3 Electrophoretic analysis of COSM nanoparticle

The ability of COSM polymer to form stable nanoparticles with plasmid DNA was ascertained by agarose gel electrophoresis. Nanoparticles were prepared at weight ratios ranging from 1:1 to 1:20. However ratios below 10 did not retard plasmid DNA effectively (data not shown) and ratios above 10 to 20 showed effective DNA retardation as seen in Fig 47A. The luminance inside the wells refers to the plasmid that is retained strongly by the interaction of COSM polymer. The binding strength between the polymer COSM and DNA was further established by treating the samples with DNase enzyme that would degrade any exposed DNA. However in Fig 47B it was clearly showed that the lanes do not have any smear of degraded DNA while the luminance is still retained in the wells. On the other hand, the first well had naked DNA treated with DNase which was completely degraded

and the last lane had smear of control DNA without DNase treatment. Furthermore, in another analysis, the same DNase treated nanoplex ratios were incubated for 30 min with hepain, a highly negatively charged biomolecule. The principle of competitive affinity binding will prompt COSM polymer to unpack the bound DNA and interact with heparin, thereby releasing plasmid DNA. This was observed in Fig 47C as the lanes started to display the DNA smear which is released due to heparin binding to the COSM polymer.

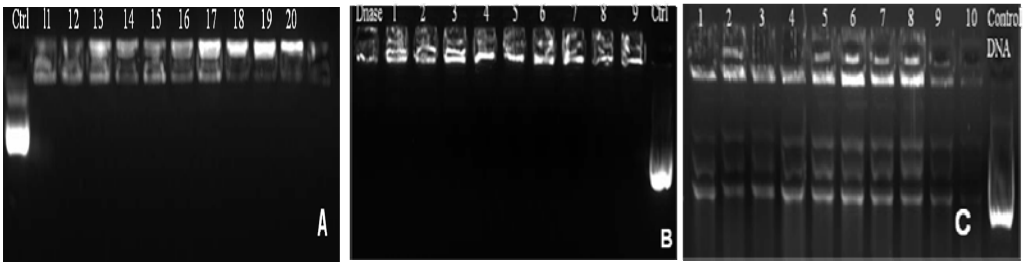

Fig 47: Agarose gel electrophoresis is performed on pDNA/COSM nanoparticles. A) The DNA retardation ability of the nanoparticle is determined. Lane 1 is pDNA alone. Lanes 2 -11 have nanoparticles in the ratios 1:11, 1:12, 1:13, 1:14, 1:15, 1:16, 1:17, 1:18, 1:19, 1:20. B) Protection of pDNA against DNase. Lanes 1-9 contain the same ratios and lanes on the either ends of the gel are pDNA treated with DNase enzyme and pDNA alone respectively. C) Release of pDNA from COSM on treatment with heparin. Lanes 1-10 represent the ratios 11-20 and pDNA alone as the control.

4.5.3 Blood compatibility and Cytotoxicity study of COSM polymer

4.5.3.1 Hemolysis and RBC aggregation

The increase in cationic density of the polymer motivate better cellular interactions that may produce undesired interactions with the blood components

which can finally end up with RBC aggregation and cell lysis. Therefore preliminary evaluation of blood compatibility of COSM polymer was demonstrated by hemolysis and RBC aggregation analysis. At four different concentrations of COSM polymer (1 mg/mL) till the maximum 100 μg, it was observed that the haemolytic activity was very less and within the 1 % permissible value (Appendix A4-Table 4). The hemolysis activity of COSM was compared to the 100 % hemolysis by Triton X-100 and 0 % hemolysis by normal saline. Next RBC aggregation was determined to be absent even when red blood cells were incubated with 100 μL of COSM and the morphology of the RBC remained unaffected as in Fig 48A. Normal saline treated RBC did not cause any aggregation as in Fig 48B and the image was similar to that of COSM treated RBC. Thus COSM was validated to be non haemolytic while PEI treated RBC in Fig 48C showed the toxic effect of the polymer in the form of aggregation and clumping of cells with lysis. COSM did not elicit any initial unwanted responses and therefore could be exploited for intravenous administration.

4.5.3.2 Plasma protein interaction with COSM polymer

Interaction of COSM polymer with blood plasma proteins is a prerequisite parameter that needs to be investigated. Any interaction would lead to protein adsorption followed by reduction in the protein composition of the plasma which eventually would result in absence of protein bands while doing native PAGE. On the other hand normal saline do not influence plasma protein adsorption and protein are observed as bands in the gel. In Fig 48D, the coomassie blue stained gel enabled the clear visibility of protein bands in all the three lanes in the gel. This ascribed that COSM polymer did not interact and adsorb plasma proteins as similar in the case of saline treated plasma and therefore displayed the entire plasma protein bands in the

gel. Serum proteins incubated with two concentrations of 50 and 100 µg of COSM (1mg/mL) along with the saline control resulted in three lanes in the PAGE gel with similar display of protein bands indicating the absence of any kind of plasma protein interaction with the COSM polymer.

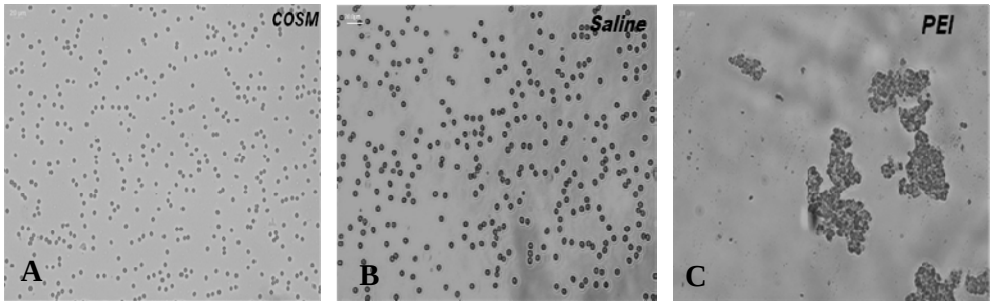

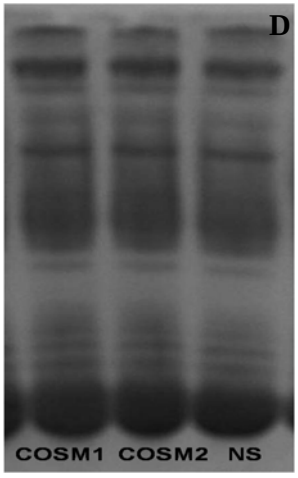

Fig 48: RBC aggregation studies with (A) COSM derivative (B) with normal saline (C) with PEI 25 kDa (20 X magnification for RBC) (D) Plasma Protein interaction with COSM (1 mg/mL); Lanes COSM1, COSM2 represent polymer in 50 &100 µg and lane NS is normal saline, the control

4.5.3.2 Cytotoxicity evaluation of COSM polymer

The polymer CON was observed to be non toxic but it is necessary to decide the toxicity of the matrix after spermine conjugation. Hence C6 cells were exposed to COSM (1 mg/mL) polymer in four different concentrations 25 µg, 50 µg, 75 µg and 100 µg suspended in MEM: DMEM/F12 Ham medium. In Fig 49, spermine derivatised chitosan ornithine conjugate was found to be completely non toxic to the cells as more than 100 % cell viability was observed. Mean while the positive

control Triton X-100 was highly toxic to the cells and the medium alone served as the negative control which had 100 % cells viable. Both chitosan (CHI) and PEI 25 kDa added in 50 µg concentration displayed toxicity to the cells. Toxicity of unmodified chitosan is due to its solubilisation in acidic medium.

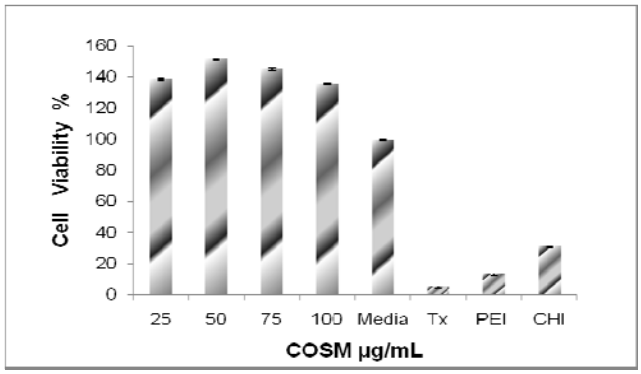

Fig 49: Cytotoxicity of COSM evaluated by MTT assay. Cell viability % of C6 glioma cells after incubation with COSM in four different concentrations. Controls were **media** that referred to medium alone and **TX** coded for Triton X-100. Other controls were **CHI**: unmodified chitosan and **PEI** (25 kDa). The values given are mean ± SD and n=3.

4.5.4 In vitro cell study with COSM/pDNA nanoparticle

4.5.4.1 Evaluation of Cellular Uptake

The polymer COSM was adopted to generate nanoparticles with plasmid DNA p53 to investigate the cellular uptake of nanoparticles. YOYO iodide is a nucleic acid intercalating agent and was used for tagging p53 before polymer complexation. It was revealed in Fig 50A that the cells treated with only YOYO tagged p53 plasmid showed absence of fluorescence in the nucleus and a diminished intensity in the vicinity of the cells. This might be due to the faint diffusion of tagged plasmid around the cells. On the other hand, Fig 50B displayed the cells incubated

with COSM nanoparticles for 4 h which had a prominent bright green fluorescence in the Hoeschst stained nucleus that represented an efficient cellular uptake of COSM nanoparticles. The fluorescence was spread all over the cells which affirmed that CON nanoparticles were able to transfer the YOYO tagged plasmid to the nucleus of the cells. Additionally as shown in Fig 50C, the confocal microscopic image with orthogonal z-stacking of the cells apparently depicted the green fluorescence of homogenous distribution of COSM/tagged pDNA nanoparticles inside the cell and nucleus that suggested efficient cellular internalization of the nanoparticles. The cell uptake results were found to be consistent with flow cytometry histogram in Fig 50D that showed excessive uptake of COSM nanoparticles. The fluorescence shift was ascertained with the histogram of the unstained cells in Fig 50E.

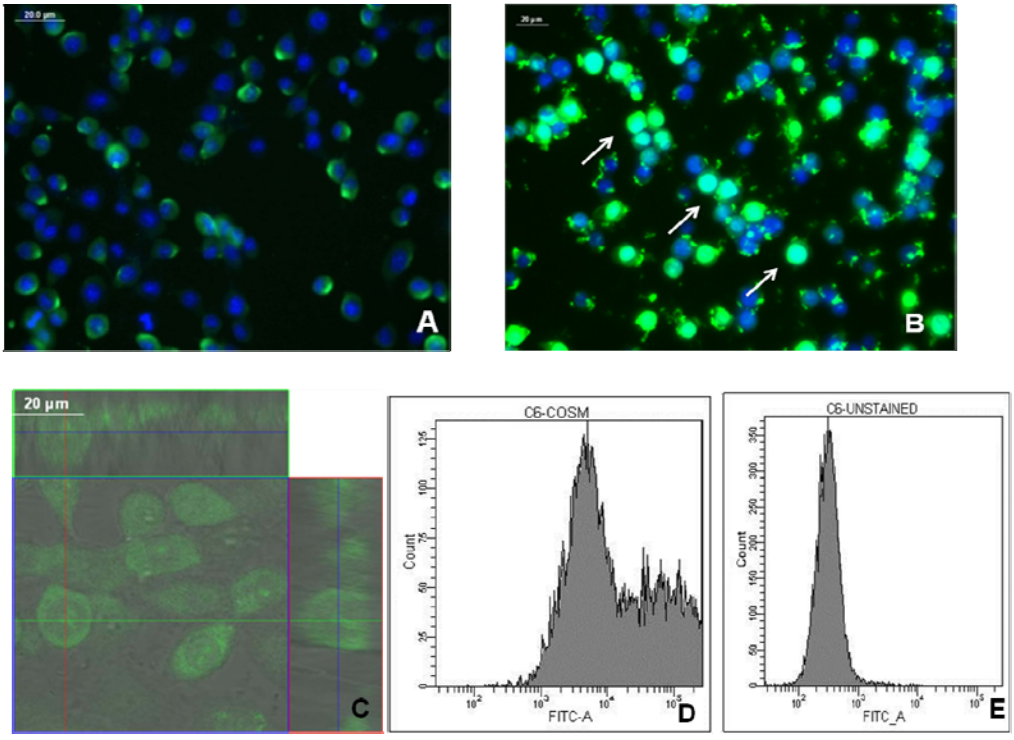

Fig 50: Fluorescence microscopic image of A) control C6 cells with only YOYO tagged pDNA and B) YOYO labelled pDNA/COSM nanoparticles in 1:15 ratio

(w/w) after 4h incubation. Arrows indicate the cell uptake of COSM nanoparticles. C) Confocal fluorescent images of cell uptake of YOYO labelled pDNA/COSM nanoparticles merging images of both the bright field and green filter after 4 h. Magnification is 40 X and scale bar size is 20 μm. Representative histograms of pDNA fluorescence from flow cytometry analysis of D) cells incubated with COSM/pDNA nanoparticles E) Unstained cells as control

4.5.4.2 Endocytosis inhibition Study

Identification of the specific endocytic pathways adopted by these COSM nanoparticles for cellular uptake is helpful for better understanding of the intracellular trafficking mechanism. Hence endocytosis inhibitors designated for each pathway were used to block the COSM nanoparticle entry. In parallel to fluorescent images, images were also captured with confocal microscope embedded with z-stacking to unravel the accumulation of the nanoparticles throughout the cell. Both images are shown adjacent to each for every inhibitor study in Fig 51 to comprehend the pathways. It was observed in Fig 51A and B, that both inhibitors chlorpromazine and dynasore seemed to restrict the free inward movement of nanoparticles as the fluorescence intensity got subsided in the cell citing that clathrin mediated dynamin dependent pathway is likely to be used for cell uptake. The confocal image result (Fig 51A1 and B1) also supported the finding. Significant reduction of fluorescence was observed in the cells treated with amyloride inhibitor in Fig 51C and C1, suggesting that macropinocytosis pathway also influence the nanoparticle internalization. The inhibitor filipin obstructed the caveolae pathway and presented cells with a faltered fluorescence in Fig 51D and D1, which pointed out that only partial inhibition of COSM/pDNA nanoparticle cell uptake has taken place. By using

ornithine and spermine as the inhibitors to block the ligand specific receptors, the plasmid associated fluorescence in the nucleus has been curtailed which proposed the perception of a receptor mediated cellular entry of COSM nanoparticles (Fig 51E-F and 51E1-F1). The confocal microscopic images of cells treated with the respective inhibitors also maintained the same pattern of the fluorescent visualized images. It clearly showed that the overlay images of cells in the bright field background had sparsity of fluorescence emitted by the plasmid assisted COSM nanoparticles. The orthogonal analysis by z-stacking enabled an in depth view of the localisation of the tagged nanoparticles inside the cells and demonstrated the reduction of nanoparticles within cells when treated with inhibitors. In COSM nanoparticle mediated gene delivery also the clathrin pathway with dynamin mediated, macropinocytosis and ligand specific receptor pathways were identified to play major roles in facilitating gene transfer to cells.

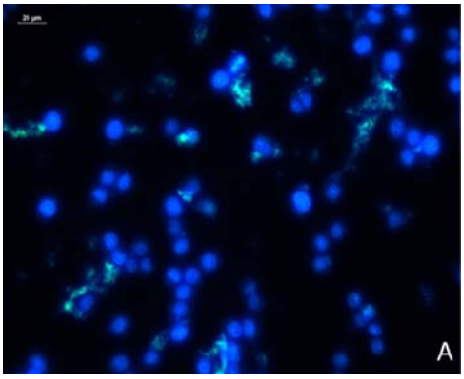

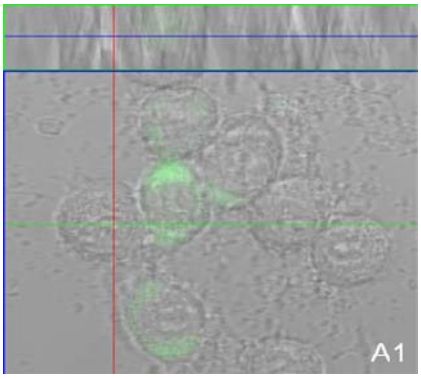

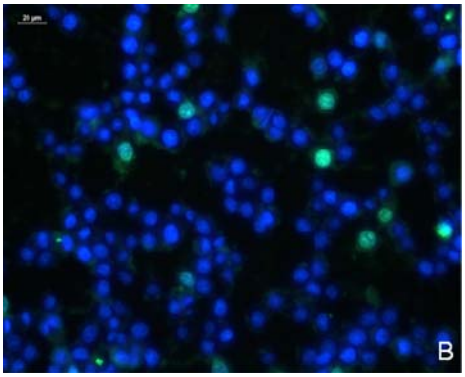
B

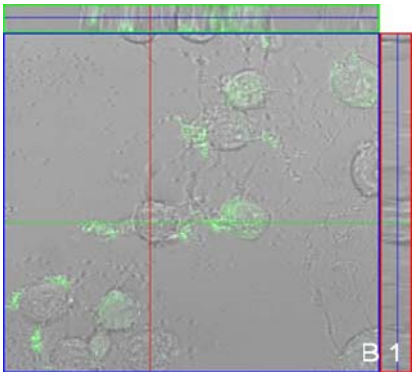
B 1

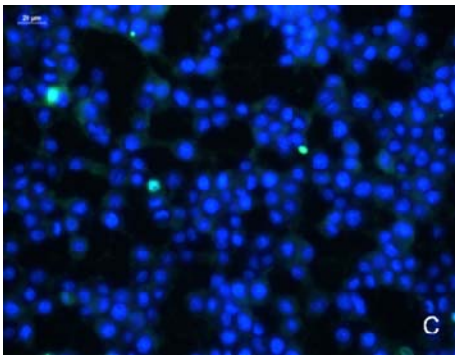
C

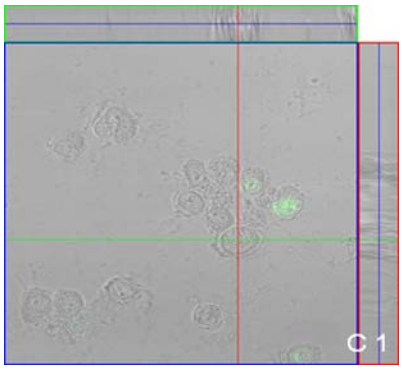
C 1

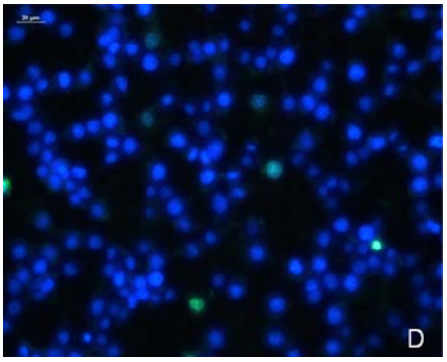
D

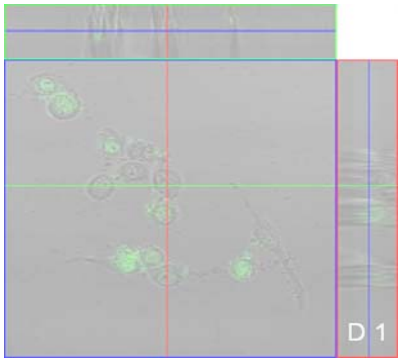
D 1

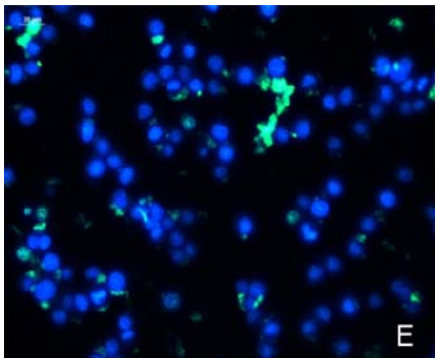
E

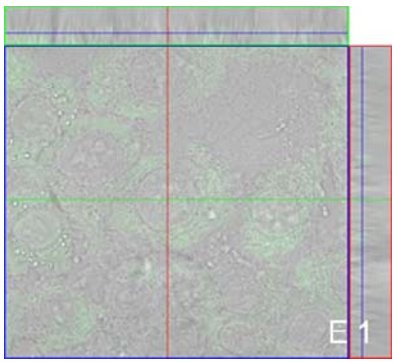
E 1

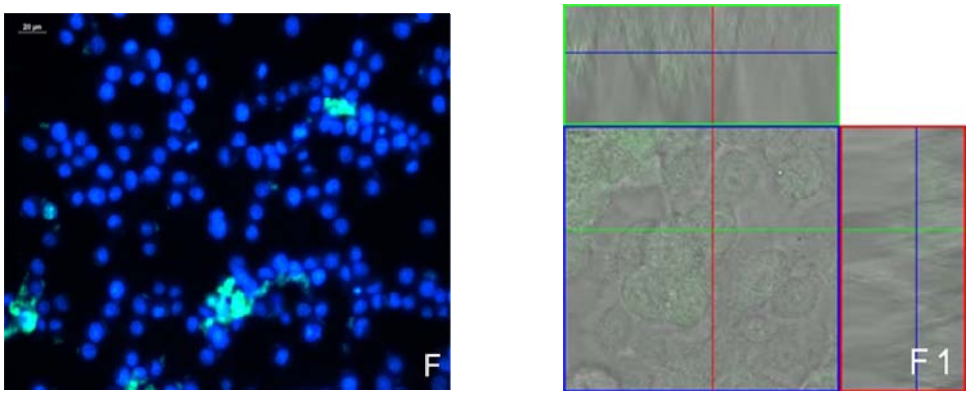

Fig 51: Representative fluorescent and confocal images of endocytosis inhibition study with COSM/pDNA complexes in ratio 1:16 (DNA/COSM) in C6 glioma cells. Magnification and scale bar is 40 X and 20 µm respectively. Fluorescent images of cells from (A) to (F) treated with a separate endocytic inhibitor prior incubation with COSM nanoparticles. Therefore (A) represent chlorpromazine treated cells B) Dynasore treated cells C) Amiloride treated cells D) Filipin treated cells E) Ornithine and F) spermine treated cells. Images A1 to F1 represented the z-stacking confocal images of the same inhibitor studies.

4.5.4.3 Transfection with p53 Gene expression

The *in vitro* gene transfer of COSM derivative was recognized with the live dead assay conducted on C6 glioma cells where in the gene expression of p53 was made feasible by transporting the plasmid as cargo by COSM nanoparticles. Apoptosis was brought about by p53 expression and dead cells were stained by the ethidium homodimer dye that provided the red fluorescence in the cells. As more than 90 % of cells were transfected with p53 in Fig 52A and live cells which would have been stained green with calcein AM were very much negligible to detect. The result was easily adjudged by comparing to the controls that constituted C6 cells which had only the p53 plasmid that presented the live cells with green stain (Fig

52B) and C6 cells transfected with PEI/p53 nanoparticles that furnished red stained dead cells (Fig 52C).

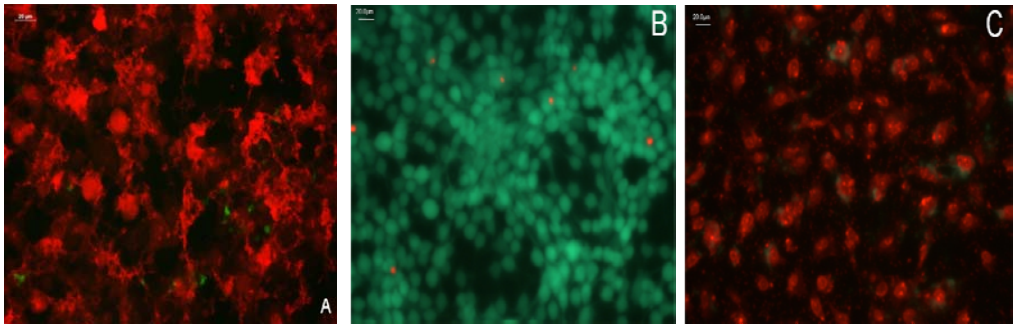

Fig 52: Transfection Assessment via Live Dead assay in C6 cells. Fluorescent images of C6 cells transfected with A) COSM/p53 plasmid nanoparticles, B) p53 plasmid alone C) PEI/p53 transfected cells. Magnification and scale bar is 40 X and 20 μm respectively.

4.5.4.4 Intracellular Nanoparticle trafficking

Unpacking of nanoparticles in the cell was explored by investigating the cytosolic movement of tagged COSM/p53 nanoparticles. The nanoparticles were prepared in the 1:16 ratio and tagging was done for COSM polymer with TRITCI and p53 plasmid with YOYO iodide. The C6 cells were treated with the dual tagged nanoparticles for 4 h incubation period for cellular uptake. Qualitative assessment of intracellular trafficking was possible by fluorescence microscopy observations. Polymer distribution was seen around the Hoeschst stained nucleus in Fig 53A with red fluorescence emitted by the COSM polymer and culminated by a bright green fluorescence of the YOYO tagged pDNA. The images of the three filters in Fig 53B revealed the final superimposed image of the nanoparticle trafficking to be clearly visible with the red fluorescence of the polymer localised within the vicinity of the cell without entering into the nucleus. On other hand, the predominance of cells with

green fluorescence dispersed throughout each cells indicated that good amount of COSM nanoparticle that has been internalised effectively due to the merits of the incorporated ligands spermine and ornithine into the polymer chitosan. The study offered an initial understanding of the ability of COSM to allow feasible intracellular trafficking and unpacking of the nanoparticles which supported the earlier results of effectual cell uptake and transgene expression.

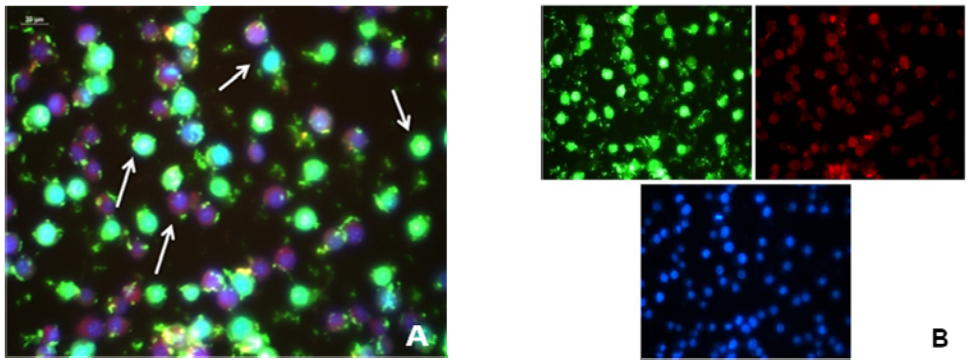

Fig 53: Nanoparticle trafficking in the cell. Fluorescent images of cells A) Overlay image of the cell uptake of COSM/p53 nanoplexes. B) images with the three filters; green filter for YOYO tagged plasmid; red filter for TRITCI tagged COSM and p53 blue filter for Hoeschst stained nucleus. Magnification and scale bar is 40 X and 20 μm respectively.

CHAPTER 5 DISCUSSION

Cancer research has always been summoned with various kinds of treatment and gene therapy has lately been the current endeavour towards a lasting hope of cure. The interest in gene therapy has been reinforced than ever before, after the advent of nanotechnology which has shown promise in renovating the existing techniques of gene delivery. The most significant challenge for gene delivery is the need of an ideal vector or carrier that could execute the task effectively and safely. Viruses were the notable vectors which had the inherent ability to exploit the host machinery for gene transfer and provide gene expression. However the safety issues with viral vectors were a deep concern and they were replaced by non viral systems that mainly included biodegradable polymers. Both synthetic and natural polymers with biodegradable property are present but among those, the amine rich polysaccharide chitosan has shown immense scope in being manipulated as a non viral gene delivery system. But then chitosan had solubility only at acidic pH and had low transfection efficacy which limited its biological application. In an approach to resolve this, certain ligands were introduced into the chitosan backbone whose advantages would be adjunct to chitosan and improve its capability of gene transfer. Ligands which were biologically present and which conveyed stealth property were preferred as they caused less rejection response from the body. Hence conjugates such as the sugar galactose, polyamine spermine, PEG diamine, the polyamino acid protamine and the amino acid ornithine were regarded for the conjugation study with chitosan. Most of them were frequently found in the physiological system and therefore might not be considered foreign by the defence system of our body.

Moreover they also proffered site specific delivery with endocytosis pathway preferences and systemic stability. Coupling more than one ligand to chitosan polymer allowed multifunctional disposition to the central polymer backbone that included targetability, sensitivity and evasion from the RES cells, which were integrated together in the chitosan based nanoparticles for efficient gene transfer. In this work, we have attempted to synthesize four bioconjugated chitosan polymer and have evaluated the physicochemical and biological characterisations of each derivative for cancer therapy.

5.1 Spermine grafted galactosylated chitosan for improved nanoparticle mediated gene delivery

Introduction of chemical groups into chitosan with an intermediate molecular weight range resulted in a derivative with enhanced gene expression and cellular uptake. Substitution in chitosan has now became an indispensable tool which assured enhanced transfection (Strand et al., 2010) for designing chitosan based nanoparticles or polyplexes that maintained an optimum balance between polyplex stability and polyplex unpacking. The incorporation of spermine and galactose in chitosan was validated by carrying out colorimetric TNBS assay. The method provided the percentage value of free amine groups and the polymer named GCSM showed a greater presence of free amine groups when compared to the parent compounds GC and chitosan. The extra amine content would facilitate for overall positive charge required for GCSM polymer to bind effectively to the nucleic acids. The FTIR spectrum of GCSM revealed prominent peaks at 3346 cm^{-1} and 3116.8 cm^{-1} specific to the broad hydroxyl group that has been contributed by galactose moiety to

chitosan. Spermine conjugation has been ascertained by the amide peaks at 1648 cm^{-1} and 1595 cm^{-1} which stood for the successful conjugation of spermine into the galactosylated chitosan.

^{1}H NMR ascertained the successful grafting of galactose and spermine into chitosan. The protons conferring high intensity peaks between 3.811 ppm and 3.645 ppm revealed the substitution of lactobionic acid groups. Besides the specific signal at 1.07 ppm of spermine, an increase in amine group signals between 3.07 and 2.98 ppm in the polymer was contributed from spermine during chitosan conjugation. Hence both FTIR and ^{1}H NMR validated the conjugation of both galactose and spermine in the chitosan to derive the product GCSM. On comparison with PEI, a highly buffering agent, GCSM polymer buffered less as seen in Fig. 5. Though being less, GCSM had far more buffering capacity than the unmodified chitosan. The hypothesis related to proton buffering capacity for certain polymers remark the capability of a polymer that is engulfed inside an endosome (Mintzer & Simanek, 2009) to disrupt the membranes by causing differences in pH prevailing both inside and outside of vesicle. In general, the polyplexes are directed into the endosome wherein the amine groups present on the GCSM polymer tend to enhance the positive charge within the vesicle and this accumulation of a single charge will create a whole imbalance in the endosome leading to its swelling and disruption (Lai & Lin, 2009). GCSM polymer was observed to show more buffering nature than unmodified chitosan which would facilitate the release of nanoparticles into the cytoplasm that could be subsequently sequestered towards the nucleus by yet to be discovered mechanisms.

Nanoparticle formation is the most crucial step for generating a polymeric gene carrier in which the surface charge and the average diameter of the particle size are important factors to be considered. The presence of positive and negative charges between GCSM and DNA resulted in complex coacervation. The opposite charges on the polymer complexes upon self assembly will have the overall charge rapidly neutralized till the charge becomes positive. The concentrations of GCSM and calf thymus DNA mixed at varying ratios determine the stability, integrity and charge of the nanoparticles (Strand et al., 2010). On investigation of various ratios, it was observed that the lower ratios gave rise to larger sizes with more of negative charge intensity indicating that proper condensation of the DNA with the polymer was not carried out as desired. Ratios between 12 and 17 showcased a consistent size and zeta potential within 500 nm and above 17 showed poor results in terms of both. Hence this range was focussed to obtain an optimum size and consequently ratios 15 and 16 gave a consistent size value.

Though polymer concentration was quite high in these ratios, the surface charge did not get raised to very high values. Similar range of zeta potential was observed by (Kim et al., 2004) who prepared nanoparticles with galactosylated chitosan and DNA. The zeta value of chitosan of molecular weight 120 kDa was 25 mV. The presence of galactose side chain deduced the charge density and sometimes it could be hypothesized that the high Mw of 120 kDa of chitosan might overweigh the less Mw of galactose and spermine resulting in an electrostatic repulsion of the ionic groups in chitosan (Chen et al., 2007) which would not allow proper packaging of nucleic acid inside. This would lead to entanglement of the rigid chain of chitosan with DNA, along with its side chains of galactose and spermine hanging loosely,

thereby causing merely equilibrium of the charges. Interestingly, this type of polyplex condensation are governed by two concomitant effects known as “re-entrant condensation” and “charge inversion”, where increase in polyion content has hardly any effect on the overall charge distribution on the nanoplex (Bordi et al., 2007). However, at times only a slight positive charge is preferred over very high surface charges for cell culture studies, as previous reports (Germershaus et al., 2008) showed the chances of cytotoxicity when the amount of amine groups were increased. This confirmed the relationship between high charge density and toxicity (Lv et al., 2006). The surface charge of naked ctDNA was around−17.9, whereas the surface charge for complexes made of varying GCSM and ctDNA ratios were found to range from 10 to 13 mV, which was obviously a desirable cationic charge to mediate transfection. As ratio 15 had a slight higher zeta when compared to the other ratios, nanoplex of this particular ratio was considered along with its optimum size for our later experiments.

Particle size plays an important role in transferring genes to the cells and we tried to obtain nanoparticles of size within 250 nm range to facilitate the uptake of the particles. The morphological observation by TEM displayed a distorted spherical shape with a size distribution slightly smaller than that measured by the Zetasizer. A similar observation of smaller sizes occurred for Chen et al. (2007) and it is likely that dried nanoparticles were used in TEM experiment while in Zetasizer the particles were analysed in liquid dispersion. As chitosan possessed inherent swelling property, GCSM would be expected to swell in suspension which resulted in a large hydrodynamic size when measured by the Zetasizer. The shape had more or less of globular appearenace which depicted that the shape is resulted in order to strike the

balance between packaging stability and intracellular disassembly of complexes (Strand et al., 2010; Reitan et al., 2009). The surface images obtained from AFM also supported the TEM size images, clearly displaying the distinct boundary of each nanoparticle without any aggregation. Both TEM and AFM images emphasized the formation of spheroid shapes of the nanoparticle created due to the localized bending or distortion of GCSM when bound to plasmid DNA. These kind of shapes for chitosan based DNA nanoparticles acquired from TEM and AFM had been noticed in other few report too (Zhang et al., 2008).

The integrity of the nanoparticle to remain stable in biological system is one of the parameters that need to be elucidated. And for this the electrophoretic mobility of the nanoparticle was analysed which clearly showed the retardation movement of DNA, hardly passing out from the wells. The bands are bright and luminescent stating that GCSM polymer was able to constrict DNA, hence over shielding it from the attack of any enzymes. This was further validated by applying DNase treatment on nanoparticles in which the figure showed certain fluorescent DNA fragments in the wells. Despite the presence of the nuclease, GCSM polymer was able to protect ctDNA from enzyme digestion. On heparin displacement of DNA from the complexes, the lanes revealed the presence of DNA smear as same as the lane showing enzyme untreated control DNA. The control well without any fluorescence appeared to have their DNA completely degraded. Hence, the ratios conferred the integrity of GCSM nanoparticle and succeeded in showing resistance to nuclease attack.

A vital perspective that needs to be reckoned with is that the the polymer should be non toxic in systemic circulation (Huang et al., 2004). Hence GCSM

nanoparticles were recognized to be blood compatible with very limited hemolysis and negligible RBC aggregation. Protein adsorption study of the chitosan derivative presented serum protein bands in the gel after treating with GCSM polymer which demonstrate that the polymer does not illicit any interactions with the proteins in the blood plasma to form complexes and the proteins therefore was displayed as bands in the gel. Literature evidence cited that chitosan (Erbacher et al., 1998) showed negligible level of toxicity and even with further vector modifications on this parent polymer, the viability of the cells remains unchanged. In addition, hepatocyte targeting galactosylated chitosan gene carriers conjugated with PEI (Kim et al., 2005) and pullulan-spermine based nanoparticles (Thakor et al., 2009) also reported low cytotoxicity. Hence, GCSM nanoparticle having chemical combinations of galactose and spermine on the parent chitosan backbone demonstrated up to 80 % of cell viability supporting the above reports.

The potential of liver targeted gene delivery is one of the major concerns for developing an efficient nanoparticle for gene transfer. Liver is susceptible to many disease states like hepatoma carcinoma which needs to be addressed (Nguyen & Ferry, 2004) and its accessibility to the entire organ system by systemic circulation has invited attention for therapeutic gene delivery. Since liver cell surface have large number of asialoglycoprotein receptors (ASGPR) that recognize sugar ligands, the attachment of galactose residues into chitosan backbone would serve the purpose of targeted delivery. Efficient gene transfer into the HepG2 cells should therefore demonstrate a complete internalization of the nanoparticle inside the cell. The transfer of gene by the nanoplex to nucleus is identified by YOYO iodide labeling of the plasmid that enabled its fluorescent microscopic observation. Although YOYO

iodide was recently argued to be not an effective marker for studying intracellular trafficking (Escoffre et al., 2009), the fluorescent intensity produced by this dye was far exceeding than compared to other covalent dyes. YOYO also featured high binding affinity to dsDNA and when unbound to DNA, it exhibited extremely low fluorescence level. The dye was not affected by pH which made it more attractive than fluorescein which might be affected by pH changes in tissues (Perry et al., 2008). Polyplex labeled with FITC was adopted for cell uptake experiment without any inhibitor treatment and that was used for comparison of intracellular inhibition studies.Therefore with the prevailing GCSM nanoparticle also, a fairly large amount of hoarding of nanoparticles in and around the nucleus was observed.

Uptake is mediated by different pathways of the endocytosis mechanism (Rejman et al., 2005) and each inhibitors of the distinct pathway were used for investigating the actual pathway that would be likely to be adopted by GCSM nanoparticle for its internal trafficking in the cytoplasm. HepG2 cells were treated with inhibitors namely chlorpromazine and filipin that inhibit the clathrin and caveolae pathways. Meanwhile galactose and asialofetuin ligands can bind to asialoglycoprotein receptor (ASGPR) and block receptor mediated endocytosis. It was observed that the inhibitors of clathrin and caveolae did not prevent GCSM nanoparticle from entering the cell clearly stating that GCSM nanoparticles did not depend much on the above two pathways for its trafficking process. On the contrary, the application of asialofeutin and glucose as inhibitors revealed a marked reduction in the distribution of GCSM nanoparticles which indicated that receptor mediated endocytosis is the much preferred pathway for cellular entry for GCSM nanoparticles, when compared to the other two mentioned pathways.

Similarly, substitution of galactose and spermine in chitosan revealed a considerable increase in gene transfer. The efficiency was evaluated with aid of the luciferase assay and on comparison with PEI 25 kDa control which is known to be a highly effective cationic gene vector (Kunath et al., 2003), the transfection efficiency of GCSM vector was measured. Between two ratios, transfection seemed to be slightly higher in the lower ratio which may infer that the polymer at that particular DNA/polymer (w/w) ratio was able to provide a dense condensation of DNA. There were pioneer experiments on transfection efficiency of chitosan based on parameters defining the pH of the transfection media, amine to phosphate ratio (N/P) and the amount of pDNA optimized for nanoparticle preparation (Sato et al., 2001; Huang et al., 2004; Thakor et al., 2009). In these earlier reports the involvement of serum in the media did not cause any inhibition in transfection mediated by chitosan nanoparticles and hence the entire cell culture studies for GCSM nanoparticles were carried out in presence of 10 % FBS. The results were also complementing to the fact that serum had very little detrimental effect on transfection when glycosylated chitosan is adopted for nanoparticle formation (Sato et al., 2001, Srinivasachariet al., 2006). Moreover live dead assay also substantiated enhanced transfection which was comparable to the cells treated with PEI/p53 nanoparticles. Hence receptor mediated uptake allowed a more rapid means of ligand targeted internalization providing enhanced transfection with a prospective for controlled delivery into the cells.

5.2 Protamine conjugated PEG diamineylated chitosan derived polyplex for enhanced cell uptake and gene delivery.

Among cationic polymers, chitosan based nanoparticles or polyplexes has been largely studied for polycation mediated gene delivery system as the polymer boasts of being biocompatible and biodegradable (Buschmann et al., 2013). The reactive groups in the polymer allow the feasibility for tailor made modulation in the chemical structure and the primary amine groups composition favour chemical reactions to occur as well as create electrostatic bonds with oppositely charged molecules like nucleic acid and induce DNA condensation to a tightly packed complex constructs, all of which benefit a nanoparticle mediated non viral delivery system. Gene delivery has become an important strategy to combat cancer progression and eligible polymer vectors are in a constant need to carry the gene of interest to the tumour sites. Hence chitosan based nanoparticles with appropriate modifications were nominated as suitable vectors for gene delivery.

In this study, diaminopolyethylene glycol with terminal amine groups and protamine has been chosen for chitosan derivatisation. This is because PEG diamine would provide the stealth property required for chitosan nanoparticles to be more biocompatible and the end amine groups act as the linker for conjugation with protamine that is a suitable polycation to promote better DNA condensation and cellular gene transfer (Casettari et al., 2012). PEG diamine is anticipated to prevent any ionic interactions between nanoparticles and charged biomolecules during circulation due to the presence of the PEG chain, leading to prolonged exposure to tumour cells by passive tumour targeting via enhanced permeability retention effect

(EPR). Since PEGylation would convey non-immunogenicity, clearance from the blood would be slower facilitating a better tumour therapeutic approach. Protamine is a cocktail of basic amino acids with arginine being a dominant substituent (Lewis et al., 2004) which is known for conceivable cell membrane penetration and DNA translocation. Initial attempts to conjugate chitosan with protamine yielded nanoparticles with sizes in micrometer range and unsteady shifts of anionic and cationic surface charge on the nanoparticles. This might be due to incomplete condensation of DNA with the protamine modified chitosan which impaired the complete formation of a polycation nanoparticle. But the present effort of grafting diaminopolyethylene glycol to the chitosan polymer prior conjugation with protamine readily redefined the derivative property to augment protamine binding in the next step that resulted in protamine conjugated diamine PEGylated chitosan (CDP) nanoparticles of favourable size and zeta potential.

In protamine grafted diamine PEGylated chitosan, the primary amine compositon has been increased than the unmodified chitosan as determined by the TNBS assay, which indicate the presence of the conjugates in the chitosan derivative. And the FTIR spectra also revealed the hydroxyl and amide peaks of PEG and protamine conjugation in the CDP polymer. Moreover ^{1}H NMR data enabled a clear depiction of the specific proton signals of PEG diamine and protamine in the chitosan backbone. The thermal property by DSC also observed a different thermal peak for CDP when compared to the parent compound chitosan which indicated the formation of CDP product. All the above physicochemical characterisation confirmed the successful conjugation of both PEG diamine and protamine into the chitoan backbone.

Cationic polymer that promoted endosomal escape is a sought after attribute for non viral systems to accomplish gene transfer. In protamine grafted diamine PEGylated chitosan, the amine groups in protamine are titratable which lead to proton buffering in the endosome that could create an influx of protons in the endosomal matrix. Accumulation of H+ ions resulted in acidification of the endosome and to balance the charges, there would be a rapid inward gush of chloride ions and water into the endosome which gave way to the osmotic expansion of the endosome. In this way the amassed protons offer the endosome to act as a sponge adsorbing the entire water molecules eventually causing the swelled endosome to rupture and liberate the CDP nanoparticles into the cytosol. This proton sponge hypothesis (Behr, 1997) has been widely accepted concept for delivering polycation based nanoparticles into the cell. Hence any polycation with large number of amine groups should mediate the endosome buffering and the polymer polyethyleneimine is the best example for such a polycation.

Chitosan, though being a polycation caused very meagre level of protonation and the endosomal acidification was elevated when the amine rich polysaccharide is grafted with residues like protamine. But the buffering capacity of CDP was very low when compared to PEI and endosomal escape was successively performed due to the ionisation behaviour of chitosan backbone to promote proton sponge effect (Richard et al., 2013). It is proposed that the CDP derivative would employ excess charge dissipated from chitosan derivative during polyplex formation such that there would be loose ends of the polymer chain that is not complexed with DNA which enable similar acidification kinetics and chloride hoarding that allowed endosome lysis.

In an aqueous milieu, the combination of both cationic and anionic components facilitate the compact binding of DNA by the CDP derivative and pushes the nucleotides further into the core of the entwined chains of CDP polymer enabling a kind of packaging that prevent the gene from unwinding itself from the complexed structure. The energetics of this complex is responsible for the nanoparticle formation otherwise both polymer and DNA exist as long chains of molecules when not in contact. Hence the physical parameters of CDP nanoparticles also would be different from the individual components and determination of both size and surface charge established the success of CDP nanoparticle formation. The nanoparticle size and surface charge is represented as function of the w/w ratio of CDP and DNA and was monitored by dynamic light scattering. There was inconsistency in values for size at very low ratios < 4 and at ratios >8 wherein optimal sizes within 200 nm were obtained in the range between 4 and 8. This discrepancy in size and charge is caused by the effect of reentrant condensation experienced by the polyions in solution (Bordi et al. 2007).

It is not necessary that there should be corresponding decrease in size and increase in charge depending on the density of the polycation as the whole process of polyelectrolyte complex formation is governed by both long range electrostatic bonds and short lived attractive interactions. An equilibrium between these forces lead to charge inversion and size saturation that influence the average size and overall electrical charge which might vary for each nanoparticle ratios. Moreover the transfer of genes across the cell has certain level of dependency towards the the size and shape of the molecule and therefore size within 100-200 nm is desirable for cellular gene translocation (Gaumet et al., 2008). In addition to this an overall

cationic surface charge, defined by the zeta potential is a crucial parameter to bind effectively to the nucleic acid and to surface glycoproteins of the cell membrane bilayer. Very high zeta potential for polymer could also induce cytotoxicity and therefore a satisfactory zeta potential is exhibited at ratios within 4 and 8 which demonstrated effective cell uptake and cell viability.

The DLS measurements of the nanoparticles were obtained as the culminated average values of sizes in the solution and the hydration property also enhanced the diameter of the nanoplexes and therefore the morphological examination with the help of TEM confirmed the exact size range. TEM image of the dried sample of CDP ratio 7 exposed the actual size of nanoparticles belonging within 150 nm, with most of them appearing close to 100nm and below. Uniform distribution of spherical and compact CDP nanoparticles suggested proper DNA condensation and hydrophilic exterior reduced interactions between complexes thus avoiding agglomeration. The size transition is partly due to unique feature of chitosan that display re-entrant condensation and charge inversion that affects the morphology of the nanoparticles (Amaduzzi et al., 2014). Hence the size obtained for the particular ratio was in agreement with the size determined by DLS measurement and has satisfied the desired polyplex size requirements for gene delivery.

Evidently it is necessary to evaluate further the physical integrity of CDP nanoparticles and the polymer-DNA condensation capacity was determined by agarose gel electrophoresis. The method can separate charged objects and influence the mobility of the nanoparticles in a uniform electric field (Kowalczyk et al., 2011). As the proportion of CDP was increased at different ratios, the movement of pDNA in the gel was retarded which was represented by the bright luminance retained in the

wells indicating the ethidium bromide intercalated DNA wound by the CDP polymer chains. This evinced that the polymer CDP is able to protect DNA and shield it properly from nuclease attack maintaining the integrity of the nucleotide. Further affirmation on the solidarity in the CDP nanoplexes were performed with DNase protection assay which revealed that the polyplexes continued to protect DNA from nuclease activity with practically negligible release of the gene from the electrostatic interaction of the CDP derivative. In case the absence of DNA smear in the lanes in the gel indicated complete degradation rather than being hidden, this was verified by treating the samples with heparin which promoted DNA dissociation from the complexes. Competitive affinity binding will occur for the nanoparticles in the presence of the highly negative charged heparin molecule and CDP polymer would tend to loosen the interactions with DNA for binding to heparin. This resulted in exclusive DNA release which advocated that CDP derivative was indeed able to tightly pack the DNA into the nanoparticle core and consolidated the whole complex against enzymatic degradation.

It is a matter of concern to know the compatibility of blood and a foreign material like the polymer CDP which in general terms would provoke complicated body responses. A safe polymeric based non viral system should not face any kind of interference from the blood cells during its circulatory movement and facilitate minimal interactions that are not detrimental. The use of certain biological relevant conjugates and polyethylene glycol has been able to accomplish better biocompatibility to the polymer. Conjugation with PEG is the most noted approach of generating safe polymeric derivatives as they contribute the ‘steric stabilization’ nature which helps the polymer based nanoconjugates to evade unwanted reactions

with blood and immune cells. In this study, the polymer CDP was introduced to red blood cells to investigate the response from the most prominent cells of the blood supply. The results from both hemolysis and red blood cell aggregation disclosed healthy cells without any lysis or aggregation in the presence of the CDP derivative. The percentage of hemolysis was very much below the permitted 1 % value and microscopic images of red blood cells revealed the cells to be identical with the RBC treated with only saline. The results were similar to an earlier report with protamine derivative (Thomas et al., 2010) which also supported protamine derivatised compound to be compatible with red blood cells. Another issue to pertain to is the study of the physicochemical properties of the polymer on the serum proteins known as opsonins that get adsorbed onto any nanomaterial. Considering the high surface energy that exists on nanomaterials, the process of protein adsorption or opsonisation around the polymer could not be ruled out (Xu et al., 2007). Here also the role of PEG is significant to produce steric stabilization and avert the serum proteins from interacting with the polymer. Even at a very high concentration, CDP derivative did not adsorb the serum proteins and hence protein bands were distinctly seen in the native PAGE gel as observed in the same way as in saline treated serum.. It is therefore assumed that the CDP derivative could be well tolerated in the physiological fluids, reduce the recognition by the reticuloendothelial system that is responsible for serum clearance and prolong the circulation time of the nanoparticles in order to arrive at the tumour sites.

The positive charges in the CDP polymer are necessary for nanoparticles to gain adherence to the cells but this should not evoke any membrane perturbation that might damage the cell. Hence the elucidation of cell viabiliy is a decisive factor to

progress the CDP nanoparticles study for *in vitro* analysis. It was observed that cell viability was significantly higher for all the four concentrations of the CDP polymer which depicted that the attachment of both protamine and PEG diamine in the chitosan backbone proved to be non toxic for the polymer to be compatible with the cells. The lack of toxicity with the CDP derivative was comparable to that of the medium alone treated cells and wholly different from the toxic effect by Triton X-100 and polymer like PEI.

The major focus in the incorporation of both PEG diamine and protamine into the chitosan backbone was to modulate the derivative with plus points of the two conjugates that would allow permissible gene delivery to the cells. PEG diamine acted both as the linker and stealth provider to the derivative while protamine cast membrane permeability and nuclear localisation cues for the derivative to arrive at the cell and the nucleus. Glioma cells represented the most malignant tumour condition of the central nervous system and constituted 77 % of all the different types of brain tumour cells (Béduneau et al., 2007; Caffo et al., 2014). Despite surgical treatment regime, brain tumour continues to end up with the highest mortality once the high grade glioma is diagnosed. Patients hardly survive for more than a year and chemotherapy is a failed attempt since the intravenously administered drugs are relatively impermeable to the blood brain barrier (BBB) that separate the circulatory system from cerebral parenchyma.

At this juncture, nanoparticle based systems might provide a solution to deliver the specific anticancer agents or therapeutic genes across the BBB. The blood brain barrier is characterised mainly by endothelial cells that comprise specific endocytosis pathways which restrict the free movement of substances across the

cells. Therefore chitosan based nanoconjugates were explored in *in vitro* C6 cells of glioma to recognize the effectual possibility of gene delivery. The effect of functionlisation was demonstrated with cell uptake experiment in C6 glioma cells that very well depicted bright green fluorescent cells across the field of view. The cellular internalization of CDP nanoparticles was further estimated with flow cytometry and around 90 % CDP nanoparticles found their way inside the nucleus indicating that CDP nanoparticle was able to adhere to the cell surface and gain access inside.

Once CDP nanoplex has entered the cell, it is essential to learn by which pathway that the nanoparticle was recruited across the cell. This study would prove to be beneficial as nanoparticles could be customized to enter the specific endocytosis pathways and localize to the desired subcellular organelles. The glioma cells were treated with CDP/YOYO tagged plasmid nanoparticle that had the desirable cationic surface charge, spherical shape and size that is almost 100nm which evidently would be recognized by the receptors of the different pathways (Sahay et al., 2010). The fluorescence of YOYO tagged plasmid/CDP nanoparticles enabled clear visibility of the location of the nanoparticles in the cells. But in the presence of certain chemicals that acted as inhibitors of the various commonly used pathways, the fluorescence was diminished with scanty distribution.

The pathway mediated by clathrin coat proteins were impeded by chlorpromazine and was found to have very minimal inhibition against the entry of CDP nanoparticles since the fluorescent nanoparticles seemed to be localised in the cell. And in other three pathways also, there was only very small degree of inhibition as observed in the case of dynamin dependent clathrin mediated pathway that was

blocked by dynasore, macropinocytosis blocked by amiloride and receptor mediated pathway blocked by protamine conjugate. However caveolae pathway blocked by filipin showed comparatively good inhibition with very faint fluorescence in and around the cells that suggested the likelihood of preventing free movement of CDP nanoparticles into the cell. Earlier reports (Priya et al., 2014) showed that protamine based nanoconjuagtes chose caveolae pathway above others for cellular entry and this has been found to be true with nanoparticles formed from protamine grafted PEG diamineylated chitosan derivative also.

The extend of successful delivery of CDP nanoparticle in tumour cells could be manifested only in terms of transgene expression which is the main therapeutic goal at the end of any non viral gene delivery system application. Transfection efficiency of CDP nanoparticles was interpreted from the qualitative result obtained with the Live Dead assay on cells treated with CDP/p53 plasmid. The assay introduced calcein and ethidium homodimer dyes to stain the live and dead cells respectively. Since p53 plasmid is responsible for apoptosis, cells which got transfected with p53 gene that underwent apoptosis lead to disruptions in the cell membrane that permitted the diffusion of the red stain ethidium homodimer that preferentially stained cells with damaged cell membrane. The control that was transfected with PEI based nanoparticles had cell death while the cells treated with p53 alone showed live cells that were stained green. The toxic condition in the cells clearly represented the effective transfer of the gene mediated by the non toxic polymer CDP. Consequently the cell death caused by p53 expression proposed that CDP nanoparticles were able to unpack the vector complex with plasmid DNA p53 being transferred to the nucleus for the desired expression of the gene and its protein.

5.3 Enhanced intracellular uptake and endocytic pathway selection mediated by ornithine grafted chitosan polycation for gene delivery

Chitosan is a versatile polymer due to certain intrinsic properties that the naturally derived polymer possessed which included low toxicity, optimal biocompatibility, suitability for high loading and condensing ability for polyanionic molecules. The polymer is subjected to widespread research by modifying existing versions of chitosan polymer to achieve an ideal colloidal vector. It is known that functionalizing chitosan with amino acids, those which are generally present in the human system would aid in biocompatibility and gene delivery to the tumour cells. Ornithine, a precursor of polyamines such as spermine and spermidine could serve as a tumour targeting moiety for nanoparticles since the abnormal proliferating cells such as the tumor have elevated polyamine metabolism. Therefore an attempt was performed to derivatize chitosan with ornithine.

Studies have also reported that an intermediate molecular weight range for chitosan was befitting for nanoparticle formulations (Alex et al., 2011).The intermediate molecular weight range around 120 kDa of chitosan was adopted for ornithine conjugation. On the basis of primary amine composition of the CON derivative with TNBS assay, the conjugation of ornithine was confirmed with the excess amount of amines found in the synthesized derivative. Moreover, the chemical composition of CON derivative was also ascertained with FTIR and ^{1}H NMR. In CON FTIR spectrum, the saccharide structure of chitosan retained at 1068cm^{-1} (skeletal vibrations of C-O-C stretching) while the amide peaks has been shifted to 1631$cm^{-1}$and 1535cm^{-1} in comparison with the chitosan spectrum. The

shift in the amide bond indicated the incorporation of ornithine into chitosan. Given the presence of peaks of ornithine and chitosan in the ^{1}H NMR spectrum also affirmed the gafting of chitosan with ornithine. The DSC analysis showed the thermal peak to vary in the synthesized CON derivative from the unmodified chitosan which indicated the formation of CON polymer.

Endosomal escape is another essential parameter necessary for cationic nanoparticles to execute gene delivery to nucleus for expression. The endosomal release of DNA is brought about by the proton sponge effect of polymeric nanoparticles that refers to its buffering property (Lundqvist et al., 2008). Ornithine grafted chitosan was able to provide a strong buffering capacity in the endosomal pH range than compared to the unmodified chitosan. This optimal buffering range would enable endosomal release without causing much toxicity to the cells. Although buffering ability is less compared to PEI, the presence of both secondary and tertiary amine groups responsible for its broad buffering ability is also one of its factors to be highly toxic.

In aqueous state, CON polymer formed complexes with DNA and bound tightly so as to attain the nanosize that was confirmed by determining the hydrodynamic diameter of the complexes. The ratios that resulted featured a balance between the opposite charges of both polymer and DNA producing optimal sizes within 150nm range. It is well known that size and surface charge of the nanoparticles have a great influence on the basic nature of complexes in physiological conditions (Carlstedt et al., 2012). Therefore an optimal size within 100nm was chosen for further *in vitro* studies.

In TEM image analysis it could be argued that the shape is dependent on the affinity binding property of the opposite charges present in both polymer and DNA which influence the shape of nanoparticles. Chitosan ornithine derived nanoparticles on association with DNA tend to appear irregular in shape instead of absolute spherical shapes. Coincidently similar type of distorted shapes of chitosan DNA constructs have also been reported (Sajomsang et al., 2011).

DNA retardation in agarose gel electrophoresis is another supporting factor that confirmed the intact binding ability of CON polymer with DNA. The effect of CON polymer in DNA binding was assessed by observing the retention of DNA inside the wells due to the strong interaction between CON and plasmid DNA. Both DNase degradation and heparin release showed that the nanoparticles protected DNA against enzymatic attack and maintained the integrity. In addition to this, compatibility of red blood cells with the CON polymer was addressed to ensure that the physiological fluid system of our body is able to tolerate the effects of nanoparticles. Aggregation of red blood cells could arise only when the reactive groups in CON polymer cause unwanted reactions with the erythrocytes. Nevertheless, no significant toxic effect was identified for CON polymer with the red blood cells as CON derivative components were physiologically biocompatible and biodegradable. Polycationic nanoparticles (Lundqvist et al., 2008) mask DNA from the circulating proteins to a certain degree and therefore polymer CON when subjected to native gel electrophoresis displayed absence of any protein interactions. The bands obtained were similar to the bands seen with normal saline which is the control, indicative of minor protein adsorption that may not cause immunological

responses. The presence of bands in the gel indicated that CON polymer is compatible with the serum and is able to ward off any protein adsorption.

Cell viability is necessary for the polymer to be used further and hence reagent MTT was implemented to compare the metabolism of live cells from those affected cells in response to the addition of CON polymer. The modified derivative of chitosan with ornithine has demonstrated a good level of viability even on treatment with a maximum of 100 μg concentration, almost similar in comparison to the control of untreated cells. This supports the rationale that incorporation of surface modifications in biocompatible chitosan produced negligible toxicity (Lai & Lin, 2009). Lack of toxicity for chitosan ornithine conjugate suggested that no harm could occur to cells when they would be treated with CON nanoparticles.

Gene delivery to glioma cells (Fueyo et al., 1999) had gained rapid interest as these cells act as active targets for local gene therapy due to their complete localization into the central nervous system and devoid of remote metastases. Therefore the efficacy of CON nanoparticle was further investigated in glioma cells to evaluate the complete internalisation of the nanoparticles. The dye YOYO iodide had been adopted for fluorescent microscopy imaging as it is unaffected by any pH variations (Gao et al., 2013). The fluorescence intensity produced by this dye after binding specifically to nucleic acids is very high when compared to other covalent dyes. As YOYO is cell impermeant, only nanoparticles with YOYO tagged DNA would gain entry inside the cell and reveal green fluorescence. Ornithine in chitosan modification encouraged the localisation of the tagged plasmid in the proximity of Hoechst stained nuclear regions and hence affirmed cellular entry. This has also been

ascertained in literature that ornithine residues mediate efficient gene transfection in cell lines (Perry et al., 2008).

Nanoparticles enter the cells via the endocytic pathways and selective inhibition of the different pathways was initiated to identify the relevant intracellular track adopted by CON nanoparticle for cell internalisation. Hence glioma cells were treated separately with each inhibitor specific to the known pathways before cell incubation with the nanoparticles (Kumar et al., 2011). Caveolae and macropinocytosis were not inhibited much as nanoparticle crowding was observed in the cytoplasm. Inhibiton of clathrin mediated endocytosis was observed with least cell uptake and this was further validated with cells treated with the inhibitor dynasore (Ivanov, 2008) that inhibit the activity of the molecule dynamin which caused scission of clathrin coated vesicles containing the engulfed nanoparticles. Dynamin independent clathrin mediated mechanism route also prevails in cells which might be the reason for very faint fluorescence uptake in dynasore treated cells. However, most of the nanoparticles were barred extensively from entering the nucleus which clearly emphasized that clathrin mediated pathway depending on dynamin scission is the primary pathway for uptake of chitosan ornithine nanoplexes.

Since enhanced cellular internalisation of CON nanoparticles occurred, the transfection efficiency of CON nanoparticles was analysed with the Live Dead assay on cells treated with CON/p53 plasmid complexes. The p53 gene was expressed in the cells which resulted in the apoptosis state and the dead cells allowed the diffusion of ethidium homodimer dyes which is specific for damaged cells, thus enabling detection of red fluorescence in the cells. Very less live cells were present that indicated the effective uptake of CON nanoparticles inside the cell, causing cell

death. The presence of only the p53 plasmid does not facilitate transfection which was inferred from the control cells that showed the green stained viable cells. Hence CON polymer turned out to be an effective non viral delivery system for transgene expression.

5.4 Nanoparticle mediated gene expression and intracellular trafficking by spermine derivatized chitosan ornithine conjugate (COSM).

The previous matrix chitosan ornithine conjugate was able to meet the basic requirements of an effective gene delivery system in terms of DNA condensation, endososmal escape, cell viability and transgene expression. Although ornithine incorporation into the chitosan backbone has improved its solubility and transfection property, an additional specificity for the derivative was incorporated to enhance its attributes. In chitosan-ornithine conjugate, the conjugate ornithine is a very low molecular weight amino acid that has been an active candidate involved in most of the biochemical pathways that occured in the cells. However it is well known that conjugation of certain target ligands such as folic acid and transferrin (Kim et al., 2006) to polysaccharide matrixes uplift the gene delivery efficacy of the derivatives. And therefore it would be desirable to achieve a chitosan conjugate that possessed specificity in tumour targeting and limit its exposure to the surrounding normal cells.

Such a similar functional biomolecule is the polyamine spermine, which is already reported as a suitable polycation (Alex et al., 2011) for non viral gene delivery. The targeting groups are often selected to be unique biomolecules that are associated with the signal transduction in the cells for proliferation and tumour

suppressing cues which have receptors that would be highly regulated and overly expressed in the tumour cells. Polyamines are widely recognized amine rich organic molecules that play a significant role in regulating cell's normal functions and haemostasis stature. In this regard, ornithine is one of the precursors in the polyamine biosynthesis cascade that lead to the formation of one of the main polyamines, spermine. Incorporation of spermine has been the reason for certain natural polysaccharides like dextran to be reformed into a matrix suitable for gene delivery purposes (Hosseinkhani et al., 2004).

Spermine is a tetra amine, a higher polyamine that has wide spectra of regulatory roles at genome level which include DNA condensation to gene modulation. In the polyamine biosynthetic pathway, the rate limiting step is the conversion of ornithine into the first and the simplest diamine, the putrescine. The enzymatic reaction is driven by the catalytic enzyme ODC whose encoding gene is greatly influenced by tumour promoters. Attachment of further aminopropyl groups into putescine leads to the formation of spermine and spermidine in the cells (Minois et al., 2011). Tumour cells will have high metabolism rate than normal cells and hence the growth factors and tumour promoters influence the ODC gene to upregulate polyamines that is necessary for cell proliferation. In addition to this, the uncontrolled growth of tumour cells will induce cues to attract extracellular polyamines that are needed to drive excessive metabolism (Gerner et al., 2004). This becomes an advantage for nanoconjugates that have spermine residues which are likely to be deviated from its normal route to tumour localised regions and are entrapped by the enhanced permeation effect. In course of action, the transfer of a

therapeutic gene of interest to the tumour site mediated by the nanoconjugates is strikingly possible.

In this work, spermine was grafted to the chitosan ornithine matrix with this objective in mind and using DSC/DMAP, the hydroxyl groups of chitosan is activated to react with the amine group in spermine. The conjugation was confirmed by FTIR, ^{1}H NMR and DSC which affirmed that the grafting of the polyamine has occurred and have been well integrated into the chitosan backbone. Progressive acidification of the endosome is an essential strategy for cationic polymer to dispense the release of nanoparticles that would be captured inside the endosome during its cell entry. The buffering capacity was quite reasonable for chitosan ornithine but further conjugation with spermine has extended the buffering range for the derivative COSM. Hence nanoparticles formed with COSM would cause the swelling and rupture of endosome which help them to escape from being directed towards lysosome for degradation. Although PEI is the best buffering agent, the amine groups that conveyed this attribute is also responsible for making the polymer highly cytotoxic. The titration curve of COSM resisted the acidification at a range much lower than the usual pH 5-6 range seen in polymers like PEI. However this did not preclude the derivative from proton induction in the endosome and therefore any plausible correlation between high pH range of buffering and the transfection ability of the derivative does not favour in the case of chitosan based derivative.

Alternative to this, a recent report had suggested that the ionisation behaviour of chitosan is the significant parameter that results in the proton sponge effect similar to that of PEI and bring forth the endosomal release of nanoparticles (Richard et al., 2013). It is interesting to note that the polymer backbone actually play a pivotal in

inducing endosome acidification rather than the conjugated residues since a similar situation exists for the polyamine/PK core-shell nanoparticles where the acid-degradable PK shell induce cytosolic release while spermine promote the DNA complexation and biocompatibile nature (Cho & Kwon, 2011).

Since COSM derivative has the suitable buffering ability to conduct endosomal escape, the amine groups in the COSM polymer that allocate this distinction are also able to render strong interactions with pDNA to develop nanoparticles or nanoplexes. In accord with this, the dynamic light scattring mechanism allowed the determination of the mean diameter and surface charge of the COSM nanoparticles and fostered optimal size range and positive zeta potential that could result in a satisfactory cell uptake. Ratios below 10 gave nanoparticles with very large dimensions of microsize and varying surface charges that ascribed poor nanoparticle formation. But higher ratios from 11-20, though produced nanoparticle size range within 200-300 nm, bestowed an attractive zeta potential of range 30 mV to 37 mV. The surface charge could make a marked difference in the association of these COSM nanoparticles with the tumour cell surface and assign greater cellular penetration (Wang et al., 2011).

Among the nanoparticles, the least size range and zeta potential of a particular COSM/pDNA nanoparticle ratio 1:16 was adopted for TEM observation that disclosed the actual size dimension to be falling within 200 nm range. Accordingly, the hydrodynamic property was responsible for the larger size in nanoparticles during DLS measurements as the sample is in solution phase while the dried nature of the sample in TEM analysis validates the COSM nanoparticles dimensions (Kanatani et al., 2006). The resulted nanoparticle size and shape of

ellipsoidal pattern were commonly observed for chitosan based systems for gene delivery.

In follow up to this, agarose gel electrophoresis enabled to infer the integrity of COSM nanoparticles from the electrophoretic movement of the COSM nanoparticles and DNA released which conceded the capability of COSM derivative to bind with pDNA and produced stable nanoparticles that protected the nucleic acid from DNase enzyme degradation. The condensation ability is mainly contributed by the presence of spermine in the nanoparticle since the conjugate is widely used for DNA isolation (Feuerstein et al., 1986). Spermine is capable of forming electrostatic interactions with the phosphate groups of the DNA without any base specific interactions thus maintaining DNA integrity at the same time (Shao et al., 2012). Actually this property is of good advantage for the COSM nanoparticles during its systemic delivery.

The compatibility of COSM derivative with the systemic components mainly the red blood cells was addressed with hemolysis and RBC aggregation study. Hemolytic activity by COSM derivative was in effect negligible though the COSM nanoparticles showed a very high zeta potential. Also there was devoid of any RBC aggregation and the cells were intact and maintained their morphology in the presence of very high concentration of COSM derivative. An increase in the positive charge is a desirable trait which also ensures unwanted interaction between the polymer and negatively charged red blood cells leading to cell damage and aggregation. This was actually perceived in the red blood cells treated with PEI polymer which is also a known polycationic polymer. On the contrary, this did not occur to red blood cells treated with spermine functionalised chitosan-ornithine

conjugate and this advanage might be the due to the presence of naturally relevant conjugates like spermine and ornithine that is inherently present in the biological systems.

Another benchmark for COSM compatibility is to assess the interaction of COSM derivative with serum proteins. Serum proteins also referred to as opsonins lead to a process termed opsonisation where serum proteins are adhered to the polymer surface enabling easy identification by the mononuclear phagocytic system (MPS) system to clear the polymer from the circulation (Xu et al., 2007). Therefore when a polycation is run in a PAGE gel, reduction in the protein bands is expected which evaluate the polymer protein interaction. Nevertheless, COSM derivative did not favour any protein adsorption and therefore the serum proteins were vividly present in the Coomassie blue stained gel and appeared in the same manner as how the saline treated serum showed. This approved the chances for COSM nanoparticles to remain in circulation for a prolonged period without being noticed much by the reticuloendothelial sytem and reach the targeted tumour sites. The non toxicity of COSM was affirmed furthermore with another reported matrix that had both chitosan and spermine as constituents (Jiang et al., 2011).

When polymer comes in contact with *in vitro* cells, they should be non toxic and COSM derivative was found to be extremely non toxic to the cells, rather a slight improvement in the cell viability was observed in cells treated with the polymer. The marginal rise in cell proliferation might be due to the presence of spermine, which is a polyamine that is constantly metabolised in the cells for their normal functions. And as tumour cells are used for cytotoxicity analysis, the likelihood of an extensive

polyamine transporter system for polyamine cellular uptake might have engrossed the feasible entry of COSM nanoparticles.

In this study, COSM derivative fulfilled the essential prerequisites to encourage an effective cellular uptake and this was manifested in the glioma cell line with proficient distribution of YOYO fluorescence in the nucleus of the cells. Obviously chitosan ornithine had produced significant cell uptake of the nanoparticles, it was very much noticeable that spermine functionalized chitosan ornithine complexed plasmid treated cells also had a larger influx of the nanoparticles. The cellular recognition of COSM nanoparticles is largely due to the elevated level of polyamine metabolism in glioma cells. Therefore the craving for polyamine has induced the cells to recognize the COSM/pDNA nanoplexes as an essential nutrient, triggering the suitable endocytic pathways for COSM nanoparticle engulfment and allowed the schematic ingress of COSM nanoplexes to the cells. The cells treated with only YOYO tagged plasmid had faint fluorescenece in the cytosol or in the proximity of the cells indicating that cells do permit a meagre amount of DNA to be internalized by the act of pinocytosis. But the fluorescence is very much faded and scarce when compared to the fluorescence brought about by COSM nanoparticles. The fluorescence was observed to be spread uniformly over the transfected cells rather than seen in small portions. This embarked that COSM derivative was able to translocate the pDNA to the cell and unpack its cargo into the host cell nucleus. This made COSM derivative a preferable non viral gene delivery system and the results obtained from flow cytometry and confocal microscope also agreed with the potent uptake of COSM nanoparticles.

It would be useful if the endocytosis pathway could be exploited in a manner that could regulate the trafficking of the COSM nanoparticle and enable better transgene expression. In this line, therefore study of intracellular translocation was initiated by implementing endocytosis inhibition study. The inhibitors are chemicals that block the check points in each endocytosis cascade and affect the facile cell uptake. Clathrin mediated pathway with dynamin dependent was blocked with chlorpromazine and dynasore that revealed an apparent reduction in the nuclear localisation of fluorescent tagged nanoparticles. This represented the dependency of the COSM nanoparticles in employing the clathrin pathway with dynamin for cellular internalization. Inhibiton of the macropinoytosis pathway by amiloride proved to be difficult for the cells to permit easy entry of COSM nanoplexes thereby linking the usage of macropinocytosis for COSM cell uptake. Since COSM derivative has both ornithine and spermine in its chemical structure, blocking the receptor mediated pathway with the same conjugates was adopted in order to verify the fact. Eventually a fair amount of fluorescence depletion was observed that would explain the promising role of ligand attached polymer nanoparticles to avail cellular entry using receptor mediated pathway. In this regard, either the cationic transport system or polyamine transport system must be responsible for the cell uptake which is an area that requires indepth investigation. The caveolae pathway inhibition showed cells having a detectable amount of fluorescence indicating that this pathway would be the last rung on the ladder of preference of endocytosis pathway for intracellular trafficking of COSM nanoparticles. However similar strategy of endocytosis was found in other spermine conjugated derivatives too (Kanatani et al., 2006; Alex et al., 2011). Since endocytosis of nanomedicines is still a field that is

continuously explored (Sahay et al., 2010) evidence of the role of these pathways are important findings for futuristic study with chitosan based nanoparticles.

The employment of multiple pathways for cell uptake of COSM nanoparticles aided an improvement in the transgene expression. The transfection efficiency was profoundly observed to be very high as the apoptosis signals from the plasmid p53 DNA was exemplified in the treated C6 cells. An impressive fluorescent image of cells with bright red fluorescence representing the expression p53 plasmid in the nucleus was observed. Cells that were treated with p53 plasmid alone showed the green stained live cells which helped to comprehend and differentiate the cells which had the effect of p53 expression mediated by COSM nanoparticles. Although apoptotic expression has caused a slight morphological change in the dead cells, there is no such eruption or complete lysis of the cells thus avoiding any detrimental effect to the surrounding tissues.

In general most of the papers based on non viral gene delivery systems have not been successful to explain the actual principle behind the unpacking of polymer/DNA complex which continue to be a popular topic of research and scientific debate. Since COSM derivative has found to be a promising candidate for gene delivery, an attempt has been adopted to study the intracellular unpacking of the nanoparticles by close examination of the trafficking of the tagged polymer and DNA. The fluorescent images disclosed the presence of red fluorescence like a halo around the cells with very bright green fluorescence inside the cells indicating that localisation of the polymeric nanoparticles occur in the cytosolic areas of the cells and the tagged DNA was able to cross the nuclear membrane and emit green fluorescence in the nucleolar regions. It could be argued that the electrostatic force

that is present between the phosphate groups of the nucleic acid and spermine conjugated chitosan ornithine polymer is dependent on the salt concentration of the physiological ionic environment (Luan & Aksimentiev, 2010) which may result an interplay of electrostatics and hydrodynamics that lead to relaxation of the DNA/polymer complex with eventual release of the nucleic acid. This plasmid trafficking study alone could not affirm the unpacking mechanism of nanoparticles and as to establish that statement it requires several novel experiment strategies and tools to completely elucidate the phenomenon which is yet to be unravelled.

CHAPTER 6 SUMMARY AND CONCLUSION

In a broad sense, gene therapy propose to treat cancer at the genetic level that could be accomplished either by replacement of the defective gene with a therapeutic gene or with a functional gene delivery that expressed the protein which prove to be cytotoxic. The direct exposure of the therapeutic gene to tumour cells is implausible as naked gene is susceptible to enzymatic cleavage during its initial journey in the systemic circulation. Hence the transfer of the gene of interest into the tumour cells is the greatest challenge that impedes gene therapy to be a reality. An approach to resolve this is the introduction of gene carriers or vectors designed from natural polymers combined with the concept of nano to ensure an effective gene delivery system.

Chitosan has been considered as a potential polymer for development of nano vectors but has its own demerits of being insoluble in neutral pH that influence the biocompatibility property along with low gene delivery efficacy. The polymer is reported to be feasible for chemical modification which enables a strategic incorporation of ligands that would allow better solubility and enhanced cellular uptake of the gene vectors leading to gene expression. Tumour cells possess equivalent characteristics and biology of a normal cell except that those features would be much enhanced and structured than the normal cells which redirect circulating nutrients and cellular factors towards the tumour cells for massive progression. This trait has been manipulated to decide in the choice of ligands to be embedded in the chitosan polymer that might serve as tumour targeting agent and at the same time may supplement solubility to chitosan and provide transgene expression. The physicochemical parameters have crucial influence in the

modulation of chitosan derived nanoparticles which includes molecular weight, degree of deacetylation, cationic charge density and pH dependency to cite a few. In this thesis, the very high molecular weight of chitosan is reduced by sodium nitrite depolymerisation to arrive at an intermediate molecular weight range of 120-130 kDa in which very few work has been reported. The bioconjugated chitosan derivative was initiated with the depolymerised chitosan and suitable ligands which included sugar, polyamino acid, amino acid and polyamine were substituted into the chitosan polymer for synthesis of nanoparticles with the specificity.

Firstly, the introduction of galactose and spermine into chitosan which rendered both dissolution and tumour targeting property was attempted. Conjugation with galactose alone did not confer the required cationic density for the nanoparticle to adhere and integrate into the anion charged cell membrane and therefore the positive charges were compensated by spermine addition. Chemical characterisation was confirmed with FTIR and ^{1}H NMR with the sizes of the synthesised nanoplexes well within the 200 nm range validated by both TEM and AFM observation. Cationic charge density was in an optimal range within +15 mV that conveyed a reasonable buffering capacity for the GCSM nanoparticles much higher than chitosan as well as displayed DNA gel retardation ability. Compatibility of the GCSM derivative with biological system was established with negligible red blood cell hemolysis and aggregation, absence of plasma protein adsorption and non cytotoxic to *in vitro* cell lines. Since galactose moiety has been used in chitosan derivitization which is recognized by asialoglycoprotein receptors prevalent in liver cells, cell culture studies were carried out in HepG2 cell lines to investigate the extent of a ligand targeted delivery by GCSM nanopaarticles. The Hep G2 cell lines indeed had a good

cell uptake of GCSM nanoparticles and endocytosis pathways preferred by this particular chitosan derivative was found to be mostly the receptor mediated pathway. Gene delivery efficacy was measured with both luciferase gene expression and qualititative assessment of p53 apoptotoic expression that conveyed enhanced transfection ability for the derivative. Even though transfection was very much pronounced, the transfection efficiency was still lesser than PEI transfected cell lines in the case for luciferace expression while apoptosis expression was similar for both GCSM and PEI nanoparticles.

Secondly in another strategy to derivatise chitosan, ligands such as protamine, an arginine rich polyamino acid was conjugated but the synthesized derivative of chitosan protamine failed to enhance solubility and had an impaired DNA condensation ability as steady distribution of positive charge was not present. Hence to stabilize the chitosan nanoparticles, PEG diamine was grafted at first to chitosan since PEG has the property of steric stabilization followed by protamine substitution. This indeed gave way to CDP derivative which was soluble at neutral pH whose conjugation was characterised by TNBS assay, FTIR, ^{1}H NMR and DSC analysis followed by slightly higher buffering capacity range than GCSM polymer and unmodified chitosan. The favourable size range and spheroidal shape of almost 100 nm established by DLS and TEM analysis prevented DNA migration in the gel towards the negative electrode and protected against DNase degradation. Blood compatibility of CDP was tested with red blood cells and blood plasma that showed minimal hemolysis and aggregation of red blood cells when in contact with CDP derivative and at the same time did not cause opsonisation that often lead to the removal of proteins from the blood plasma. Hence CDP did not provoke any

unwanted reactions with blood which mark the derivative to be suitable for *in vivo* study. Cell viability with C6 glioma cells was very well observed with CDP derivative and with the help of fluorescence microscope and flow cytometry, the cell uptake of CDP nanoparticles was also efficiently revealed with fluorescence of YOYO tagged pDNA inside the cells. This was followed by endocytosis inhibition study to unravel the pathway responsible for the efficient cell uptake and it was conceivable that caveolae pathway had a major role in recruiting the nanoparticles inside the cell. The transfer of gene to the nucleus was accomplished by CDP nanoparticles that were clearly shown by the Live Dead assay using p53 gene expression that lead to apoptosis. Cells treated with p53 plasmid alone did not execute cell death while cells treated with CDP nanoparticles had the apoptotic gene delivered to the nucleus and caused gene expression. However protamine was the only substituent in CDP derivative that favoured a tumour targeting specificity. Therefore to further enhance diverse targeting ability for chitosan, other biologically relevant conjugates were considered.

One such strategy was the adoption of the amino acid ornithine, which was part of the arginine biogenesis pathway and an extensively used amino acid for a variety of biochemical process in the cells. Incorporation of ornithine into the depolymerised chitosan backbone enhanced the solubility of chitosan in neutral pH and conjugation was confirmed by FTIR, ^{1}H NMR and DSC analysis. The amines in the chitosan derivative were responsible for protonation that provided a higher acid base titration for CON derivative than chitosan as well as a good zeta potential charge of +17 mV that yielded nanoplexes of 100 nm size. The size range was ascertained by TEM and AFM showing an ellipsoidal kind of shape and the CON

nanoplexes were able to retard DNA in the wells of the gel thus packing it tightly and masking it from nuclease degradation. Hemolysis and red blood cell aggregation hardly occurred when chitosan ornithine conjugate was treated with red blood cells and the derivative did not adsorb any serum proteins in presence of blood plasma indicating that CON did not elicit any systemic reactions. Both this experiments finally made it aware that CON was blood compatible and safe to be used for *in vivo* conditions. CON derivative did not cause any disturbance to the cell viability in C6 glioma cells and hence was adopted for further cell uptake and transfection studies. Both fluorescence and flow cytometry investigated the cell uptake of CON nanoparticles to be very high and endocytosis pathway inhibition study was evaluated to determine the pathways that encouraged efficient cell uptake. Fluorescent and confocal observation unravelled that clathrin mediated endocytosis with dynamin dependency as the primary cell uptake pathway for CON nanoparticles. Transfection efficiency was demonstrated by p53 gene expression that showed cell death in the glioma cell lines without causing any lysis or burst release of the cells. Since the derivative CON was considered non toxic, the apoptosis state of cells was only brought about by CON nanoparticle which succeeded in transferring the p53 gene to cells followed by gene expression.

Our previous study with GCSM derivative has pursued us to realise the benefits of the polyamine spermine which is also one of the candidates in the ornithine biogenesis pathway and therefore an attempt was made to combine the effect of polyamine to the CON conjugate. Chitosan ornithine conjugate was further reformed with spermine conjugation which maintained the enhanced solubility for chitosan derivative and chemical characterisation was established with FTIR, ^{1}H

NMR and DSC analysis. It was demonstrated that the primary amine composition has increased which corresponded to the enhanced buffering capacity much higher than the other synthesized derivatives. The cationic surface density of the COSM nanoparticles was around +30 mV which is a highly recommended zeta potential for cell uptake and size range came within the 200 nm range as given by TEM observation. The steric hindrance of two charged conjugates might be the reason for slight increase in nanoparticles size for COSM when compared to the nanoparticle size formed from CON. Nevertheless the DNA retardation ability was well maintained by COSM derivative during the migration of COSM nanoparticles and effectively shielded the gene from enzymatic cleavage. The capability of COSM derivative to be compatible with *in vivo* conditions was established by performing basic haematological related studies that included blood hemolysis study which showed negligible haemolytic activity within 1 % permissible value, non occurrence of erythrocyte aggregation and absence of plasma protein interaction with the derivative. Simultaneously COSM derivative proved to be non toxic in C6 glioma cells and offered very much cell viability which indicated that tumour cell lines extensively utilised polyamines for their metabolism. Excellent cell uptake was noticed with fluorescent images that were supported further by confocal which showed the COSM nanoparticle localised within the cell and nucleus and flow cytometry also estimated the high count of cells that had the tagged nanoparticles. Furthermore investigation of the endocytosis pathway revealed that COSM nanoparticle utilised multiple pathways for their cellular entry with major share driven by the clathrin dynamin dependent and ligand receptor pathways suggesting that a receptor recognizing the polyamine is predominating the cellular uptake of

COSM nanoaparticles. Finally gene expression is the ultimate goal for nanoparticle mediated gene delivery and with aid of live dead assay the transfection efficiency was demonstrated with p53 apoptosis expression that caused the death of cells leaving very little live cells. The profound cell uptake and intracellular nanoparticle trafficking indicated that COSM nanoparticles effectively entered the cells and caused nanoparticle diaassembly that enabled the release and transfer of p53 gene to nucleus for apoptosis expression.

Until now, an impeccable gene delivery system is a faraway reality for cancer therapy but all the four bioconjugated chitosan derivatives had met the essential prerequisites to be an effective nanoparticle gene delivery system and however COSM derivative was found to be the most promising among them. The derivative had the attributes of enhanced solubility, enhanced buffering capacity that did not cause any toxic effect both at systemic and cellular levels and the presence of spermine conjugate has resulted in outstanding cell uptake that lead to exclusive transgene expression.

It would be very much beneficial to incorporate future study with COSM derivative with a focus on the polyamine pathway study by adopting cell lines that are devoid of this pathway. Moreover gene expression analysis could be tried with other therapeutic genes like VEGF (Vascular endothelial growth factor) also along with real time PCR estimation. And finally *in vivo* studies also could be attempted to establish further the potentiality of the particular derivative for gene delivery.

REFERENCES

Acheampong DO, Zhang J, Wang M (2013) Angiogenesis and cancer therapy. *Int J Pharm Sci Rev Res* 4(6): 2021-2027.

Alex SM, Rekha MR, Sharma CP (2011) Spermine grafted galactosylated chitosan for improved nanoparticle mediated gene delivery. *Int J Pharm* 410(1-2): 125-37.

Alexis F, Pridgen EM, Langer R, Farokhzad OC (2010) Nanoparticle technologies for cancer therapy. *Handb Exp Pharmacol* 197: 55-86.

Amaduzzi F, Bomboi F, Bonincontro A, Bordi F, Casciardi S, Chronopoulou L, et al. (2014) Chitosan-DNA complexes: Charge inversion and DNA condensation. *Colloids Surf B Biointerfaces* 114: 1-10.

Arvizo RR, Miranda OR, Moyano DF, Walden CA, Giri K, et al. (2011) Modulating pharmacokinetics, tumor uptake and biodistribution by engineered nanoparticles. *PLoS ONE* 6(9): e24374.

Awotwe-Otoo D, Agarabi C, Keire D, Lee S, Raw A, Yu L, Habib MJ (2012) Physicochemical characterization of complex drug substances: evaluation of structural similarities and differences of protamine sulfate from various sources. *AAPS J* 14(3): 619–626.

Azzam T, Eliyahu H, Makovitzki A, Linial M, Domb AJ (2004) Hydrophobized dextran-spermine conjugate as potential vector for in vitro gene transfection. *J Control Release* 96(2):309-23.

Béduneau A, Saulnier P, Benoit JP (2007) Active targeting of brain tumors using nanocarriers. *Biomaterials* 28(33): 4947- 67.

Behr JP (1997) The proton sponge: a trick to enter cells the viruses did not exploit. *Chimia* 51: 34–6.

Benjaminsen RV, Mattebjerg MA, Henriksen JR, Moghimi SM, Andresen TL (2013) The possible "proton sponge " effect of polyethylenimine (PEI) does not include change in lysosomal pH. *Mol Ther* 21(1): 149-57.

Benns JM, Mahato RI, Kim SW (2002) Optimization of factors influencing the transfection efficiency of folate–PEG–folate-graft-polyethylenimine *J Control Release* 79: 255–269.

Bergens G, Benjamin LE (2003) Tumorigenesis and the angiogenic switch. *Nat Rev Cancer* 3(6): 401-410.

Bertrand N, Wu J, Xu X, Kamaly N, Farokhzad OC (2014) Cancer nanotechnology: The impact of passive and active targeting in the era of modern cancer biology. *Adv Drug Deliv Rev* 66: 2–25.

Bordia F, Camettia C, Sennatoa S, Viscomia D (2007) Radiofrequency dielectric loss relaxation in polyion-induced liposome aggregates. *J Colloid Interface Sci* 309: 366–372.

Bray F, Jemal A, Grey N, Ferlay J, Forman D (2012) Global cancer transitions according to the Human Development Index (2008–2030): a population-based study. *Lancet Oncol* 13: 790–801.

Buschmann MD, Merzouki A, Lavertu M, Thibault M, Jean M, Darras V (2013) Chitosans for delivery of nucleic acids. *Adv Drug Deliv Rev* 65: 1234–1270.

Caffo M, Raudino G, Caruso G (2014) Nanotechnology and Brain Tumors Drug Delivery. *Recent Pat Nanomed* 3(1): 26-36.

Cai LL, Liu P, Li X, Huang X, Ye YQ, Chen FY, et al. (2011) RGD peptide-mediated chitosan-based polymeric micelles targeting delivery for integrin-overexpressing tumor cells. *Int J Nanomedicine* 6:3499-508.

Cairns RA, Harris IS, Mak TW (2011) Regulation of cancer cell metabolism. *Nat Rev Cancer* 11: 85-95.

Calvo MB, Figueroa A, Pulido EG, Campelo RG, Aparicio LA (2010) Potential role of sugar transporters in cancer and their relationship with anticancer therapy. *Int J Endocrinol* 2010: 1-14.

Canton I, Battaglia G (2012) Endocytosis at the nanoscale. *Chem Soc Rev* 41(7): 2718-39.

Carlstedt J, Lundberg D, Dias RS, Lindman B (2012) Condensation and decondensation of dNA by cationic surfactant, spermine, or cationic surfactant−cyclodextrin mixtures: macroscopic phase behavior, aggregate properties, and dissolution mechanisms. *Langmuir* 28: 7976−89.

Casé AH, Picola IPD, Zaniquelli MED, Fernandes JC, Taboga SR, Winnik FM, Tiera MJ (2009) Physicochemical characterization of nanoparticles formed between DNA and phosphorylcholine substituted chitosans. *J Colloid Interface Sci* 336, 125–133.

Casettari L, Vllasaliu D, Castagnino E, Stolnik S, Howdle S, Illum L (2012) PEGylated chitosan derivatives: Synthesis, characterizations and pharmaceutical applications. *Prog Polym Sci* 37:659-685.

Chang KL, Higuchi Y, Kawakami S, Yamashita F, Hashida M (2010) Efficient gene transfection by histidine-modified chitosan through enhancement of endosomal escape. *Bioconjug Chem* 21(6): 1087–1095.

Chari RVJ (1998) Targeted delivery of chemotherapeutics: tumor activated prodrug therapy *Adv Drug Deliv Rev* 31: 89 – 104.

Chen Y, Mohanraj VJ, Wang F, Benson HAE (2007) Designing chitosan–dextran sulfate nanoparticles using charge ratios. *AAPS Pharm Sci Tech* 8: 1-9.

Cheng Yi, Luo X, Betz J, Buckhout-White S, Bekash O, Payne GF, Bentley WE, Rubloff GW (2010) In situ quantitative visualization and characterisation of chitosan electrodeposition with paired sidewall electrodes. *Soft matter* 6: 3177-3183.

Chlebowski RT, Anderson GL (2012) Changing concepts: menopausal hormone therapy and breast cancer. *J Natl Cancer Inst* 104 (7): 517-27.

Cho SK, Kwon YJ (2011) Polyamine/DNA polyplexes with acid-degradable polymeric shell as structurally and functionally virus-mimicking non viral vectors. *J Control Release* 150(3): 287-97.

Chua TC, Liauw W, Koong HN, Esquivel J (2011) Surgical therapies in metastatic colorectal cancer with a potential for Cure. *Am J Clin Oncol* 34(3): 326-331.

Conner SD, Schmid SL (2003) Regulated portals of entry into the cell. *Nature* 422: 37−44.

Cuenca AG, Jiang H, Hochwald SN, Delano M, Cance WG, Grobmyer SR (2006) Emerging implications of nanotechnology on cancer diagnostics and therapeutics. *Cancer* 107(3): 459–466.

Dash M, Chiellini F, Ottenbrite RM, Chiellini E (2011) Chitosan – a versatile semisynthetic polymer in biomedical applications. *Prog Polym Sci* 36: 981–1014.

Dikshit R, Gupta PC, Ramasundarahettige C, Gajalakshmi V, Aleksandrowicz L, Badwe R et al. (2012) Cancer mortality in India: a nationally representative survey. *Lancet* 379: 1807–16.

Dominska M, Dykxhoorn DM (2010) Breaking down the barriers: siRNA delivery and endosome escape. *J Cell Sci* 123(8): 1183-9.

Dufes C, Muller JM, Couet W, Olivier JC, Uchegbu IF, Schätzlein AG (2004) Anticancer drug delivery with transferrin targeted polymeric chitosan vesicles. *Pharm Res* 21(1): 101-7.

Edelstein ML, Abedi MR, Wixon J (2007) Gene therapy clinical trials worldwide to 2007--an update. *J Gene Med* 9(10): 833-42.

Eliyahu H, Joseph A, Azzam T, Barenholz Y, Domb AJ (2006) Dextran-spermine-based polyplexes--evaluation of transgene expression and of local and systemic toxicity in mice. *Biomaterials* 27(8): 1636-45.

Eliyahu H, Joseph A, Schillemans JP, Azzam T, Domb AJ, Barenholz Y (2007) Characterization and in vivo performance of dextran-spermine polyplexes and DOTAP/cholesterol lipoplexes administered locally and systemically. *Biomaterials* 28(14): 2339-49.

Eliyahu H, Makovitzki A, Azzam T, Zlotkin A, Joseph A, Gazit D, Barenholz Y, Domb AJ (2005) Novel dextran-spermine conjugates as transfecting agents: comparing water-soluble and micellar polymers. *Gene Ther* 12(6): 494-503.

Eliyahu H, Siani S, Azzam T, Domb AJ, Barenholz Y (2006) Relationships between chemical composition, physical properties and transfection efficiency of polysaccharide-spermine conjugates. *Biomaterials* 27(8): 1646-55.

Elsabahy M, Nazarali A, Foldvari M (2011) Non-viral nucleic acid delivery: key challenges and future directions. *Curr Drug Deliv* 8(3): 235-44.

El-Sayed A, Futaki S, Harashima H (2009) Delivery of macromolecules using arginine-rich cell-penetrating peptides: ways to overcome endosomal entrapment. *AAPS J* 11(1): 13-22.

El-Sayed A, Khalil IA, Kogure K, Futaki S, Harashima H (2008) Octaarginine- and octalysine-modified nanoparticles have different modes of endosomal escape. *J Biol Chem* 283(34): 23450-61.

Endoh T, Ohtsuki T (2009). Cellular siRNA delivery using cell-penetrating peptides modified for endosomal escape. *Adv Drug Deliv Rev* 61: 704-709.

Engel S, Heger T, Mancini R, Herzog F, Kartenbeck J, Hayer A, Helenius A (2011) Role of endosomes in simian virus 40 entry and infection. *J Virol* 85(9): 4198-211.

Erbacher P, Bettinger T, Belguise-Valladier P, Zou S, Coll JL, Behr JP, Remy JS (1999a) Transfection and physical properties of various saccharide, poly(ethylene glycol), and antibody-derivatized polyethylenimines (pei). *J Gene Med* 1(3): 210–22.

Erbacher P, Zou S, Bettinger T, Steffan AM, Remy JS (1998) Chitosan-based vector/DNA complexes for gene delivery: biophysical characteristics and transfection ability. *Pharm Res* 15, 1332–1339.

Escoffre JM, Bellard E, Golzio M, Teissi J, Rols MP (2009) Transgene expression of transfected supercoiled plasmid DNA concatemers in mammalian cells. *J Gene Med* 11: 1071–1073.

Fang N, Chan V, Mao HQ, Leong KW (2001) Interactions of phospholipid bilayer with chitosan: effect of molecular weight and pH. *Biomacromolecules* 2(4): 1161–1168.

Feuerstein BG, Pattabiramant N, Marton LJ (1986) Spermine-DNA interactions: A theoretical study. *Proc Nad Acad Sci USA* 83: 5948-5952.

Floor SL, Dumont JE, Maenhaut C, Raspe E (2012) Hallmarks of cancer: of all cancer cells, all the time? *Trends Mol Med* 18(9): 509-515.

Fueyo J, Manzano CG, Yung WKA, Kyritsis AP (1999) Targeting in gene therapy for gliomas. *Arch Neurol* 5: 445-59.

Gao JQ, Lv Q, Li LM, Tang XJ, Li FZ, Hu YL, Han M (2013) Glioma targeting and blood-brain barrier penetration by dual-targeting doxorubincin liposomes. *Biomaterials* 34(22): 5628-39.

Gaumet M, Vargas A, Gurny R, Delie F (2008) Nanoparticles for drug delivery: the need for precision in reporting particle size parameters. *Eur J Pharm Biopharm* 69(1): 1-9.

Germershaus O, Mao SR, Sitterberg J, Bakowsky U, Kissel T (2008) Gene delivery using chitosan, trimethyl chitosan or polyethylenglycol-graft-trimethyl chitosan block copolymers: establishment of structure–activity relationships *in vitro*. *J Control Release* 125: 145–154.

Gerner EW, Meyskens FL Jr (2004) Polyamines and cancer: old molecules, new understanding. *Nat Rev Cancer* 4(10):781-92.

Ginn SL, Alexander IE, Edelstein ML, Abedi MR, Wixon J (2013) Gene therapy clinical trials worldwide to 2012 – an update. *J Gene Med* 15: 65–77.

Goesmann H, Feldmann C (2010) Nanoparticulate Functional Materials. *Angew Chem Int Ed* 49: 1362–1395.

Gordon DJ, Resio B, Pellman D (2012) Causes and consequences of aneuploidy in cancer. *Nature Rev Genet* 13: 189-203.

Ha CH, Sirisoma NS, Kuppusamy P, Zweier JL, Woster PM, Casero JRRA (1998) The natural polyamine spermine functions directly as a free radical scavenger. *Proc. Natl. Acad. Sci. U.S.A.* 95, 11140–11145.

Hamman JH (2010) Chitosan based polyelectrolyte complexes as potential carrier materials in drug delivery systems. *Mar Drugs* 8(4): 1305–1322.

Hanahan D, Weinberg RA (2000) The hallmarks of cancer. *Cell* 100: 57–70.

Hanahan D, Weinberg RA (2011) Hallmarks of cancer: the next generation. *Cell* 144: 646–674.

Hashimoto M, Morimoto M, Saimoto H, Shigemasa Y, Sato T (2006) Lactosylated chitosan for dna delivery into hepatocytes: the effect of lactosylation on the physicochemical properties and intracellular trafficking of pdna/chitosan complexes. *Bioconjugate Chem* 17: 309−316.

Haugsten EM1, Zakrzewska M, Brech A, Pust S, Olsnes S, Sandvig K, Wesche J (2011) Clathrin- and dynamin-independent endocytosis of FGFR3--implications for signaling. *PLoS One* 6(7): e21708.

Hayashi Y, Yamauchi J, Khalil IA, Kajimoto K, Akita H, Harashima H (2011) Cell penetrating peptide-mediated systemic siRNA delivery to the liver. *Int J Pharm* 419(1-2): 308-13.

Hongliang D, Xiaoqing C, Guangxi Z (2013) Advances in the targeting molecules modified chitosan-based nanoformulations. *Curr Drug Targets* 14(9): 1034-52.

Hosseinkhani H, Azzam T, Tabata Y, Domb AJ (2004) Dextran–spermine polycation: an efficient non viral vector for in vitro and in vivo gene transfection. *Gene Ther* 11: 194–203.

Huang M, Khor E, Lim LY (2004) Uptake and cytotoxicity of chitosan molecules and nanoparticles: effects of molecular weight and degree of deacetylation. *Pharm Res* 21: 344–353.

Huynh NT, Roger E, Lautram N, Benoît JP, Passirani C (2010) The rise and rise of stealth nanocarriers for cancer therapy: passive versus active targeting. *Nanomedicine (Lond)* 5(9): 1415-1433.

Igarashi K, Kashiwagi K (2010) Modulation of cellular function by polyamines. *Int J Biochem Cell Biol* 42(1): 39-51.

Illum L (1998) Chitosan and its use as a pharmaceutical excipient. *Pharmaceut Res* 15: 1326–1331.

Illum L, Gill IJ, Hinchcliffe M, Fisher AN, Davis SS (2001) Chitosan as a novel nasal delivery system for vaccines. *Adv Drug Deliv Rev* 51: 81–96.

Ivanov AI (2008) Pharmacological inhibition of endocytic pathways: is it specific enough to be useful? *Methods Mol Biol* 440: 15-33.

Jain RK, Stylianopoulos T (2010) Delivering nanomedicine to solid tumors. *Nat Rev Clin Oncol* 7(11):653-64.

Jayakumar R, Chennazhi KP, Muzzarelli RAA, Tamura H, Nair SV, Selvamurugan N (2010) Chitosan conjugated DNA nanoparticles in gene therapy. *Carbohyd Polym* 79: 1–8.

Jemal A, Bray F, Center MM, Ferlay J, Ward E, Forman D (2011) Global Cancer Statistics *Ca Cancer J Clin* 61: 69–90.

Jeong JH, Kim SW, Park TG. (2007) Molecular design of functional polymers for gene therapy. *Prog Polym Sci* 32: 1239–1274.

Jiang HL, Kwon JT, Kim EM, Kim YK, Arote R, Jere D, Jeong HJ, Jang MK, Nah JW, Xu CX, Park IK, Cho MH, Cho CS (2008) Galactosylated poly(ethylene glycol)-chitosan-graft-polyethylenimine as a gene carrier for hepatocyte-targeting. *J Control Release* 131: 150–157.

Jiang HL, Lim HT, Kim YK, Arote R, Shin JY, Kwon JT, et al. (2011) Chitosan-graft-spermine as a gene carrier in vitro and in vivo. *Eur J Pharm Biopharm* 77(1): 36-42.

Jiao CY, Delaroche D, Burlina F, Alves ID, Chassaing G, Sagan S (2009) Translocation and endocytosis for cell-penetrating peptide internalization. *J Biol Chem* 284: 33957–33965.

Jintapattanakit A, Maob S, Kissel T, Junyaprasert VB (2008) Physicochemical properties and biocompatibility of N-trimethyl chitosan: effect of quaternization and dimethylation. Eur. J. Pharm. Biopharm. 70: 563–571.

Jokerst JV, Lobovkina T, Zare RN, Gambhir SS (2011) Nanoparticle PEGylation for imaging and therapy. *Nanomedicine (Lond)* 6(4): 715-28.

Joshy KS, Sharma CP (2012) Blood compatible nanostructured lipid carriers for the enhanced delivery of Azidothymidine to brain. *Adv Sci Lett* 4: 1–9.

Junghans M, Kreuter J, Zimmer A (2000) Antisense delivery using protamine-oligonucleotide particles. Nucleic Acids Res. 28: e45.

Junghans M, Kreuter J, Zimmer A (2001) Phosphodiester and phosphorothioate oligonucleotide condensation and preparation of antisense nanoparticles *Biochim. Biophys. Acta* 1544: 177 –188.

Kamaly N, Xiao Z, Valencia PM, Radovic-Moreno AF, Farokhzad OC (2012) Targeted polymeric therapeutic nanoparticles: design, development and clinical translation. *Chem Soc Rev* 41(7): 2971-3010.

Kanatani I, Ikai T, Okazaki A, Jo J, Yamamoto M, Imamura M, Kanematsu A, Yamamoto S, Ito N, Ogawa O, Tabata Y (2006) Efficient gene transfer by pullulan-spermine occurs through both clathrin- and raft/caveolae-dependent mechanisms. *J Control Release* 116(1): 75-82.

Kasaai M, Arul J, Charlet G (2000) Intrinsic viscosity–molecular weight relationship for chitosan *J Polym Sci B Polym Phys* 38(19): 2591–2598.

Kean T, Thanou M (2010) Biodegradation, biodistribution and toxicity of chitosan. *Adv Drug Deliv Rev* 62: 3–11.

Khalil IA, Kogure K, Futaki S, Harashima H (2006) High density of octaarginine stimulates macropinocytosis leading to efficient intracellular trafficking for gene expression. *J Biol Chem* 281: 3544–3551.

Kim E, Lee BS, Pyo HB, Song HW, Kim YP, Choi IS, Kim HS (2008) Fabrication of nonbiofouling surface and its application to surface plasmon field enhanced fluorescence spectroscopy. *Biochip J* 2: 103–110.

Kim TH, Jiang HL, Park IY, Kim YK, Cho MH, Nah JW (2006) Chemical modifications of chitosan as gene carriers. *Biomater Res* 10(3): 110-116

Kim TH, Park IK, Nahb JW, Choia YJ, Choa CS (2004) Galactosylated chitosan/DNA nanoparticles prepared using water-soluble chitosan as a gene carrier. *Biomaterials* 25: 3783–3792.

Kim TK, Kim SI, Akaike T, Cho CS (2005) Synergistic effect of poly (ethylenimine) on the transfection efficiency of galactosylated chitosan/DNA complexes. *J Control Release* 105: 354–366.

Knight DK, Shapka SN, Amsden BG (2007) Structure, depolymerization, and cytocompatibility evaluation of glycol chitosan. *J Biomed Mater Res A* 83A: 787–798.

Kosuge M, Takeuchi T, Nakase I, Jones AT, Futaki S (2008) Cellular internalization and distribution of arginine-rich peptides as a function of extracellular peptide concentration, serum, and plasma membrane associated proteoglycans. *Bioconjug Chem* 19: 656–664.

Kowalczyk B, Lagzi I, Grzybowski BA (2011) Nanoseparations: Strategies for size and/or shape-selective purification of nanoparticles. *Curr Opin Colloid Interface Sci* 16(2): 135–148.

Kumar A, Yellepeddi VK, Davies GE, Strychar KB, Palakurthi S (2010) Enhanced gene transfection efficiency by polyamidoamine (PAMAM) dendrimers modified with ornithine residues. *Int J Pharm* 392(1-2): 294-303.

Kumar A, Yellepeddi VK, Vangara KK, Strychar KB, Palakurthi S (2011) Mechanism of gene transfection by polyamidoamine (PAMAM) dendrimers modified with ornithine residues. *J Drug Target* 19(9):770-80.

Kunath K, Harpe AV, Fischer D, Petersen H, Bickel U, Voigt K, Kissel T (2003) Low-molecular-weight polyethylenimine as a non-viral vector for DNA delivery: comparison of physicochemical properties, transfection efficiency and in vivo distribution with high-molecular-weight polyethylenimine. *J Control Release* 89: 113–125.

Lahtz C, Pfeifer GP (2011) Epigenetic changes of DNA repair genes in cancer. *J Mol Cell Biol* 3, 51-58.

Lai WF, Lin MCM (2009) Nucleic acid delivery with chitosan and its derivatives. J Control Release 134: 158–168.

Lee JY, Choi YS, Suh JS, Kwon YM, Yang VC, Lee SJ, Chung CP, Park YJ (2011) Cell-penetrating chitosan/doxorubicin/TAT conjugates for efficient cancer therapy. *Int J Cancer* 28(10): 2470-80.

Leong KW, Mao HQ, Truong-Le VL, Roy K, Walsh SM, August JT (1998) DNA Polycation nanospheres as non-viral gene delivery vehicles, *J Control Release* 53 183–193.

Lewis JD, de Jong ME, Bagha SM, Tang A, Gilly WF, Ausió J (2004) All roads lead to arginine: the squid protamine gene. *J Mol Evol* 58(6): 673-80.

Liu CW, Lin WJ (2012) Polymeric nanoparticles conjugate a novel heptapeptide as an epidermal growth factor receptor-active targeting ligand for doxorubicin. *Int J Nanomedicine* 7:4749-67.

Liu D, Wu W, Ling J, Wen S, Gu N, Zhang X (2011) Effective PEGylation of iron oxide nanoparticles for high performance in vivo cancer imaging. *Adv Funct Mater* 21: 1498–1504.

Liu TC, Kirn D (2008) Gene therapy progress and prospects cancer: oncolytic viruses. *Gene Ther* 15: 877–884.

Lu P, Weaver VM, Werb Z (2012) The extracellular matrix: A dynamic niche in cancer progression. *J Cell Biol* 196(4): 395–406.

Luan B, Aksimentiev A (2010) Electric and electrophoretic inversion of the DNA charge in multivalent electrolytes. *Soft Matter* 6: 243–246.

Lundqvist M, Stigler J, Elia G, Lynch I, Cedervall T, Dawson KA (2008) Nanoparticle size and surface properties determine the protein corona with possible implications for biological impacts. *Proc Natl Acad Sci* U S A 105: 14265-14270.

Lv HT, Zhang SB, Wang B, Cui SH, Yan J (2006) Toxicity of cationic lipids and cationic polymers in gene delivery. *J Control Release* 114: 100–109.

Ma DX, Shi NQ, Qi XR (2011) Distinct transduction modes of arginine-rich cell-penetrating peptides for cargo delivery into tumor cells. *Int J Pharm* 419(1-2): 200– 208.

Mao S, Shuai X, Unger F, Simon M, Bi D, Kissel T (2004) The depolymerisation of chitosan: effects on physicochemical and biological properties. *Int J Pharm* 281: 45–54.

Mao S, Sun W, Kissel T (2010) Chitosan-based formulations for delivery of DNA and siRNA. *Adv Drug Deliv Rev* 62: 12–27.

McMahon BJ, Kwaan HC (2012) Thrombotic and bleeding complications associated with chemotherapy. *Semin Thromb Hemost* 38(08): 808-817.

Minois N, Carmona-Gutierrez D, Madeo F (2011) Polyamines in aging and disease.*Aging (Albany NY)* 3(8): 716–732.

Mintzer MA, Simanek EE (2009) Non viral vectors for gene delivery. *Chem Rev* 109(2): 259-302.

Moreira C, Oliveira H, Pires LR, Simo ˜es S, Barbosa MA, Peˆgo AP (2009) Improving chitosan-mediated gene transfer by the introduction of intracellular buffering moieties into the chitosan backbone. *Acta Biomater* 5: 2995–3006.

Morille M, Passirani C, Vonarbourg A, Clavreul A, Benoit JP (2008) Progress in developing cationic vectors for non-viral systemic gene therapy against cancer. *Biomaterials* 29(24-25): 3477-96.

Morris VB, Sharma CP (2010) Folate mediated histidine derivative of quaternised chitosan as a gene delivery vector. *Int J Pharm* 389 (1–2): 176–185.

Mourya VK, Inamdar NN (2008) Chitosan-modifications and applications: opportunities galore. *React Funct Polym* 68, 1013–1051.

Mumper RJ, Wang J, Claspell JM, Rolland AP (1995) Novel polymeric condensing carriers for gene delivery. *Proc Intl Symp Controlled Rel Bioact Mater* 22: 178-179.

Muzzarelli RAA (2009) Chitins and chitosans for the repair of wounded skin, nerve, cartilage and bone. *Carbohyd Polym* 76: 167–182.

Nam HY, Kwon SM, Chung H, Lee S-Y, Kwon S-H, Jeon H, Kim Y, Park JH, Kim J, Her S, Oh Y-K, Kwon IC, Kim K, Jeong SY (2009) Cellular uptake mechanism and intracellular fate of hydrophobically modified glycol chitosan nanoparticles. J Control Release. 135: 259–267.

Nazir S, Hussain T, Ayub A, Rashid U, MacRobert AJ (2014) Nanomaterials in combating cancer: therapeutic applications and developments. *Nanomedicine* 10(1): 19-34.

Neamnark A, Suwantong O, Bahadur RK, Hsu CY, Supaphol P, Uludağ H (2009) Aliphatic lipid substitution on 2kDa polyethylenimine improves plasmid delivery and transgene expression. *Mol Pharm* 6(6): 1798-815.

Nel AE, Mädler L, Velegol D, Xia T, Hoek EMV, et al. (2009) Understanding biophysicochemical interactions at the nano–bio interface. *Nat Mater* 8: 543 – 557.

Neu M, Fischer D, Kissel T (2005). Recent advances in rational gene transfer vector design based on poly (ethyleneimine) and its derivatives. *J Gene Med* 7: 992–1009.

Nguyen TH, Ferry N (2004) Liver gene therapy: advances and hurdles. *Gene Ther* 11 (Suppl 1) S76–84.

Niemantsverdriet M, van Goethem MJ, Bron R, Hogewerf W, Brandenburg S, Langendijk JA, van Luijk P, Coppes RP (2012) High and low LET radiation differentially induce normal tissue damage signals. *Int J Radiat Oncol Biol Phys* 83(4): 1291-7.

No HK, Meyers SP, Prinyawiwatkul W, Xu Z (2007) Applications of chitosan for improvement of quality and shelf life of foods: A Review. *J Food Sci* 72(5): 87-100.

Orlandi PA, Fishman PH (1998) Filipin-dependent inhibition of cholera toxin: evidence for toxin internalization and activation through caveolae-like domains. *J Cell Biol* 141: 905–915.

Palmer AJ, Wallace HM (2010) The polyamine transport system as a target for anticancer drug development. *Amino Acids* 38: 415–422.

Parhiza H, Shier WT, Ramezani M (2013) From rationally designed polymeric and peptidic systems to sophisticated gene delivery nano-vectors. *Int J Pharm* 457: 237–259.

Pedro SA, Cabral-Albuquereque E, Ferreira D, Sarmento B (2009) Chitosan: An option for development of essential oil delivery systems for oral cavity care? *Carbohyd Polym* 76: 501-508.

Perry HAD, Amer F, Saleh A, Aojula H, Pluen A (2008) YOYO as a dye to track penetration of LK15 DNA complexes in spheroids: use and limits. *J Fluoresc* 18: 155–161.

Pietras K, Östman A (2010) Hallmarks of cancer: Interactions with the tumor stroma. *Exp Cell Res* 316: 1324–1331.

Prabhakar U, Maeda H, Jain RK, Sevick-Muraca EM, Zamboni W, et al. (2013) Challenges and key considerations of the enhanced permeability and retention effect for nanomedicine drug delivery in oncology. *Cancer Res* 73(8): 2412-7.

Preissner S, Dunkel M, Hoffmann MF, Preissner SC, Genov N, et al. (2012) Drug cocktail optimization in chemotherapy of cancer. *PLoS ONE* 7(12): e51020.

Priya SS, Rekha MR, Sharma CP ((2014) Pullulan–protamine as efficient haemocompatible gene delivery vector: Synthesis and in vitro characterization. *Carbohyd Polym* 102: 207– 215.

Reitan NK, Maurstad G, Davies CL, Strand SP (2009) Characterizing DNA condensation by structurally different chitosans of variable gene transfer efficacy. *Biomacromolecules* 10: 1508–1515.

Rejman J, Bragonzi A, Conese M (2005) Role of clathrin- and caveolae-mediated endocytosis in gene transfer mediated by lipo- and polyplexes. *Mol Ther* 12: 468–474.

Rekha MR, Sharma CP (2009) Blood compatibility and in vitro transfection studies on cationically modified pullulan for liver cell targeted gene delivery. *Biomaterials* 30: 6655–6664.

Richard I, Thibault M, De Crescenzo G, Buschmann MD, Lavertu M (2013) Ionization behavior of chitosan and chitosan-DNA polyplexes indicate that chitosan has a similar capability to induce a proton-sponge effect as PEI. *Biomacromolecules* 14(6): 1732-40.

Riva R, Ragelle H, Rieux Ad, Duhem N, Je´roˆme C, Pre´at V (2011) chitosan and chitosan derivatives in drug delivery and tissue engineering. *Adv Polym Sci* 244: 19–44.

Sahay G, Alakhova DY, Kabanov AV (2010) Endocytosis of nanomedicines. *J Control Release* 145(3):182-95.

Sajomsang W, Gonil P, Ruktanonchai UR, Pimpha N, Sramala I, Nuchuchua O, Saesoo S, Chaleawlert-umpon S, Puttipipatkhachorn S (2011) Self-aggregates formation and mucoadhesive property of water-soluble β-cyclodextrin grafted with chitosan *Int. J. Biol. Macromol* 48: 589-95.

Sato T, Ishii T, Okahata Y (2001) In vitro gene delivery mediated by chitosan. Effect of pH, serum and molecular mass of chitosan on the transfection efficiency. *Biomaterials* 22: 2075–2080.

Shao Q, Goyal S, Finzi L, Dunlap D (2012) Physiological levels of salt and polyamines favor writhe and limit twist in DNA. *Macromolecules* 45(7): 3188–3196.

Shelma R, Sharma CP (2011) Development of lauroyl sulfated chitosan for enhancing hemocompatibility of chitosan. *Colloids Surf. B* (84) 561-570.

Shmueli RB, Anderson DG, Green JJ. Electrostatic surface modifications to improve gene delivery (2010) *Expert Opin Drug Deliv* 7(4): 535–550.

Sigismund S, Confalonieri S, Ciliberto A, Polo S, Scita G, Di Fiore PP (2012) Endocytosis and signaling: cell logistics shape the eukaryotic cell. *Physiol Rev* 92: 273−366.

Snyder SL, Sobocinski PZ (1975) An improved 2, 4, 6-trinitrobenzenesulfonic acid method for the determination of amines. *Anal Biochem* 64: 284–288.

Soetens O, Crabeel M, El Moualij B, Duyckaerts C, Sluse F (1998) Transport of arginine and ornithine into isolated mitochondria of Saccharomyces cerevisiae. *Eur J Biochem* 258(2): 702-9.

Soliman H (2013) Immunotherapy strategies in the treatment of breast cancer. *Cancer Control* 20(1): 17-21.

Sonawane ND, Szoka, FC Jr, Verkman AS (2003) Chloride accumulation and swelling in endosomes enhances DNA transfer by polyamine-DNA polyplexes. *J Biol Chem* 278: 44826-44831.

Song B, Zhang W, Peng R, Huang J, Nie T, Li Y, Jiang Q, Gao R (2009) Synthesis and cell activity of novel galactosylated chitosan as a gene carrier. *Colloids Surf B Biointerfaces* 70(2): 181-6.

Soto AM, Sonnenschein C (2010) Environmental causes of cancer: endocrine disruptors as carcinogens. *Nat Rev Endocrinol* 6: 363-370.

Srinivasachari S, Liu Y, Prevette LE, Reineke TM (2007) Effects of trehalose click polymer length on pDNA complex stability and delivery efficacy. *Biomaterials* 28, 2885–2898.

Strand SP, Issa MM, Christensen BE, Vårum KM, Artursson P (2008) Tailoring of chitosans for gene delivery: novel self-branched glycosylated chitosan oligomers with improved functional properties. *Biomacromolecules* 9: 3268–3276.

Strand SP, Lelu S, Reitan NK, Davies CL, Artursson P, Vårum KM (2010) Molecular design of chitosan gene delivery systems with an optimized balance between polyplex stability and polyplex unpacking. *Biomaterials* 31: 975–987.

Sudheesh K, Shukla SK, Mishra AK, Arotiba OA, Mamba BB (2013) Chitosan-based nanomaterials: A state-of-the-art review. *Int J Biol Macromol* 59: 46-58.

Tan PH, Chan CL, George AJ (2006) Strategies to improve non-viral vectors--potential applications in clinical transplantation. *Expert Opin Biol Ther* 6(6): 619-30.

Thakor DK, Teng YD, Tabata Y (2009) Neuronal gene delivery by negatively charged pullulan–spermine/DNA anioplexes. *Biomaterials* 30: 815–1826.

Thomas JJ, Rekha MR, Sharma CP (2010) Dextran-protamine polycation: An efficient non viral and haemocompatible gene delivery system. *Colloids Surf B Biointerfaces* 81: 195–205.

Tian F, Hu YLK, Zhao B (2003) The depolymerisation mechanism of chitosan by hydrogen peroxide. J Mater Sci 38: 4709–4712.

Tsuchiya Y, Ishii T, Okahata Y, Sato T (2006) Characterization of protamine as a transfection accelerator for gene delivery. *J of Bioact and Compat Polym* 21: 519-537.

Venkatesh S, Smith TJ (1998) Chitosan-membrane interactions and their probable role in chitosan-mediated transfection, *Biotechnol Appl Biochem* 27 (3): 265–267.

Vercauteren D, Rejman J, Martens TF, Demeester J, De Smedt SC, Braeckmans K (2012) On the cellular processing of non-viral nanomedicines for nucleic acid delivery: Mechanisms and methods. *J Control Release* 161: 566–581.

Verma A, Stellacci F (2010) Effect of Surface Properties on Nanoparticle–Cell Interactions. *Small* 6(1): 12–21.

Vermeulen K, Bockstaele DRV, Berneman ZN (2003) The cell cycle: a review of regulation, deregulation and therapeutic targets in cancer. Cell *Prolif* 36: 131–149. 131.

Vile RG, Russell SJ, Lemoine NR (2000) Cancer gene therapy: hard lessons and new courses. *Gene Ther* 7(1): 2-8.

Vineis P, Wild CP (2014) The cancer wars 1 Global cancer patterns: causes and prevention. *Lancet* 383: 549–57.

Wagner V, Dullaart A, Bock AK, Zweck A (2006) The emerging nanomedicine landscape. *Nat Biotechnol* 24: 1211 – 1217.

Wang C, Pham PT (2008) Polymers for viral gene delivery. *Expert Opin Drug Deliv* 5(4): 385-401.

Wang J, Byrne JD, Napier ME, DeSimone JM (2011) More effective nanomedicines through particle design. *Small* 7: 1919–1931.

Wang XL, Xu R, Lu ZR (2009a) A peptide-targeted delivery system with pH sensitive amphiphilic cell membrane disruption for efficient receptor-mediated siRNA delivery. *J Control Release* 134: 207-213.

Williams JA, Bridge G, Fowler LJ, John RA (1982) The reaction of ornithine aminotransferase with ornithine. *Biochem J* 201(1): 221–225.

Williams K (1997) Interactions of polyamines with ion channels. *Biochem J* 325: 289-297.

Won YY, Sharma R, Konieczny SF (2009) Missing pieces in understanding the intracellular trafficking of polycation/DNA complexes. *J Control Release* 139: 88–93.

Xu LC, Siedlecki CA (2007) Effects of surface wettability and contact time on protein adhesion to biomaterial surfaces. *Biomaterials* 28(22): 3273-83.

Xu Y, Takai M, Ishihara K (2009) Protein adsorption and cell adhesion on cationic, neutral, and anionic 2-methacryloyloxyethyl phosphorylcholine copolymer surfaces. *Biomaterials* 30(28): 4930-8.

Yang S, May S (2008) Release of cationic polymer-DNA complexes from the endosome: A theoretical investigation of the proton sponge hypothesis. *J Chem Phys* 129: 185105.

Yang SJ, Lin FH, Tsai KC, Wei MF, Tsai HM, Wong JM, Shieh MJ (2010) Folic acid-conjugated chitosan nanoparticles enhanced protoporphyrin IX accumulation in colorectal cancer cells. *Bioconjug Chem* 21(4): 679-89.

Youn JI, Park SH, Jin HT, Lee CG, Seo SH, Song MY, Lee CW, Sung YC (2008) Enhanced delivery efficiency of recombinant adenovirus into tumor and mesenchymal stem cells by a novel PTD. *Cancer Gene Ther* 15(11): 703-12.

Yu H, Deng C, Tian H, Lu T, Chen X, Jing X (2011) Chemo-physical and biological evaluation of poly(l-lysine)-grafted chitosan copolymers used for highly efficient gene delivery. *Macromol Biosci* 11: 352–361.

Zhang C, Wang QT, Liu H, Zhang ZZ, Huang WL (2011) Advancement and prospects of tumor gene therapy. *Chin J Cancer* 30(3): 182–188.

Zhang H, Zhu D, Song L, Liu L, Dong X, Liu Z, Leng X (2011) Arginine conjugation affects the endocytic pathways of chitosan/nanoparticles. *J Biomed Mater Res A* 98(2): 296-302.

Zhang X, Pan SR, Hu HM, Wu GF, Feng M, Zhang W, Luo X (2008) Poly(ethylene glycol)-block-polyethylenimine copolymers as carriers for gene delivery: effects of PEG molecular weight and PEGylation degree. *J. Biomed. Mater. Res. A.* 84: 795–804.

Zhang Y, Yang Y, Tang K, Hu X, Zou G (2008) Physicochemical characterization and antioxidant activity of quercetin-loaded chitosan nanoparticles. *J Appl Polym Sci* 107: 891–897.

Zheng F, Shi X-W, Yang G-F, Gong L-L, Yuan H-Y, Cui Y-J, et al. (2007) Chitosan nanoparticle as gene therapy vector via gastrointestinal mucosa administration: Results of an *in vitro* and *in vivo* study. *Life Sci* 80: 388–396.

Zhu XL, Du YZ, Yu RS, Liu P, Shi D, Chen Y, et al. (2013) Galactosylated chitosan oligosaccharide nanoparticles for hepatocellular carcinoma cell-targeted delivery of adenosine triphosphate. *Int. J. Mol. Sci* 14: 15755-15766.

LIST OF PUBLICATIONS & CONFERENCES ATTENDED

Piña M, Alex SM, Arias F, Santos M, Rodriguez-Cabello J, Rehka MR, Sharma CP (2015) Elastin-like recombinamers with acquired functionalities for gene-delivery applications. *J Biomed Mater Res A* doi: 10.1002/jbm.a.35455. [Epub ahead of print]

Alex SM, Sharma CP (2014) Enhanced intracellular uptake and endocytic pathway selection mediated by hemocompatible ornithine grafted chitosan polycation for gene delivery. *Colloids Surf B Biointerfaces* 1; 122:792-800

Alex SM, Sharma CP (2012) Nanomedicine for gene therapy. *Drug Dev Trans Res* 1:10-14.

Alex SM, Rekha MR, Sharma CP (2011) Spermine grafted galactosylated chitosan for improved nanoparticle mediated gene delivery. *Int J Pharm* 10;410(1-2):125-37.

Alex SM and Sharma CP (2012) Ligand targeted and polyamine substitution in chitosan for efficient nanoparticle mediated gene delivery. (Oral Presentation in the International Conference on Biomaterials (BIDTE) conducted by the Society of Biomaterials and Artifcial Organs of India held in Chennai, Jan 5-7). *Received First Prize (Bajpai-Sahay Award).*

Alex SM and Sharma CP. (2012) Improved uptake of nucleic acid by ornithine incorporated chitosan polyplexes. (Poster presentation in the 10th International conference on Nanomedicine and Drug Delivery (Nano DDS), USA, Dec 6-7.)

APPENDICES

A1- Table 1. Percentage hemolysis of GCSM polymer in four ascending concentrations. The values given are mean ± SD and n=3.

Amount of GCSM polymer (µg/mL)	% hemolysis
25	0.352 ± 0.24
50	0.410 ± 0.13
75	0.528 ± 0.36
100	0.645 ± 0.48
Triton X-100	1 ± 0.32

A2- Table 2. Percentage hemolysis of CDP polymer in four ascending concentrations. The values given are mean ± SD and n=3.

Amount of CDP polymer (µg/mL)	% hemolysis
25	0.317 ± 0.37
50	0.508 ± 0.11
75	0.636 ± 0.34
100	0.674 ± 0.111
Triton X-100	1 ± 0.28

A3- Table 3. Percentage hemolysis of CON polymer in four ascending concentrations. The values given are mean ± SD and n=3.

Amount of CON polymer (µg/mL)	% hemolysis
25	0.363 ± .006
50	0.426 ± 0.021
75	0.439 ± 0.007
100	0.453 ± 0.001
Triton X-100	1 ± 0.008

A4- Table 4. Percentage hemolysis of COSM polymer in four ascending concentrations. The values given are mean ± SD and n=3.

Amount of COSM polymer (µg/mL)	% hemolysis
25	0.234 ± .091
50	0.352 ± 0.20
75	0.410 ± 0.57
100	0.469 ± 0.06
Triton X-100	1 ± 0.46

Fig A5: Infrared spectroscopy for evaluation of chemical groups in the functional entities of the GCSM derivative. FTIR spectrum of galactosylated chitosan (GC).

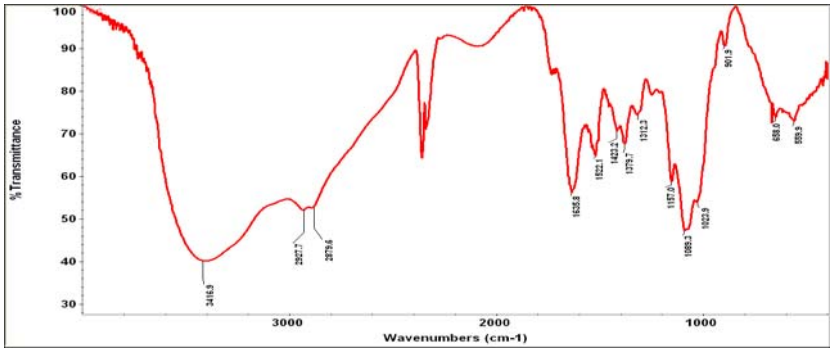

Fig A6: Infrared spectroscopy for evaluation of chemical groups in the functional entities of the CDP derivative. FTIR spectrum of diamine PEGylated chitosan (CD).